Investigation of parasporins, the cytotoxic proteins from the bacterium *Bacillus thuringiensis*

VIDISHA KRISHNAN

SUBMITTED FOR THE DEGREE OF DOCTOR OF PHILOSOPHY

DEPARTMENT OF BIOCHEMISTRY

SCHOOL OF LIFE SCIENCES

UNIVERSITY OF SUSSEX

2013

Declaration

WORK NOT SUBMITTED ELSEWHERE FOR EXAMINATION

I hereby declare that this thesis has not been submitted in whole or in part to this or any other University for the award of a degree.

Vidisha Krishnan

ABSTRACT

The cytotoxic activities of proteins from the normally insecticidal *Bacillus thuringiensis* against human cancer cell lines were investigated. Cry41Aa toxin derived from the *Bacillus thuringiensis* strain A1462, which shows activity against human cancer cell lines is structurally related to the toxins synthesized by commercially produced transgenic insect-resistant plants, with the exception of an additional C-terminal beta-trefoil ricin domain. To test whether this putative carbohydrate binding domain is responsible for the cytotocidal activity of Cry41Aa against cancer cell lines, we developed an efficient expression system for the toxin and created a deletion mutant lacking the ricin domain. Both Cry41Aa and its deletion mutant were stably expressed and found to have almost identical activities against the HepG2 cancer cell line *in vitro*. Our results suggest that the acquisition of the ricin domain was not responsible for Cry41Aa having toxicity to human cancer cells and more subtle changes have resulted in the evolution of mammalian cancer cell toxicity. We further attempted to identify those differences that are responsible for the divergence in activity between the cancer-killing toxins and their insecticidal counterparts. We also studied the cell-killing activity of other uncharacterized *Bacillus thuringiensis* crystal toxins including Cry51 and Cry65 whose targets are not known so far.

Acknowledgements

I sincerely express my immense gratitude to my supervisor, Dr. Neil Crickmore for his kind and patient guidance and active involvement in all stages of this project from its inception. Neil is not only an outstanding scientist but a great teacher and a wonderful person. I am indebted to him for all that I have learnt and continue to learn from him and I express my profound respect to him.

With gratitude I acknowledge Dr. Lynne Mayne for introducing me to Cell Biology skills.

My special thanks to Dr. Michelle West for the excellent facilities, expertise and advice. To all her wonderful, approachable and friendly lab members for extending every aid cheerfully and promptly.

To Ali who is always in our thoughts.

To Mark, Paul, Zenas, Ruchir and the undergrads including Natalie, Laura, Laurence, Heather and everyone with whom I have worked for all the wonderful times that I had with them in the lab.

Finally, I would like to thank my wonderful, amazing kids Ash and Babhravi for all their love and support. They always inspire me to do my best. To Krishnan for annoying me for close to two decades—besides for the innumerable print-outs! To my wonderful grand-dad and grand –mum for their unconditional love and providing me the best possible facilities in India and all that I have learnt from them. To all my family and friends who have always been there for me.

I wouldn't have been able to do this without you all!

Vidisha.

Table of Contents

Abbreviations

AC	Adenylate cyclase
APN	Aminopeptidase-N
ATP	Adenosine 5’- triphosphate
BSA	Bovine serum albumin
Bt	*Bacillus thuringiensis*
Bp	base pairs
BT-R1	*Bacillus thuringiensis* midgut cadherin receptor in *M. sexta*
Cry	Crystal
Cyt	Cytolytic
DTT	Dithiothreitol
DMEM	Dulbecco’s modified Eagle’s medium
DMSO	Dimethyl sulphoxide
E. coli	*Escherichia coli*
FBS	Fetal bovine serum
FPLC	Fast protein liquid chromatography
GPI	glycosylphosphatidyl-inositol
IPTG	Isopropyl β-D-thiogalactopyranoside
kDa	Kilo Dalton
l	Litre
LB	Luria Bertani
SDS	Sodium dodecylsulfate
OD	Optical density
ORF	Open reading frame

PAGE	Polyacrylamide gel electrophoresis
PBS	Phosphate buffered saline
PCR	Polymerase chain reaction
PKA	Protein kinase A
PS	Parasporin
PSG	Penicillin, streptomycin, and glutamine
RFU	Relative Fluorescence Unit
RGB	Resolving gel buffer
RLU	Relative Luminescence Unit
RSS	Rapid size screen
SD	Standard deviation
SGB	Stacking gel buffer
TEMED	N,N,N’,N’-tetramethylethylenediamine
Vip	Vegetative insecticidal protein

1. Introduction

1.1 General Introduction

The toxicity of a naturally occurring organism is a striking phenomenon. As we introspect at the history of naturally occurring toxins, be they of bacterial or plant origin, we find that once their physical and chemical parameters are understood, these substances can be of considerable medical and economic importance (Schmitt et al., 1999; Sandvig and Deurs, 2000; Goodsell, 2001).

Bacterial protein toxins have been long employed as biological tools to elucidate several mechanisms in agriculture and medicine. Gram-positive entomopathogenic bacteria have received substantial attention as biological control agents due to their potential to control insect pests in agriculture and insect vectors of human diseases. *B. thuringiensis* δ-endotoxins provide a valuable alternative to synthetic insecticides for controlling insect pests. Sprays comprising of sporulated Bt have not only been employed for pest control in agriculture, sprays of *B. thuringiensis* subsp. *israelensis* (Bti) have also been used to control disease-carrying vectors such as mosquitoes and blackflies (Becker, 2000). Besides sprays, *B. thuringiensis* genes expressing the entomocidal Cry proteins have been engineered into crop plants, rendering them resistant to several insect pests (Barton et al., 1987; Vaeck et al., 1987; de Maagd et al., 1999; Tabashnik, 2010). *B. thuringiensis* is safe to the environment, humans and non-target organisms owing to its narrow host range alongside its

efficacy in controlling varied insect pests (Bulla et al., 1975; Drobniewski, 1994; Mendelsohn et al., 2003; Walter et al., 2010; Bravo et al., 2011, 2012).

Recently *B. thuringiensis* toxins have been isolated that possess preferential activity against human cell lines and in particular cancer cell lines. These toxins have been suggested as being non-insecticidal (Mizuki et al., 1999, 2000; Ohba et al., 2009). Study of this class of toxin has implications not only in medical research as potential therapies for certain cancers or as diagnostic agents but also in the risk assessment of Bt toxins being used and developed for insect control in agriculture. It is imperative to carry out the risk assessment of food and feed derived from genetically engineered Bt plants. Although there have been reports of modified Bt on non-target human cells (Mesnage et al., 2012), various assessments carried out to check for the safety of commercial Bt toxins as sprays or transgenic plants have found them to be environmentally friendly with no known adverse effects to non-target species (Kapur et al., 2010; Caquet et al., 2011).

1.2 *Bacillus thuringiensis*

Isolated by the Japanese bacteriologist Ishiwata from diseased silkworm *Bombyx mori* larvae in 1901 and scientifically described by Berliner in 1911 (Heimpel & Angus, 1958), *B. thuringiensis* is currently the leading biorational pesticide which is safe to the environment. The bacterium is gram-positive, rod-shaped, aerobic endospore-forming and characterised by the presence of protein crystals within

the cytoplasm of its sporulating cells that are toxic towards insects. These insecticidal crystal (Cry) proteins produced during the stationary phase of the bacterium's growth cycle have been used as biopesticides against a wide range of agricultural insect pests belonging to several orders including Lepidoptera (butterflies and moths), Diptera (flies and mosquitoes), Coleoptera (beetles and weevils), Hymenoptera (wasps and bees) and Orthoptera (locust) (Hofte & Whiteley, 1989; de Maagd et al., 2001). Some of the Cry toxins have been reported to show activity against non-insect species particularly the nematodes, mites and protozoa (de Maagd et al., 2001; Wei et al., 2003).

1.3 *B. thuringiensis* taxonomy and genetics

B. thuringiensis is closely related to the ubiquitous soil bacterium *Bacillus cereus*, an opportunistic pathogen that causes food poisoning (Gonzalez, 1981; Drobniewski, 1993). Molecular characterisation techniques such as 16S and 23S rRNA sequence analysis (Ash et al., 1991; Rössler et al., 1991; Akhurst et al., 1997; te Giffel et al., 1997), AFLP analysis (Keim et al., 1997; Jackson et al., 1999), multilocus enzyme electrophoresis (Helgason et al., 2000) have failed to discriminate *B. thuringiensis* isolates from *B. cereus*, crystal formation being the most significant criterion for distinguishing between the two. Thus both *B. thuringiensis* and *B. cereus* belong to the *Bacillus cereus* group that also entails the mammalian pathogen *B. anthracis*, *B. mycoides*, *B. pseudomycoides* and a psychrotolerant strain *B. weihenstephanessis* which are able to grow at low temperatures of 7ºC and below (Lechner et al., 1998; Jensen et al., 2003). High genetic relatedness has resulted in them being regarded as members of a single

species, *Bacillus cereus sensu lato* (Daffonchio et al., 2000; Helgason et al., 2000). *B. cereus* is actually considered as the parental species. The other members of the taxa including *B. thuringiensis* and *B. anthracis* are in fact the derivatives of *B. cereus* that have acquired large extrachromosomal elements that encode for the crystal toxins of *B. thuringiensis* or the pX01- lethal toxin of *Bacillus anthracis* (Gonzalez et al., 1981; Agaisse et al., 1999; Okinaka et al., 1999; Read et al., 2003; Hu et al., 2009). It has been reported that transfer of δ-endotoxin encoding plasmids from *B. thuringiensis* to *B. cereus* results in the production of crystalline inclusions in the recipient *B. cereus* strain rendering it indistinguishable from *B. thuringiensis* (González et al., 1982; Battisti et al., 1985). Further, it has been reported that *B. thuringiensis* can incur loss of production of δ-endotoxins either due to loss of plasmid or changes in gene expression. *B. thuringiensis* strain thus cured of its *cry*- encoding plasmid cannot be phenotypically distinguished from the *B. cereus* strain (Aronson, 1993; Eilenberg et al., 2000). However, they retain the status of separate species due to remarkably different distinct virulence phenotype (Helgason et al., 2000).

The genome of *B. thuringiensis* strains range from 2400 to 5700 kb present as choromosomal and extrachromosomal elements (Carlson et al., 1994, 1996). The crystal toxin genes are found on the extrachromosomal DNA in the form of large circular plasmids (Kronstad et al., 1983; Ward & Ellar, 1983), although chromosomal homologs have also been identified (Carlson & Kolsto, 1993). Plasmids in *B. thuringiensis* strains range from 4.56 to 228 kb (Gonzalez & Carlton, 1980; Lereclus et al., 1982; Baum & Gonzalez, 1992). *B. thuringiensis* harbours a plethora of transposable elements including insertion sequences and

transposons, often located in the vicinity of the toxin gene, thus facilitating intra/ inter molecular genome mobility (Battisti et al., 1985; Green et al., 1989).

1.4 Ecology and prevalence

The search for genetic diversity of *B. thuringiensis* has led to its isolation worldwide from diverse habitats, thus reporting the mesophilic *B. thuringiensis* to be indigenous to many environments having an optimal growth temperature at approximately 25-35ºC (Martin & Travers, 1989; Bernhard et al., 1997). Strains have been isolated worldwide from diverse environments including soil (DeLucca et al., 1979, 1981; Carozzi et al., 1991; Hastowo et al., 1992; Hossain et al., 1997), stored grain dusts (DeLucca et al., 1984), mills (Meadows et al., 1992), foods (Damgaard et al., 1996; Rosenquist et al., 2005; Frederiksen et al., 2006), insect cadavers (Damgaard et al., 1997; Hansen et al., 1998; Eilenberg et al., 2000), freshwater (Espinasse et al., 2003), phylloplanes of conifer and decidual leaves (Collier et al., 2005; Bizzarri & Bishop, 2007), rhizosphere (Manonmani et al., 1991), annelids (Hendriksen & Hansen, 2002), crustaceans (Swiecicka & Mahillon, 2006) and insectivorous mammals (Swiecicka et al., 2002; Swiecicka & De Vos, 2003). Hence with an unclear ecology, this ubiquitous bacterium may be best described as an opportunist pathogen. However in spite of such complex ecology, it has been suggested the bacterium mainly reproduces in an insect cadaver (Raymond et al., 2010). Hence this suggests that the presence of the *B. thuringiensis* in these environments is transient in nature. The persistence of *B. thuringiensis* spores and toxins in various diverse environments have been well

researched (West et al., 1984; Petras & Casida, 1985) reporting the viability of spores to be several years.

An insight into the true ecological roles of *B*. *thuringiensis* might prove to be vital for improving the reliability of risk assessment and for developing efficient methodologies for isolation of novel *B. thuringiensis* strains harbouring useful δ-endotoxin genes.

1.5 Virulence factors

The bacterium produces a repertoire of virulence factors during vegetative and stationary phases of its growth that contribute to its pathogenicity (Hansen & Salamitou, 2000). The crystal toxins of *B. thuringiensis* are considered to be the major virulence factors which impart entomopathogenic properties to the bacterium. Most of the insecticidal properties of the bacterium are derived from the δ-endotoxin present in both the crystalline inclusion and in the spore coat. Production of toxin constitutes only one of the factors contributing to the pathogenicity of the bacterial strain. The crucial contribution of its spores in its pathogenicity has also been noted for instance in case of *Galleria mallonella* larvae (Li et al., 1987). Beside some of the other important non-specific virulence factors thought to contribute in its pathogenicity include phospholipases (Henner et al., 1988; Lechner et al., 1989; Zhang et al., 1993), bacteriocins (Barboza-Corona et al., 2009), haemolysins (Pendleton et al., 1973; Heierson et al., 1986; Budarina et al., 1994; Bouillaut et al., 2005; Nisnevitch et al., 2010), α-exotoxins (Krieg, 1971; Mohd-Salleh et al., 1980), β-exotoxins (Levinson et al., 1990; Carlberg et al., 1995; Perani et al., 1998), enterotoxins, inhibitor A (InhA) (Zhang

et al., 1993; Fedhila et al., 2002, 2003), proteases (Brar et al., 2009), chitinases (Tantimavanich et al., 1997; Kramer & Muthukrishnan, 1998; Sampson & Gooday, 1998; Liu et al., 2002; Arora et al., 2003) and antibiotics including Zwittermicin A (ZmA) (Stabb et al., 1994; Silo-Suh et al., 1998). Most of the virulence factors' gene expression are regulated by the transcriptional activator, phospholipase C regulator (PlcR) which has been thought to activate at least 45 genes (Agaisse et al., 1999; Gohar et al., 2008). The PlcR regulon is vital for the pathogenicity of both *B. cereus* and *B. thuringiensis* and is highly reduced or abolished by the disruption of *PlcR* gene (Salamitou et al., 2000).

In addition to the specific Cry toxins produced during the stationary phase in the sporulating cells, the bacterium also produces insecticidal proteins during its vegetative growth phase, termed as Vip proteins (vegetative insecticidal proteins) which are unrelated and differ remarkably to the Cry toxins (Schnepf et al., 1998). Although produced during the different stages of the *B. thuringiensis* life cycle, both Cry and Vip proteins share a common narrow range of target insect pests with no significant harmful effects on non-target organisms.

1.6 Vip toxins

Vip toxins have been classed as Vip1, Vip2, Vip3 and Vip4. One hundred and two *vip* genes have been sequenced so far and have been ranked by percentage amino acid sequence identity in accordance to the *B. thuringiensis* Cry toxin nomenclature (Crickmore et al., 2013) which has resulted in Vip1A (5 members),

Vip1B (4), Vip1C (1), Vip1D (1), Vip2A (11), Vip2B (4), Vip3A (66), Vip3B (5), Vip3C (4) and Vip4A (1). Vip1A and Vip2A are binary toxins encoded by a single operon (Shi et al., 2004) and when used in combination, are highly toxic to the agricultural pest the western corn rootworm *Diabrotica virgifera* infesting corn plants (Fang et al., 2007). They demonstrate a typical binary relationship of A+B type wherein Vip2 is the cytotoxic A-domain and part of Vip1 contains the receptor-binding B-domain and a possible translocation domain (de Maagd et al., 2003). Vip3 toxins share no sequence homology to Vip1A and Vip2A toxins. The 88.5 kDa Vip3 proteins possess insecticidal activity against crucial lepidopteran pests of maize and cotton including *Spodoptera litura* and *Helicoverpa zea*. They have been found to be active against a wide spectrum of lepidopteran larvae. Vip1 and Vip4 show homology to *Clostridium perfringens* iota domain Ib toxins. Vip2 is homologous to Ia component of the iota toxin. The Vip proteins are secreted during the vegetative stage of the growth commencing at the mid-log phase as well as during sporulation (Estruch et al., 1996).

1.7 Bt δ-endotoxins

The Bt δ-endotoxins are the major virulence factors that have been known to impart pathogenic properties to the bacterium against specific insects (Agaisse et al., 1999). The δ-endotoxins of *B. thuringiensis* can be divided into two major families, Cry and Cyt.

Most *B*. *thuringiensis* δ-endotoxin genes reside on plasmids (Gonzalez et al., 1981; Kronstad et al., 1983) which appear to be transmissible or conjugative in

nature (González et al., 1982). A defining feature of a *cry* gene is its expression during the stationary phase of the growth cycle. Their products generally accumulate in the mother cell compartment to form a crystal inclusion accounting for 20- 30% of the dry weight of the sporulated cells. The very high level of crystal protein synthesis in *B. thuringiensis* and its co-ordination with the stationary phase are controlled by a variety of mechanisms occurring at the transcriptional, post-transcriptional and post-translational levels (Schnepf et al., 1998). Although a vast number of *cry* genes for instance *cry1Aa*, *cry1Ab*, *cry2Aa*, *cry4Aa*, *cry15Aa* studied so far show expression in the mother cell and are dependent on sporulation sigma factors σ^E and/or σ^K (Brizzard et al., 1991; Brown, 1993; Yoshisue et al., 1993a, 1993b; Agaisse & Lereclus, 1995; Dervyn et al., 1995), expression of c*ry* genes such as *cry3Aa* is sporulation independent. Cry3Aa is produced during the vegetative growth phase of the bacterium, although at a lesser extent than during the stationary phase. The *cry3A* promoter is weakly functional during the vegetative growth phase and is activated at the end of the exponential growth. The promoter of the *cry3Aa* gene resembles the promoter recognised by the primary sigma factor σ^A of the vegetative cells. Cry3A expression is increased in Spo0A mutants which are unable to initiate sporulation (Agaisse & Lereclus, 1994; Baum & Malvar, 1995; Salamitou et al., 1996).

As of the start of 2013, there were 290 distinct Cry and Cyt toxins based on amino acid sequence identity. Currently the primary sequence identity among toxin sequences forms the basis of nomenclature of Cry and Cyt δ-endotoxins (Crickmore et al., 1998). In 1989, Hofte & Whiteley classified the then 14 different crystal toxins into 5 groups Cry I, II, III, IV and CytA based on sequence

similarities and host specificity. The ever expanding list of *B. thuringiensis* toxin genes rendered it difficult to retain such a form of nomenclature leading to the formation of a new revised system of nomenclature which classed toxin genes solely on the relatedness between the protein sequences. A committee assigns Cry toxins to distinct holotypes based on percentage amino acid sequence identity. Each holotype is assigned a primary (Arabic numeral), secondary (uppercase letter) and tertiary rank (lowercase letter) representing approximately 45%, 78% and 95% identity respectively. Quarternary rank (indicated by Arabic numeral too) denotes identical sequences which differ only slightly. Hence, those toxins differing only in quarternary rank most likely possess identical specificities and potencies. The new system removes the need to bioassay each new toxin against a series of organisms as the original nomenclature would demand (Crickmore et al., 1998). >700 *cry* genes had been sequenced to date and have been assigned to 279 holotypes. 36 *cyt* genes have been sequenced and have been assigned to 11 holotypes (Crickmore et al., 2013).

1.7.1 Cyt δ-endotoxins

Cyt toxins from *B. thuringiensis* are cytolytic to various insects and mammalian cells including erythrocytes. Three major classes of Cyt toxins, Cyt1, Cyt2 and Cyt3, have been identified. Cytolytic toxins have generally been characterised from various strains of *B. thuringiensis* possessing activity towards mosquitos and other dipteran insects. Unlike the *B. thuringiensis* Cry δ-endotoxins, Cyt toxins exhibit a broad cytolytic activity *in vitro* and are highly specific to dipteran larvae *in vivo*. High hydrophobicity and the ability to bind to certain membrane lipids have resulted in the broad cytolytic properties of the Cyt1Aa toxins. The mechanism of action is unclear and may be either pore-forming (Promdonkoy &

Ellar, 2000, 2003) or detergent-like (Butko, 2003). Like the Cry toxins, the Cyt toxins are synthesised as protoxins. Small peptide amino acids are removed from the N and C- termini to activate the toxin (Armstrong et al., 1985). For instance in case of Cyt2A, 32 amino acid residues and 15 amino acid residues are cleaved from N and C-terminal ends respectively by proteinase K treatment yielding a monomeric protein with haemolytic activity (Koni & Ellar, 1994). Non-receptor mediated binding of Cyt toxins to the synthetic lipid membrane has been observed (Thomas & Ellar, 1983b; Gill et al., 1987; Bravo et al., 2007). This is in contrast with the receptor mediated activity of Cry toxins. The X-ray structure of the Cyt2A toxin depicts a single domain of α/β architecture consisting of six α-helices and seven β-sheets (Li et al., 1996). The cytolytic toxins possess activity against mosquitos with Cyt1Aa and Cyt2Aa possessing the highest activity. The presence of a ricin domain (cd00161; pfam 00652) has been detected in the inactive Cyt1Ca (Berry et al., 2002). There is evidence of synergism between Cyt and Cry toxins for instance Cyt1Aa synergising the mosquitocidal activity of Cry11Aa (Wirth et al., 2003; Perez et al., 2005; Oestergaard et al., 2007). Synergism was detected between Cyt1A and Cry10Aa toxin of *B. thuringiensis* subsp. *israelensis* (Hernandez-Soto et al., 2009). Further, co-expression of Cyt2Aa2 and Cry4Ba in *E. coli* resulted in high synergism against *Aedes aegypti* and *Culex quinquefasciatus* larvae (Promdonkoy et al., 2005).

1.8 Cry δ-endotoxins

The 279 distinct crystal toxins of *Bacillus thuringiensis* can be further divided into a number of distinct homology groups (Table 1.1 and Figure 1.1) (de Maagd et al., 2003). The three -domain Cry proteins constitute the biggest class comprising of 249 Cry toxins. Intriguingly, members of the three-domain Cry proteins are also

present in other obligate bacteria for instance *Penibacillus popilliae*, a causal agent of milky disease of scarabaeid larvae, the parasporal crystal protein of which contains CryBP1 (Cry18Aa1) which shows 40% sequence identity to Cry2 polypeptides of *B. thuringiensis* (Zhang et al., 1997). The three-domain Cry protein members, Cry16 and Cry17 are found in *Clostridium bifermentans* (Barloy et al., 1998). The Mtx group of toxins form the second largest class made up of 9 members. Members of the Mtx group consists of the conserved domain that belongs to *Clostridium epsilon* toxin ETX / and *Bacillus* mosquitocidal toxin MTX2 superfamily (ETX/MTX2; pfam 03318). The Bin toxins constitute the third largest group with three different basic members (primary rank) and seven subtypes. Additionally, the other Cry toxins phylogenetically unrelated to above include the unique Cry6, Cry22, Cry37, Cry55 and Cry46. The Cry6 toxins were isolated from *B. thuringiensis* strains active on nematodes. Cry6A has been found to be active against nematode species (Wei et al., 2003) and on certain coleopterans including corn rootworm (Thompson et al., 2001). Cry6 toxin depicts homology to the conserved chromosome segregating protein, SMC family of proteins (TIGR: 02169). Cry22 proteins were initially isolated from *B. thuringiensis* strains active on ants (Payne et al., 1997). Later the activity of Cry22 was reported against coleoptera for instance corn rootworm (Mettus-Light & Baum, 2000) and boll weevil (Isaac et al., 2001). X-ray crystallographic studies reveal that the protein has an elongated six domain structure consisting of four cadherin-like domains flanked by a 242-residue N-terminal domain and a C-terminus of 142 residues with a fold analogous to the domain III of the three-domain Cry proteins, implicating a binding function (Rydel et al., 2003). Cry55Aa1 is thought to be a nematicidal protein (Guo et al., 2008). Cry55Aa2 might possess activity against

coleopteran pests (Bradfisch et al., 1999). Cry34 members are not related to other Bt crystal proteins; however, they are homologous to binary toxins from *B. sphaericus* with 26-29% sequence identity (de Maagd et al., 2003). Cry46, a mammalian cell-killing toxin is a β-pore forming hydralysin-like toxin (UniProtKB/Swiss-Prot: Q52SK7.3) (Ito et al., 2004).

Not all the Cry toxins isolated were insecticidal. Recently a number of non-insecticidal Cry toxins have been isolated that have been found to possess activity against human cancer cell lines. These Cry toxins have been grouped into a separate class called parasporins mainly due to their unique cytotoxic activity (Mizuki et al., 2000). Parasporins-1 (Cry31), Parasporins-3 (Cry41) and Parasporins-6 (Cry63) are the typical 3-domain toxins. Parasporin-2 (Cry46) is a hydralysin- like toxin while Parasporin-4 (Cry 45) and Parasporin-5 (Cry64) are Mtx-like toxins.

Table 1.1 List of Bt toxins and their classification based on homology groups 3 Domain Toxins | Bin Group Toxins | Mtx Group Toxins | Parasporins

Cry1Aa	Cry1Ab	Cry1Ac	Cry1Ad	Cry1Ae	Cry1Af	Cry1Ag	Cry1Ah	Cry1Ai	Cry1Ba	Cry1Bb				
Cry1Bc	Cry1Bd	Cry1Be	Cry1Bf	Cry1Bg	Cry1Bh	Cry1Bi	Cry1Ca	Cry1Cb	Cry1Da	Cry1Db	Cry1Dc	Cry1Ea		
Cry1Eb	Cry1Fa	Cry1Fb	Cry1Ga	Cry1Gb	Cry1Gc	Cry1Ha	Cry1Hb	Cry1Ia	Cry1Ib	Cry1Ic				
Cry1Id	Cry1Ie	Cry1If	Cry1Ig	Cry1Ja	Cry1Jb	Cry1Jc	Cry1Jd	Cry1Ka	Cry1La	Cry1Ma	Cry1Na	Cry1Nb		
Cry2Aa	Cry2Ab	Cry2Ac	Cry2Ad	Cry2Ae	Cry2Af	Cry2Ag	Cry2Ah	Cry2Ai	Cry2Aj	Cry2Ak	Cry2Ba			
Cry3Aa	Cry3Ba	Cry3Bb	Cry3Ca	Cry4Aa	Cry4Ba	Cry4Ca	Cry4Cb	Cry4Cc						
Cry5Aa	Cry5Ab	Cry5Ac	Cry5Ad	Cry5Ba	Cry5Ca	Cry5Da	Cry5Ea	Cry6Aa	Cry6Ba	Cry7Aa	Cry7Ab	Cry7Ba	Cry7Bb	
Cry7Bb	Cry7Ca	Cry7Cb	Cry7Da	Cry7Ea	Cry7Fa	Cry7Fb	Cry7Ga	Cry7Gb	Cry7Gc	Cry7Gd	Cry7Ha	Cry7Ia	Cry7Ja	Cry7Ka
Cry8Aa	Cry8Ab	Cry8Ac	Cry8Ad	Cry8Ba	Cry8Bb	Cry8Bc	Cry8Ca	Cry8Da	Cry8Db	Cry8Ea	Cry8Fa	Cry8Ga		
Cry8Ha	Cry8Ia	Cry8Ib	Cry8Ja	Cry8Ka	Cry8Kb	Cry8La	Cry8Ma	Cry8Na	Cry8Pa	Cry8Qa	Cry8Ra	Cry8Sa	Cry8Ta	
Cry9Aa	Cry9Ba	Cry9Bb	Cry9Ca	Cry9Da	Cry9Db	Cry9Dc	Cry9Ea	Cry9Eb	Cry9Ec	Cry9Ed	Cry9Ee	Cry9Fa	Cry9Ga	
Cry10Aa	Cry11Aa	Cry11Ba	Cry11Bb	Cry12Aa	Cry13Aa	Cry14Aa	Cry14Ab	Cry15Aa	Cry16Aa	Cry17Aa	Cry18Aa	Cry18Ba	Cry18Ca	
Cry19Aa	Cry19Ba	Cry20Aa	Cry20Ba	Cry21Aa	Cry21Ba	Cry21Ca	Cry21Da	Cry22Aa	Cry22Ab	Cry22Ba	Cry22Bb	Cry23Aa	Cry24Aa	
Cry24Ba	Cry24Ca	Cry25Aa	Cry26Aa	Cry27Aa	Cry28Aa	Cry29Aa	Cry30Aa	Cry30Ba	Cry30Ca	Cry30Da	Cry30Db	Cry30Ea	Cry30Fa	Cry30Ga
Cry31Aa	Cry31Ab	Cry31Ac	Cry31Ad	Cry32Aa	Cry32Ab	Cry32Ba	Cry32Ca	Cry32Cb	Cry32Da	Cry32Ea	Cry32Eb	Cry32Fa	Cry32Ga	
Cry32Ha	Cry32Hb	Cry32Ia	Cry32Ja	Cry32Ka	Cry32La	Cry32Ma	Cry32Mb	Cry32Na	Cry32Oa	Cry32Pa	Cry32Qa	Cry32Ra	Cry32Sa	Cry32Ta
Cry32Ua	Cry33Aa	Cry34Aa	Cry34Ab	Cry34Ac	Cry34Ba	Cry35Aa	Cry35Ab	Cry35Ac	Cry35Ba	Cry36Aa	Cry37Aa	Cry38Aa	Cry39Aa	Cry40Aa
Cry40Ba	Cry40Ca	Cry40Da	Cry41Aa	Cry41Ab	Cry41Ba	Cry42Aa	Cry43Aa	Cry43Ba	Cry43Ca	Cry43Cb	Cry43Cc	Cry44Aa	Cry45Aa	
Cry46Aa	Cry46Ab	Cry47Aa	Cry48Aa	Cry48Ab	Cry49Aa	Cry49Ab	Cry50Aa	Cry50Ba	Cry51Aa	Cry52Aa				
Cry53Aa	Cry53Ab	Cry54Aa	Cry54Ab	Cry54Ba	Cry55Aa	Cry56Aa	Cry57Aa	Cry58Aa	Cry59Aa	Cry59Ba				
Cry60Aa	Cry60Ba	Cry61Aa	Cry62Aa	Cry63Aa	Cry64Aa	Cry65Aa	Cry66Aa	Cry67Aa	Cry68Aa	Cry69Aa	Cry69Ab			
Cry70Aa	Cry70Ba	Cry70Bb	Cry71Aa	Cry72Aa										
Cyt1Ab	Cyt1Aa	Cyt1Ba	Cyt1Ca	Cyt1Da	Cyt2Aa	Cyt2Ba	Cyt2Bb	Cyt2Bc	Cyt2Ca	Cyt3Aa				
Vip1Ab	Vip1Aa	Vip1Ac	Vip1Ba	Vip1Bb	Vip1Ca	Vip1Da			Sip1					
Vip2Ab	Vip2Aa	Vip2Ac	Vip2Ad	Vip2Ae	Vip2Af	Vip2Ba	Vip2Bb							
Vip3Ab	Vip3Aa	Vip3Ac	Vip3Ad	Vip3Ae	Vip3Af	Vip3Ag	Vip3Ah	Vip3Ba	Vip3Bb	Vip3Ca	Vip4Aa			

The list of Bt toxins has been taken from Bt nomenclature database (http://www.lifesci.sussex.ac.uk/home/Neil_Crickmore/Bt/). Parasporins, a sub-class of Bt toxins, have been taken from the parasporin nomenclature database (http://parasporin.fitc.pref.fukuoka.jp/list.html). The homology group classification is taken from the published paper (de Maagd et al., 2003). The Cry toxins phylogenetically unrelated are highlighted with different colours. These toxins are Cry6, Cry22, Cry37, Cry55 and Cry 46. Cry34 members (light green) are not related to other Bt crystal proteins, however they are homologous to binary toxins from *B. sphaericus* (de Maagd et al., 2003).

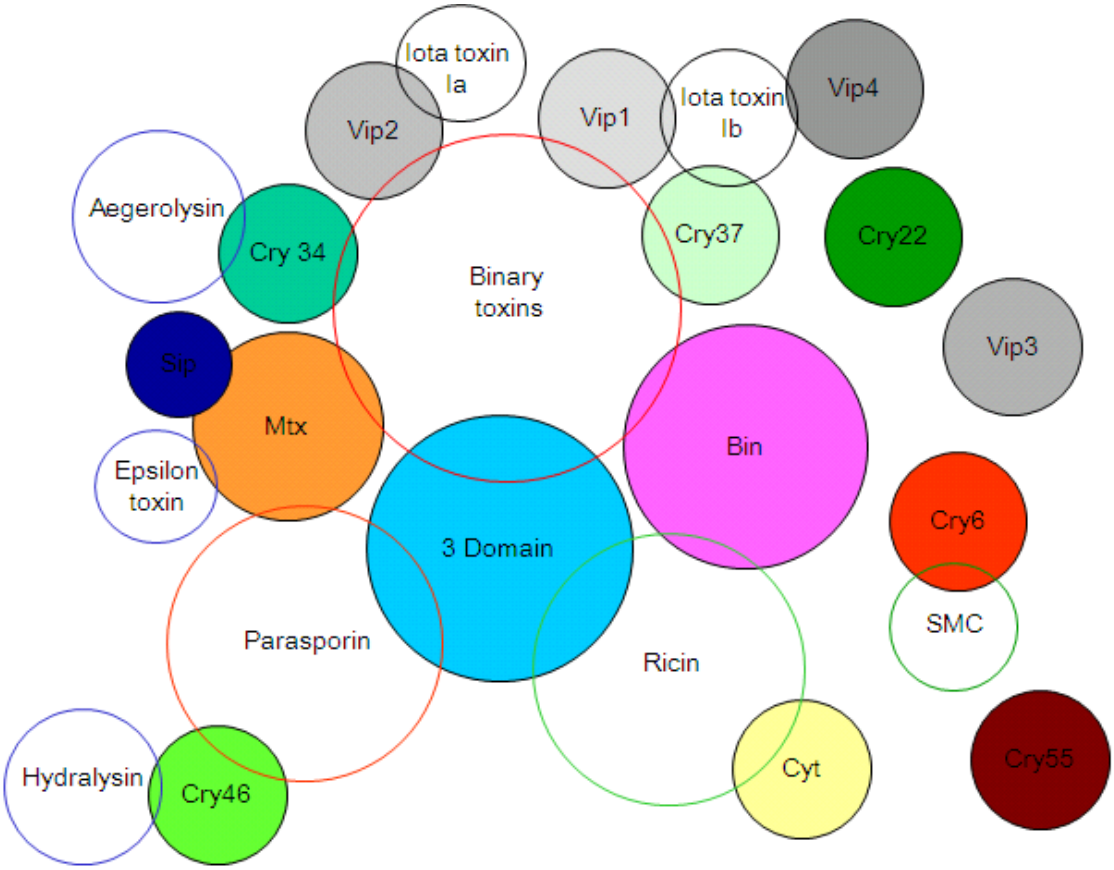

Figure 1.1. Venn diagram depicting homology of Bt proteins to the conserved domains and protein families found in a diverse group of organisms. The homology group classification is taken from the published paper (de Maagd et al., 2003). The conserved domains and protein families have been identified using CD search or BLAST, NCBI. The identifiers where applicable are given in the text.

1.9 The Mtx Group

Mtx2 and Mtx3 are widely distributed among mosquitocidal *Lysinibacillus sphaericus* strains. They are related to each other and also to various other bacterial toxins such as cytotoxin of *Pseudomonas aeruginosa*, the epsilon toxin of *Clostridium perfringens*, the alpha toxin of *Clostridium septicum* and aerolysin from *Aeromonas hydrophila*. *B. thuringiensis* toxins in this group include Cry15Aa, Cry23Aa, Cry33Aa, Cry38Aa, Cry45Aa, Cry51Aa, Cry60Aa, Cry60Ba and Cry64Aa. Most of the Bt toxins belonging to this subgroup need further characterisation. Cry15Aa protein from *B. thuringiensis* subsp. *thompsoni* possesses significant homology to Mtx2 and Mtx3 toxins. Cry15Aa requires its unrelated helper 40kDa protein for crystallisation and full toxicity against *M. sexta* (Brown & Whiteley, 1992; Rang et al., 2000; Naimov et al., 2008). The 29 kDa Cry23 in combination with the 13-14 kDa Cry37 is toxic against certain coleoptera for instance boll weevil (Donovan et al., 2000). The sequence of Cry37 bears no significant homology to the existing proteins in the public databases. The three dimensional structure of the binary Cry23/Cry37 complex resembles that of proaerolysin (Figure 1.5, p. 32) (Rydel et al., 2001). *cry33Aa* and *cryNT32* are arranged in an apparent operon similar to the Bt subsp *thompsoni* genes (de Maagd et al., 2003). Not much is known about the protein Cry53 from *Bacillus thuringiensis cameroun* strain. Cry38 is isolated from the *B. thuringiensis* strain that produces Cry34/Cry35 (Baum et al., 2004). Cry45 is a parasporin that is a mammalian cell killing toxin from *Bacillus thuringiensis* with no known insecticidal activity. Cry51 is related to Cry15A and Cry33A which may possess some insecticidal activity (Huang et al., 2007). Cry60s (Cry60Aa/Ba) are putative new mosquitocidal toxins (Sun & Park, unpublished). Cry64 is a new parasporin

classed as parasporin 5 with no known insecticidal activity (Ekino et al., unpublished). The host specificities of the Mtx group of toxins investigated so far widely differ ranging from Lepidoptera for Cry15 to Coleoptera for Cry23 and Cry38 and *in vitro* cytotoxicity against mammalian cancer cell lines for the non-insecticidal Cry45Aa (Lee et al., 2000). Although these proteins demonstrate a low sequence similarity yet they share a conserved sequence motif comprising of an amphipathic loop region flanked by two Ser/Thr-rich regions with each other as well as with protein toxins from a variety of organisms (Naimov et al., 2008).

1.10 The Bin group

The Bin group toxins comprising of 3 basic members (primary rank) form the third largest group of the Bt crystal toxins based on homology groups. Since these Cry toxins share sequence similarities to the individual components of the binary toxin from mosquitocidal *L. sphaericus* and are themselves mostly part of a binary toxin, they have been classed into Bin group of crystal toxins. The mosquitocidal activity of *L. sphaericus* is due to the presence of 'Bin' (binary) toxin produced during sporulation. Bin mosquitocidal protein consists of two proteins the toxic Bin A of 42 kDa and the binding moiety Bin B of 52 kDa (Charles et al., 1996; Wirth et al., 2010). Both components are required for full toxic activity thus implicating a binary toxin mode of action (Broadwell et al., 1990). The members of the Bin group are Cry35, Cry36 and Cry49. All three Cry35A toxins have a carbohydrate binding Ricin-type β-trefoil [cd00161; pfam 00652] domain at the N terminus. Cry49Aa is a binary toxin and appears to rely on the presence of a second three-domain protein Cry48Aa. Cry36 is toxic on its own.

1.10.1 The Binary toxins

Cry proteins that exerts toxicity together whereas individually they are not toxic are grouped as binary toxins. The toxicity appears to rely on the presence of the second Cry protein. For instance such association is observed in case of Bt three-domain protein, Cry48Aa with Bin-like protein, Cry49Aa derived from *L. sphaericus*. These are the two component toxins wherein insect toxicity is achieved in the presence of the second accessory protein. The necessity for both components for pathogenicity has been demonstrated. Other such complexes include Cry34/Cry35; Cry23/Cry37 and Vip1/Vip2. Cry35 proteins are only active in the presence of the unrelated Cry34 against western corn rootworm (Ellis et al., 2002). 29 kDa Cry23 protein functions effectively only in conjunction with 13-14 kDa Cry37 protein on certain coleopterans (Donovan et al., 2000). The various binary toxins studied so far have been illustrated in Figure 1.2.

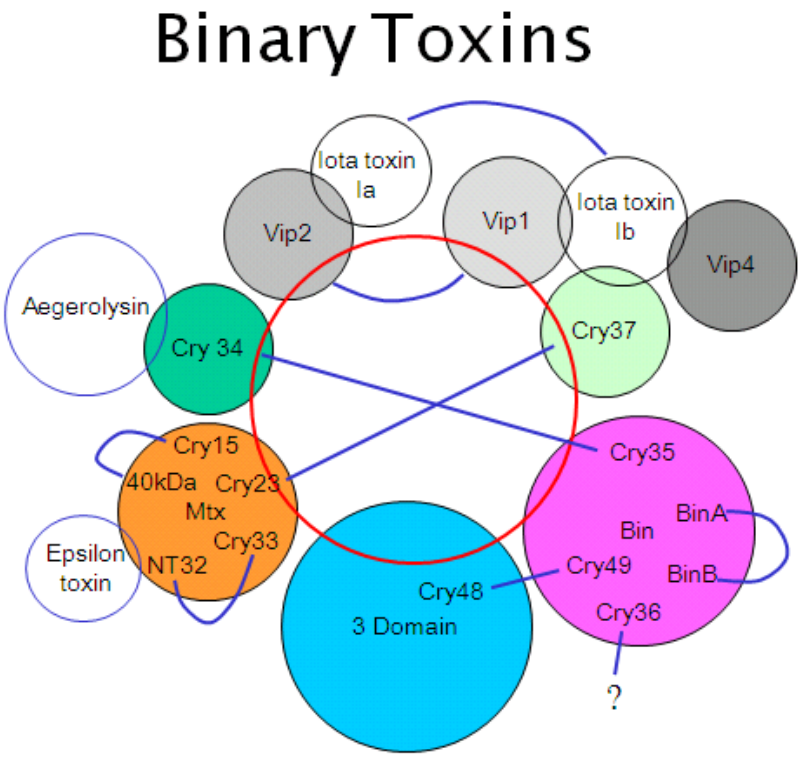

Figure 1.2. The various members of the binary toxins. The Bt toxins which rely on each other for toxicity and form complexes with each other are joined by blue lines. ? indicates that the associations of Bin Cry36 is not known. The corresponding homology groups and conserved domains are also indicated in the diagram.

1.11 The three-domain Cry toxins

The three-domain Cry toxins have been extensively used as biological insecticides for several decades now. They are active against several insect orders including Lepidoptera, Diptera, Coleopteran and Hymenoptera. They have also been found to be active against nematodes (Figure 1.3). These toxins share distinct three dimensional structures comprising of three domains.

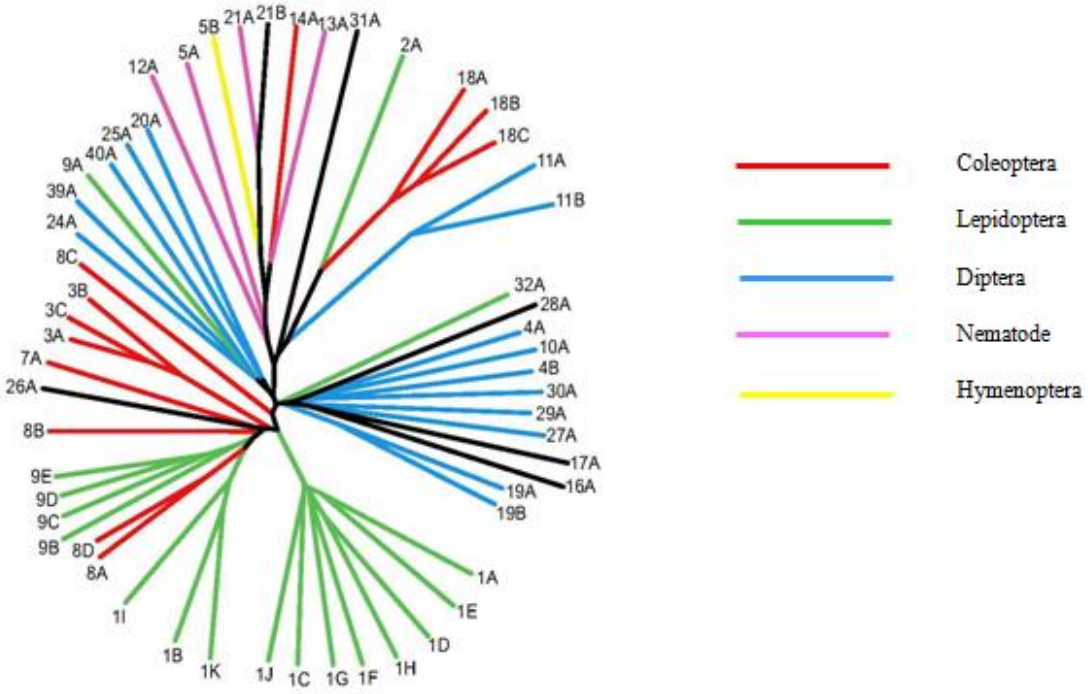

(de Maagd et al., 2003)

Figure 1.3. Specificity of the three-domain toxins to various insect orders.

A common three-domain structure of the activated Cry1Aa (Grochulski et al., 1995), Cry2Aa (Morse et al., 2001), Cry3A (Li et al., 1991), Cry3Bb (Galitsky et al., 2001), Cry4Aa (Boonserm et al., 2006), Cry4Ba (Boonserm et al., 2005) and Cry8Ea1(Guo et al., 2009) toxins has been revealed by X-ray crystallography. Domain I is comprised of seven α-helices and domains II and III are made up of mostly β-sheets (Figure 1.4). While domain I plays a crucial role in pore formation, receptor binding and host specificity has been ascribed to domains II and III. Five blocks of amino acids are found to be conserved amongst the majority of Cry toxins (Hofte & Whiteley, 1989). Amino acid sequence alignment of the Cry toxins reveals the presence of three additional blocks outside the active core at the carboxyl terminal halves of these sequences (Schnepf et al., 1998).

Domain I: Domain I, corresponding to the N-terminus comprises of seven α-helix bundle which is organised into a highly conserved central helix (helix α-5) surrounded by six helices which are amphipathic in nature. Helix 5 contains the conserved block1. The central location thus implicates its role in maintaining the structural integrity of the helix bundle. The helices 4 and 5 are possibly responsible for membrane insertion and pore formation (Li et al., 1991). Domain I is analogous to other pore forming toxins such as colicin A and diphtheria toxin (Parker et al., 1992). An alternative to the above idea that the hydrophobic hairpin between α4 and α5 initiates the membrane insertion, is the possibility that helices 5 and 6 juxtaposed to each other open up in a penknife fashion before inserting into the membrane (Hodgman & Ellar, 1990).

Domain II comprises of three anti parallel β-sheets joined in a Greek Key topology forming a β-prism. The first β strand of Domain II and helix 7 of domain I include the conserved block 2. Surface-exposed loops of β-sheets bears semblance to immunoglobin antigen-binding sites (Schnepf et al., 1998). The β-prism fold is similar to that of various plant lectins for instance Jacalin (Bourne et al., 1999; Meagher et al., 2005). This suggests the role of domain II in receptor binding.

Domain III is a β- sandwich structure comprising of two twisted anti parallel β-sheets displaying a jelly-roll topology. Conserved blocks 3, 4 and 5 lie on one of the three buried strands within domain III. The domain III is thought to aid in maintaining the integrity of the toxin molecule possibly by masking it from proteolysis within the gut of the target insect (Li et al., 1991).

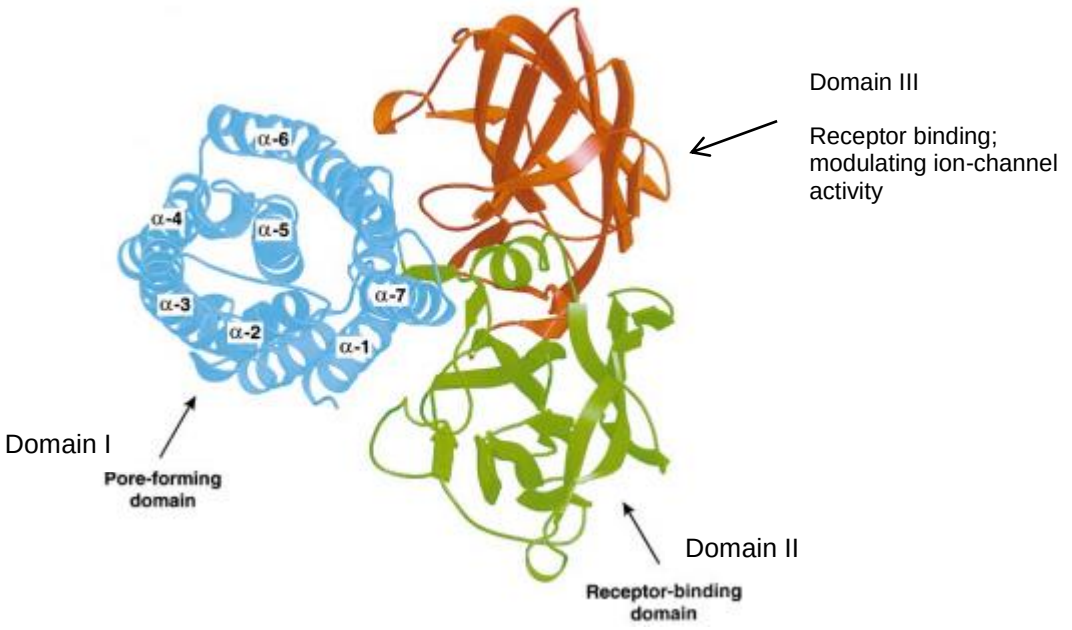

(Aronson & Shai, 2001)

Figure 1.4. Schematic representation of the structure of the three domain toxin Cry3A.

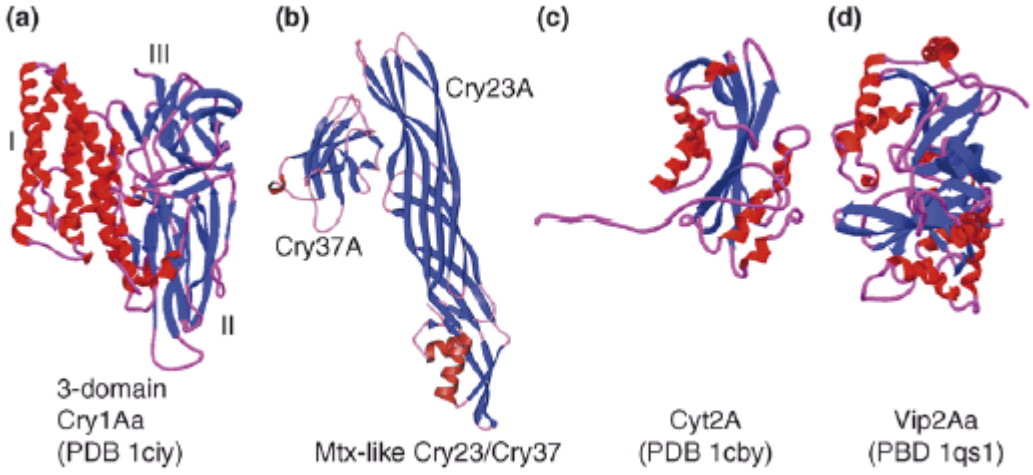

(Bravo & Soberón, 2008)

Figure 1.5. Structures of various Bt crystal proteins representing the various classes of the toxins. Helices are indicated in red, β-sheets are indicated in blue and the coils are indicated in purple.

1.12 Split toxins

It has been observed in some of the Cry proteins that a pair of adjacent genes separated by intergenic region encode the typical N and C terminal regions of Bt δ endotoxins as two separate proteins. They are termed as split toxins. These split toxins have more than one Open Reading Frame (ORF) separated by an intergenic region. One of the ORF's usually contains homology blocks 1-5 as described by Hofte & Whiteley (1989) and is the typical N-terminus present in most Bt δ endotoxins. The second ORF usually encode homology blocks 6-8, the C-terminal region of longer protoxins.

Thirteen such *cry* gene pairs have been found in *B. thuringiensis.* The first genes of these pairs are *cry5Ad* (Lenane et al., 2008), *cry10Aa* (Thorne et al., 1986), *cry19Aa* (Rosso & Delecluse, 1997), *cry24Ba* (Ohgushi et al., 2005), *cry30Ba* (Ito et al., 2006), *cry39Aa* (GenBank accession BAB72016), *cry40Aa* (GenBank accession BAB72018), *cry40Ba* (GenBank accession BAC77648), *cry41Aa/Ab* (Yamashita et al., 2005), *cry41Ba* (GenBank accession HM461871), *cry42Aa* (GenBank accession BAD35166) and *cry44Aa* (Ito et al., 2006) (Figure 1.6).

Cry5Ad and orf2-5Ad differ from the other split toxins in that they occur within a Cry5A (Cry5Aa, Cry5Ab, Cry5Ac) family in which the other members encode a single open reading frame containing all eight homology blocks (Lenane et al., 2008).

The carboxy- terminal ends containing homology blocks 6-8 in the longer Cry δ endotoxin genes gets cleaved during the proteolytic activation of *B. thuringiensis* protoxins. A possible function as a molecular chaperone helping in the crystallization of Cry proteins has been suggested (Bietlot et al., 1990; Park et al., 2000; Barboza-Corona et al., 2012).

The cause of the segmentation of the *cry* toxin genes into separate open reading frames has not been elucidated. Previously such gene configuration was observed in mosquitocidal strains. But recently this has been observed in the *cry41* parasporin genes. Typically, the region separating the open reading frames shows no homology to any known transposons or insertion sequences. Possibly the segregation into various open reading frames resulted due to recombination or transposition event. It would interesting to investigate if such gene structure in the split toxins actually confer any advantage to the bacterium or if it's a mere evolutionary process in which the intergenic region was lost in other Bt δ endotoxin *cry* genes and the homology blocks 1-8 were found together on a single ORF, or that these split toxins evolved from a full length δ-endotoxin gene.

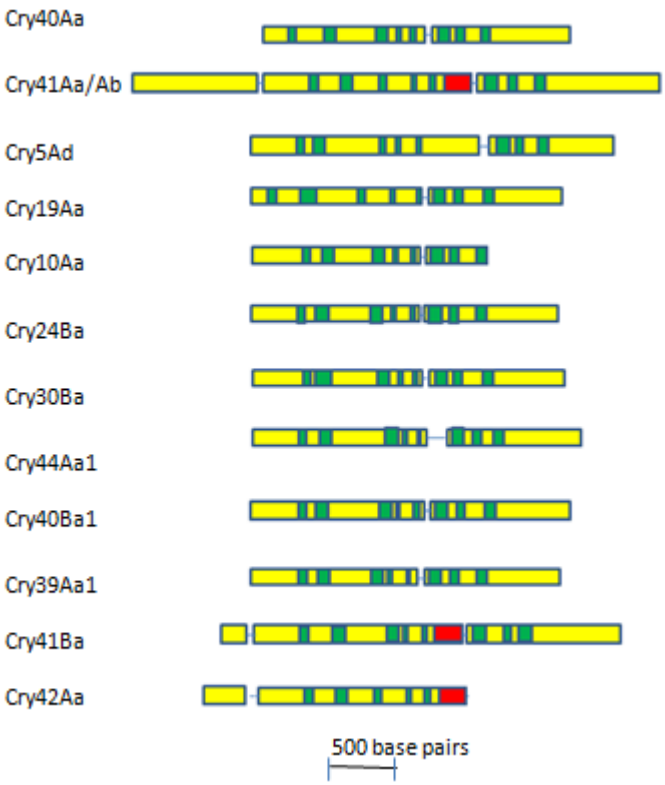

Figure 1.6. Schematic representation of the split toxins. The green boxes denote the eight conserved blocks of Cry toxins. The red box denotes homology to the conserved ricin domain [cd00161; pfam 00652].

1.13 Mode of action

A multistep process of cell killing has been proposed for the insecticidal three domain toxins. Pore formation and signal transduction are two hypotheses being put forward, pore formation mode being the most widely accepted and consistent with various studies (Vachon et al., 2012). The preliminary steps of toxin solubilisation in the midgut lumen, activation by gut proteases and binding to the primary receptor cadherin are shared by both the hypotheses. The pore formation model further suggests that binding to the primary receptor in the microvilli of the midgut cells induces proteolytic cleavage of helix α1 and causes oligomerization of the toxin followed by binding to a secondary receptor, for instance aminopeptidase (APN) or alkaline phosphatase (ALP). Recently, the possibility of a "ping-pong" binding mechanism with cadherin and aminopeptidase N receptors has been proposed for toxin action by Paccheco et al. (2009). This report suggests that the Cry toxin first binds to the highly abundant but low-affinity APN facilitating the concentration of the toxin at the midgut brush border membrane for the subsequent binding to cadherin resulting in the oligomerization of the toxin which then binds again to the APN with a high affinity leading to the insertion of the oligomer and pore formation (Pacheco et al., 2009). The signal transduction model which was based on studies conducted on insect cell lines proposes that the interaction of the Cry toxin with the primary receptor cadherin triggers a cascade pathway mediating the activity of protein G which in-turn activates adenylyl cyclase that further augments the cyclic adenosine monophosphate levels activating protein kinase A and leading to cell death (Zhang et al., 2006). The models are depicted in the Figures 1.7 (p. 43) and 1.8 (p. 44). The further details of toxin mechanism are given in the following sections.

1.13.1 Solubilisation and proteolytic activation

After ingestion by a susceptible insect, the crystal protoxins are released by solubilisation in the gut. For most lepidopterans the alkaline milieu of midgut is presumed to be crucial for disruption of intramolecular disulphide bridges formed due to 16-18 cysteine residues at the carboxy terminal (Bietlot et al., 1990). Differences in the extent of solubilisation possibly result in the variable degree of toxicity among Cry proteins. The solubility of crystals containing multiple toxins may be affected by the presence of specific Cry toxins as in case of *B. thuringiensis* subsp. *aizawai* HD-133 which contains Cry1Ab, Cry1Ac and Cry1D. HD-133 strain cured of Cry1Ab gene solubilised at higher pH as compared to the non-mutated HD-133 crystals (Aronson et al., 1991). In the neutral or slightly acidic midguts of coleopteran larvae, proteolytic treatment by a serine protease chymotrypsin yields a soluble Cry3A δ-endotoxin product which retains its full toxicity (Carroll et al., 1997).

Solubilisation is followed by activation of the Cry protoxins by trypsin- and chymotrypsin-like midgut proteases in insects (Tojo & Aizawa, 1983). The 130 kDa Cry1A family of protoxins are cleaved at both N and C-termini to yield active toxic cores of 55-67 kDa (Schnepf et al., 1998). Only a small peptide <100 amino acids are removed from the N terminal. The C terminal half gets cleaved sequentially in ~10 kDa fragments resulting in a conformational change within the toxic core (Choma et al., 1991).

1.13.2 Receptor binding

The activated crystal toxin binds to the specific membrane protein receptors on the gut epithelium of the susceptible insects (Hofmann et al., 1988). The process of binding is a two-stage one involving reversible and irreversible steps. The reversible binding involves a low affinity interaction between the toxin and the membrane receptor whilst the irreversible binding includes tight binding between the receptor and insertion of toxin into the membrane (Hofmann & Luthy, 1986; Van Rie et al., 1989; Ihara & Himeno, 2008). A myriad of such high–affinity toxin binding sites in the insect midguts have been reported (Pigott & Ellar, 2007). The best characterised amongst the protein receptors identified so far include a glycosylphosphatidyl-inositol (GPI) -anchored aminopeptidase-N (APN) (Knight et al., 1994; Sangadala et al., 1994; Gill et al., 1995), cadherin-like receptors (CADR) in lepidopterans (Nagamatsu et al., 1998, 1999). Glycolipids constitute an important class of Cry toxin receptors in nematodes (Griffitts et al., 2005). Other Cry toxin receptors include a GPI anchored alkaline phosphatase (ALP) (Fernandez et al., 2006), a 270-kDa glycoconjugate (Valaitis et al., 1997) and a 252-kDa protein (Hossain et al., 2004).

The widely accepted view is that the activated toxin inserts into the membrane of the susceptible insect and forms pores after toxin-receptor interaction. As proposed by Knowles & Ellar (1987), the pore resulted in the death of the insects. Bravo et al. (2004) further developed this model of pore formation suggesting that a toxin oligomerization precedes the toxic pore formation.

1.14 Bravo-Soberon model

The Bravo-Soberon model is based on experiments with Cry1Ab and the tobacco hornworm, *Manduca sexta.* It predicts the binding of proteolytically activated monomeric Cry1Ab toxin to the cadherin receptor BT-R1 followed by cleavage of domain I helix α1 by membrane bound proteases. The monomer then oligomerises to the tetrameric form which binds to the receptor APN and forms association with lipid rafts further inserting into the membrane forming pores of 0.5-1nm in diameter thus resulting in osmotic cell lysis and insect death (Bravo et al., 2007). This sequential event in the pore formation pathway was elucidated by temporal differences in the immunoprecipitation of BT-R1 and APN by Cry1Ab (Bravo et al., 2004). Co-precipitation of Cry1Ab with BT-R1 decreased over time whilst 4-fold increase of Cry1Ab-APN precipitation was noted. In addition the previous reports suggested a 100-fold greater affinity of the receptor Bt-R1 for Cry1Ac as opposed to APN (Vadlamudi et al., 1993; Sangadala et al., 1994). This suggests that the binding of Cry1Ab to Bt-R1 and APN is sequential in nature. Alternatively, Pigott & Ellar (2007) highlighted that due to the low abundance of cadherin as compared to other Cry1Ab receptors, the possibility exists that high affinity, low concentration cadherin receptors get rapidly saturated with Cry1Ab as compared to APN receptors. The nicking of α-helix 1 upon binding of BT-R1 and subsequent cleavage was proved by N-terminal sequencing which showed its presence in Cry1Ab monomers that were activated by *M. sexta* gut juice in-vitro but was absent from Cry1Ab oligomers produced by incubation with BBMV (Brush border membrane vesicles) (Gomez et al., 2002). Bravo et al. (2004) indicated the presence of BT-R1 in the soluble fraction of iodoxano gradient centrifugation of solubilised *M. sexta* BBMV. APN co-precipitated with lipid rafts.

Incubation of BBMV with Cry1Ab prior to solubilisation results in BT-R1 co-fractionating with lipid rafts if APN is not cleaved of its GPI anchor. This suggests the association of BT-R1 –Cry1Ab complex to lipid rafts via APN.

1.15 The “ping-pong” sequential binding model

Based on the observations on the binding of Cry1Ab mutants to *Manduca sexta* receptors, cadherin and APN, Pacheo et al. (2009) proposed a ping pong binding mechanism. The model suggests involvement of domain II loop 3 in the first binding event with the high abundance, low affinity, APN receptor which serves to locate the monomeric toxin in the vicinity of the microvilli. This interaction is followed by a high affinity binding to the cadherin receptor Bt-R1 that involves participation of other regions of domain II besides loop 3, such as loops α-8 and 2. Interaction with Bt-R1 triggers cleavage of helix α-1 and oligomerization of the toxin. The oligomeric structure binds with high affinity to APN through other regions of the toxin, such as the domain III β16–22 region, whilst remaining associated with Bt-R1 through loop 3. This mediates the insertion of the oligomeric structure into the membrane suggesting a “ping-pong” binding mechanism (Figure 1.8) (Pacheco et al., 2009).

1.16 Zhang-Bulla model

The Zhang-Bulla model is based upon experiments conducted on undifferentiated *Trichoplicus ni* ovarian cells expressing *M. sexta* cadherin BT-R1 and rules out the possibility of dependence of cytotoxicity on pore formation. The model proposes that a cell signalling pathway is activated leading to cell death

by binding of the receptor Bt-R1 by monomeric Cry1Ab (Zhang et al., 2005, 2006). The model suggests that the cyclic–AMP (cAMP) pathway is activated by Cry toxins. The activated Cry toxins upon binding to BT-R1 stimulate G protein which in turn activates AC causing an increase in intracellular cAMP production that further activates PKA. PKA activation causes the destabilisation of the cytoskeleton and formation of ionic pores leading to cell lysis (Zhang et al., 2008).

Since the model is based on limited experiments using undifferentiated *T. ni* ovarian cells *in vitro*, there is no further evidence that Cry1Ab demonstrates similar means of toxicity *in vivo* or in other cell lines. Furthermore, it was noted that several Cry toxins which led to the increase of cAMP levels in *M. brassicae* demonstrated no toxicity (Knowles & Farndale, 1988).

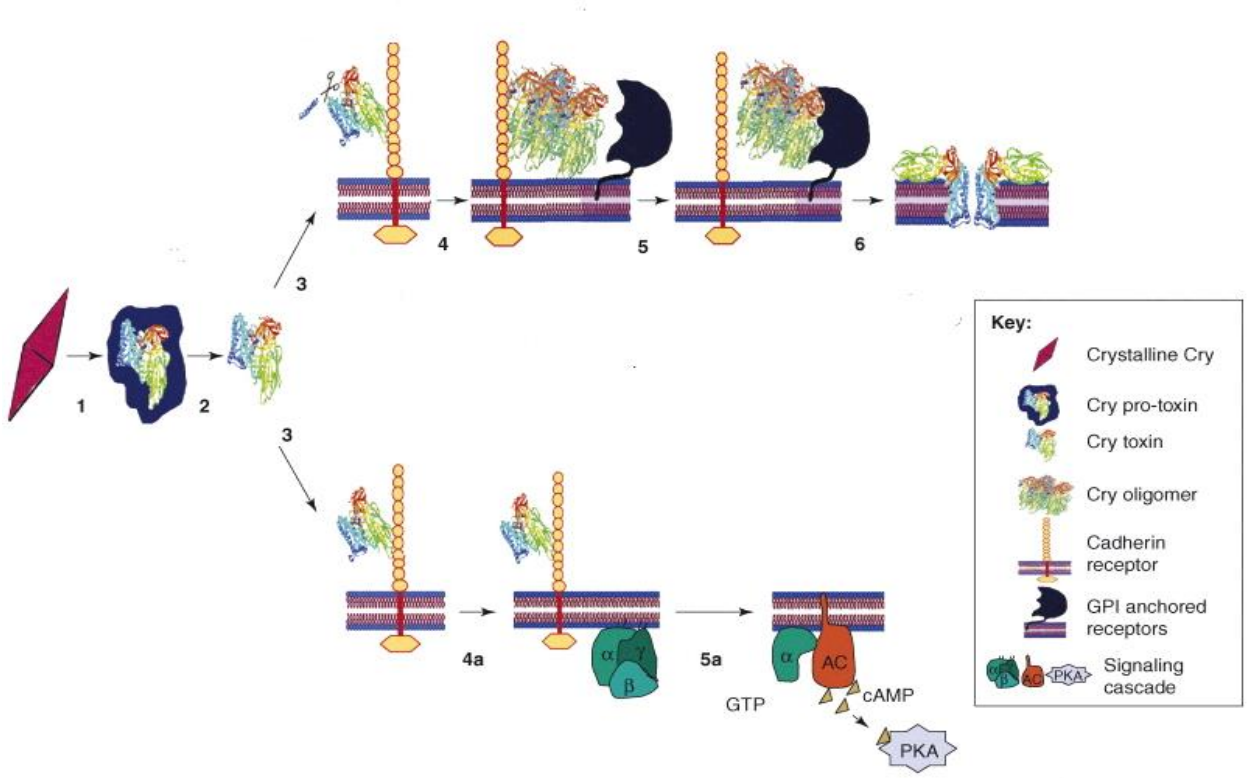

(Bravo & Soberón, 2008)

Figure 1.7. The two hypotheses put forth for the mechanism of action for the Bt Cry toxins: pore formation model (top) and signal transduction model (bottom). The preliminary steps of toxin solubilisation in the midgut lumen (1), activation by gut proteases (2) and binding to the primary receptor cadherin (3) are shared by both the hypotheses. The pore formation model further suggests that binding to the primary receptor in the microvilli of the midgut cells induces proteolytic cleavage of helix α1 (3) and induces oligomerization of the toxin (4) followed by binding to a secondary receptor (5). The toxin then inserts itself into the membrane, thereby forming a pore (6). The signal transduction model proposes that the interaction of the Cry toxin with the primary receptor cadherin triggers a cascade pathway mediating the activity of G protein (4a) which in-turn activates adenylyl cyclase (5a) that further augments the cyclic adenosine monophosphate levels activating protein kinase A and leading to cell death.

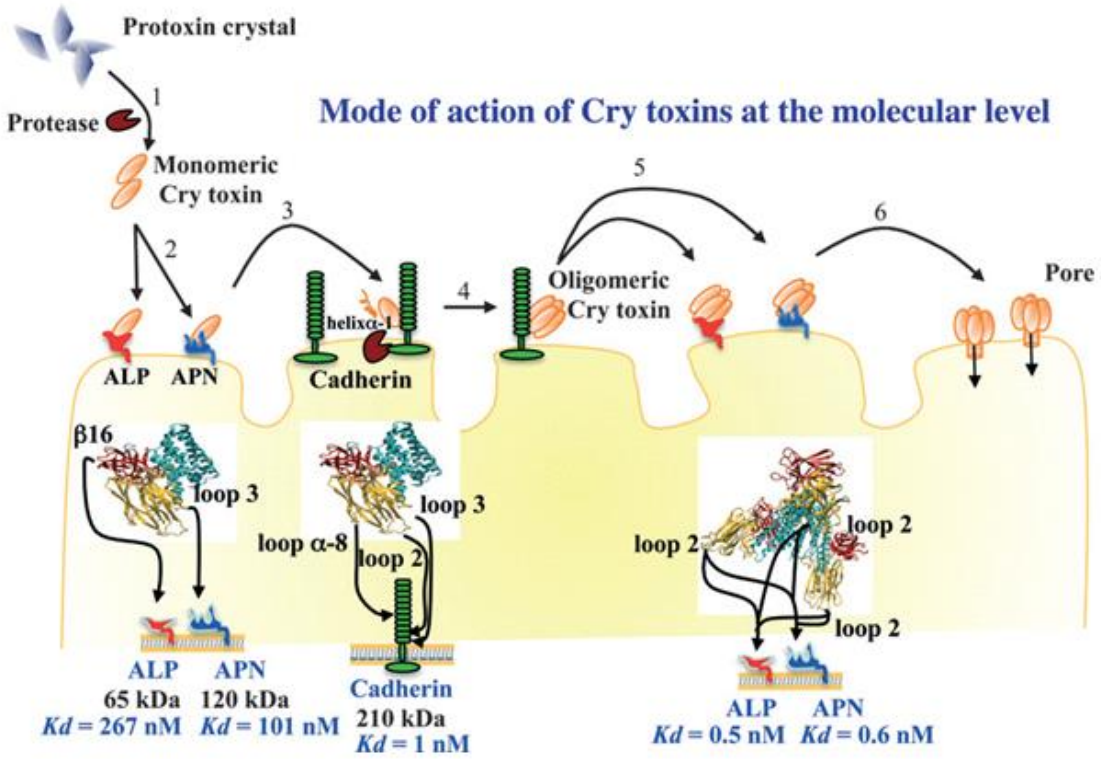

(Pardo-López et al., 2013)

Figure 1.8. Schematic representation of the "ping-pong" binding mechanism as suggested by Pacheo et al., 2009. 1. The 3-domain Cry protoxin is solubilised in the midgut lumen and activated by the gut protease generating 65kDa toxin fragment. 2. 65-kDa Cry1Ab monomer binds to low- affinity APN and ALP receptors through domain II loop 3. 3. The monomer binds Bt-R1 cadherin receptor through domain II loops α-8, 2, and 3 in a high-affinity interaction which induces cleavage of the N-terminal end of the toxin including α-1 of domain I. 4. Formation of a 250-kDa oligomer 5. The oligomer binds Bt-R1 through loop 3 and to high -affinity APN and ALP through domain III. 6. Membrane insertion of the 250-kDa oligomer and pore formation after APN interaction.

1.17 Parasporins

Besides the insecticidal toxins, certain Bt toxins have been isolated from non-insecticidal strains that are found to be selectively active against human cancer cell lines (Kim et al., 2000; Lee et al., 2000b; Mizuki et al., 2000; Yamashita et al., 2000).

The proteins derived from some of these non-insecticidal strains have been classed into a new family of Bt endotoxins known as parasporins, toxins that exhibit cytocidal activity preferentially killing human cancer cell lines (Mizuki et al., 2000). The non-hemolytic and preferential cytotoxic activity distinguishes them from the insecticidal Cyt proteins (Mizuki et al., 1999; Schnepf et al., 1998). No reports have yet been published indicating the presence of these cytotoxic crystal proteins in insecticidal strains. Indiscriminate cytotoxicites of parasporal inclusions derived from two mosquitocidal reference strains, *israelensis* and *kyushensis* to human cells, fish and insect cells has been reported. However, the cytotocidal activity has been attributed to the Cyt toxins (Thomas & Ellar, 1983a; Mizuki et al., 1999).

Currently, based on amino acid sequence analysis, these proteins have been categorised into 6 families, Parasporin (PS) - 1-6, purified from various Bt strains. Differences in molecular weight, structure and target cell specificity set them apart from each other.

Parasporin-1 (Cry31), parasporin-3 (Cry41) and parasporin-6 (Cry63) are 3-domain toxins like most insecticidal Cry proteins, with PS-3 being a split-toxin containing an additional Ricin-like/β-trefoil domain ($(QXW)_3$ motif). Parasporin-2 (Cry46) is a hydralysin like toxin while parasporin-4 (Cry 45) and parasporin- 5 (Cry64) are Mtx-like toxins homologous to *Clostridium perfringens* ε –toxin whose cell- killing mechanism involves oligomerization of the toxin in the lipid rafts and formation of pores in the cell membrane (Table 1.2).

These six different parasporins have been isolated mainly from Japan, Vietnam and Canada. There are also reports of occurrence of the parasporins from soils in India (Poornima et al., 2010). Recently parasporins have been isolated from a Caribbean island indicating the global dispersion of the *B. thuringiensis* strains producing the cancer killing crystal toxin (Gonzalez et al., 2011).

This class of mammalian cell killing toxins could not only be harnessed as potential therapies for certain cancers but also be useful in providing a risk-assessment of Bt toxins being used for controlling insect pests in agriculture.

Table1.2. List of various parasporin toxins isolated so far

Parasporin	Cry toxin Nomenclature	Type
Parasporin 1	Cry31Aa/b/c/d	Three-domain Cry toxin
Parasporin 2	Cry46Aa	Hydralysin-like toxin
Parasporin 3	Cry41Aa/b	Three-domain Cry toxin
Parasporin-4	Cry45Aa	Epsilon/Mtx-like toxin
Parasporin 5	Cry64Aa	Epsilon/Mtx-like toxin
Parasporin 6	Cry63Aa	Three-domain Cry toxin

Parasporins and their corresponding crystal toxin nomenclature have been taken from the parasporin nomenclature database (http://parasporin.fitc.pref.fukuoka.jp/list.html), the link to which is provided in the Bt nomenclature database. The homology group has either been determined using CD search, NCBI or BLAST, NCBI. The identifiers are mentioned in the text.

1.17.1 Parasporin-1 (Cry31A)

Parasporin-1 is a three domain non-insecticidal *B. thuringiensis* toxin that preferentially possesses cytotoxic activity against human cancer cell lines. So far, parasporin 1 has been isolated from ten strains of *B. thuringiensis* from soils of Japan, Vietnam and also from parasitic dead two-spotted spider mites from orchard apples in Canada (Jung et al., 2007; Uemori et al., 2008). Parasporin-1 is produced as an 81 kDa inclusion protein. This three domain toxin exhibited a low sequence similarity to existing Cry and Cyt proteins.

Protease treatment by trypsin yields the active form of parasporin-1 which is a heterodimer made up of 15 and 56 kDa subunits. This proteolytic processing is

a pre-requisite for the toxin to be active against the cancer cell lines as observed in case of *B. thuringiensis* Cry toxins (Lightwood et al., 2000). Intriguingly, the cytotoxic activity of Parasporin-1Aa1 appeared to be protease specific. Parasporin-1Aa1 when treated with trypsin and proteinase K exhibited cytotoxic activity. However, cytotoxic activity against HeLa cells, as assessed by MTT assay, sharply decreased at concentrations of proteinase K above 60 µg/ml possibly due to the broad specificity of the protease used leading to further digestion of high molecular weight protein bands of parasporin-1. No cytotoxicity was observed when the protein was treated with chymotrypsin (Mizuki et al., 2000; Katayama et al., 2005) whereas in PS1Aa2 (Cry31Aa2) only trypsin generated the cytotoxic fragments. The protein treated with chymotrypsin or proteinase K exhibited no cytotoxicity. The trypsin activation occurs by N-terminal processing (Jung et al., 2007). The parasporin-1 protein preferentially exerts its cytotoxic effects against certain cell lines especially HeLa, MOLT-4 and HL60 cell lines. It demonstrates a moderate cytotoxicity to Sawno and HepG2 cells but is non-toxic to the cells obtained from normal tissues, peripheral blood T cells and MRC-5 cell line (Table 1.3, p. 57). This suggests that a specific receptor is required for the parasporin-1 protein. The role of receptors in the insect toxicity has been well-documented in the case of *B. thuringiensis* insecticidal Cry proteins which exhibits specific insecticidal activity as opposed to Bt Cyt toxins which are toxic to both insects and human cells (Gill & Hornung, 1987; Gill et al., 1992; Schnepf et al., 1998).

Specific cell death as caused by Parasporin-1 differs from the mode of activity normally exhibited by pore forming insecticidal Cry or Cyt proteins of *B.*

thuringiensis. This is evident by the absence of lactate dehydrogenase (LDH) release and lack of penetration of propidium iodide in HeLa cells as well as no alteration in the membrane potential of the cells treated with Parasporin-1Aa1. Parasporin-1 treatment is marked by attenuation of cellular protein and DNA synthesis and rapid increase in intracellular calcium ions. A large influx of extracellular calcium ions was observed in cells which were treated with parasporin-1Aa1, resulting in the apoptotic death of the target cell. The apoptotic cell death is further strengthened by the fact that a decline of PS1Aa1 cytotoxic activity is observed by synthetic caspase inhibitors and the PS1Aa1 treatment leads to degradation of apoptosis-related proteins, procaspase-3 and poly (ADP-ribose) polymerase in HeLa cells. A delayed cytopathy of 8-10 h is observed in case of sensitive cell lines treated with parasporin-1 unlike that observed in case of other parasporin toxins which cause immediate cell death of the sensitive cell lines after treatment. Thus, Parasporin-1 appears to cause cell death by a novel mechanism by increasing the intracellular calcium ion concentration, not reported in any other bacterial cytotoxic protein. Still, the exact mechanisms of its action and pathways need further clarification (Katayama et al., 2007).

1.17.2 Parasporin-2 (Cry46Aa)

Parasporin-2 is a hydralysin- like toxin targeting mostly human liver and colon cancer cells. PS2Aa1 lacks the conserved blocks of the insecticidal Cry proteins and is homologous to hydralysin, a β-pore forming toxin from Hydra, a Cnidaria (Sher et al., 2005). PS2 shares no homology to most of the existing *B. thuringiensis* Cry or Cyt toxins. A low homology is seen with Cry15 belonging to Mtx-like group (Brown & Whiteley, 1992). The ~37 kDa protein on proteinase-K treatment yields a cytotoxic ~30 kDa fragment that exhibits notable cytotoxicity to certain human cancer cell lines. The digestion occurs on both the N and C termini of the protein removing 51 and 36 residues from the respective termini (Kitada et al., 2006). The active protein is selectively cytotoxic to HepG2 and Jurkat cell lines and less toxic to HeLa and normal hepatocyte cells (Ito et al., 2004). The cytotoxic effect of parasporin-2 is non-apoptotic causing swelling and fragmentation of the susceptible cells possibly altering the ion permeability of the cells. The initial step is the specific binding of the activated toxin to a putative receptor in the lipid raft of the plasma membrane of the sensitive cells followed by the formation of oligomers of PS2Aa in plasma membrane leading to pore formation and cell lysis (Abe et al., 2008). Thus the cell killing mechanism is similar to various pore forming toxins like hydralysins, aerolysin from *Aeromonas hydrophila* and epsilon toxin from *Clostridium perfringens* (Kitada et al., 2006).

The crystal structure of active parasporin-2 has been determined. The active protein is mainly composed of long β-strands aligned with its long axis imparting it an unusual elongated shape. It exhibits similarity to aerolysin type β –pore forming toxin. Three distinct domains can be identified in the molecule. A short α-

helix sandwiches a small β-sheet and probably serves as the target binding module (Figure 1.9a). Domain 2 and Domain 3 are β sandwiches possibly involved in oligomerization and pore formation (Akiba et al., 2009).

Domain 1 is comprised of four short α-helices (H1-H4) and a small four stranded anti-parallel β-sheets (S2-3 and S11-12). H1 helix borders domain 2 whereas H2 and H3 sandwich the β-sheet. Domain 1 is enriched with aromatic residues particularly histidine, phenylalanine, tryptophan and tyrosine. As put forth for the *Clostridium perfringens* epsilon toxins, these exposed aromatic residues might be the putative binding sites for the membrane receptors of the susceptible cancer cells (Akiba et al., 2009).

Domain 2 is a β sandwich domain that contains a β-hairpin (S8-9) and a twisted five -stranded β-sheet (S5-6, S7, S10-11 and S13) that are anti- parallel. At the interface of domain 2 and domain 3, the five stranded β-sheet is re-organised into three-stranded and two-stranded anti-parallel β-sheets. These two β-sheets form a β-sandwich which constitutes domain 3.

Despite the low sequence similarity of circa 26%, parasporin-2 shares a remarkable structural similarity with the aerolysin- type β-PFT's (pore forming toxins) (Figure 1.9b, c & d).

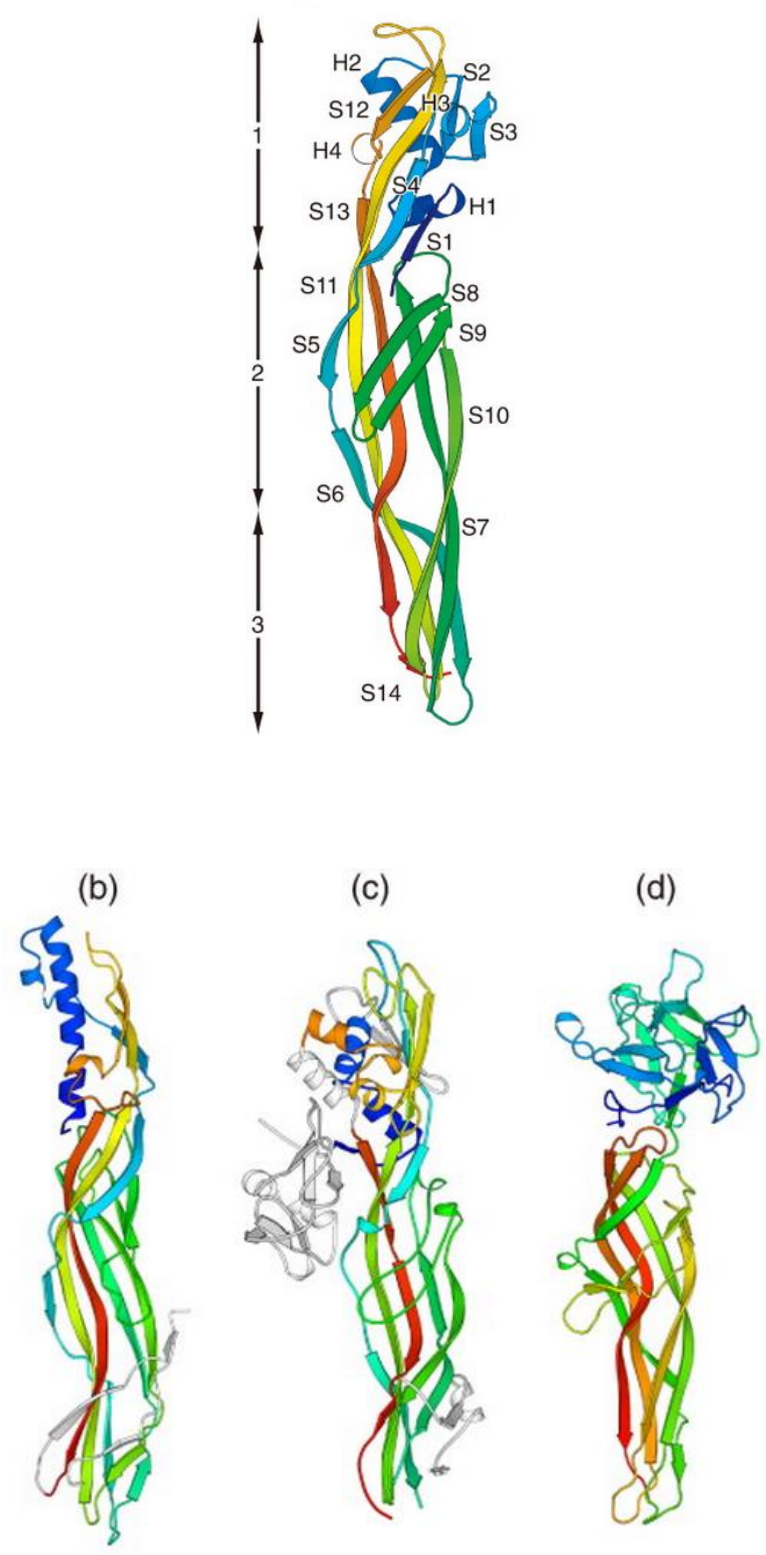

(Akiba et al., 2009)

Figure 1.9. Ribbon representation of the structural homologues of parasporin-2. (a) is the structure of activated parasporin-2 (Akiba et al., 2009). (b) is the epsilon toxin from *C. perfringens* (Cole et al., 2004). (c) is the aerolysin toxin from *A. hydrophila* (Parker et al., 1994). (d) is the Hemolytic lectin from *L. sulphurous* (Mancheño et al., 2005).

1.17.3 Parasporin-3 (Cry41Aa and Cry41Ab)

The 88 kDa proteins classed as parasporin-3 were isolated from the *B. thuringiensis* strain A1462 from soils of Tokyo in Japan and was first reported by Yamashita et al. (2005). They reported that the proteinase K activated protein of 64 kDa was selectively cytotoxic to human cancer cell lines HepG2 (liver) and HL60 (myeloid luekemia cells). Amongst all the parasporins isolated so far, Parasporin-3 possesses the narrowest cytotoxicity spectrum affecting only the above cell lines (Yamashita et al., 2005). Little is known about parasporin-3 which is notably similar to the insecticidal Cry proteins of *B. thuringiensis* in terms of amino acid sequence but differs remarkably in its selective cytotoxic activity against the human cancer cell lines.

The amino acid sequences of the parasporin-3 derived from the *B. thuringiensis* strain A1462 exhibit a remarkable similarity to the Bt insecticidal three-domain Cry toxins possessing the conserved domains of the insecticidal Cry1 toxins as described by Schnepf et al. (1998) and are thus predicted to possess a typical three-domain structure. Parasporin-3, found as the second gene (*ORF2*) in a three gene operon, is similar to several *B. thuringiensis* split toxins as enlisted in Section 1.12. The third gene (*ORF3*) of parasporin-3 resembles the C-terminus of the larger Cry1A-type toxins containing the conserved blocks 6-8, the role of which still needs investigation.

A schematic representation of the parasporin-3 toxin and a *B. thuringiensis* Cry1 toxin is shown below in Figure 1.10, depicting the conserved blocks of the two proteins.

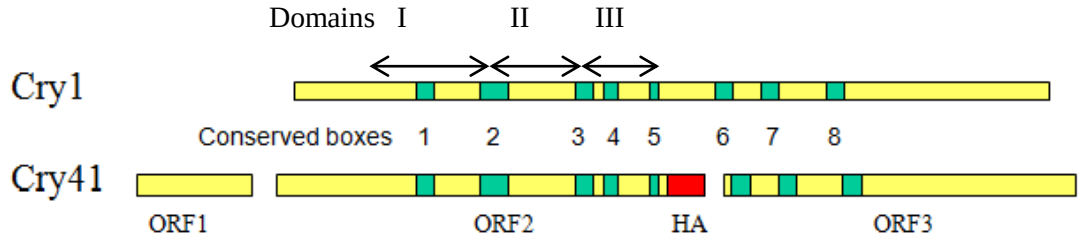

Figure 1.10. Conserved blocks of Bt insecticidal Cry1 protein and Cry41 (parasporin-3). The green boxes denote the eight conserved blocks of cry toxins. The red box denotes homology to the conserved ricin domain [cd00161; pfam 00652].

Additionally ORF2 possesses a conserved domain belonging to Ricin superfamily. This is most similar to HA-33 like domain present in *Clostridium botulinum* type C mammalian neurotoxin (Figure 1.11) that causes botulism disease characterised by muscular paralysis in humans and animals (Tsuzuki et al., 1990). The HA-33 component is responsible for haemagglutination and aggregation of erythrocytes caused by the toxin complex from *Clostridium botulinum*. The presence of glutamine-any residue-tryptophan (QxW) pattern is observed in the sequence of the *ORF2* gene. This is the characteristic feature of ricin-like lectin domains, $(QxW)_3$ domains (hereafter referred to as ricin domain) and the internal repeats as QxW repeats (Hazes, 1996). Whether ricin domain has a role to play in the cytotoxicity of the parasporin-3, or is just present as a non-functional domain in ORF2 awaits clarification.

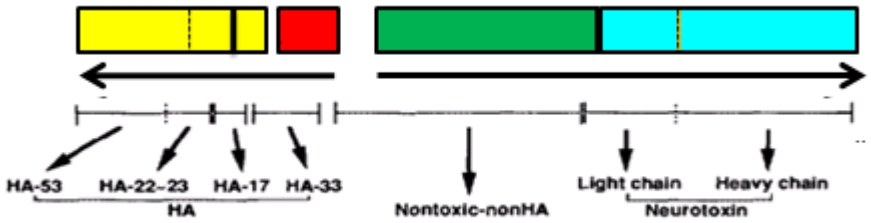

Figure 1.11. Gene organisation of 16S progenitor toxin of *Clostridium botulinum* type C. This comprises of a neurotoxin (turquoise box) in conjunction with non-toxic components designated as Nontoxic-non HA (green box) and hemagglutinin. HA is composed of subcomponents with molecular masses of 53, 22-23, 17 (yellow box) and 33 kDa (red box) (Adapted from Fujinaga et al., 1994).

1.17.4 Parasporin-4 (Cry45Aa)

Parasporin-4 is a ~30 kDa Epsilon/Mtx-like cytotoxic protein isolated from *Bacillus thuringiensis* strain A1470. The active parasporal protein exhibits strong cytotoxicity against human leukemic T cells. As with other parasporins, proteolytic processing is indispensable for the toxin activity. The protease treatments yield a ~27 kDa active form of the toxin selectively cytotoxic against colonic, uterine and blood cancer cells. The protein retained its cytolethal activity when processed both by alkaline proteinase K and acidic pepsin (Okumura et al., 2005, 2006).

PS4 treatment causes swelling of the susceptible cells marked with nuclear shrinkage causing the bursting of the ballooned cells within 24 hours of its administration (Okumura et al., 2011). Circular Dichroism revealed PS4 to be a β-sheet dominated protein. Parasporin-4 is homologous with various *B. thuringiensis* Cry toxins including Cry15, Cry33 and Cry14. It also shows homology with various pore-forming toxins such as ε-toxin from *Clostridium*

perfringens. Most of the pore-forming toxins are dependent on cholesterol for their activity (Hang'ombe et al., 2004). Insecticidal Cry toxins from *B. thuringiensis* have been reported to be pore forming toxins (Schnepf et al., 1998) with Cry1A (Zhuang et al., 2002) and Cry4Ba (Kanintronkul et al., 2005) believed to be cholesterol- dependent. Parasporin-2 also needs cholesterol for its cytotoxic activity (Kitada et al., 2009). However parasporin-4 activity seemed independent of cholesterol. Cytotoxicity of parasporin-4 was not altered in case of cholesterol-depleted CACO-2 cells. Thus parasporin-4 seems to be a pore forming toxin whose activity is independent of cholesterol that thus differs from aerolysin-type and cholesterol dependent toxins (CDC) such as streptolysin O of *S. pyogenes*, pnemolysin of *streptococcus pneumonia* (Tilley et al., 2005) and perfringolysin of *C. perfringens*. Parasporin-4 binds non-specifically to the plasma membrane of the susceptible cells and oligomerises to form pores only in the target cells causing cell death (Okumura et al., 2011).

1.17.5 Parasporin-5 (Cry64Aa)

Parasporin-5 has been isolated in 2009 by Ekino & Shin (unpublished) from the Bt strain A1100. Not much has been reported for PS5. Sequence analysis reveals that PS-5 is an Epsilon/Mtx like toxin.

1.17.6 Parasporin-6 (Cry63Aa)

Parasporin-6 (Cry63Aa) has been isolated from *B. thuringiensis* strains M109 and CP84 (Nagamatsu et al., 2010). Sequence analysis suggests that it is a three-domain Cry toxin. The proteolytically active toxin was cytotoxic towards human hepatocyte cancer HepG2 cells and uterus cervix cancer HeLa cells (Table 1.3). The treatment was accompanied by swelling of the cells and formation of vacuoles in the cytoplasm of the sensitive cells (Nagamatsu et al., 2010). Not much work has been reported on this mammalian Cry toxin.

Each parasporin studied so far is endowed with its own mechanism for inducing cell death. PS1 activates apoptotic signalling due to increased levels of calcium ions. PS2 acts as a cytolysin which causes permeabilization of the plasma membrane with target cell specificity. PS4 is a cholesterol independent pore-forming toxin. The mode of action of PS3, PS5 and PS6 still needs investigation. The cytotoxicity spectrum of the parasporins isolated and investigated so far is summarised in Table 1.3. Although each of the parasporins differed in their specificity to different cell types, human HepG2 liver carcinoma cell line is susceptible to all of them (Table 1.3).

Table 1.3 Cytotoxicity spectrums of parasporins

CELL LINE	ORIGIN	PS1	PS2	PS3	PS4	PS5	PS6
HUMAN							
MOLT 4	Leukemic T cell	++	++++	-	-		
JURKAT	Leukemic T cell	-	++++	-	-		
HL60	Myeloid Leukemia	+++	++++	++	+++		
HeLa	Uterus cervix cancer	+++	-	-	-		+
TCS	Uterus cervix cancer	-	-	-	-		
Sawano	Uterus cancer	-	++++	-	-		
HepG2	Hepatocyte cancer	++	++++	++	++		++++
A549	Lung cancer	-	+++	-	-		
CACO-2	Colon cancer	-	+	-	-		+
T cell	Normal T cell	-	+++	-	-		
UtSMC	Normal uterus	-	++	-	-		
HC	Normal Hepatocyte	-	-	-	-		
MRC-5	Normal Lung	-	+	-	-		
MONKEY							
Vero	Kidney	-	??	-	-		
RODENT							
PC12	Pheochromocytoma	??	??	??	++		

(Adapted from Ohba et al., 2009)

The levels of cytotoxicity, based on EC_{50} calculated using cell proliferation assays were denoted as follows: extremely high, ++++; high, +++, moderate, ++, low, + and non- toxic, -.? indicates not tested

1.18 Present work

Chapter three studies the cytotoxic effect of various Cry proteins from native strains of *B. thuringiensis* on human cancer cell lines. Chapter four describes the attempted heterologous expression of *cry41Aa* (Parasporin-3) gene and its various mutants in *E. coli*. Chapter five summarises the creation of homologous expression systems for parasporin-3. It also investigates whether the putative carbohydrate binding beta-trefoil ricin domain domain present at the C-terminal of *cry41Aa* gene is responsible for the cytotocidal activity of Cry41Aa against cancer cell lines. Chapter six analyses the Mtx-type Cry51 and three-domain Cry65 toxins and evaluates their activities against cancer cell lines.

2. Materials and Experimental protocols

2.1 General materials

2.1.1 Bacterial strains

2.1.1.1 *E. coli*

2.1.1.1.1 JM109 procured from Promega was used for T-vector cloning, subcloning, transformation, and in some instances for protoxin expression.

Genotype*: end A1, rec A1, gyr A96, thi, hsd R17, rel A1, sup E44, ⊿[lac-pro AB], [F' traD36 , proAB, lacIqZ⊿M15]*.

2.1.1.1.2 BL21(DE3)

An *E. coli* strain with DE3, a λ prophage carrying the T7 RNA polymerase gene under the control of *lac* UV5 promoter. BL21(DE3) permits high-efficiency protein expression of a gene cloned with its own ribosome binding site under the control of a T7 promoter.

Genotype: *F^- ompT gal dcm lon hsdS_B (r_B^- m_B^-) λ(DE3 [lacI lacUV5-T7 gene 1 ind1 sam7 nin5]).*

2.1.1.1.3 GM2163

This is Dam^- Dcm^- strain which does not methylate DNA and is resistant to chloramphenicol. *E. coli* GM2163 was used to obtain unmethylated DNA for ease of transformation in *B. thuringiensis* since it was observed by Macaluso & Mettus (1991) that some *B. thuringiensis* strains restrict uptake of methylated DNA and

hence unmethylated plasmid DNA is a requisite for efficient transformation of *B. thuringiensis.*

Genotype: *ara14, leuB6, thi, fhuA31, lacY1, tsx78, galK2, supE44, hisG4, rpsL136 (Str^r), xyl5, mtl1, dam13:Tn9 (Cm^r), dcm6, mcrB1, hsdR2, mcrA.*

2.1.1.2 *Bacillus thuringiensis*

2.1.1.2.1 *Bacillus thuringiensis* native strain A1462 donated by BFRI, JAPAN.

2.1.1.2.2 *Bacillus thuringiensis* strain Sbt012 isolated from China.

2.1.1.2.3 *Bacillus thuringiensis* subspecies *kurstaki* HD73 that produces insecticidal Cry1Ac toxin.

2.1.1.2.4 IPS 78/11, a crystal free (acrystalliferous) strain of *Bacillus thuringiensis* subsp *israelensis.*

2.1.1.2.5 *Bacillus thuringiensis* strain 4D7, a crystal free derivative of *Bacillus thuringiensis* subspecies *kurstaki,* was obtained from Bacillus Genetic Stock Center, Department of Biochemistry, Ohio State University.

2.1.1.2.6 *Bacillus thuringiensis* strain 4Q7, a crystal free plasmid-cured strain of *Bacillus thuringiensis* subsp *israelensis,* was obtained from Bacillus Genetic Stock Center, Department of Biochemistry, Ohio State University.

2.1.2 Plasmids

2.1.2.1 Plasmid vectors

2.1.2.1.1 pSVP27A, an *E. coli* –Bt expression vector: This is an *E. coli* / *B. thuringiensis* shuttle vector with the Cyt1A promoter from the *cyt1A* toxin gene of *B. thuringiensis* subsp. *israelensis* upstream of the cloned target gene (Crickmore & Ellar, 1992; Crickmore et al., 1994). The vector, pSVP27 possesses attributes of the *E. coli* / *B. thuringiensis* shuttle vector, pSV2 which is used in cloning genes in *E. coli* via the multiple cloning site for expression in *B. thuringiensis.* The vector possesses origin of replication for both *E. coli* and *B. thuringiensis*. The vector carries chloramphenicol and ampicillin resistance genes.

2.1.2.1.2 pGEM-T vector procured from Promega was employed for cloning PCR products amplified using Taq DNA polymerase which adds adenine (A) to the 3' end of its PCR products. It possesses an origin of replication in *E. coli* and an ampicillin resistance gene.

2.1.2.1.3 pET3a Expression vector procured from Novagen which possesses an origin of replication in *E. coli*, ampicillin resistance gene, T7 IPTG inducible promoter and a multiple cloning site.

2.1.2.2 Recombinant plasmids

2.1.2.2.1 Plasmid pGC-I harbouring the gene that encodes Cry41Aa1 (PS3Aa1) toxin from BFRI, JAPAN.

2.1.2.2.2 Recombinant *cry51Aa1* cloned into the shuttle vector pHT304 with its own promoter and conferring resistance to erythromycin from the collaborators (Ming Sun's lab, Huazhong Agricultural University, Wuhan) in China.

2.1.2.2.3 Recombinant Cry65Aa: Cry65Aa1 was isolated from *B. thuringiensis* strain SBt003 by Sun et al., 2010 (unpublished). Recombinant *cry65* cloned and expressed in the Bt recombinant strain BMB1281 and conferring resistance to chloramphenicol was sent by the collaborators from China.

2.1.2.2.4 pGEMCry1Ac: Insecticidal *cry1Ac* gene cloned into pGEM-T vector and expressed in *E. coli* JM109.

2.1.3 Insect populations

2.1.3.1 *Plutella xylostella* strains

2.1.3.1.1 NO-QA: Cry1Ac resistant population. The field-collected insecticidal Cry1Ac resistant population was obtained from the Max Planck Institute for Chemical Ecology (Thuringia, Germany) and maintained in the laboratory on a diet of six-week-old Chinese cabbage (*Brassica pekinensis*) at 25°C under a 16 h photophase.

2.1.3.1.2 G-88: Cry1Ac susceptible population. A subpopulation of Gen-88 adapted to artificial diet (Gen-88 D) was obtained from Dr. Ben Raymond, Centre for Ecology and Hydrology (Oxford, UK) and maintained in the lab on a sterile artificial Hoffman's diet at 25°C under a 16 h photophase.

2.1.3.1.3 LAB-UK: Cry1Ac susceptible population maintained in the laboratory on a diet of six-week-old Chinese cabbage (*Brassica pekinensis*) at 25°C under a 16 h photophase.

2.1.4 Human cancer cell lines

2.1.4.1 A549 (human lung carcinoma), an anchorage dependant (adherent) cell line was kindly provided by Dr. Lynne Mayne, University of Sussex, UK.

2.1.4.2 HepG2 (human Caucasian hepatocyte carcinoma), an adherent cell line was purchased from ECACC, Salisbury, UK.

2.1.4.3 HeLa (human cervical cancer), an adherent cancer cell line was kindly provided by Dr. Michelle West, University of Sussex, UK.

2.1.5 Culture media

The cell lines mentioned above were routinely maintained in the medium DMEM (Dulbecco's modified Eagle media) supplemented with 10% FBS (Fetal Bovine Serum) and 2% PSG (Penicillin, Streptomycin, and Glutamine) as recommended by the supplier.

2.1.5.1 Sub-culture Routine

The cells were kept in sterile polystyrene 80 cm^2 flasks (Nunc) with filter cap and sub-confluent cultures (70-80%) were trypsinised (Trypsin/EDTA 1X containing 0.05% Trypsin and 0.53 mM EDTA) and split bi-weekly in case of HeLa and A549

cells and weekly in case of HepG2 cells depending on the seeding ratio. The cells were grown in a standard, cell culture incubator at 37°C/5%CO_2 humidified air.

2.1.6 Miscellaneous reagents and kits used for cell assays

2.1.6.1 Etoposide (Sigma), a derivative of podophyllotoxin and topoisomerase II inhibitor was prepared as 10 mg/ml stock solution in DMSO and diluted to the appropriate concentration in tissue culture medium.

2.1.6.2 Trypan Blue Solution (Gibco®), 0.4%.

2.1.6.3 CellTiter-Blue cell viabillity assay kit from Promega.

2.1.6.4 CellTiter-Glo luminescent cell viability assay kit from Promega.

2.1.7 Bacterial culture media

2.1.7.1 LB (Luria –Bertani) media

Tryptone: 10 g

Yeast Extract: 5 g

NaCl: 10 g

Water to 1 litre. The pH was adjusted to 7.5 with 5 M NaOH.

2.1.7.2 LB agarose plates: Luria –Bertani media solidified with 15 g/l agar.

2.2 Experimental protocols

2.2.1 Design of PCR primers for amplification of DNA fragments

The primers were designed by analysing the specific target sequence and their properties and suitability assessed by using PCR Primer Stats (SMS on www.bioinformatics.org). The primers were further crosschecked using the programme PRIMER SELECT from the DNASTAR software package. The appropriate primers are listed in the relevant chapters.

2.2.2 PCR amplification of DNA

The open reading frames and the DNA fragments of the crystal genes under investigation were amplified using the appropriate primers as listed in the relevant chapters. The PCR amplification reactions were performed using either Taq or Pfu DNA polymerase as mentioned in the relevant chapters. High fidelity Expand long range PCR kit from Roche was used according to the manufacturer's instructions for generation of PCR products with 3'A- overhangs to enable cloning into the pGEM-T vector possessing 3' T- overhangs. High Fidelity *pfu* DNA polymerase-based PCR amplification system from Stratagene, Pfu Ultra Hotstart Master mix was used in many instances for amplification of DNA fragments. High fidelity PCR master mix from Roche was also employed in certain instances as mentioned in the relevant chapters.

PCR contents for a 50 µl volume whilst employing High fidelity Expand long range PCR kit from Roche were 1 pmol/µl (1 µM) of Forward and Reverse primers each, 10 µl of 5X Expand Long Range Buffer (Roche), 10-500 ng of template DNA, 2.5

µl of nucleotide mix, 0.7 µl of Expand Long Range Enzyme mix and 35.3 µl of water. In case of using Pfu Ultra Hotstart Master mix from Stratagene or High Fidelity Master mix from Roche, the contents were as follows: 0.5 µl of 100 pmol/µl Forward and Reverse primers each, 0.5 µl of template DNA, 25 µl of the master mix (2.5 U per 50 µl reaction) and 23.5 µl of sterile distilled water. The initial denaturation was set up at 95°C for 2 min. The annealing temperature used for amplification usually varied between 55-60°C. The extension time was based on the size of the target DNA, set up as 30 seconds per kb of DNA to be amplified for targets which were more than 10kb. PCR reactions were generally run for 30 cycles. PCR amplicons were analysed and visualised by electrophoresis on a 1% (w/v) agarose gels and staining with a fluorescent nucleic acid dye GelRed.

2.2.3 Purification of PCR amplicons

2.2.3.1 Column purification of the PCR amplicons

The PCR amplified products were purified using QIAquick PCR Purification kit (Qiagen) according to the manufacturer's instructions.

2.2.3.2 Gel isolation of the DNA fragments

In some instances the PCR amplicons and the desired DNA fragments were isolated from the agarose gel and purified using a simple bind-wash-elute protocol based QIAquick Gel Extraction kit (Qiagen) according to the manufacturer's instructions.

2.2.4 Ligation of the purified PCR amplicons

The purified PCR products were either self- ligated or ligated to the desired vector for the formation of the desired construct using either 2X Rapid Ligation buffer (Promega) or T4 DNA Ligase buffer 10X (Promega).

Purified PCR amplicons were ligated into pGEM-T or pGEM-T easy vectors vector using 2X Rapid Ligation buffer (Promega). For ligation of other purified PCR amplicons, T4DNA Ligase buffer 10X (Promega) was used. Ligation reactions were typically assembled as follows: 0.1-1 weiss units of T4 DNA ligase, 1 µl of Ligation Buffer and 3:1 Molar ratio of vector: insert DNA. Sterile distilled water was added to make the volume to 10 µl. The reaction mix was incubated 2-3 h at room temperature and further kept on ice.

1 µl of the above ligation mix was used for transformation into 50 µl of competent *E. coli* cells by electroporation.

2.2.5 Transformation of bacterial strains with plasmids

2.2.5.1 Transformation of *E. coli* strains by electroporation

A fresh colony of *E. coli* strain was used to inoculate 100 ml of L. Broth. Cells were grown with vigorous aeration at 37°C to mid-log phase, until they reached an OD_{600} of 0.4-0.8. The cells were harvested by centrifugation at 15,000 *g* for 10 min in sterile centrifuge bottles in SLA-1500 rotor. The cells were then washed extensively to eliminate all salts. The cell pellet was washed in 100 ml cold

distilled water and further centrifuged at 15,000 *g* for 10 min in SLA-1500 rotor. The pellet was resuspended in 1 ml of cold distilled water and transferred to an Eppendorf tube. The cells were centrifuged for a further 2 min at 16,000 *g* rpm and resuspended in 200 µl of cold water. 50 µl of the competent *E. coli* cells, thus prepared were mixed with 1 µl of the DNA to be transformed and then pipetted into a sterile electroporation cuvette containing electrodes. A short electric pulse of 1.8 kV, 200 Ω, 25 µF is applied to the cells for the uptake of DNA. The cells were then incubated with broth and allowed to express the antibiotic resistance gene for 30-60 min prior to plating. Transformed cells were plated out on LB-agar plates containing the antibiotic ampicillin at a concentration of 100 µg/ml and incubated at 37°C overnight to obtain the colonies with the desired DNA.

2.2.5.2 Transformation of *Bacillus thuringiensis* strains

Plasmids were transformed into various strains of *B. thuringiensis* by electroporation. The Bt cells were rendered electrocompetent using the same methodology as that used for competent *E. coli* cells with few modifications. The fresh Bt cultures were grown at 30°C in a shaking incubator until they reached an OD_{600} of 0.4-0.8. The cells were harvested and competent Bt cells were prepared as described above. Electroporation was carried out using the same protocol as outlined in Section 2.2.5.1. However following electroporation, the cells were incubated with broth at 30°C without shaking and allowed to express the antibiotic resistance gene for 60 min prior to plating. Transformed cells were plated out on LB-agar plates containing the antibiotic chloramphenicol at a concentration of 5 µg/ml and incubated at 30°C overnight to obtain the colonies with the desired DNA.

2.2.6 Rapid size screen of the *E. coli* transformants

To identify the desired clone, rapid size screening was performed. The rapid size screen (RSS) solution consisted of 100 µl of 500 mM EDTA, 1 g of 10% sucrose, 150 µl of 10% SDS, 2.5 ml of 0.5 M NaOH, 600 µl of 1.4 M KCl and 6.5 ml of water. The dye Bromophenol blue was added to the solution.

25 µl of the above RSS solution (pre-warmed) was added to the Eppendorf tubes. Individual bacterial colonies were picked by a sterile toothpick and resuspended in the solution. The tube was incubated in water bath at 37°C for 5 min followed by incubation in ice for 5 min. The samples were centrifuged at 11,000 *g* for 5 min. 10 µl of the sample was loaded on to a 1% agarose gel. Plasmids with insert ran slower than the plasmids carrying no insert and were chosen for further analyses.

2.2.7 Extraction of plasmid DNA from transformed bacterial strains

2.2.7.1 Extraction of plasmid from *E. coli* transformants

Small scale plasmid preparations were carried out using QIAprep Spin Miniprep kit (Qiagen) that follows a simple bind-wash-elute protocol as per the manufacturer's recommendations.

2.2.7.2 Extraction of plasmid from *B. thuringiensis* transformants

Plasmid DNA was extracted from *B. thuringiensis* by using QIAprep Spin Miniprep Kit from Qiagen. Freshly grown transformed Bt cells were resuspended in 250 µl of Buffer P1 containing 10 mg/ml lysozyme and incubated in water bath at 37°C for 30 min to 1 h to enhance the lysis of the cell wall. 250 µl of lysis Buffer P2 was added to the tube and gently inverted 4-6 times and the rest of the protocol as mentioned above in case of *E. coli* (Section 2.2.7.1) was carried out according to the manufacturer's instructions.

2.2.8 Analyses of extracted plasmids

The sequence integrity of all the plasmid constructs was verified by restriction analysis and sequencing.

2.2.8.1 Restriction analysis of extracted plasmids

The extracted plasmids were subjected to restriction analysis. All digestions in this study were performed using restriction enzymes and their associated buffers purchased from NEB (New England Biolabs). Digestions were carried out according to manufacturer's recommendations for the optimal temperature and buffer conditions for each enzyme used. Restriction digestion was performed on the plasmids thus extracted to verify the correct size of the insert. Typically, 1 µg of plasmid DNA was digested with 0.5 µl of restriction enzyme (10 U/µl) and 1 µl of corresponding buffer (10X) in which the enzyme shows maximum activity. The total volume was made up to 10 µl by adding water. The reaction was incubated in water bath at 37°C for 1 h and the digest verified on a 1% agarose gel.

2.2.8.2 DNA sequence analysis

The plasmid DNA products were sequenced to confirm the integrity or presence of desired inserts or deletions at the junctions by dideoxy chain termination method (MWG, Germany).

2.2.9 Expression and harvesting of the protein

2.2.9.1 Expression and harvesting of the protein from *E. coli* JM109

Fresh transformed colony of desired plasmid in *E. coli* JM109 was grown in LB medium supplemented with the appropriate antibiotic. 100 ml of L-broth was inoculated with the culture of interest and appropriate antibiotic usually 100 µg/ml of ampicillin for JM109 and grown for three days at 37°C. After three days of growth, the resultant inclusion bodies of the recombinant crystal gene were harvested. The culture thus grown was centrifuged at 20,000 *g* for 10 minutes. The pellet was resuspended in 30 ml of sterile distilled water, sonicated for 1 min 4 times and then re-centrifuged and finally resuspended in 5 ml of water. The protein was checked on the 7.5% SDS-PAGE as described in Section 2.2.10.

2.2.9.2 Expression and harvesting of protein from *E. coli* BL21(DE3)

Expression plasmids were transformed into *E. coli* BL21(DE3) cells and the transformant of interest was grown in LB medium supplemented with ampicillin (100 µg/ml) until optical density of 0.5 was obtained at 600 nm. Protein expression was then induced by the addition of 0.5 mM IPTG. The induced culture was grown

for 24 h at 37°C in a shaker at 175 rpm. The protein was harvested after 24 hours of growth as discussed above. Protein samples were analysed by SDS-PAGE.

2.2.9.3 Expression and harvesting of protein from *Bacillus thuringiensis*

The wild type-Bt isolates and the Bt transformants harbouring the plasmid of interest were grown on LB agar plates supplemented with appropriate antibiotic, when necessary for 3-5 days at 30°C. Sporulated cells were scrapped off the plates and suspended in 30 ml of sterile distilled water. The cells were then harvested and subjected to extensive washing procedure as described above in Section 2.2.9.1. The protein was analysed by SDS-PAGE.

2.2.10 Analysis of harvested proteins by SDS-polyacrylamide gel electrophoresis

The harvested proteins were resolved on a SDS-PAGE (sodium dodecyl polyacrylamide gel electrophoresis). The size of the crystal toxin was assessed using either 7.5% or 12% SDS-PAGE based on the method described by Laemmli (1970). Smaller molecular weight proteins were resolved on 12% SDS gels. Polyacrylamide gels were prepared from materials supplied by Bio-Rad.

For 7.5% gel, Resolving gel solution consisted of 2 ml of water, 1 ml of Resolving Gel Buffer (18.18 g Tris, 0.4 g SDS, distilled water to 100 ml, pH 8.8), 1 ml Acrylamide/bis-Acrylamide mixture, 30% solution (Sigma), 8 µl of 400 mg/ml

ammonium per sulphate solution (freshly made) and 4 µl of TEMED. For 12% SDS-PAGE gel, the volume of distilled water used was 1400 µl and the volume of acrylamide/bis-Acrylamide used was 1600 µl, the volumes of remaining ingredients being the same.

Stacking gel solution remained same for both 7.5 and 12% gels and consisted of 1ml of distilled water, 500 µl of Stacking gel Buffer (6.06 g Tris, 0.4 g SDS, Water to100 ml, pH 6.8), 333 µl Acrylamide/bis-Acrylamide mixture, 4 µl of and 2 µl of TEMED.

Protein samples were mixed with 2X sample buffer (1:1) (2 g SDS, 6 mg EDTA, 20 mg Bromophenol blue, 5 ml Resolving gel buffer, 50% (v/v) glycerol, 5% β-mercaptoethanol) and boiled for 3-5 min before loading on the SDS gel. Electrophoresis was performed at 200V for approximately 30 min using 1X Tris-glycine-SDS Buffer (0.76 g Tris, 3.6 g Glycine, 0.25 g SDS and water to 25 ml) followed by 30 min staining using Coomassie Brilliant Blue R dye (Sigma). The samples were then destained using the solution comprising of methanol, water and glacial acetic acid (10:9:1).

2.2.11 Estimation of protein concentration

The Bio-Rad protein assay kit based on the method described by Bradford (1976) was employed to estimate the concentration of the solubilised and the trypsin-treated protein samples with BSA (bovine serum albumin) as the standard. The

assay involves the addition of the acidic dye, Coomassie Brilliant Blue G-250 to the protein solution and subsequent measurement of the absorbance at 595 nm with spectrophotometer. Briefly, 1 part of the dye reagent, Coomassie Brilliant Blue G-250 (Bio-Rad) was diluted with 4 parts of sterile distilled water and filtered through Whatman filter to get rid of the particulates. Five dilutions of the protein standard, BSA at 10mg/ml ranging from 0.2 to 1mg/ml was prepared in order to get a linear range. 20 µl of each standard and protein sample solutions were pipetted to the disposable polystyrene cuvettes. 980 µl of the diluted dye reagent was added to each cuvettes and vortexed. The reaction mix was incubated for at least 5 min before measuring the absorbance at 595 nm. A curve of protein concentration (mg/ml) of the standard versus the OD_{595} was plotted and the concentration of the unknown protein samples deduced based on their absorbance.

2.2.12 Characterisation of the expressed proteins

Solubilisation and activation of crystal proteins

The protein samples were dispensed in an Eppendorf tube and centrifuged for 5 min at 11,000 *g*. The supernatant was discarded and the pellet resuspended in 50mM sodium carbonate buffers at various pH ranging from 8.0 to 11.0. In some instances, as mentioned in the relevant chapter, an acidic buffer was also used to solubilise the proteins. DTT at the final concentration of 1mM was added to the samples to carry out solubilisation in a reducing environment. The sample was incubated at 37°C, water bath for 1 h. After incubation, the reaction mix was centrifuged and the supernatants were analysed by SDS-PAGE. Similarly, either the solubilised proteins or protein extracts were processed by varied

concentrations of various proteases including proteinase K (Sigma), trypsin (Sigma), chymotrypsin (Sigma) and gut extracts from *Plutella xylostella* populations prepared in the corresponding solubilising buffer.

2.2.13 Purification of the protein samples

2.2.13.1 Purification of proteins by sucrose density gradient

To separate the crystalline inclusions from the spores, a differential ultracentrifugation through a discontinuous sucrose gradient was performed based on the method described by Thomas & Ellar (1983a). The sucrose gradient comprised of three layers of 10 ml each with concentrations in the ascending order of 1.97 M (67.4 g of sucrose in 100 ml of water), 2.1 M (71.8 g of sucrose in 100 ml water), and 2.3 M (78.7 g in 100 ml water) sucrose added slowly to the sides of a 38 ml polycarbonate round centrifuge tubes (Nalgene). 1 ml of the washed and sonicated crystal-spore mixture was applied to each tube band the centrifugation was set up at 72,000 *g* at 4^0C for 16 h in an SW28 rotor using an Optima LE-80K Ultracentrifuge (Beckman).

The layer of interest approximately 1-5 ml (present in the bottom part of the middle sucrose layer) was removed, diluted 10-fold in ice-cold distilled water and was centrifuged at 25,000 *g* at 4^0C for 15 min in a SS-34 rotor. The pelleted crystalline inclusions were resuspended in 0.5 ml of sterile distilled water for further solubilisation and trypsin activation.

2.2.13.2 Dialysis

The protein samples containing DTT were dialysed using a 25 kDa MWCO Micro DispoDialyzer (Sigma) against 50 mM Tris buffer pH 8 overnight on a magnetic stirrer at 4°C to remove DTT and low molecular weight contaminants. Briefly, 100 µl of the sample was placed into the dialyzer and immersed in approximately 500 ml of 50 mM Tris buffer, pH 8. Dialysis was carried out at 4^0C overnight with constant stirring. The dialysed samples were analysed on the 7.5% SDS-PAGE and their concentration was determined and further frozen at -20^0C for cell assays.

2.2.13.3 Anion exchange chromatography-FPLC

Purification of the solubilised crystal toxins were performed using AKTA FPLC (GE Healthcare). The solubilised protein samples were applied to an anion-exchange column, Resource Q (Amersham Pharmacia Biotech, UK) at a flow rate of 1 ml/min at 4°C in 50 mM sodium carbonate buffer, pH10.5 and were eluted with an increasing linear gradient of 1 M sodium chloride. 1 ml fractions were collected and analysed on SDS-PAGE.

2.2.14 Feeding regimens for artificial rearing of *Plutella xylostella* G-88 population

G-88 was maintained on an aseptic artificial Hoffman's diet at 25^0C under a 16 h photophase. The artificial diet comprised of the following ingredients: 32 g wheat germ, 15 g casein, 13 g sucrose, 6.4 g yeast, 4.3 g Wesson's salt mix, 0.4 g cholesterol, 0.4 g methyl paraben and 0.7 g sorbic acid measured and blended in 357 ml of boiling sterile distilled water containing 5.4 g agar. The blended mixture was then rendered sterile by autoclaving. The autoclaved mix was then allowed to cool down to 40^0C. 0.1 g vanderzant vitamin mixture (Sigma), 2.0 g of ascorbic acid and 0.4 g choline chloride aseptically measured and dissolved in 50ml of sterile distilled water were then added to the above cooled autoclaved mix. The diet was supplemented with 1 ml of the antibiotic rifampicin (25 mg/ml stock prepared in methanol).

The diet thus prepared was then dispensed 20 ml each into 50 ml of sterile plastic cups and covered with cling film and stored at 4^0C for further rearing and bioassays.

2.2.15 Toxicity assays

The toxic activity of the protein samples were evaluated on the insects and human cancer cells.

2.2.15.1 Assay of insecticidal activity

The toxicity of protein samples to the cabbage pest, *Plutella xylostella* were evaluated using leaf-dip and diet-based bioassays based on the method described by Sayyed et al. (2000).

2.2.15.1.1 Leaf-dip bioassay

The protein samples to be assayed for the insecticidal activity were diluted in a sterile distilled water-triton (50 µg/ml triton X-100) solution. Chinese cabbage leaf discs (were dipped for 10 s into the resulting protein solutions and allowed to air dry at ambient temperature for 1-2 hours. The discs were placed in sterile petridishes (5 cm diameter) containing filter paper moistened with distilled water. Five second-instar larvae were introduced into each disc and incubated at 25^0C for 3 days after which the mortality was assessed. Larvae which failed to exhibit any coordinated movement upon prodding with blunt ended sterile forceps, were considered dead. Larvae fed on Leaf discs dipped in just sterile distilled water-triton (50 µg/ml triton X-100) solution was used as a negative control. Larvae fed on Leaf discs dipped in insecticidal Cry1Ac at 3 mg/ml was used as a positive control.

2.2.15.1.2 Diet-based assays

20 ml of sterile artificial diet were poured aseptically into a 50 ml autoclaved cup and allowed to set. The cups were treated with 100 µl of protein samples which were surface-spread and allowed to air dry at ambient temperature. Five second-instar larvae were introduced into each cups and incubated at 25^0C for 5 days. The mortality was assessed after 3 days as well as 5 days. Larvae which failed to exhibit any coordinated movement upon prodding with blunt-ended sterile forceps, were considered dead. Negative control larvae were fed on diet treated with sterile distilled water-triton (50 µg/ml triton X-100) solution. Positive control larvae were fed on diet treated with insecticidal Cry1Ac at 1 mg/ml.

2.2.15.2 Assay of cytocidal activity

2.2.15.2.1 Dye-exclusion cell viability assay

In order to measure the percentage of cell suspension that was viable, the dye trypan blue (0.4%) was used which stains the dead cells blue and leaves the viable cells unstained due to their intact cell membrane which excludes dyes like trypan blue, eosin or propidium. The assay was performed in 96 -well flat bottomed plate (Costar). 90 µl of cell suspension was dispensed in each well. 5 x 10^3 cells of A549 and HepG2 were used. The plate was then incubated at 37°C/5%CO_2 humidified air for 48 hours. After 48 hours incubation, each well received 10 µl of treatments which included Control i.e the sodium carbonate buffer, protein samples to be tested at a concentration of 1 µg per well and Etoposide, a topoisomerase II inhibitor at a concentration of 50 µM. The medium in the well was changed and the plate was incubated at 37°C/5%CO_2 humidified air for 48 hours to check for cytopathic effects. After 48 hours, the media was sucked out of the wells by the aid of a sterile Pasteur pipette. The cells were trypsinised with 100 µl of trypsin for 5 min at 37°C/5%CO_2 humidified air and dispensed into the universal flasks containing 100 µl of medium. The flasks were then centrifuged at 800 rpm for 5 min. The supernatant was discarded and pellets were resuspended in the culture medium and trypan blue (1:1). The cells were counted after 1 min using hemacytometer. The dead cells appeared blue. Percentage viability was calculated by dividing the total number of viable cells per ml of the aliquot by total number of cells per ml of aliquot multiplied by 100.

2.2.15.2.2 CellTiter-Blue cell viability assay

The levels of cytotoxicity of the proteins were assessed by using the CellTIter-Blue cell viability assay (Promega) to determine the number of viable cells in culture. The test methodology for cytotoxicity evaluation was adopted from previously published journal papers and manufacturer's instructions (Ahmed et al., 1994; Squatrito et al., 1995; Slaughter et al., 1999; O'Brien et al., 2000; Gonzalez & Tarloff, 2001; Promega, 2009). Briefly, serial dilutions of cells were made in triplicates. 90 µl of the cells were dispensed in the 96-well flat bottomed plate (Costar or nunc). The various dilutions of the cells used per well were: 1.0 x 10^4 , 5 x 10^3 cells, 2.5 x 10^3 cells,1.25 x 10^3 cells, 6.25 x 10^2 cells. Each experimental condition was set-up in triplicate to ensure well-to well consistency and for quantitating interwell variability. Cytopathic effects were observed under a phase-contrast microscopy. The assay was performed in 96 -well flat bottomed plate (black plates from Costar or clear plates from Nunc). 90 µl of cell suspension was dispensed in each well. The plate was then incubated at 37°C/5%CO_2 humidified air for 24 hours. After 24 hours incubation, each well received 10 µl of treatments.

After 24 hours of treatment, the wells were incubated with CellTiter-Blue (resazurin) reagent (Promega). 20 µl of CellTiter-Blue reagent was added aseptically to each well with 100ml of medium. The plates were placed back into the incubator. Plates were removed and reading taken after every hour for 1 h, 2 h and 4 h.

Cell cytotoxicity was measured using fluorescence by a fluorescent plate reader (GloMax –Multi Microplate Multimode reader from Promega).

Fluorescence was measured with a green filter with excitation wavelength at 525nm and emission wavelength ranging between 580-640 nm. Triplicate readings were averaged and Fluorescence reading was plotted against the cell number plated. Treatment was carried out on various cell lines including HepG2 and HeLa.

2.2.15.2.3 CellTiter-Glo luminscent cell viability assay

Cytotoxicity of the proteins was further corroborated by bioluminescent detection of ATP using CellTiter-Glo luminscent cell viability kit from Promega. This is based on quantitation of ATP which plays an important role in energy exchange processes in biological systems and hence serves as a reliable biomarker of cell viability (Crouch et al., 1993). The assay was set up according to the manufacturer's instructions.

Briefly, serial dilutions of cells were made in triplicates. 90 µl of the cells were dispensed in the recommended opaque- walled white 96-well flat and clear bottomed plate (Costar). The various dilutions of the cells used per well were: 1.0×10^4 , 5×10^3 cells, 2.5×10^3 cells,1.25×10^3 cells, 6.25×10^2 cells. Each experimental condition was set-up in triplicates to ensure well-to-well consistency and for quantitating inter-well variability. Cytopathic effects were observed under a phase-contrast microscopy. 90 µl of cell suspension was dispensed in each

well. The plate was then incubated at 37°C/5%CO_2 humidified air for 24 hours. After 24 hours incubation, each well received 10 µl of treatments. After 24 hours of treatment, the experimental plate was equilibrated at room temperature for 30 min before adding equal volume of CellTIter- Glo reagent to the volume of cell culture medium in each well. The CellTiter-Glo reagent was prepared according to the supplier's instructions. Briefly, the CellTiter-Glo buffer was thawed and equilibrated to room temperature prior to use. CellTiter-Glo substrate was equilibrated to room temperature prior to use. The thawed buffer was transferred to the amber bottle containing the CellTiter-Glo substrate and gently vortexed to reconstitute the CellTiter-Glo Reagent. The reagent was then added to the plate containing the cell culture medium as discussed above. The contents were mixed for 2 min on an orbital shaker to induce cell lysis. The experimental plate was further incubated at room temperature for 10 min to stabilise luminescent signal. The luminescence was recorded using Promega's GloMax –Multi Microplate Multimode reader. An integration time of 0.5 s per well was used. The luminescence measured was plotted against the number of cells in culture.

3. *In vitro* evaluation of anticancer activity against human cancer cells, and pathogenicity against an insect pest, of toxins derived from native *B. thuringiensis* strains

3.1 Introduction

The parasporins studied thus far have been found to possess specific cytotoxicity to different cell lines. However, a human hepatocellular carcinoma cell line, HepG2 is noted as being susceptible to all the parasporins so far investigated for their cytocidal activity (Ohba et al., 2009; Nagamatsu et al., 2010).

The present work examined two native *B. thuringiensis* strains isolated from soils of Japan and China. The work evaluates the toxic activities of the insecticidal *B thuringiensis subspecies kurstaki* HD-73 and *E. coli* expressed insecticidal Cry1Ac toxin. The toxicity of a crystal free *B. thuringiensis* strain 4D7 normally employed for expression of *B. thuringensis cry* genes was also investigated.

It was reported in a previous study in Japan that the *B. thuringiensis* strain A1462 (previously designated as 89-T-26-17) exhibits preferential activity against human cancer cells upon proteolytic activation (Yamashita et al., 2000). The strain transferred to us for further investigation. This work explores the proteins of the native strain A1462 from Japan, tests the cytotoxic activity of the native strain and further characterises the gene involved in the cytocidal activity.

We intended to investigate if the cytotoxic activity towards mammalian cells is explicit to the parasporins or whether it is also present in the insecticidal Cry proteins. This would also provide a valuable asset to the risk assessment on fauna of food derived from crops in which *B. thuringiensis* Cry toxins have been used either as crude microbial preparations or genetically engineered in plants. It has been reported that the parasporin-3 toxin exhibited strong cytocidal activity against the liver cancer cell line (HepG2) and no toxicities against several other cancer cell lines for instance A549 (lung carcinoma). Hence we aimed to further clarify if the cell killing activity is attributed to the sensitivity of the cell lines used or if it is a specific toxin-mediated action.

The present work further examines the toxicity of a soil isolate from China Sbt021, sequencing of which had identified a putative candidate toxin gene homologous and similar to the one present in *B. thuringiensis* strain A1462. The objective was to study the biological activity of the native strain Sbt021 against insect crop pests and human cancer cell lines and to characterise the genes encoding the toxin proteins. Cell viability assays and bioassays were conducted to assess the toxicity of the proteins derived from *B. thuringiensis* native strains.

3.2 Results

3.2.1 Preparation of inclusion proteins from the native strains, solubilisation, proteolytic processing and activation of the toxins

The soil isolates of *Bacillus thuringiensis* A1462 from Japan, Sbt021 from China, wild type HD73 and acrystalliferous 4D7 strains were colony purified several times before use. The strains were grown on sterile nutrient agar plates at 30°C for 4 days. Sporulation was checked under the microscope and the sporulated cells were harvested as described in Section 2.2.9.3. The proteins were analysed on a 7.5% SDS-PAGE gel. *E. coli* expressed recombinant insecticidal Cry1Ac protoxin at 4 mg/ml previously prepared in the lab was used for assays.

Parasporal inclusions of the strain *B. thuringiensis* A1462 contained protein bands of sizes 180, 150, 100, 90 and 80 kDa (Figure 3.1) as previously reported (Yamashita et al., 2005). Sbt021 inclusions contained a major protein band at 140 kDa and a minor band at 80 kDa (Figure 3.2). Btk HD-73 yielded a major protein band of 130 kDa (Figure 3.2). As expected the SDS-profile of crystal free strain 4D7 did not show any protein bands (data not shown).

Various buffers at different pH were used to solubilise the proteins as described in Section 2.2.12. The proteins were also subjected to trypsin treatment as described in Section 2.2.12. These assays were carried out in a reducing environment or a non-reducing one (data not shown). The solubilisation assays suggested that 50 mM carbonate buffer at pH 10.9 optimally solubilised the 80

kDa protein from A1462 strain in the presence of 1 mM DTT. The 80 kDa protein was detected in the supernatant (Lane 3, Figure 3.1). The other proteins of higher molecular mass were either not solubilised or were degraded. Trypsin in presence of 1 mM DTT resulted in the partial digestion of the protein bands of the native strain A1462 generating a band slightly lower than 80 kDa and a band of circa 60 kDa (Figure 3.1, lane 2). Solubilisation of protein inclusions from Sbt021 in the presence of DTT resulted in obtaining the major band of 140 kDa and minor band of 80 kDa in the soluble fraction (Figure 3.3, lane 1). Trypsin treatment in the presence of DTT yielded multiple protein bands of varying molecular masses (Figure 3.3, lane 2). The trypsin digestion of protein inclusions from HD-73 yielded two bands of circa 58 kDa (Figure 3.4). No protein bands were observed in case of crystal free 4D7 which was used as a negative control (data not shown).

The solubilised and the trypsin treated samples containing DTT were dialysed against 50 mM carbonate buffer pH 10.9 (Section 2.2.13.2). The Bradford method was employed to estimate the concentration of the protein samples with BSA as the standard (Section 2.2.11). The dialysed samples were frozen at -20 °C for further cell assays.

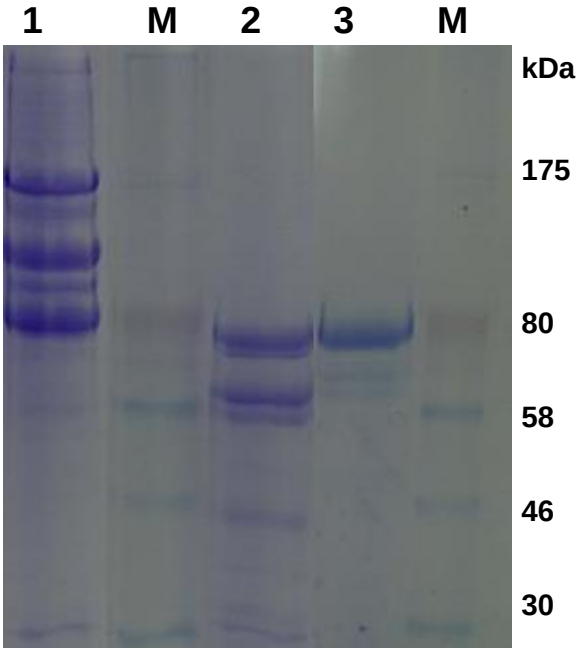

Figure 3.1. Protein analysis of the *B. thuringiensis* isolate A1462. Lane1, protein inclusions from the strain A1462; lane 2, protein treated with trypsin (1 mg/ml); lane 3, solubilised protein in sodium carbonate buffer, pH 10.9; lane M, protein marker. Solubilisation and trypsin treatment were carried out in presence of 1 mM DTT.

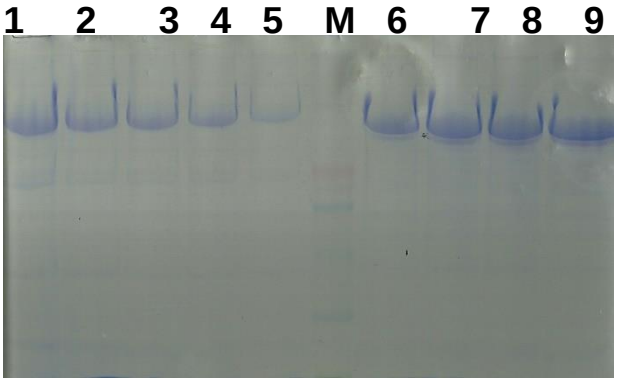

Figure 3.2. SDS-PAGE profile of *B. thuringiensis* native strains Sbt021 and HD-73. Lanes 1-5, Various dilutions of Sbt021 protein inclusions; lane M, protein marker; lanes 6-9, Various dilutions of HD-73 protein inclusions. 5, 4, 3, 2 and 1µl of the protein samples were run on the gel. The samples were diluted with sterile distilled water to make up to a total volume of 5 µl.

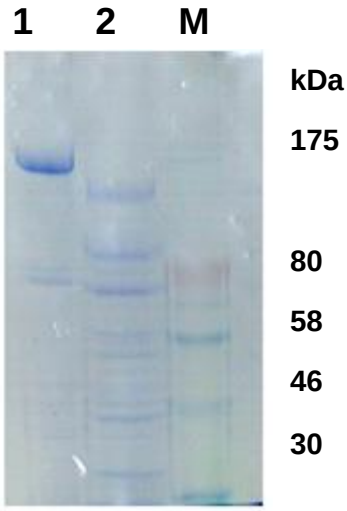

Figure 3.3. Solubilisation and proteolytic processing of protein inclusions from Sbt021. The sample was solubilised in 50 mM carbonate buffer, pH 10.9 (Lane 1) and treated with 1 mg/ml trypsin in presence of 5 mM DTT (Lane 2). Lane M represents protein marker.

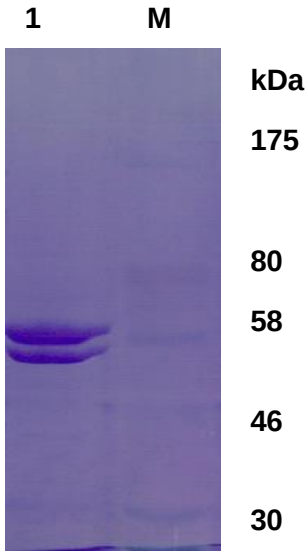

Figure 3.4. Proteolytic processing of Btk HD-73. 1 mg/ml trypsin with 5 mM DTT was used to activate the δ-endotoxin (Lane 1); protein marker (Lane M).

3.2.2 Activation and purification of recombinant Cry1Ac toxin

Recombinant Cry1Ac protoxin was activated using trypsin (1 mg/ml). A 65 kDa band was observed on the gel (Figure 3.5). AKTA FPLC was used for purifying the activated toxin fragment. The fractions were analysed on 7.5% SDS-PAGE. The activated protein was present in fractions A 8, A9, A10, A11 and A12 as evident from the SDS-PAGE gel (Figure 3.7).

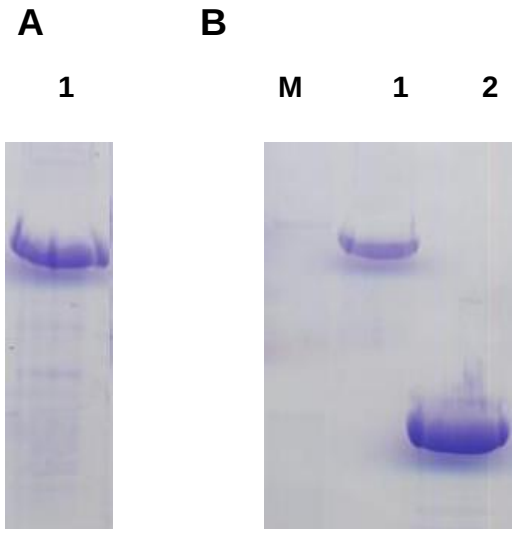

Figure 3.5. Solubilisation and proteolytic processing of the recombinant insecticidal Cry1Ac toxin. A. Lane1, recombinant Cry1Ac toxin. B. Lane M, protein marker; lane 2, solubilised Cry1Ac toxin; lane 3, proteolytically processed Cry1Ac toxin.

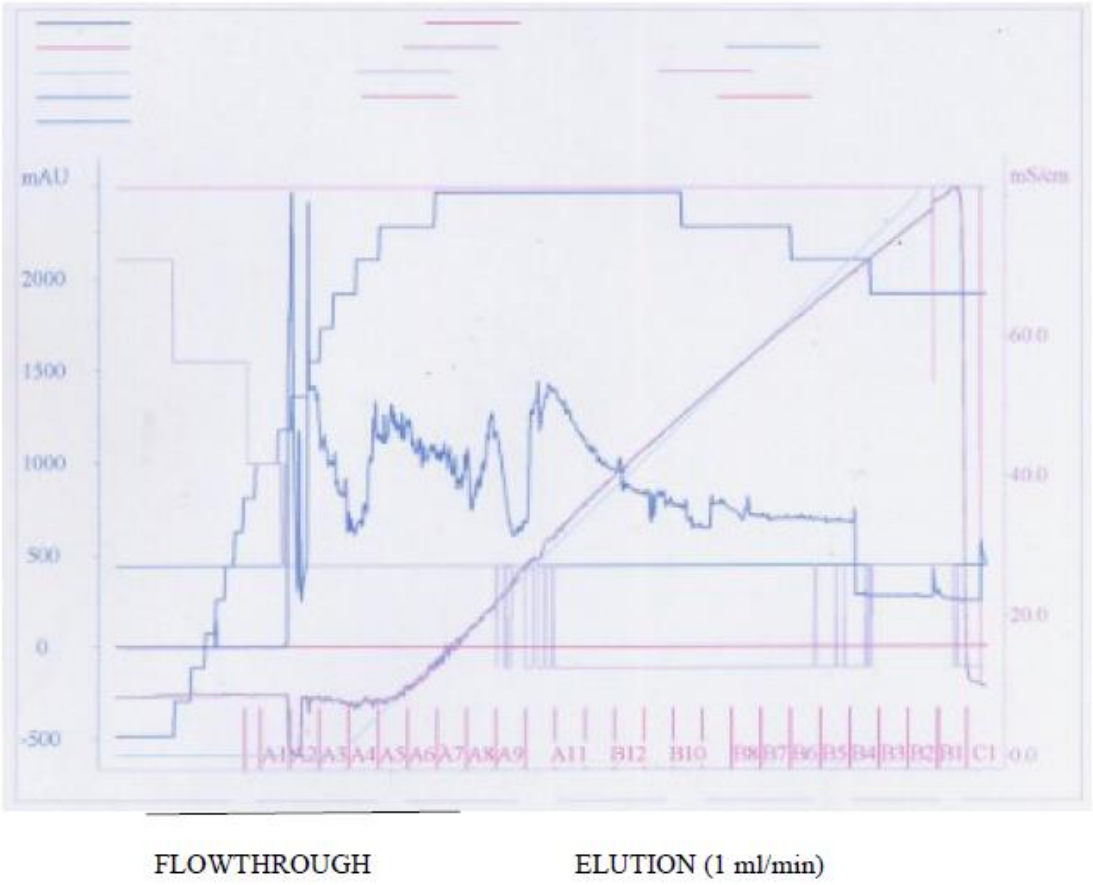

Figure 3.6. Purification of activated insecticidal Cry1Ac protein. Elution profile of activated toxin on anion exchange chromatography.

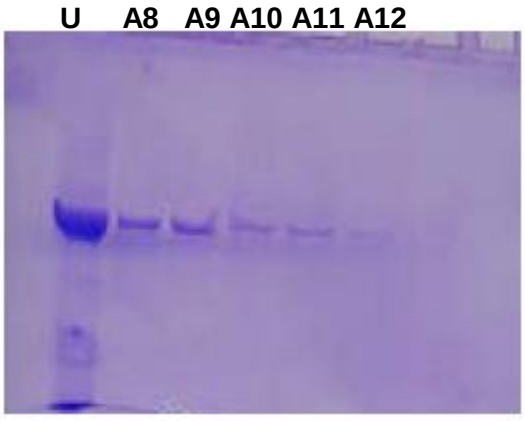

Figure 3.7. SDS-PAGE (7.5%) analysis of purified fractions of activated Cry1Ac protein. Lanes A8-A12 contain the purified activated Cry1Ac toxin. Lane U contains the un-purified trypsin activated Cry1Ac toxin.

3.2.3 Toxicity evaluation of *B. thuringiensis* proteins

3.2.3.1 Assessment of insecticidal activity

Toxicity was tested against Cry1Ac susceptible G88 populations of *Plutella xylostella* using leaf-dip and diet based assays as described in Section 2.2.15.1. No mortality was observed in the case of G88 populations treated with solubilised or trypsin treated A1462 or Sbt021 protein inclusions even at high concentrations of 0.5 mg/ml. Whereas, the insecticidal Cry1Ac and HD-73 solubilised crystals caused high larval mortality when used at concentration of 1-2 µg/ml.

3.2.3.2 *In vitro* cytocidal activity

The solubilised and the trypsin activated proteins were tested on human cancer cell lines, HepG2 and HeLa. Serial dilutions of cells were made in triplicate. 90 µl of the cells were dispensed in a 96-well flat bottomed plate (Nunc or Costar). The various dilutions of the cells used per well were: 1.0×10^4 , 5×10^3 cells, 2.5×10^3 cells,1.25×10^3 cells and 6.25×10^2 cells. Cytopathic effects were observed with an inverted phase-contrast microscope. The degree of cytotoxicity was assessed using cell viability assay techniques (CellTiter-Blue and CellTiter-Glo luminescent cell viability assays) as described in Sections 2.2.15.2.2 and 2.2.15.2.3.

Trypsin- treated *B. thuringiensis* acrystalliferous strains 4D7, HD-73 and purified trypsin-treated recombinant Cy1Ac did not elicit any morphological changes in HepG2 cells or HeLa cells as observed under the inverted phase contrast microscope (data not shown). No cytotocidal activity was observed upon treatment with these proteins as evidenced by cell viability assays. However, trypsin- treated A1462 protein caused marked morphological changes in HepG2 cells when used at a concentration of <10 µg/ml. The treatment resulted in spillage of the intracellular contents into the extracellular milieu. HeLa cells however did not exhibit any detectable morphological changes upon incubation with the same concentration of trypsin-treated A1462 protein (data not shown). Figure 3.8 shows the cell viability curves obtained for trypsin-treated Bt strain 4D7 and trypsin-treated A1462 strain in HepG2 cells with CellTiter-Blue assay. No cell-killing activity was observed when HepG2 cells were treated with the negative control, trypsin-treated 4D7. The trypsin-treated protein from *B. thuringiensis* strain A1462 induced cytotoxicity in HepG2 cells. The positive control, etoposide brought about significant cell-killing when used at a final concentration of 100 µg/ml. The cytotoxicity of trypsin-treated A1462 against HepG2 cells was further corroborated using CellTiter-Glo (Promega) (Section 2.2.15.2.3), the results of which obtained are shown in Figure 3.9. The results further substantiated that trypsin-treated A1462 is significantly cytotoxic to HepG2 cells. No cell-killing activity was observed when HepG2 and HeLa cells were administered with the trypsin-treated HD-73 used at a final concentration of 10 µg/ml. HD-73 did not affect viability of HepG2 cells (Figure 3.9). Figure 3.10 shows the cell viability of the Bt proteins on A) HepG2 cells B) HeLa cells as measured by CellTiter- Blue assay. The purified trypsin-treated recombinant Cry1Ac toxin did not affect the

cell viabilities in case of HepG2 (Figure 3.10A) and HeLa cells (Figure 3.10B). The trypsin-treated protein from *B. thuringiensis* strain A1462 induced cytotoxicity in HepG2 cells affecting the cell viability (Figures 3.10A) but failed to exhibit a comparable cytotoxicity against HeLa cells as seen by the CellTiter-blue assay when used at the same concentration of 50 µg/ml (Figure 3.10B). Trypsin-treated Sbt021 exhibited cytocidal activity against HepG2 as indicated by the CellTiter-blue assay. A comparison with trypsin-treated A1462 suggested that the degree of susceptibility of HepG2 cells to trypsin- treated Sbt021 is weak (Figure 3.10A).

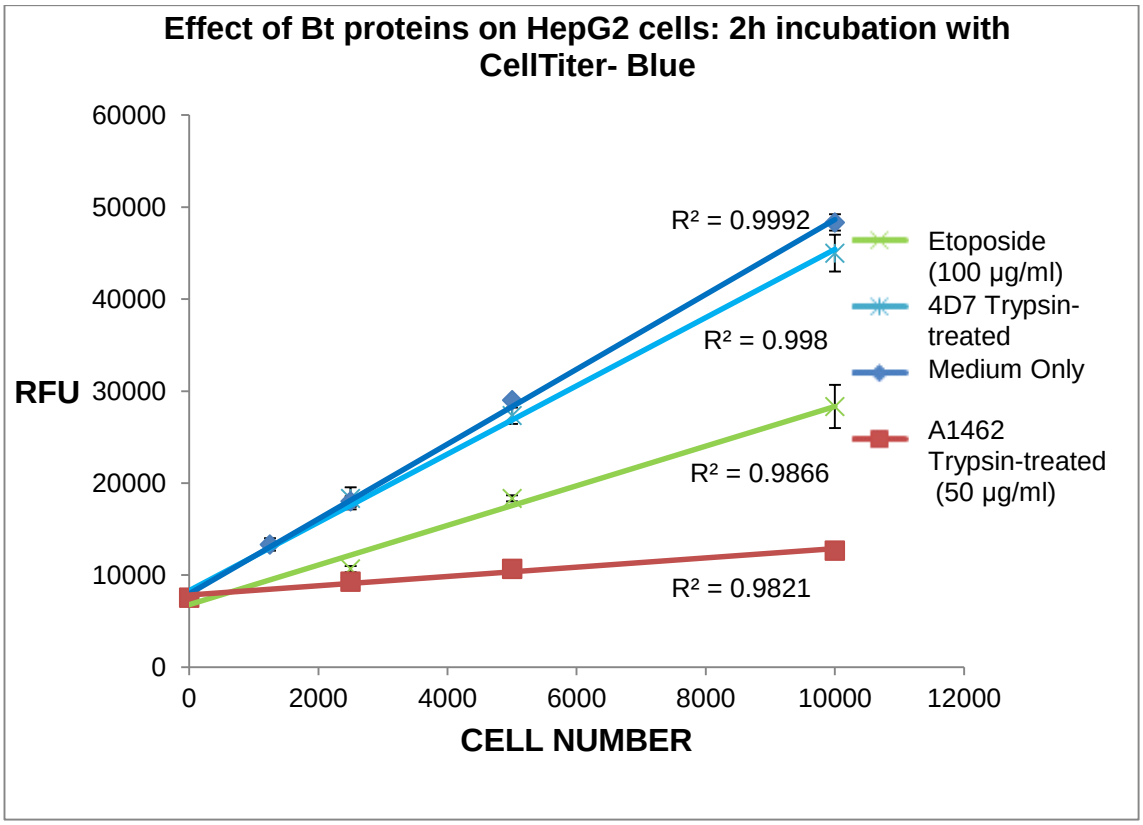

Figure 3.8. Effect of Bt proteins on viability of HepG2 cells. X-axis represents the cell number and Y- axis represents Relative Fluorescence Unit (RFU). Fluorescence was measured using a green filter with an excitation wavelength at 525 nm and emission wavelength 580-640 nm. Error bars denote SD of the mean of triplicate wells. Experiments are representative of at least five independent assays with each treatment.

Effect of Bt proteins on HepG2 cells: CellTiter-Glo assay

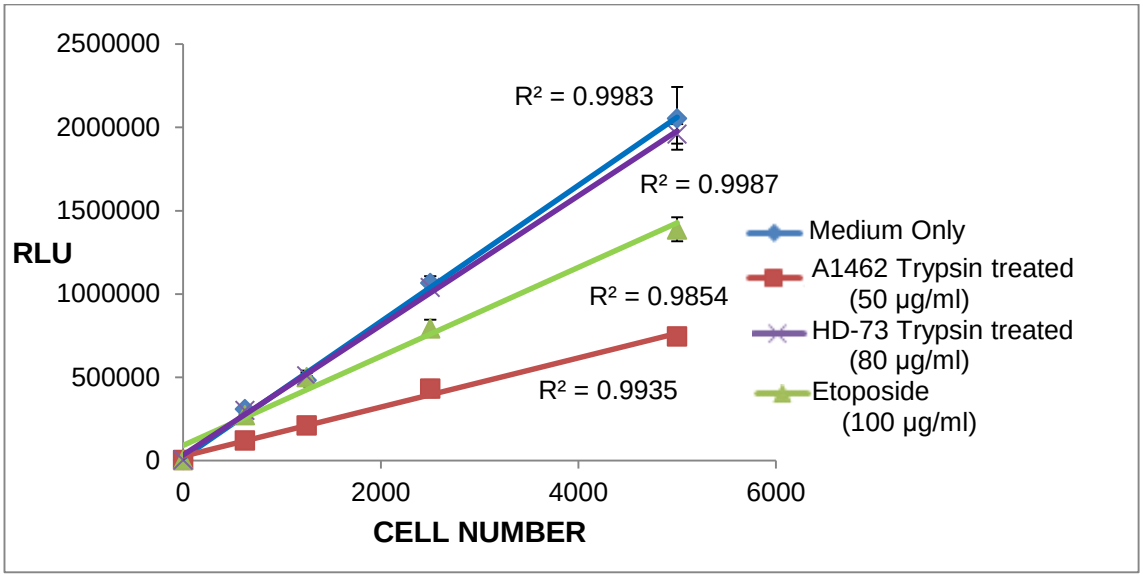

Figure 3.9. Effect of trypsin-treated A1462 and HD-73 on HepG2 cells: CellTiter-Glo Assay. Cytotoxicity of trypsin treated Bt A1462 was further corroborated by bioluminescent detection of ATP. X-axis represents the cell number and Y- axis represents Relative Luminescence Unit (RLU). Error bars denote SD for the data derived from the individual wells (triplicates). An integration time of 0.5 s was used. Experiments are representative of at least three independent assays with each treatment.

A. Effect of Bt proteins on HepG2 cells: 2h incubation with CellTiter- Blue

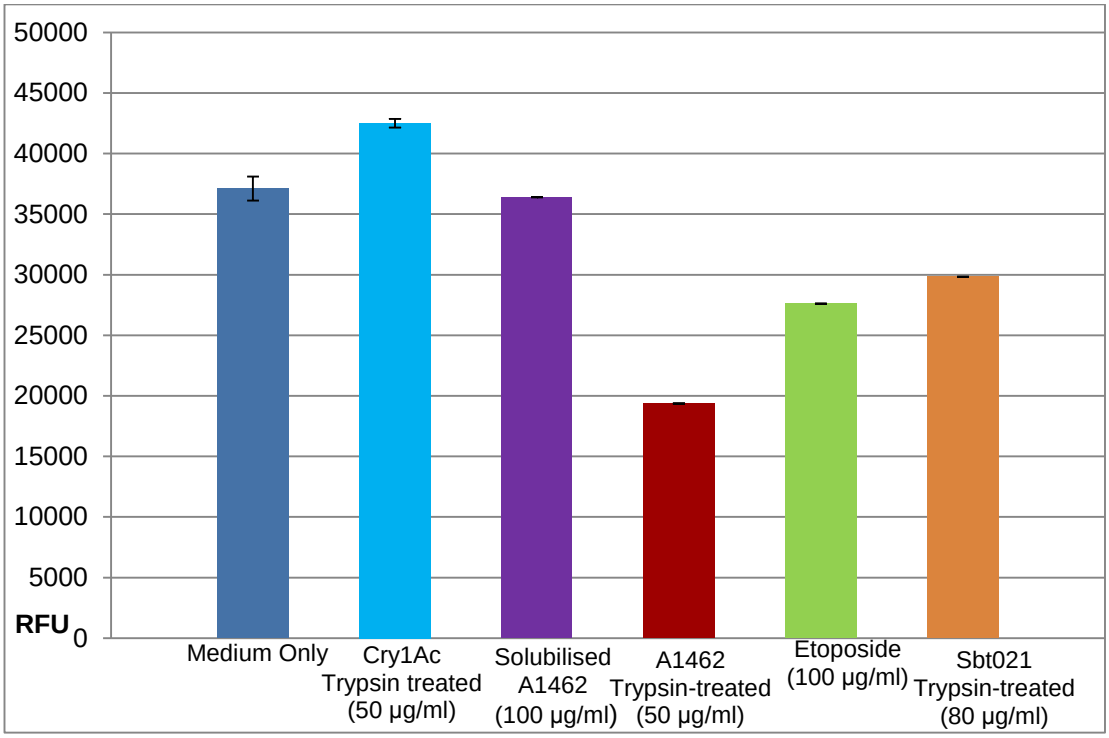

B. Effect of Bt proteins on HeLa cells: 2h incubation with CellTiter- Blue

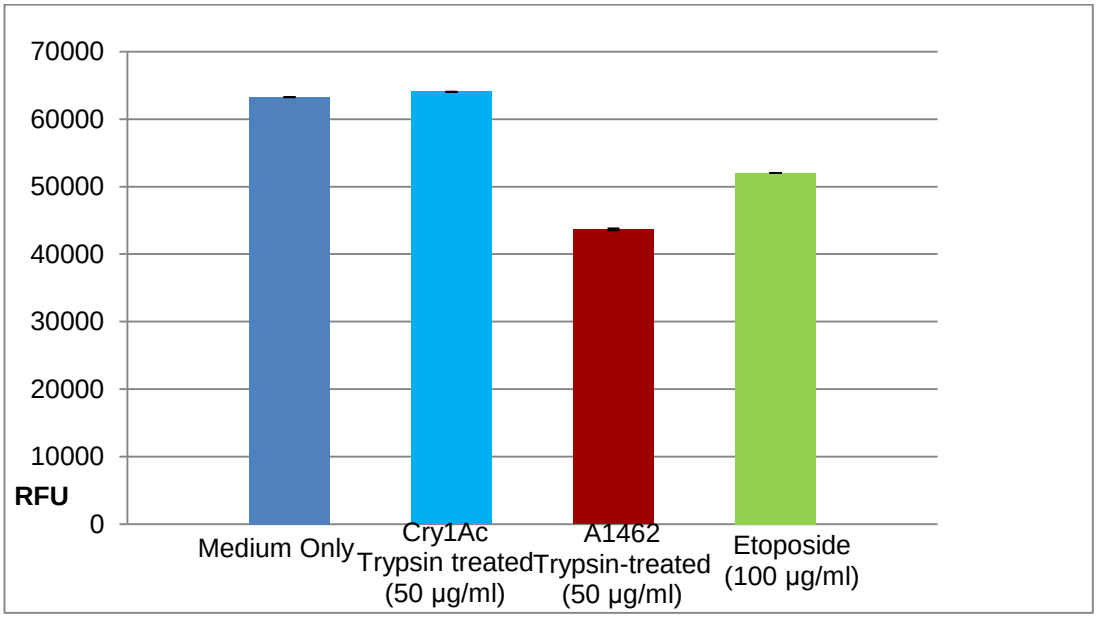

Figure 3.10. Effect of Bt proteins on (A) HepG2 (B) HeLa cells. X-axis represents the cell number and Y-axis represents Relative Fluorescence Unit (RFU). Data presented here is for 5000 cells/well. Error bars denote SD of the mean of triplicate wells. Experiments are representative of at least five independent assays with each treatment.

Dose response studies were conducted to assess if the proteins exhibited dose-dependent cytotoxicity. Figure 3.11 shows the concentration-response graphs obtained for the trypsin-treated A1462 samples on HepG2 cells with CellTiter-Blue assay. Serial dilutions of trypsin-treated inclusion proteins were prepared in 50 mm sodium carbonate buffer pH 10.9 and administered to HepG2 cells. The cytotoxicity was monitored with CellTiter -Blue as described earlier (Section 2.2.15.2.2). Maximal cell killing activity was obtained with the undiluted highest concentration of the trypsin- treated proteins. Progressive decrease in cell-killing activity was observed with decreasing concentration. Similar results were seen with trypsin-treated Sbt021 (data not shown).

Dose-response effect of trypsin-treated A1462 protein on HepG2 cells: 2h incubation with CellTiter- Blue

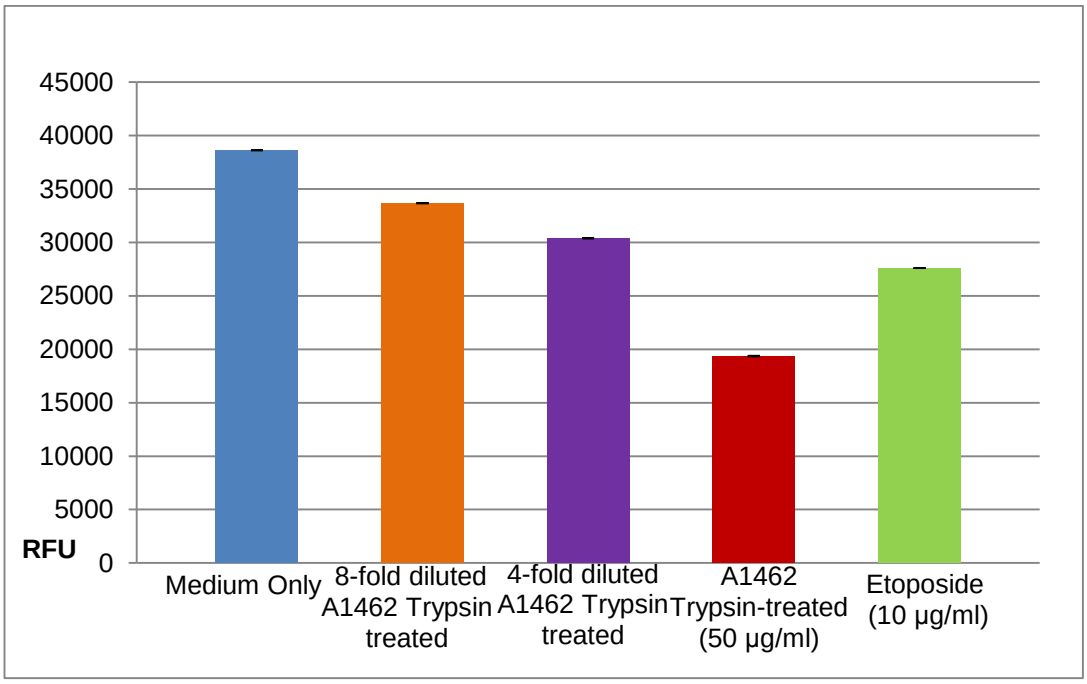

Figure 3.11. CellTiter-Blue assay indicating a dose-response analysis of trypsin-treated A1462 on viability of HepG2 cells. Y-axis represents Relative Fluorescence Unit (RFU). Data presented here is for 5000 cells/well. Error bars denote SD of the mean of triplicate wells. Experiments are representative of at least three independent assays with each treatment.

3.3 Discussion

An initial screen of *B. thuringiensis* wild type strains for *in vitro* cytotoxic activity ascertained that some of the *B. thuringiensis* strains possess activity against human cancer cells. The present studies confirmed that some of the *B. thuringiensis* inclusion proteins possess cytocidal activity against human carcinoma cell lines. The results confirm that the *B. thuringiensis* wild type strain A1462 from Japan demonstrates cytotoxic activity against human cancer cells as reported earlier (Yamashita et al., 2005). Limited cytotoxic activity was also seen for the native strain Sbt021 from China. The soils isolate A1462 exhibited cytotoxicity against human liver cancer cells (HepG2) whereas no such comparable cytotoxic activity was demonstrated against human cervical cancer (HeLa) cells. The data thus suggests varying preferential susceptibility of certain human cancer cell lines to the *B. thuringiensis* protein. HepG2 was weakly susceptible to the trypsin-treated proteins from Sbt021. No cytotoxicity was detected in case of the Lepidopteran insecticidal HD-73 strain and insecticidal Cry1Ac protein. The *B. thuringiensis* strain 4D7 did not exhibit any cytocidal activity.

Solubilised non-proteolytically treated proteins of A1462 or Sbt021 retained very low levels of cytotoxicity against HepG2 cells, this low level possibly owing to the proteolysis products generated by the action of endogenous protease. This is in agreement with the low-level of cytotoxicity observed by Lee et al. (2000a)

against MOLT-4 cells by alkali-solubilised parasporin-4 producing 89-T-34-22 strains. The proteins from the *B. thuringiensis* isolates A1462 and Sbt021 exhibited significant *in vitro* cytotoxicity to HepG2 cells only when treated with trypsin. This result can account for previously reported several findings that trypsinisation results in the cytocidal activity of *B. thuringiensis* parasporins. For instance Mizuki et al. (2000) observed that proteolytic processing is indispensable for imparting cytocidal properties to the Bt isolate 84-HS-1-11 that produces Cry31Aa1, an 81 kDa protein demonstrating preferential activity against leukemic cells. Similarly, Katayama et al. (2005) observed that parasporin-1 produced by the strain A1190 exhibits toxicity when cleaved by trypsin at two sites generating a heterodimer of 15 and 56 kDa subunits. Further, A1547 which is a parasporin-2 producer exhibits no cytotoxicity without protease digestion (Ito et al., 2004). The parasporin-4 toxin from *B. thuringiensis* strain 89-T-34-22 exhibited high cytotoxic activity against MOLT-4 cells only upon protease treatment (Lee et al., 2000a).

The cytotoxic activity thus exhibited by the inclusion proteins is selectively affecting certain types of cancer cell lines. This is in agreement with other studies that have showed cytotoxic activity associated with some *B. thuringiensis* strains. The preferential cell–killing activity of the parasporins from *B. thuringiensis* strains is similar to that demonstrated by the insecticidal Cry proteins of *B. thuringiensis* which recognise specific receptors on the susceptible insect cells. This renders them active against specific insect pests (Schnepf et al., 1998).

SDS-PAGE profiles of *B. thuringiensis* A1462 inclusions contained protein bands with molecular weight ranging from 180 to 80 kDa. This concurs with the previous study (Yamashita et al., 2005). Alkali solubilisation resulted in the obtaining of an 80 kDa band in the soluble fraction. The higher molecular mass proteins were either degraded or traces of them remained insoluble. Similar results were obtained by Kim et al. (2000) whilst investigating the cytotoxic properties of the wild type strain 90-F-45-14 which consisted of five major protein bands of molecular masses 170, 103, 73, 40 and 32 kDa. Upon alkali solubilisation of the inclusion, the higher molecular mass proteins of 170, 103 and 73 kDa could not be recovered possibly subjected to proteolytic degradation by the endogenous protease (Kim et al., 2000).

As opposed to the indiscriminate toxicity demonstrated by *B. thuringiensis* serovar *israelensis* owing to a broad-spectrum cytolysin, the Cyt1 toxin (Thomas & Ellar, 1983a; Mizuki et al., 1999), protein inclusions from the A1462 strain exhibit a selective activity against certain human cancer cell lines (Yamashita et al., 2000). There have been reports of the *B. thuringiensis* isolates being able to discriminate normal T cells from the leukaemic ones (Mizuki et al., 2000; Okumura et al., 2005).

It was observed with other *B. thuringiensis* native strains that the alkali-solubilised inclusions possess no cytotoxic activity. Proteolytic treatment of the inclusions resulted in the degradation of the protein to a lower molecular mass band which exhibited cytocidal activity against cancer cell lines (Mizuki et al., 1999; Lee et

al., 2000a; Ito et al., 2004; Yamashita et al., 2005). Our results suggested that the trypsin-treated A1462 demonstrated significant cytotoxic activity against HepG2. The solubilised A1462 lacks such significant activity thus further corroborating that proteolytic processing is indispensable for a significant cytotoxic activity.

Our results coupled with previous observations prompted us to further delve into characterisation of the protein inclusions cytotoxic to mammalian cell lines in order to assess the risk associated with the *B. thuringiensis* toxins being used in agriculture. Risk assessment being the vital aspect, it would also enable us to assess their suitability for clinical and diagnostic purposes.

In the next few chapters we aimed at analysing and determining the virulence factors that contribute to *in vitro* cytotoxicity observed in some of the *B. thuringiensis* strains.

4. Heterologous expression and characterisation of Parasporin-3 (*cry41A*) genes

4.1 Introduction

Cry41Aa and Cry41Ab parasporal inclusion proteins derived from non-insecticidal *Bacillus thuringiensis* strain A1462 have been reported to possess preferential cytotoxicity towards human cancer cell lines (Yamashita et al., 2005). These cytotoxic proteins belong to the parasporin-3 family. Amino acid analysis of the Cry41Aa and Cry41Ab responsible for the reported cytocidal activity of A1462 revealed only slight differences in their sequences thus showing a high degree of similarity.

Cry41Aa and Cry41Ab are 'split' toxins found as the second gene i.e. ORF2 in a three-gene operon. Sequence analysis of *cry41Aa* and *cry41Ab* genes detected three open reading frames in close proximity to each other and in the same orientation. Analysis of the ORFs of this operon shows that the upstream region of all the ORFs contained the putative translational signals, ribosome binding sites. The parasporin-3 *cry41Aa1* gene is found as part of a three-gene operon in which nonoverlapping reading frames are separated by short intergenic sequences. ORF1 consists of 543 base pairs encoding 180 amino acid residues with a predicted molecular weight of 19.5kDa. ORF1 has no conserved domains or blocks. ORF2 consists of 2478 base pairs encoding 825 amino acid residues with predicted molecular weight of 95.7 kDa. ORF2 contains the five conserved blocks found in many of the three-domain insecticidal Cry1A-type toxins. ORF2

is further characterised by the presence of tandem repeats of QXW/F motif in the conserved ricin domain. The ricin domain contained at the end of ORF2 is comprised of 110 amino acid residues. ORF3 consists of 2214 base pairs encoding 737 amino acid residues with a predicted molecular weight of 82 kDa. ORF3 possesses the conserved blocks 6, 7 and 8 of the larger Cry toxins (Figure 4.1).

Cry41Ab possess a similar gene organisation to Cry41Aa. ORF1 of Cry41Ab consists of 543 base pairs encoding for 180 amino acid residues depicting a high degree of percentage identity of 87.2% with ORF1 of Cry41Aa. ORF2 of Cry41Ab possesses 820 residues encoded by 2490 base pairs, showing a high degree of percentage identity of 82.7% with Cry41Aa ORF2. 735 residues of Cry41Ab ORF3 as well as 737 residues of Cry41Aa ORF3 shared a greater degree of percentage identity of 99.3% with the three conserved boxes 6, 7 and block 8 of insecticidal Cry1Ac.

Conserved domain analysis in the protein sequences of ORF2 Cry41Aa and Cry41Ab by Conserved Domain (CD) search, NCBI (Marchler-Bauer & Bryant, 2004; Marchler-Bauer et al., 2009; Marchler-Bauer et al., 2011) identified the presence of ricin-like lectin domains [cd00161; pfam 00652] in their carboxy termini, referred to as ricin domain (RD) in this and subsequent chapters. The amino acid sequence of Cry41Aa and Cry41Ab contained multiple short consensus of “Gly -X-X-X-Gln -X- Trp/Phe ” possessing the signature Q-X-W/F motifs (underlined in Figure 4.2) which form the defining characteristics of a member of the “Ricin Superfamily” (Hirabayashi et al., 1998). No function of this domain has yet been established in parasporins.

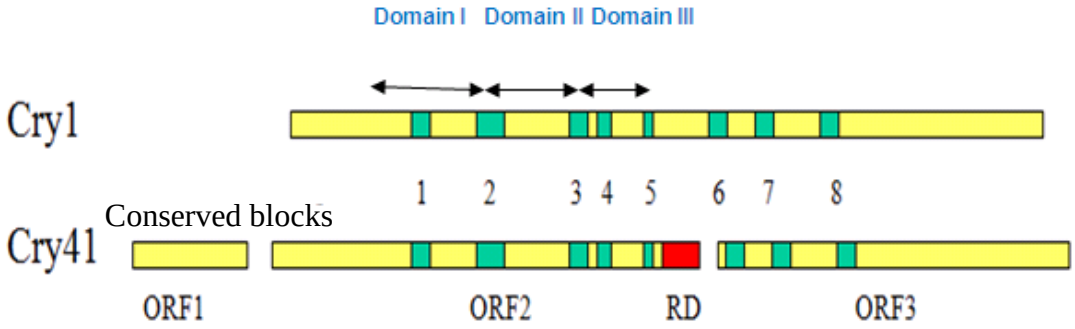

Figure 4.1. Diagrammatic representation of the domains of Cry41A (parasporin-3) and insecticidal Cry1. RD (red box) denotes the ricin-like domain at the end of ORF2 which most closely resembles that from HA-33 from *Clostridium botulinum.*

```
Cry41Aa(PS3)          MNQNCNNNGYEVLNSGKGYCQPRYPFAQAPGSELQNMGYKEWMNMCTSGDPTVLGEGYSA 60
Cry1Ac                MDNNPNINECIPYN------------------------------CLSNPEVEVLGGERIE 30
                      *::* * *     *                                  :. :  ***

Cry41Aa(PS3)          DVRDAVITSINIASYLLSVPFPPAGVAAGILGALLGLLWPTNTQAVWEAFMNTVEALINQ 120
Cry1Ac                TGYTPIDISLSLTQFLLSEFVPGAGFVLGLVDIIWGIFGPS----QWDAFLVQIEQLINQ 86
                             α1                  α2a                    α2b
                      .:  *:.::.:***  .* **.. *::. : *:: *:     *:**:  :* ****

Cry41Aa(PS3)          KLDEYARSKAISELNGLKNVLELYQDAADDWNENPGDLRNKNRVLTEFRNVNGHFENSMP 180
Cry1Ac                RIEEFARNQAISRLEGLSNLYQIYAESFREWEADPTNPALREEMRIQFNDMNSALTTAIP 146
                                 α3                        α4
                      :::*:**.:***.*:**.*: ::* ::  :*: :* :   ::.:  :*.::*. : .::*

                                BLOCK1
Cry41Aa(PS3)          SFAVRNFEVNLLPVYAEAANLHLLLLRDAVKFGEGWGMSTDPGAERDDMYRRLRSRTEIY 240
Cry1Ac                LFAVQNYQVPLLSVYVQAANLHLSVLRDVSVFGQRWGFDAATINSR---YNDLTRLIGNY 203
                              α5                              α6
                       ***:*::* **.**.:****** :***.  **: **:.: .  .*   *. *      *

Cry41Aa(PS3)          TDHCVNTYNQGLQQAKSLQANVSDYSRYPWTQYNQSGGFSYREAKGEYRGTENWNLYNAF 300
Cry1Ac                TDYAVRWYNTGLERVWGPDS------------------------------RDWVRYNQF 232
                                                                          α7
                      **:.*. ** **::. . ::                                .:*  ** *
                               BLOCK2
Cry41Aa(PS3)          RRDMTILVLDIIAQFPTYDPGLYSRPVKSELTREVYTDIRGTTWRSDANLNTIDAIENRM 360
Cry1Ac                RRELTLTVLDIVALFPNYDSRRYPIRTVSQLTREIYTNPVLENFDGSFRG-SAQGIERSI 291
                                        β1a     β1b   α8a           α8
                      **::*: ****:* **.**.  *.  . *:****:**:    .: .. .  : :.**. :

Cry41Aa(PS3)          VGSRQLQLFTWLTEMKFYIRNTGSITSYTHGDLMVGLEKKIRKTNDNDQWLPLEGQNTSY 420
Cry1Ac                RSPHLMDILNSITIYTDAHRGYYYWSGHQIMASPVGFSGPEFTFPLYGTMGNAAPQQRIV 351
                            β2        β3r     β3           β4               β5
                       ..: :::::. :*  .   *.    :.:      **:.    .    .       *:

Cry41Aa(PS3)          TRIDRPGIELGKNYWYYARTQQWFETRLLQLWANTDVLSLNAGTVGNEFWVRDVPDYRNI 480
Cry1Ac                AQLGQGVYRTLSSTLYRRPFNIGINNQQLSVLDGTEFAYGTSSNLPSAVYRKSGTVDSLD 411
                            β6                β7r     β7         β8      β9
                      :::.:   .  ..  *    :  ::.: *.:  .*:.   .:..: . .: :. .
                                                                BLOCK3
Cry41Aa(PS3)          YARSTRNHFIENHRLSWIKFEPVRDNCPFAWPGYKQLSALLFGWTHNSVDLNNIISQYRI 540
Cry1Ac                EIPPQNNNVPPRQGFSHRLSHVSMFRSGFSNSSVSIIRAPMFSWIHRSAEFNNIIASDSI 471
```

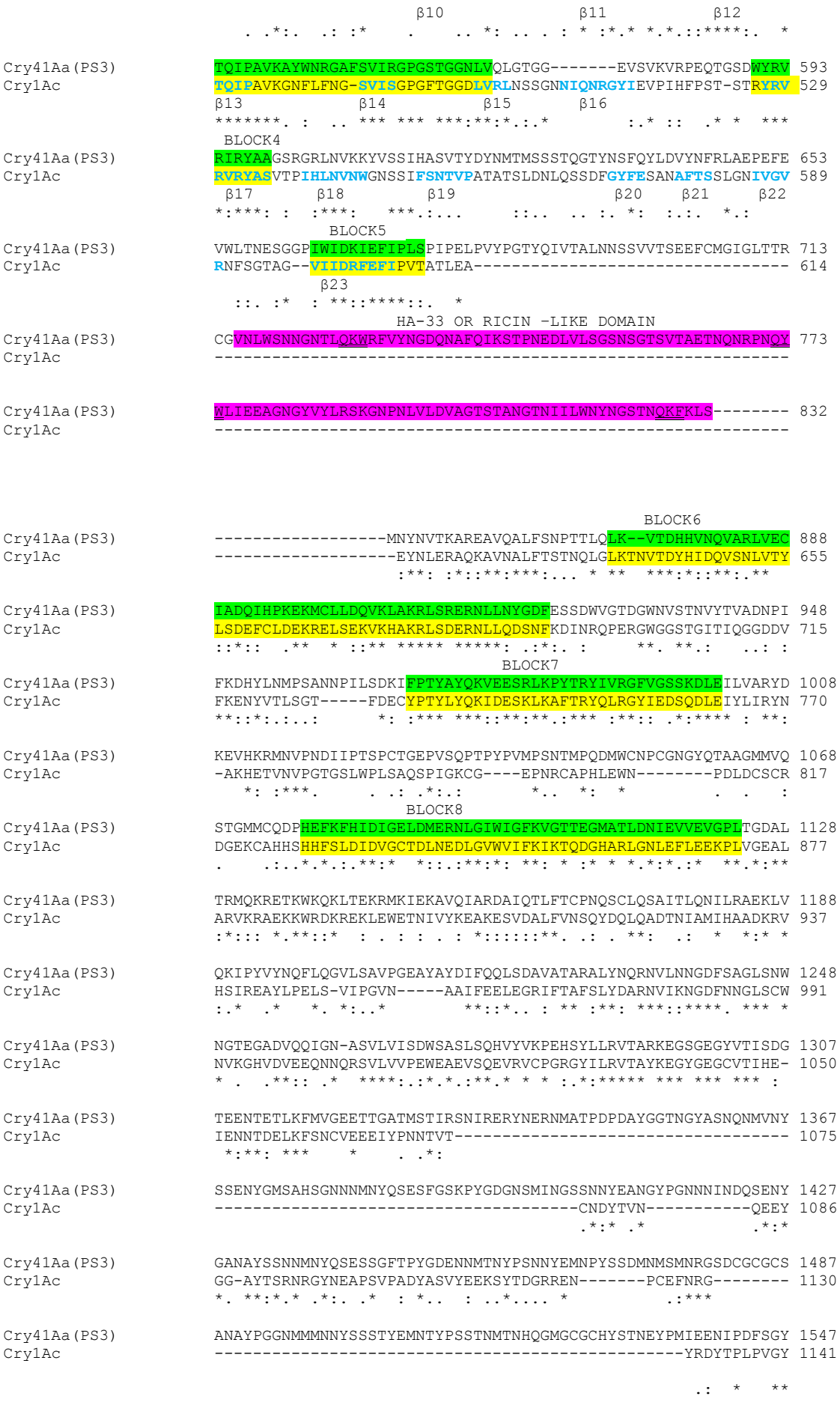
β10 β11 β12
Cry41Aa(PS3) TQIPAVKAYWNRGAFSVIRGPGSTGGNLVQLGTGG-------EVSVKVRPEQTGSDWYRV 593
Cry1Ac TQIPAVKGNFLFNG-SVISGPGFTGGDLVRLNSSGNNIQNRGYIEVPIHFPST-STRYRV 529
β13 β14 β15 β16
BLOCK4
Cry41Aa(PS3) RIRYAAGSRGRLNVKKYVSSIHASVTYDYNMTMSSSTQGTYNSFQYLDVYNFRLAEPEFE 653
Cry1Ac RVRYASVTPIHLNVNWGNSSIFSNTVPATATSLDNLQSSDFGYFESANAFTSSLGNIVGV 589
β17 β18 β19 β20 β21 β22
BLOCK5
Cry41Aa(PS3) VWLTNESGGPIWIDKIEFIPLSPIPELPVYPGTYQIVTALNNSSVVTSEEFCMGIGLTTR 713
Cry1Ac RNFSGTAG--VIIDRFEFIPVTATLEA---------- 614
β23
HA-33 OR RICIN -LIKE DOMAIN
Cry41Aa(PS3) CGVNLWSNNGNTLQKWRFVYNGDQNAFQIKSTPNEDLVLSGSNSGTSVTAETNQNRPNQY 773
Cry1Ac ----------
Cry41Aa(PS3) WLIEEAGNGYVYLRSKGNPNLVLDVAGTSTANGTNIILWNYNGSTNQKFKLS-------- 832
Cry1Ac ----------
BLOCK6
Cry41Aa(PS3) ----------MNYNVTKAREAVQALFSNPTTLQLK--VTDHHVNQVARLVEC 888
Cry1Ac ----------EYNLERAQKAVNALFTSTNQLGLKTNVTDYHIDQVSNLVTY 655
Cry41Aa(PS3) IADQIHPKEKMCLLDQVKLAKRLSRERNLLNYGDFESSDWVGTDGWNVSTNVYTVADNPI 948
Cry1Ac LSDEFCLDEKRELSEKVKHAKRLSDERNLLQDSNFKDINRQPERGWGGSTGITIQGGDDV 715
BLOCK7
Cry41Aa(PS3) FKDHYLNMPSANNPILSDKIFPTYAYQKVEESRLKPYTRYIVRGFVGSSKDLEILVARYD 1008
Cry1Ac FKENYVTLSGT-----FDECYPTYLYQKIDESKLKAFTRYQLRGYIEDSQDLEIYLIRYN 770
Cry41Aa(PS3) KEVHKRMNVPNDIIPTSPCTGEPVSQPTPYPVMPSNTMPQDMWCNPCGNGYQTAAGMMVQ 1068
Cry1Ac -AKHETVNVPGTGSLWPLSAQSPIGKCG----EPNRCAPHLEWN--------PDLDCSCR 817
BLOCK8
Cry41Aa(PS3) STGMMCQDPHEFKFHIDIGELDMERNLGIWIGFKVGTTEGMATLDNIEVVEVGPLTGDAL 1128
Cry1Ac DGEKCAHHSHHFSLDIDVGCTDLNEDLGVWVIFKIKTQDGHARLGNLEFLEEKPLVGEAL 877
Cry41Aa(PS3) TRMQKRETKWKQKLTEKRMKIEKAVQIARDAIQTLFTCPNQSCLQSAITLQNILRAEKLV 1188
Cry1Ac ARVKRAEKKWRDKREKLEWETNIVYKEAKESVDALFVNSQYDQLQADTNIAMIHAADKRV 937
Cry41Aa(PS3) QKIPYVYNQFLQGVLSAVPGEAYAYDIFQQLSDAVATARALYNQRNVLNNGDFSAGLSNW 1248
Cry1Ac HSIREAYLPELS-VIPGVN-----AAIFEELEGRIFTAFSLYDARNVIKNGDFNNGLSCW 991
Cry41Aa(PS3) NGTEGADVQQIGN-ASVLVISDWSASLSQHVYVKPEHSYLLRVTARKEGSGEGYVTISDG 1307
Cry1Ac NVKGHVDVEEQNNQRSVLVVPEWEAEVSQEVRVCPGRGYILRVTAYKEGYGEGCVTIHE- 1050
Cry41Aa(PS3) TEENTETLKFMVGEETTGATMSTIRSNIRERYNERNMATPDPDAYGGTNGYASNQNMVNY 1367
Cry1Ac IENNTDELKFSNCVEEEIYPNNTVT---------- 1075
Cry41Aa(PS3) SSENYGMSAHSGNNNMNYQSESFGSKPYGDGNSMINGSSNNYEANGYPGNNNINDQSENY 1427
Cry1Ac ----------CNDYTVN----------QEEY 1086
Cry41Aa(PS3) GANAYSSNNMNYQSESSGFTPYGDENNMTNYPSNNYEMNPYSSDMNMSMNRGSDCGCGCS 1487
Cry1Ac GG-AYTSRNRGYNEAPSVPADYASVYEEKSYTDGRREN-------PCEFNRG-------- 1130
Cry41Aa(PS3) ANAYPGGNMMMNNYSSSTYEMNTYPSSTNMTNHQGMGCGCHYSTNEYPMIEENIPDFSGY 1547
Cry1Ac ----------YRDYTPLPVGY 1141

```
Cry41Aa(PS3)          VTKTVEIFPETNRVCIEIGETAGTFMVESIELIRMDCE 1585
Cry1Ac                VTKELEYFPETDKVWIEIGETEGTFIVDSVELLLMEE- 1178

                      *** :* ****::* *****  ***:*:*:**: *:
```

Figure 4.2. ClustalW multiple sequence alignments of parasporin Cry41Aa and insecticidal Cry1Ac. Conserved blocks of Cry41Aa are highlighted in green and those of Cry1Ac are highlighted in yellow. The ricin domain (RD) of Cry41Aa is highlighted in pink. The signature Q-X-W/F motifs in the RD are underlined. Amino acid residues of Cry1Ac in bold red letters represent the α-helices of domain I (α1-7) and domain II (α8a and 8) and those in light blue letters represent the β-strands of domain II (β1a-β11) and domain III (β12-23). These secondary elements are mentioned under the alignment. In order to predict the secondary structure elements, Cry1Ac was aligned with homologous Cry1Aa whose three-dimensional structure has been resolved by x-ray crystallography (Appendix 1).

The prediction of secondary structure was facilitated using Jpred server (http://www.compbio.dundee.ac.uk/www-jpred/) in conjunction with the alignment program, Clustal W (Figure 4.3). Clustal W, revealed a few differences between the parasporin-3 and insecticidal Cry1Ac (Figure 4.3), the notable ones being the ricin domain, a 31 amino acid long region forming a loop like configuration preceding the predicted α-7 helix in Domain II from residues 261-291 in Cry41Aa and the differences at the C-terminus. Domain II loops have been well characterised in various Cry toxins including Cry3A, Cry1C and Cry1Ab (Figure 4.4). Three apical loops in Domain II of insecticidal Cry1 toxins have been implicated in receptor binding thus affecting toxicity. These three loops involved in receptor binding in insecticidal Cry vary considerably in length, sequence and confirmation (Schnepf et al., 1998; Pigott & Ellar, 2007). The predicted tertiary structures of Cry41Aa and Cry1Ac were compared using Swiss Model, a protein homology-modelling server (Guex & Peitsch, 1997; Schwede et al., 2003; Arnold

et al., 2006). The PDB file for Cry41Aa was compiled by the Swiss Model program based on the known structure of Cry1Aa (PDB code: 1ciy). Residues between 61 and 675 were modelled. The PDB file for Cry1Ac was also generated based upon the known structure of Cry1Aa (PDB code: 1ciy). Modelled residues were in the 34-611 range (Figure 4.5 and 4.6). The predicted three-dimensional structures of Cry1Ac and Cry41Aa were also visualised using FirstGlance in Jmol by uploading the PDB co-ordinate files generated by Swiss Model. No apparent equivalent of residues 261-291 in Cry41Aa is present in Cry1Ac. Note that the 31 residue insert cannot be accurately predicted by Swiss Model.

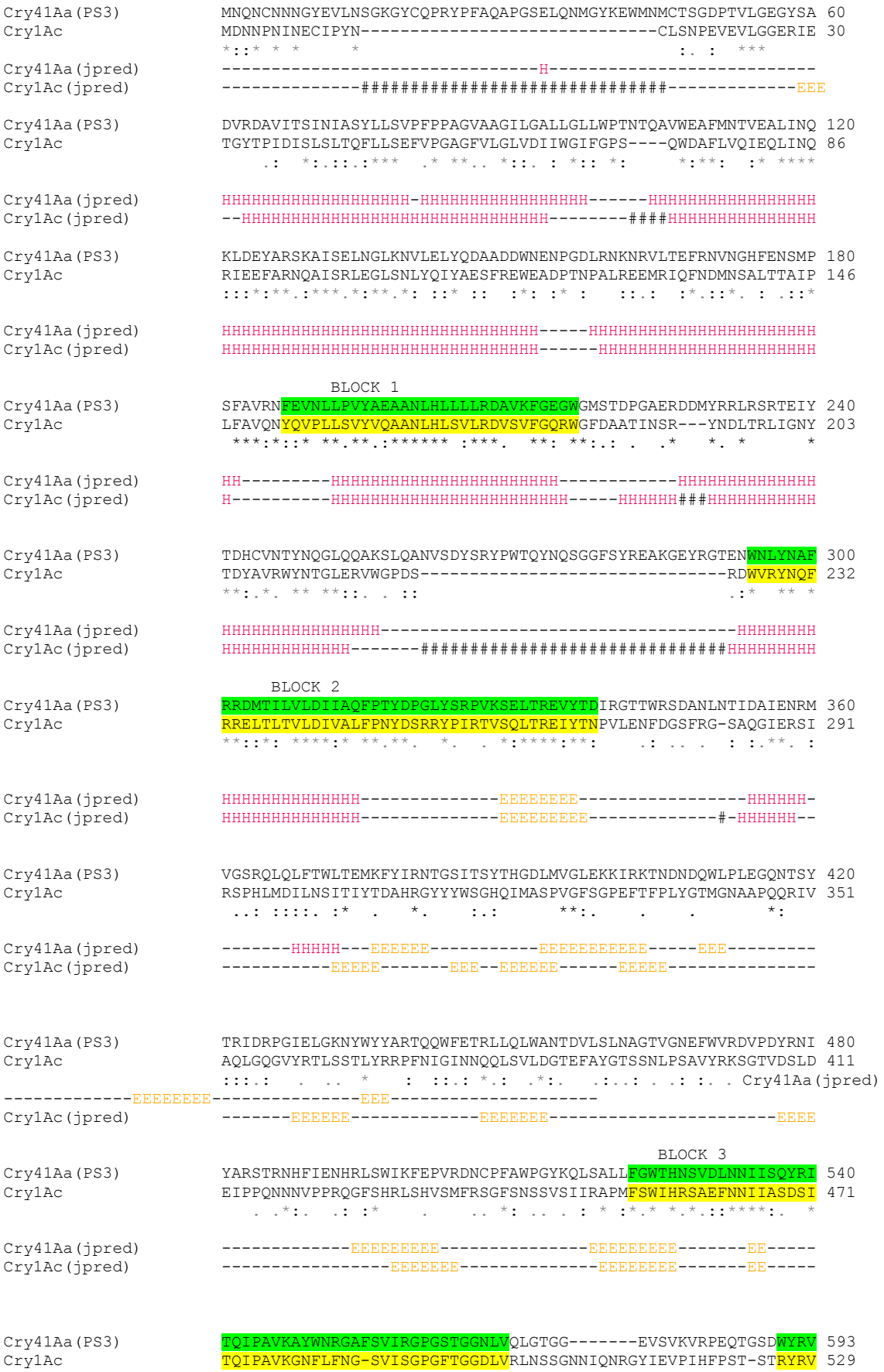
Cry41Aa(PS3) MNQNCNNNGYEVLNSGKGYCQPRYPFAQAPGSELQNMGYKEWMNMCTSGDPTVLGEGYSA 60
Cry1Ac MDNNPNINECIPYN----------CLSNPEVEVLGGERIE 30
Cry41Aa(jpred) ----------H----------
Cry1Ac(jpred) ----------##########----------EEE
Cry41Aa(PS3) DVRDAVITSINIASYLLSVPFPPAGVAAGILGALLGLLWPTNTQAVWEAFMNTVEALINQ 120
Cry1Ac TGYTPIDISLSLTQFLLSEFVPGAGFVLGLVDIIWGIFGPS----QWDAFLVQIEQLINQ 86
Cry41Aa(jpred) HHHHHHHHHHHHHHHHHH-HHHHHHHHHHHHHHHH------HHHHHHHHHHHHHHHH
Cry1Ac(jpred) --HHHHHHHHHHHHHHHHHHHHHHHHHHHHHH--------####HHHHHHHHHHHHHH
Cry41Aa(PS3) KLDEYARSKAISELNGLKNVLELYQDAADDWNENPGDLRNKNRVLTEFRNVNGHFENSMP 180
Cry1Ac RIEEFARNQAISRLEGLSNLYQIYAESFREWEADPTNPALREEMRIQFNDMNSALTTAIP 146
Cry41Aa(jpred) HHHHHHHHHHHHHHHHHHHHHHHHHHHHHH-----HHHHHHHHHHHHHHHHHHHH
Cry1Ac(jpred) HHHHHHHHHHHHHHHHHHHHHHHHHHHHHH------HHHHHHHHHHHHHHHHHHHH
BLOCK 1
Cry41Aa(PS3) SFAVRNFEVNLLPVYAEAANLHLLLLRDAVKFGEGWGMSTDPGAERDDMYRRLRSRTEIY 240
Cry1Ac LFAVQNYQVPLLSVYVQAANLHLSVLRDVSVFGQRWGFDAATINSR---YNDLTRLIGNY 203
Cry41Aa(jpred) HH---------HHHHHHHHHHHHHHHHHHHHHH------------HHHHHHHHHHHHHH
Cry1Ac(jpred) H----------HHHHHHHHHHHHHHHHHHHHHHH-----HHHHHH###HHHHHHHHHHH
Cry41Aa(PS3) TDHCVNTYNQGLQQAKSLQANVSDYSRYPWTQYNQSGGFSYREAKGEYRGTENWNLYNAF 300
Cry1Ac TDYAVRWYNTGLERVWGPDS----------RDWVRYNQF 232
Cry41Aa(jpred) HHHHHHHHHHHHHHHH----------HHHHHHHH
Cry1Ac(jpred) HHHHHHHHHHHHH-------##########HHHHHHHHH
BLOCK 2
Cry41Aa(PS3) RRDMTILVLDIIAQFPTYDPGLYSRPVKSELTREVYTDIRGTTWRSDANLNTIDAIENRM 360
Cry1Ac RRELTLTVLDIVALFPNYDSRRYPIRTVSQLTREIYTNPVLENFDGSFRG-SAQGIERSI 291
Cry41Aa(jpred) HHHHHHHHHHHHHH----------EEEEEEEE----------HHHHHH-
Cry1Ac(jpred) HHHHHHHHHHHHHH----------EEEEEEEEE----------#-HHHHHH--
Cry41Aa(PS3) VGSRQLQLFTWLTEMKFYIRNTGSITSYTHGDLMVGLEKKIRKTNDNDQWLPLEGQNTSY 420
Cry1Ac RSPHLMDILNSITIYTDAHRGYYYWSGHQIMASPVGFSGPEFTFPLYGTMGNAAPQQRIV 351
Cry41Aa(jpred) -------HHHHH---EEEEEE----------EEEEEEEEEEE-----EEE---------
Cry1Ac(jpred) ----------EEEEE-------EEE--EEEEEE------EEEEE---------- Cry41Aa(jpred)
----------EEEEEEEE----------EEE---------- Cry1Ac(jpred)
Cry41Aa(PS3) TRIDRPGIELGKNYWYYARTQQWFETRLLQLWANTDVLSLNAGTVGNEFWVRDVPDYRNI 480
Cry1Ac AQLGQGVYRTLSSTLYRRPFNIGINNQQLSVLDGTEFAYGTSSNLPSAVYRKSGTVDSLD 411
Cry41Aa(jpred) -------EEEEEE----------EEEEEEE----------EEEE
BLOCK 3
Cry41Aa(PS3) YARSTRNHFIENHRLSWIKFEPVRDNCPFAWPGYKQLSALLFGWTHNSVDLNNIISQYRI 540
Cry1Ac EIPPQNNNVPPRQGFSHRLSHVSMFRSGFSNSSVSIIRAPMFSWIHRSAEFNNIIASDSI 471
Cry41Aa(jpred) ----------EEEEEEEE----------EEEEEEEE-------EE-----
Cry1Ac(jpred) ----------EEEEEEE----------EEEEEEE-------EE-----
Cry41Aa(PS3) TQIPAVKAYWNRGAFSVIRGPGSTGGNLVQLGTGG-------EVSVKVRPEQTGSDWYRV 593
Cry1Ac TQIPAVKGNFLFNG-SVISGPGFTGGDLVRLNSSGNNIQNRGYIEVPIHFPST-STRYRV 529

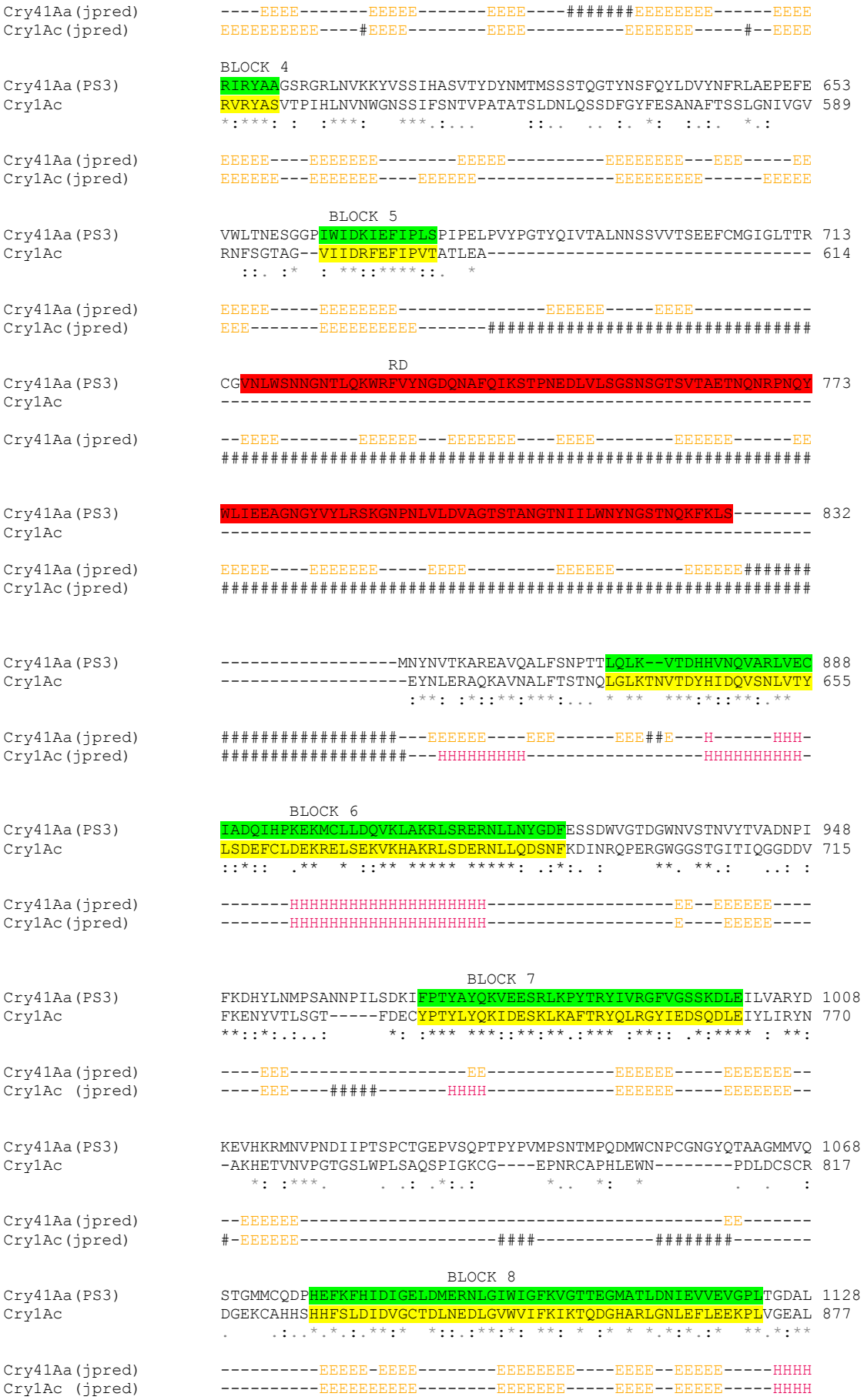
Cry41Aa(jpred)
Cry1Ac(jpred)
BLOCK 4
Cry41Aa(PS3)
Cry1Ac
BLOCK 5
RD
BLOCK 6
BLOCK 7
BLOCK 8

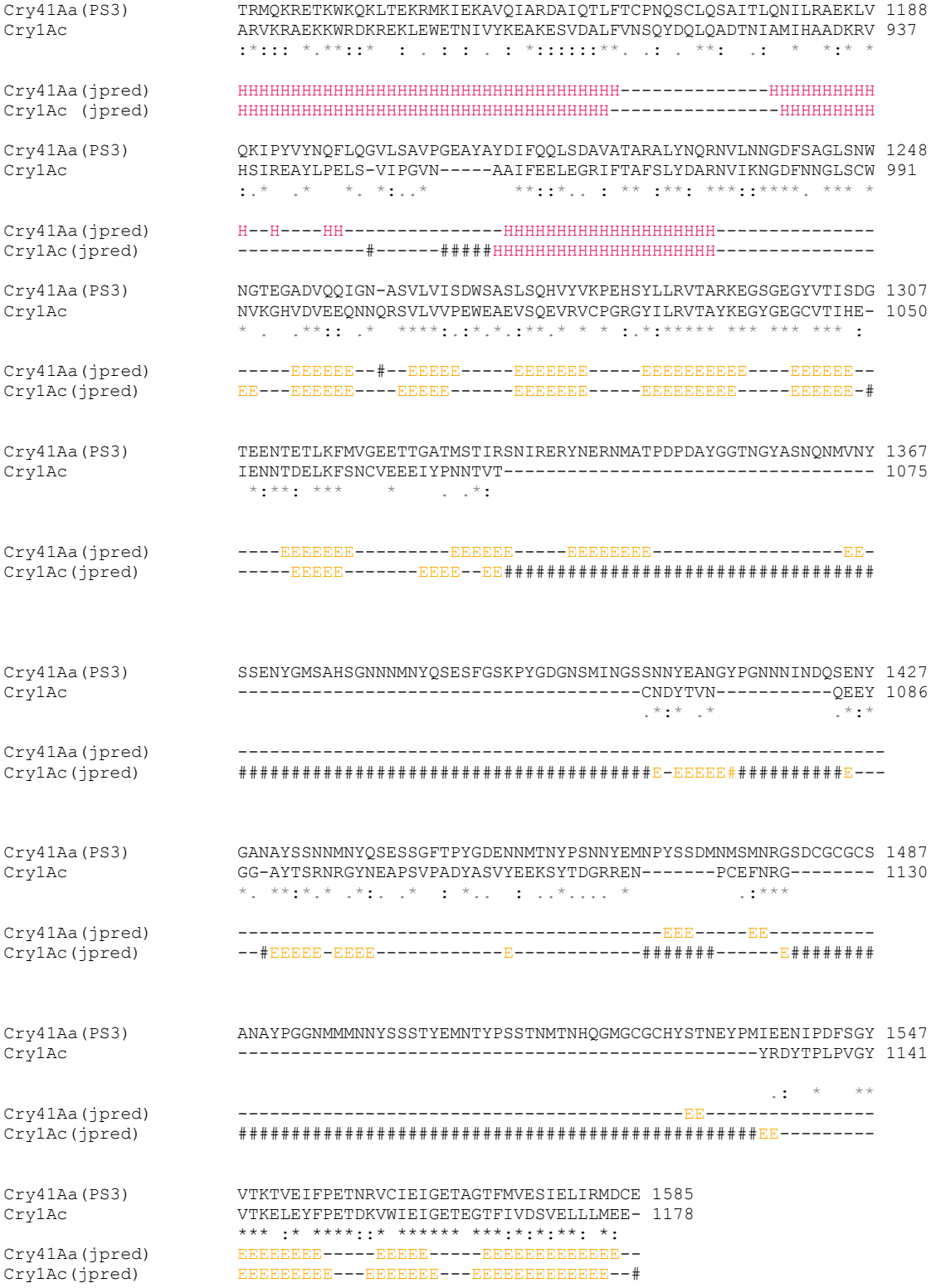

Figure 4.3. Clustal W alignments of Cry41Aa and Cry1Ac with superimposed Jpred secondary structure predictions. H represents helix. E represents sheet. – represents coil. # indicates lack of amino acid residue at a particular position upon alignment. The conserved blocks of Cry1Ac and Cry41Aa are highlighted in yellow and green respectively. Ricin domain of Cry41Aa is highlighted in red.

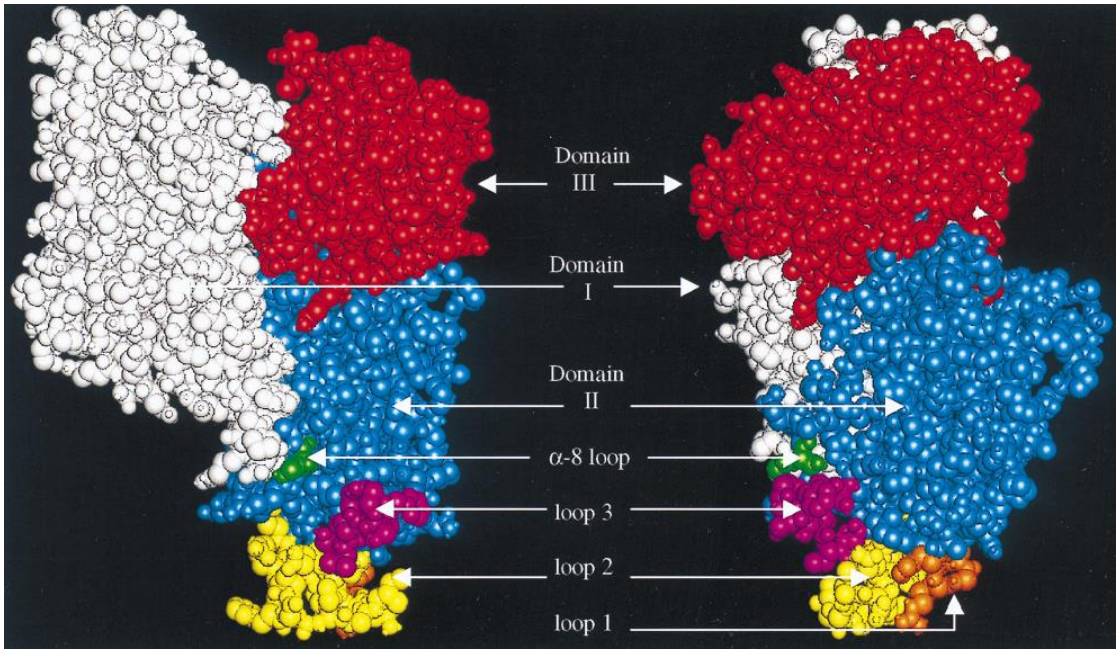

Figure 4.4. Predicted three-dimensional structure of Cry1Ab. The three domains: I (white), II (blue), III (red) and portions of domain II loops 1,2 ,3 and α-8 loops in standard (left) and rotated formats (right) are shown (Schnepf et al., 1998).

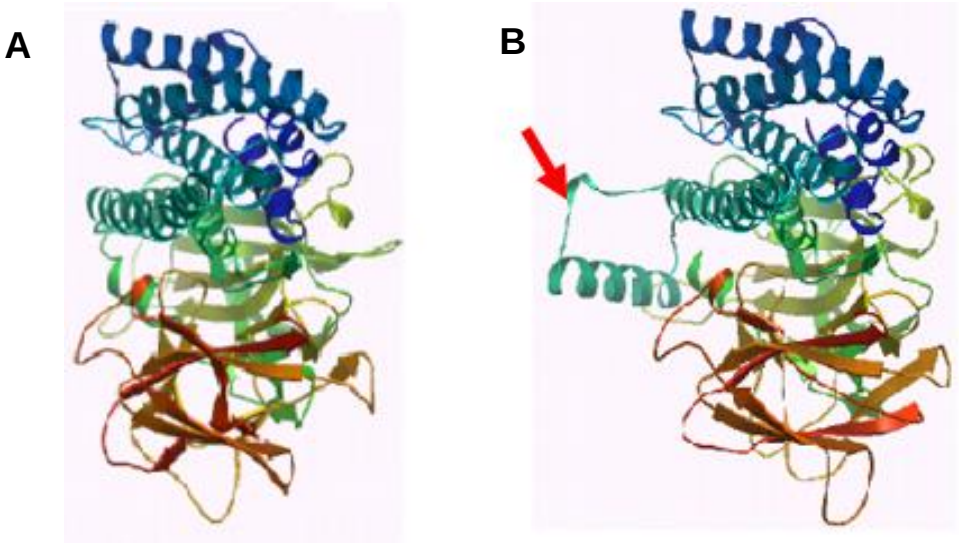

Figure 4.5. Swiss-model output of Cry1Ac (A) and Cry41Aa (B) predicted structures shown in a ribbon model. 261-291 residues of Cry41Aa form a loop-like configuration (indicated by red arrow), with no apparent equivalence in insecticidal Cry1Ac. Note this is just a representation as the 31 amino acid insert of Cry41Aa cannot be predicted accurately.

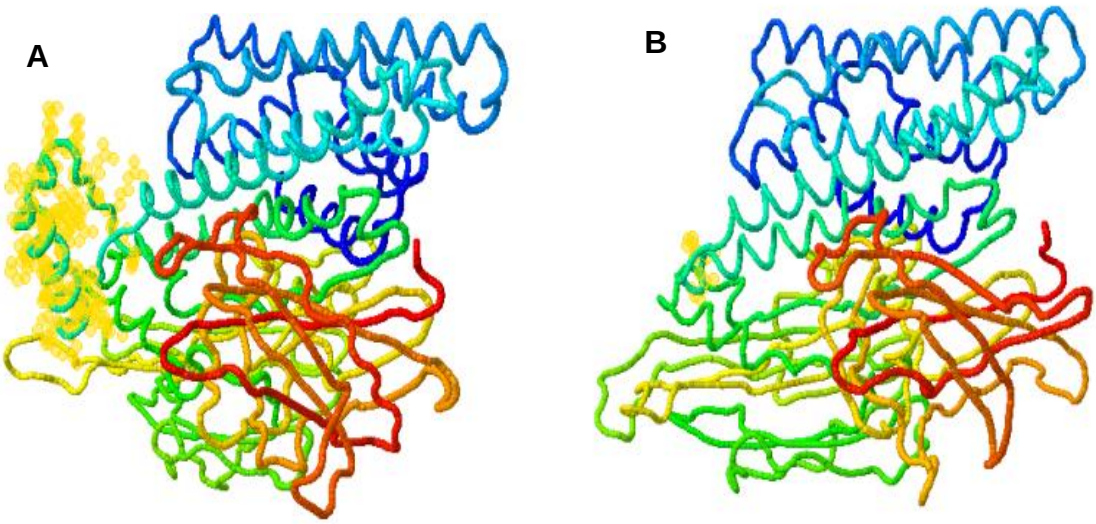

Figure 4.6.Three-dimensional predicted structures of Cry41Aa (A) and Cry1Ac (B) generated using FirstGlance in Jmol. Residues from 261-291 are marked by yellow dot- halos in case of Cry41Aa. The equivalent region (223-224) obtained by ClustalW alignment in Cry1Ac is also depicted by yellow halos.

We intended to identify the source of cytotoxicity induced by Cry41Aa and Cry41Ab parasporin inclusion proteins derived from the Bt isolate A1462. We aimed to study the roles played by various ORFs in crystal formation and toxin production, the toxicity of the domains on common agricultural pests as well as on human cancer cell lines and attempt the identification of the individual factors responsible for inducing *in vitro* cytotoxicity towards cultured mammalian cells.

This chapter describes how we attempted to develop a system for the heterologous expression of the parasporin-3 toxins from *B. thuringiensis* A1462 in *E. coli*. This system enabled us to generate mutants through deletions, domain swaps and fusion constructs. We further aimed at investigating the roles of the three open reading frames in crystal formation and expression of the parasporin

toxin. The role of parasporin Domain II was examined by creating a hybrid between the parasporin-3 and insecticidal Cry1Ac. Our next objective was to investigate the role of the ricin domain by deleting it from Cry41A thus generating the mutant Cry41AΔRD and also by fusing the RD domain to the *B. thuringiensis* insecticidal Cry1Ac toxin thus generating the recombinant Cry1AcIg. We further aimed at investigating the role of the loop-like region (residues between 261and 291) in imparting cytotoxicity to Cry41Aa by deletion. These constructs are depicted in Figure 4.7.

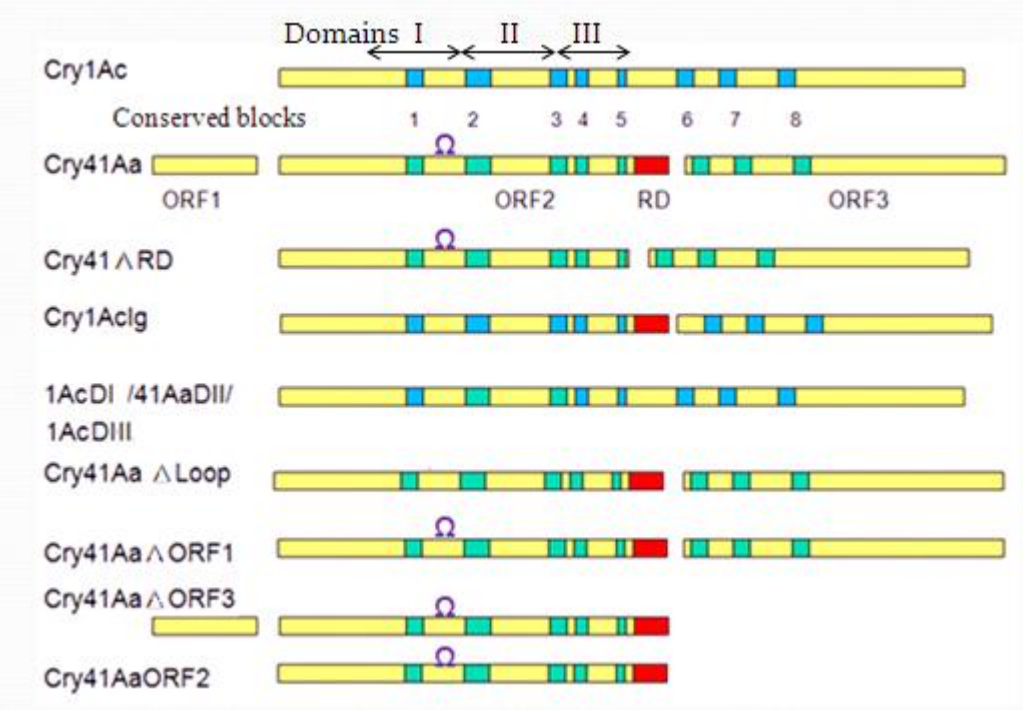

Figure 4.7. Diagrammatic representation of some of the deletions and fusion constructs attempted. The conserved blocks of Cry1Ac are indicated by blue boxes and the conserved blocks of Cry41Aa are indicated by green boxes. The red boxes indicate the ricin domain. The purple omega represents the protruding loop region.

4.2 Results

4.2.1 Expression of *cry41Aa1* gene in *E. coli* JM109

An attempt was made to express *cry41Aa* gene using its own promoter and ribosome binding site in *E. coli* strain JM109. The *cry41Aa1* gene region containing the three open reading frames was amplified by PCR using genomic DNA from *B. thuringiensis* strain A1462. The forward primer and the reverse primer were deduced from the whole genome sequence of A1462. The upstream regions of ORF1 were searched for the consensus sequences matching core promoter elements of Bt. Although a Shine-Dalgarno ribosome-binding site was found, the -10 and -35 regions of the *cry41A* gene bear no semblance to either the σ^E (-35, KMATATT; -10, CATACA-T) or σ^K (-35, GKMACA; -10, CATANNNT) consensus Bt promoter where K= G or T and M= C or A (Wong et al., 1983; Moran, 1993; Dervyn et al., 1995). Hence, the primers were designed to amplify 405 base pairs upstream of the ATG start codon of ORF1 to include any promoter site upstream of the ORF1 ATG start codon, the ribosome binding site and the terminator sequence downstream of ORF3. The transcriptional terminators were identified using TransTerm program (www.tigr.org now updated to http://www.jcvi.org/) (Ermolaeva et al., 2000). High fidelity Expand long range PCR kit (Roche) was used for generation of PCR products from the genomic DNA with 3'A-overhangs to enable cloning into the pGEM-T vector possessing 3' T-overhangs. Amplification of *cry41Aa* gene was also attempted with High Fidelity *pfu* DNA polymerase-based PCR amplification system from Stratagene. All PCR amplification reactions, whether performed using Taq or Pfu DNA polymerase, yielded a product consistent with the expected size of 6.1 kb. We opted for the PCR products generated by Roche for further studies due to higher yield and also

because it generates PCR amplicons with 3'A-overhangs. PCR amplicons were further purified using Qiagen kit (Section 2.2.3.1) and ligated into pGEM-T (Promega) according to the manufacturer's instructions (Section 2.2.4). The reaction-mix was used to transform competent *E. coli* JM109 cells by electroporation (Section 2.2.5.1). The transformants were selected on LB-agar-ampicillin plates (100 µg/ml) at 37°C. To confirm the successful formation and introduction of the plasmid into JM109 cells, the single colonies obtained were randomly selected from ampicillin containing LB agar plates and were further streaked on to LB-agar-ampicillin plates (100 µg/ml) at 37°C for increased plasmid yield. Small -scale plasmid preparations were carried using QIAprep Spin Miniprep Kit (Qiagen) (Section 2.2.7.1) and extracted plasmids were subjected to restriction analysis (Section 2.2.8) to check for colonies harbouring the desired *cry41Aa* gene operon cloned into pGEM-T vector, designated as pGEMCry41Aa (Figure 4.8). The identity of the plasmid was verified with restriction digestion and sequencing. Sequencing results obtained with the universal T7 sequencing primer confirmed the pGEMCry41Aa cassette to be as desired i.e. having *cry41Aa* gene operon with its own promoter. *E. coli* JM109 cells containing the plasmid pGEMCry41Aa were cultured in 100 ml of LB medium containing ampicillin (100 µg/ml) at 37°C for 72 h. Cells were then harvested as described in Section 2.2.9.1 and total protein extracts were analysed on a 7.5 % SDS-PAGE. A major band of ~88 kDa was observed on the gel (Figure 4.9A). Parasporal proteins thus expressed in *E. coli* strain JM109 resulted in formation of inclusion bodies as observed under phase contrast microscope (data not shown).

Inclusion bodies of recombinant Cry41Aa parasporal proteins expressed in *E. coli* JM109 were solubilised at alkaline pH under reducing milieu in presence of 1 mM DTT. The crystals were solubilised in 50 mM Na_2CO_3 (pH 9.5)/1 mM DTT at 37°C, water bath for 1 h. A major protein band of ~88 kDa was apparent on the gel (Figure 4.9B). Usually, after solubilisation protoxins must undergo proteolytic processing in order to become active toxins (Lecadet & Dedonder, 1967, Tojo & Aizawa, 1983). The crystal proteins were then digested by varied concentrations of proteinase K, trypsin, chymotrypsin and gut extracts from *Plutella xylostella* LAB-UK susceptible populations. The proteins generated by proteolytic processing with proteinase K, trypsin and gut extract from the cabbage pest, *Plutella* had a molecular mass of ~64 kDa (Figure 4.10). Although, unlike in case of the insecticidal Cry toxins wherein protease treatment generates an approximately 60 kDa protease-resistant biologically active core (de Maagd et al., 2001), higher concentrations of chymotrypsin above 2 mg/ml digested the solubilised recombinant Cry41Aa inclusions (Figure 4.10C). Similar results were obtained upon treatment with other proteinases at a high concentration (data not shown).

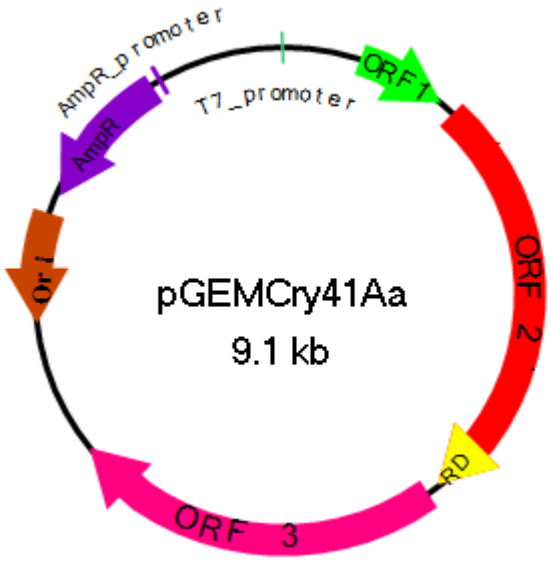

Figure 4.8. Schematic representation of the plasmid pGEMCry41Aa depicting the location of genes of the *cry41Aa* operon.

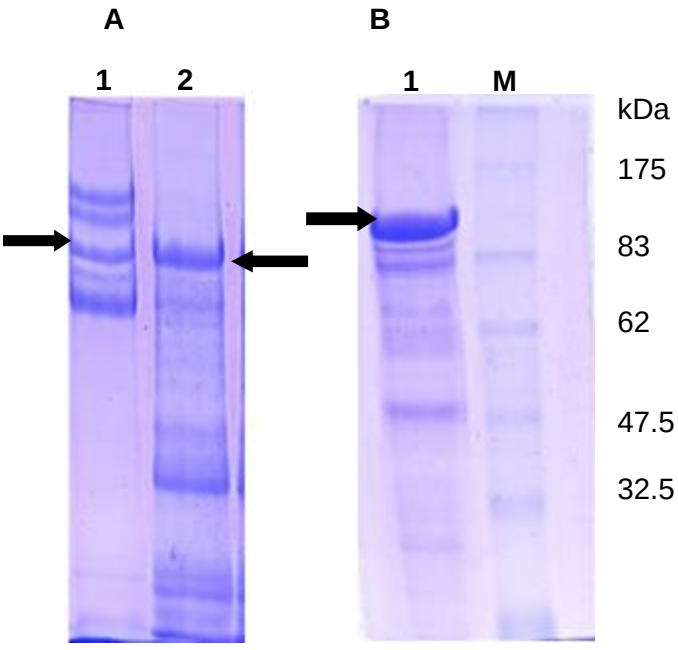

Figure 4.9. 7.5% SDS-PAGE analysis of Cry41A proteins. A. Lane 1, native parasporal inclusion proteins of Bt strain A1462; lane 2, *E. coli* JM109 expressed recombinant Cry41Aa protein inclusions. B. Lane 1, ~88kDa alkali-solubilised *E. coli* expressed recombinant Cry41Aa; lane M; molecular mass marker.

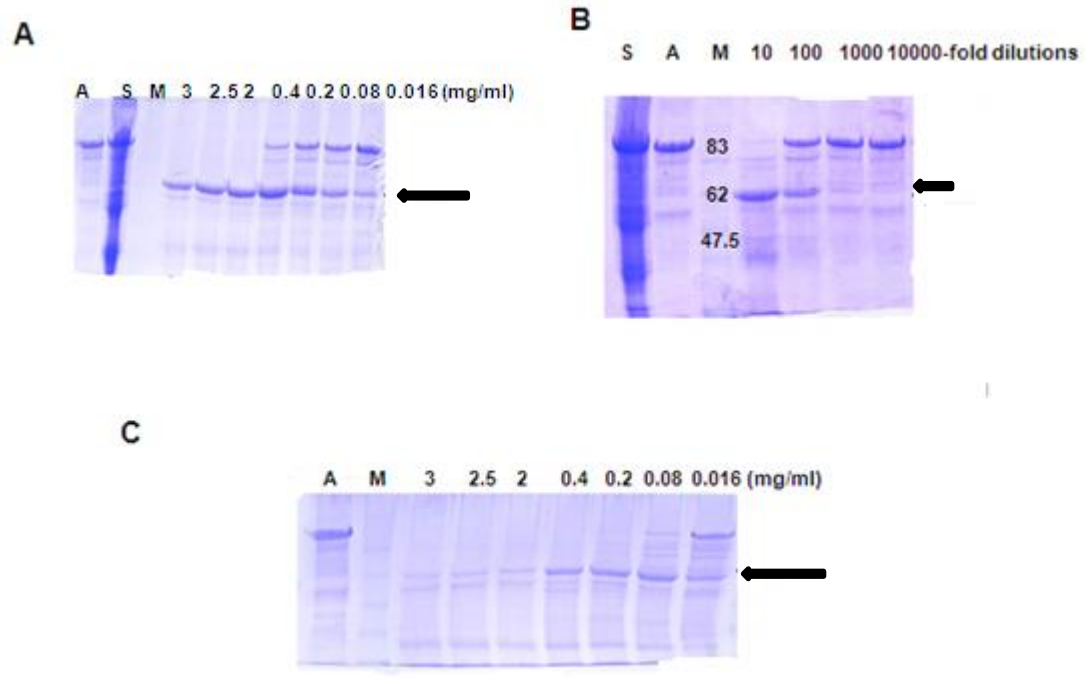

Figure 4.10. SDS-PAGE analysis of the proteolytic processing of the 88 kDa protein expressed in *E. coli.* Varied dilutions of **(A)** trypsin, **(B)** gut extract of *P. xylostella* and **(C)** chymotrypsin were used. The processed toxin fragments are indicated by the arrow. The concentrations of the proteolytic enzymes used are indicated above their respective lanes. Lane A represents alkali solubilised protein inclusions; lane M represents protein marker and lane S is the untreated total sample.

4.2.2 Domain Analysis

4.2.2.1 Investigating the roles of ORF1 and ORF3

To further investigate the involvement of various open reading frames in crystal formation and protein production, these were individually deleted from the operon. The deletions were PCR mediated as depicted schematically in Figures 4.11 and 4.12, by using primers that flanked the deleted regions and PfuUltra Hotstart from Stratagene. pGEMCry41Aa was used as the template DNA. Following amplification, PCR amplicons were self-ligated resulting in the creation of mutants, pGEMCry41ΔORF1 of 8518 base pairs with deleted ORF1 and pGEMCry41ΔORF3 of 6878 base pairs with deleted ORF3.

Deleting ORF1 had no effects either on crystal formation as observed under the phase contrast microscope (data not shown) or protein production. ~88kDa protein band was still detected on the gel and was further obtained in the soluble fraction upon alkaline treatment (Figure 4.13, lane 2). However, the resulting transformants produced smaller crystalline inclusions when *cry41Aa* gene was expressed without ORF3 as seen using the phase contrast microscope (data not shown). Upon ORF3 deletion, a major protein band at approximately 84 kDa was obtained (Figure 4.13, lane 5). However, ORF3 deletion resulted in production of proteins which were not recovered in the soluble fraction upon alkaline treatment (Figure 4.13, lane 6). The samples were further subjected to trypsin treatment as described in Section 2.2.12 and analysed on 7.5% SDS-PAGE. The samples were treated with concentrations of trypsin ranging from 2 mg/ml to 0.08 mg/ml. Trypsin at a final concentration 0.4 mg/ml and 0.08 mg/ml partially digested recombinant Cry41AaΔORF1 protein inclusions yielding a band of ~60 kDa

(Figure 4.13, lanes 3 & 4). No 60 kDa protein band was detected when recombinant Cry41AaΔORF3 inclusions were treated with trypsin (Figure 4.13, lanes 7, 8 & 9).

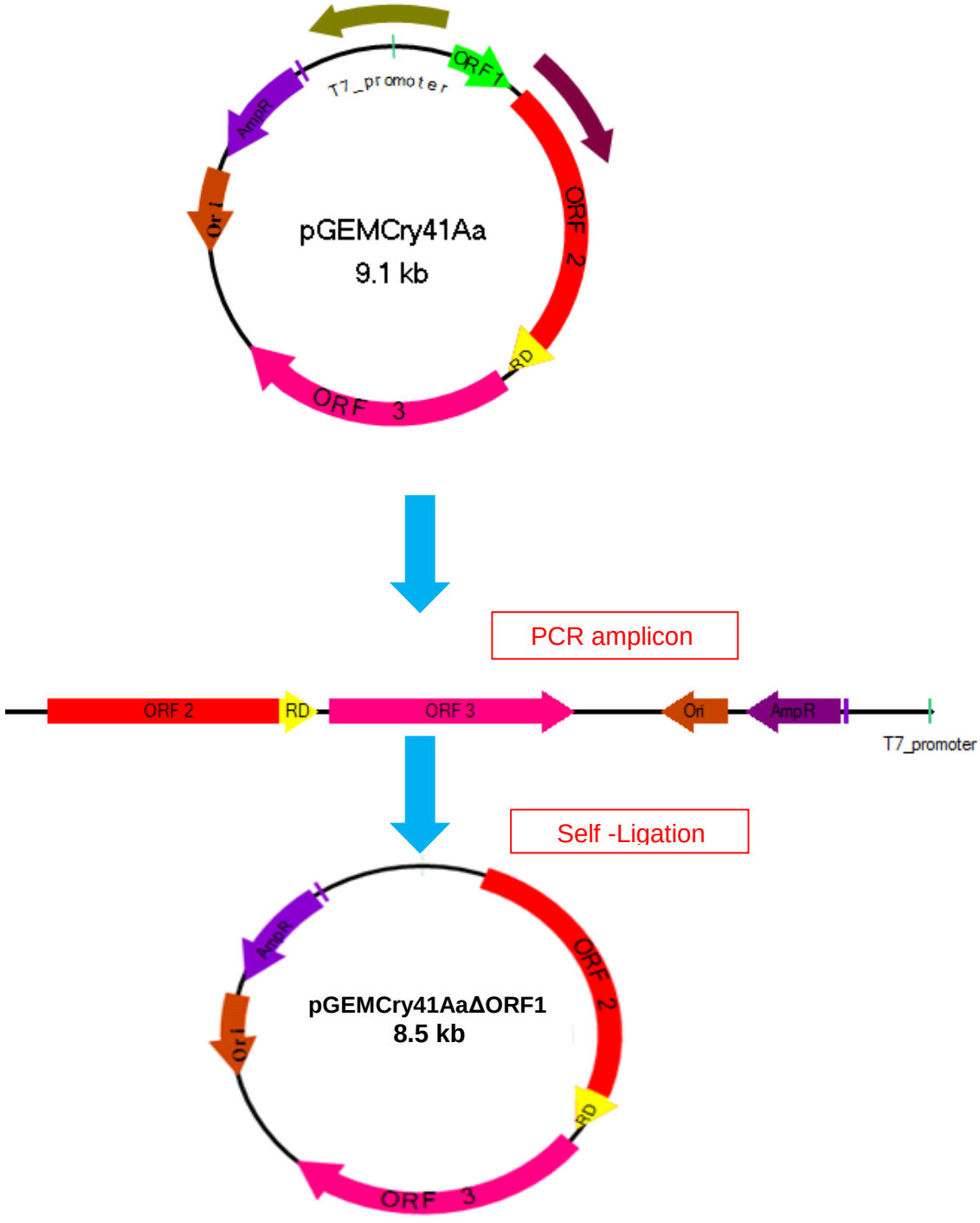

Figure 4.11. Schematic representation of the construct pGEMCry41AaΔORF1.

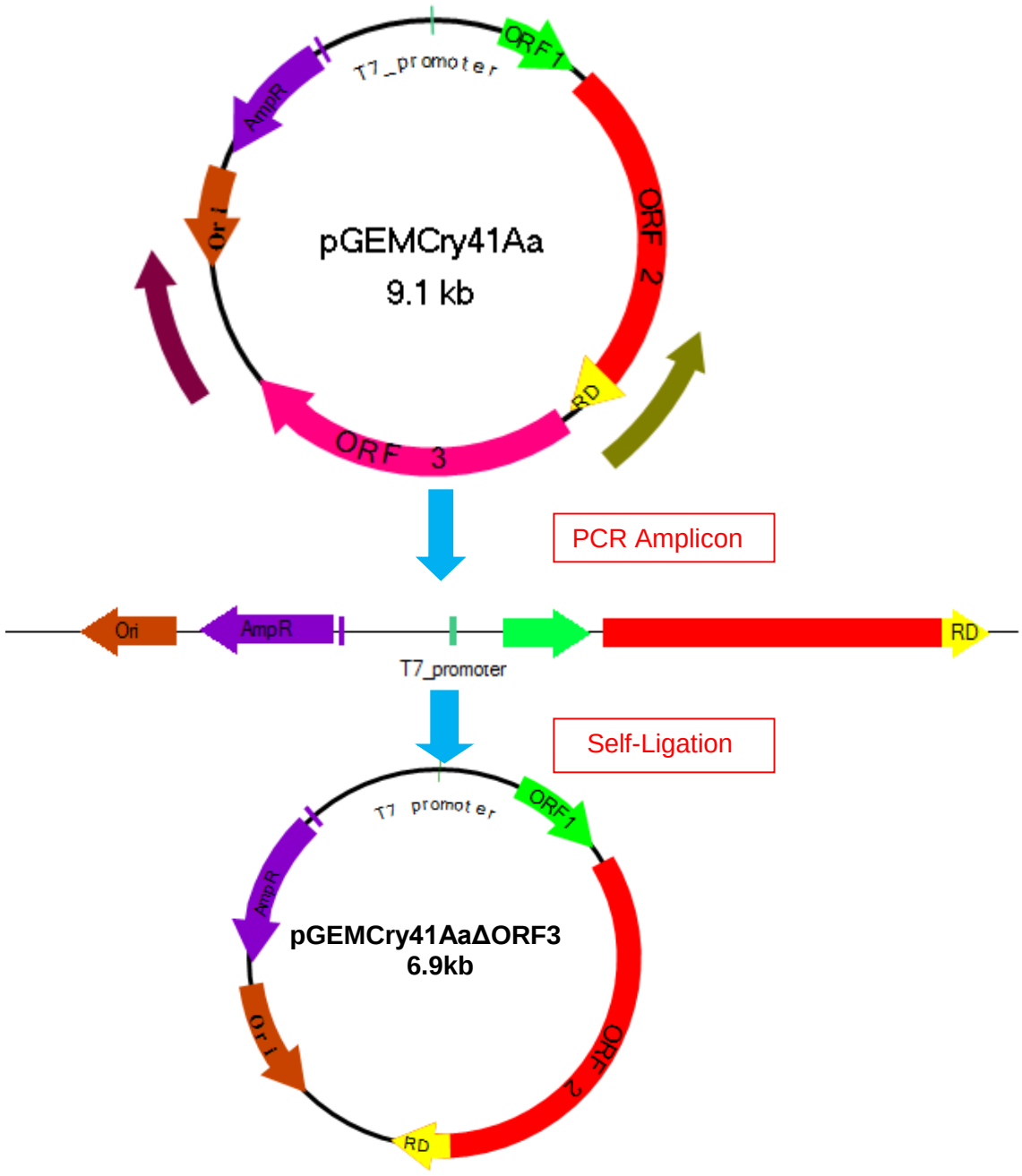

Figure 4.12. Schematic representation of the construct pGEMCry41AaΔORF3.

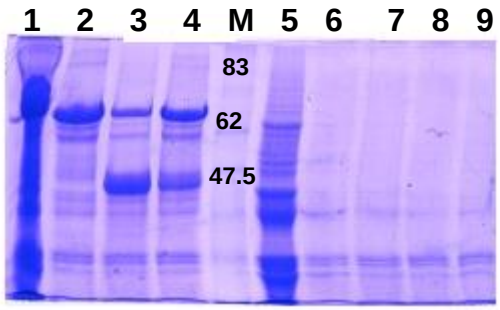

Figure 4.13. 7.5% SDS-PAGE profile depicting the effect of ORF deletions on protein production. Lanes 1-4, analysis of Cry41AaΔORF1 expressed from pGEMCry41AaΔORF1 in *E. coli* JM109 and lanes 5-9, analysis of Cry41AaΔORF3 expressed from pGEMCry41AaΔORF3 in *E. coli* JM109. Lane 1, *E. coli* pGEMCry41AaΔORF1 protein inclusions; lane 2, alkali solubilised *E. coli* expressed Cry41AaΔORF1. Lanes 3 and 4 are trypsin- treated samples. Samples were treated with 0.4 mg/ml (Lane 3) or 0.08 mg/ml (Lane 4). Lane 5, Cry41AaΔORF3 protein inclusions; lane 6, alkali solubilised sample. Lanes 7-9 are trypsin-treated Cry41AaΔORF3. Samples were treated with 2 mg/ml (Lane 7) or 0.4 mg/ml (Lane 8) or 0.08 mg/ml (Lane 9). Lane M is the protein marker in kDa.

4.2.2.2 Functional analysis of the conserved blocks of ORF3

ORF3 of parasporin-3 resembles the C-terminal half of the larger Cry toxins, a region that is believed to be important for the expression and crystallization of *B. thuringiensis* toxins. To identify regions in ORF3 which are imperative for crystal formation and protein production, deletions in ORF3 were planned.

To investigate the role of C-terminal region including block 8, the conserved region was deleted using the reverse primer from the construct pGEMCry41AaΔORF1 as diagrammatically represented in Figure 4.14. Further, in order to verify if the regions after block 8 were dispensable for crystal formation

or protein production, they were deleted as schematically demonstrated in Figure 4.15. Deleting block 8 and C-terminal residues resulted in a PCR amplicon of 6978 base pairs. Deleting residues after block 8 resulted in a PCR product of 7128 base pairs. However, these two deletions in ORF3 resulted in complete abrogation of expression. No protein band was detected on the SDS gel (data not shown).

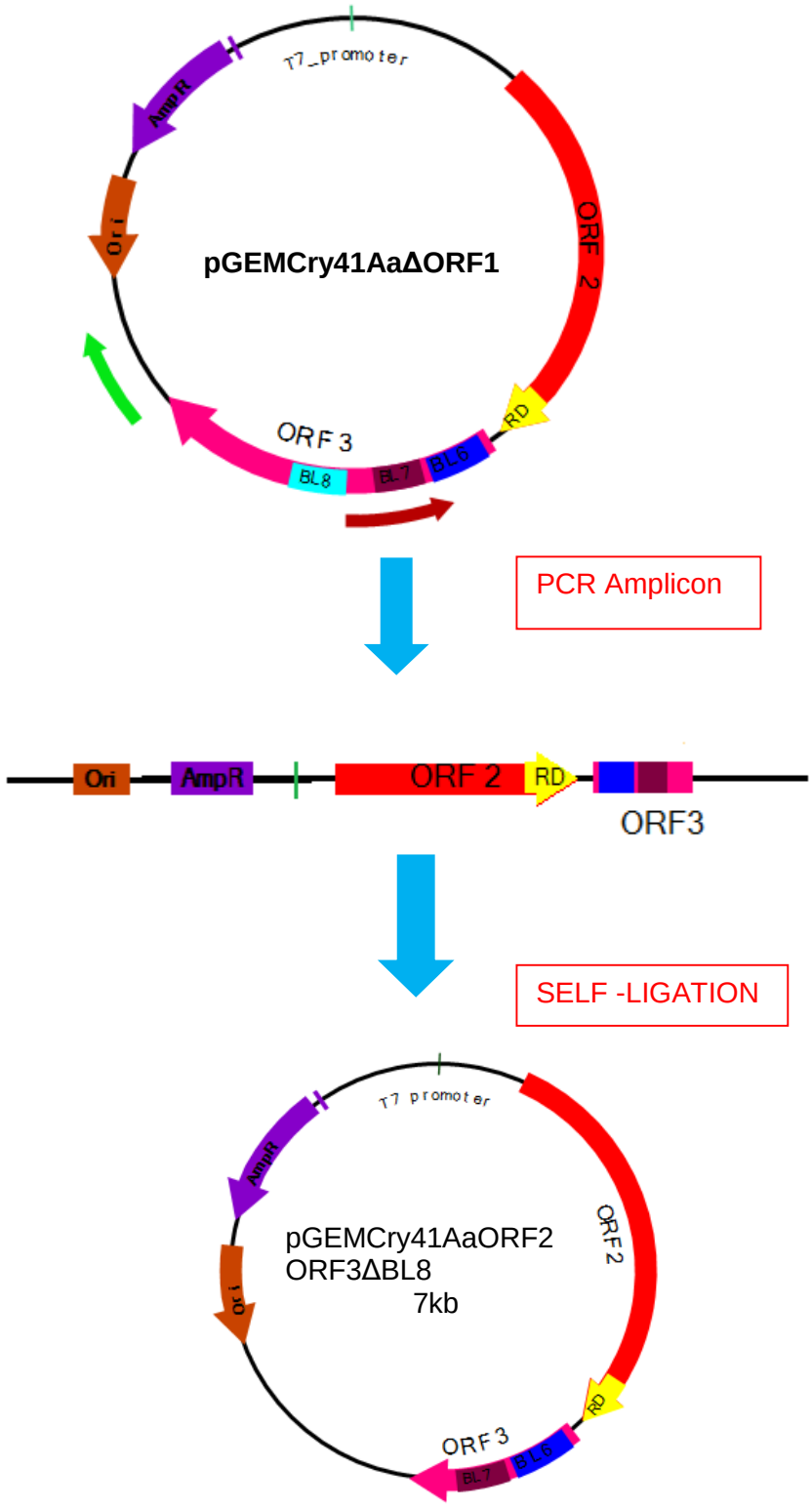

Figure 4.14. Schematic illustration of C-terminal deletion including block 8 of Cry41AaORF3 using the template pGEMCry41AaΔORF1.

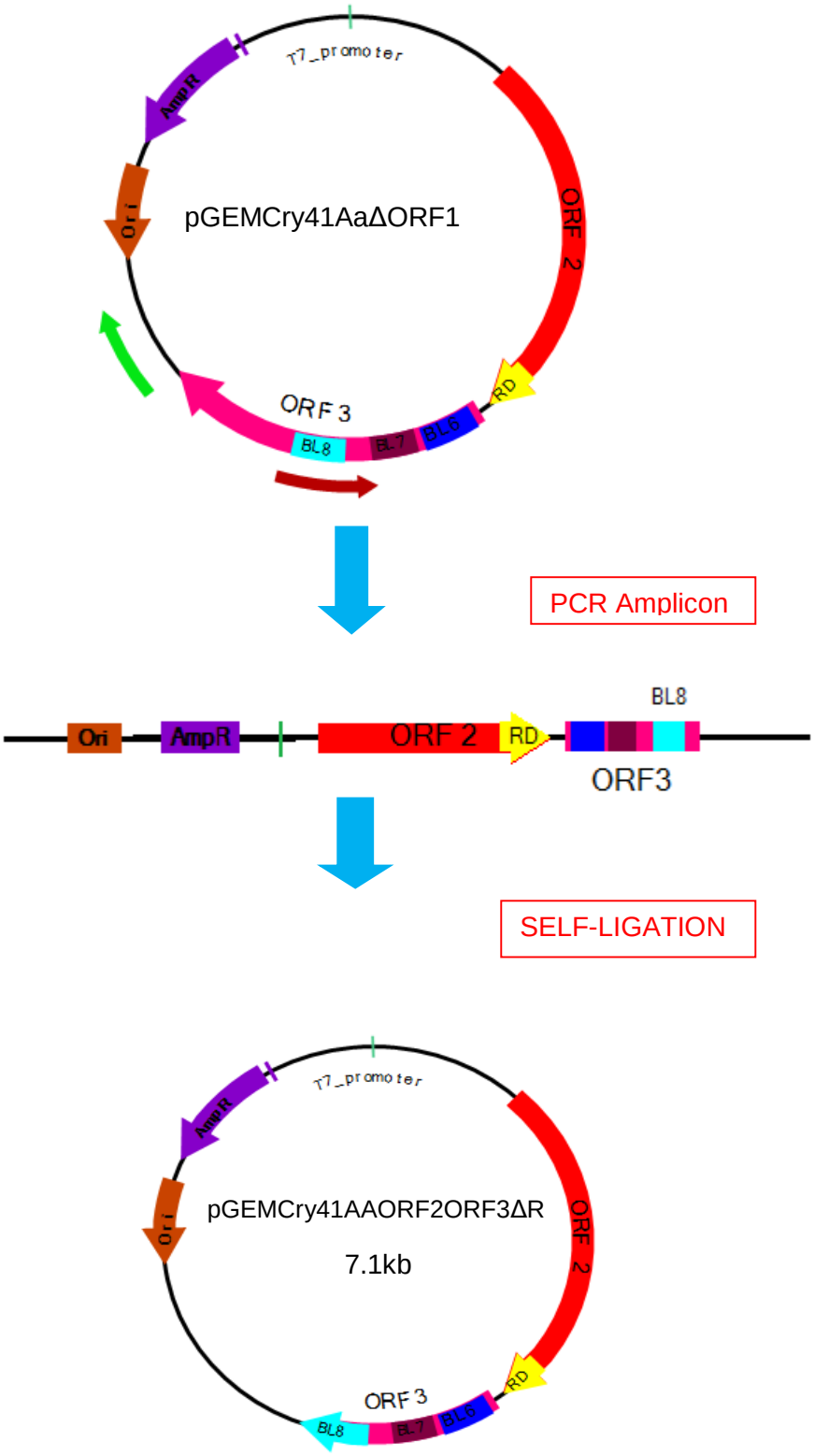

Figure 4.15. Schematic illustration of C-terminal deletion (excluding block 8) of Cry 41AaORF3.

4.2.2.4 Role of Domain II: Hybrids with insecticidal Cry1Ac

Since Domain II in insecticidal Cry proteins has been ascribed a role in the specificity of the toxin (Schnepf et al., 1998), an attempt was made to exchange and replace the domain II of insecticidal Cry1Ac with Cry41Aa domain II to create the hybrid construct designated as pGEMCry1AcDI/41AaDII/1AcDIII as schematically represented in Figure 4.16. The expression vector pGEMCry1Ac designed to express Cry1Ac in *E. coli* hosts which had native *cry1Ac* promoter, its ribosome binding site and pGEM-T vector backbone was used. The suitable junction was decided by comparing the known 3D structures of insecticidal Cry toxins including Cry1A, Cry3A. In absence of 3D structure for Cry41Aa, the suitable junction was extrapolated by aligning it with the insecticidal Cry1 toxins whose structure are known. Primers were designed to delete domain II of Cry1Ac gene contained in the plasmid pGEMCry1Ac. The primers used amplified the domains I and III resulting in the deletion of domain II as schematically illustrated in Figure 4.17 yielding a fragment of 6509 base pairs. The primers used to for amplify the domain II of Cry41Aa1 as schematically illustrated in Figure 4.17, yielded a PCR product of 519 bp. The amplified domain II from Cry41Aa was then ligated to pGEM1Ac and used to transform *E. coli* 109 to form a construct of 7106 base pairs. No expression of the hybrid could be obtained on SDS gel. The recombinant Cry1Ac is approximately 120 kDa. However, replacement of its domain II with Cry41Aa domain II, abolished its expression. No recombinant protein of desired 130 kDa was observed on the gel though crystal inclusions were observed with the phase contrast microscope (data not shown).

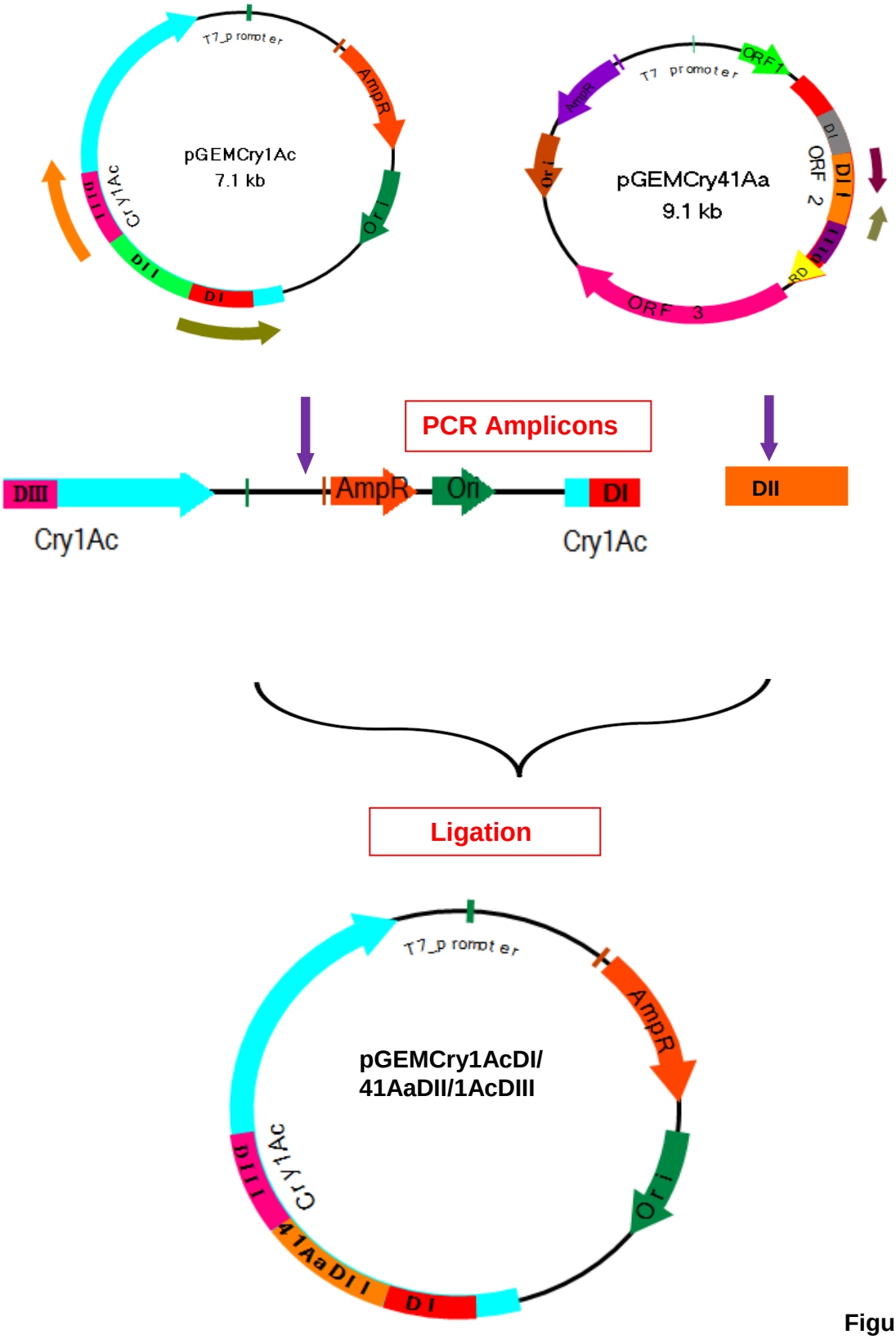

Figure 4.16. Schematic representation of construction of the hybrid pGEMCry1AcDI/41AaDII/1AcDIII.

A

The primers used for amplifying the domain II of Cry41Aa1

Forward Primer

5′-CTCACGCGAGAAGTTTATACAGATATAC-3′

Reverse Primer

5′-TACACTGTTATGAGTCCAACCAAATAAC-3′

Primers annealing to pGEMCry41Aa ORF2

158th amino acid residue of ORF2 529th amino acid

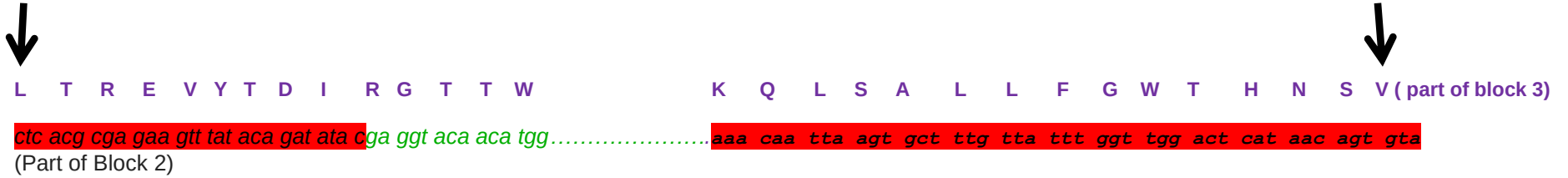

(Part of Block 2)

The PCR amplified 199 amino acid residues of Cry41Aa domain II

LTREVYTDIRGTTWRSDANLNTIDAIENRMVGSRQLQLFTWLTEMKFYIRNTGSITSYTHGDLMVGLEKKIRKTNDNDQWLPLEGQNTSYTRIDRPGIELGKNYWYYARTQQWFETRLLQLWANTDVLS
LNAGTVGNEFWVRDVPDYRNIYARSTRNHFIENHRLSWIKFEPVRDNCPFAWPGYKQLSALLFGWTHNSV

B

Primers designed to delete domain II of *cry1Ac* gene from the plasmid pGEMCry1Ac.

Forward Primer

5'GAATTTAATAATATAATTGCATCGGATAG 3'

Reverse Primer

5' TTGGGAAACTGTTCGAATTGG 3'

Primers annealing to pGEMCry1Ac DNA

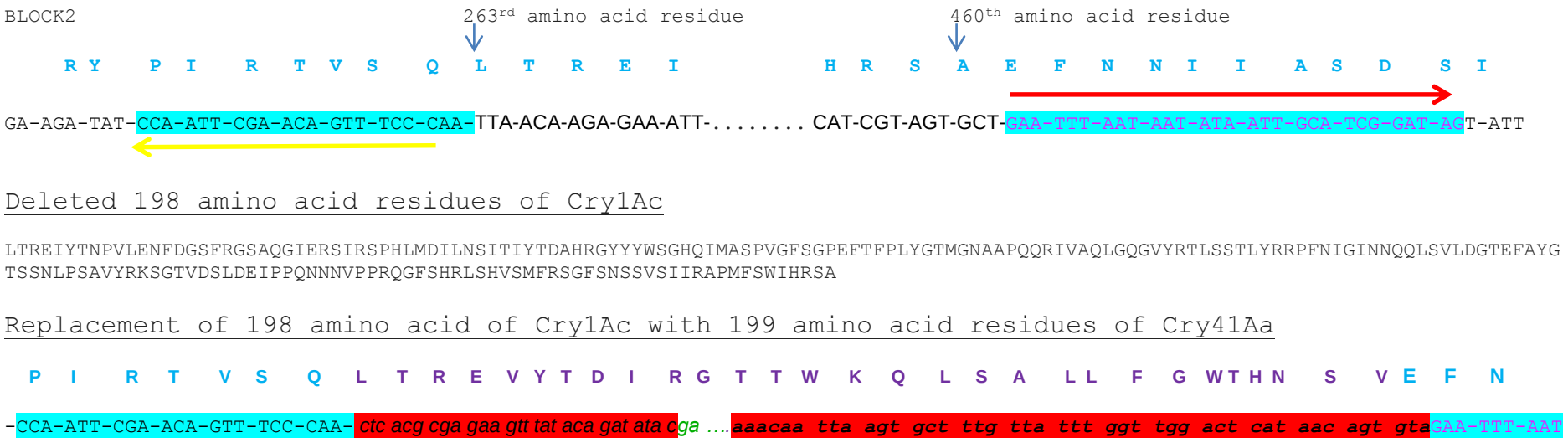

Figure 4.17. Schematic depiction of creation of the hybrid pGEMCry1AcDI/41AaDII/1AcDIII. A. Amplification of DII from pGEMCry41Aa. B. Replacement of DII of pGEMCry1Ac with the amplified Cry41Aa Domain II thus resulting in the desired hybrid construct.

4.2.3 Investigating the role of ricin domain

To test whether the beta-trefoil ricin domain present at the C-terminus of ORF2 of Cry41Aa is responsible for its cytotoxic activity against cancer cell lines, we carried out deletion of this domain from ORF2. Additionally, we intended to transfer this domain on to the insecticidal Cry1Ac toxin to investigate if it alters the specificity of the insecticidal Cry1Ac.

4.2.3.1 Deleting ricin region from ORF2 of *cry41* gene

A Cry41Aa mutant designated as pGEMCry41AaΔRD from which the ricin domain was deleted was constructed as schematically represented in Figure 4.18. Ricin domain was identified using CD search, NCBI and Motifscan (http://myhits.isb-sib.ch/cgi-bin/motif_scan). SDS-PAGE analysis detected a recombinant protein of same molecular mass i.e. 88 kDa as that of Cry41Aa expressed in *E. coli* (Figure 4.19A & B). Crystal inclusions were observed under the microscope. The mutant recombinant protein yielded a similar band of 64 kDa on proteinase K treatment as the non-mutant pGEMCry41Aa with intact ricin domain (Figure 4.19C). Trypsin-treatment too resulted in the generation of 64 kDa band (data not shown).

Forward primer:

41rddelF 5’ TAAAGGTGTGCAACTATCCCTTGAC 3’

Reverse primer:

41rddelR 5’ TCGAGTGGTTAAGCCAATACCC 3’

Primers annealing to pGEMCry41Aa/ORF2ORF3 :

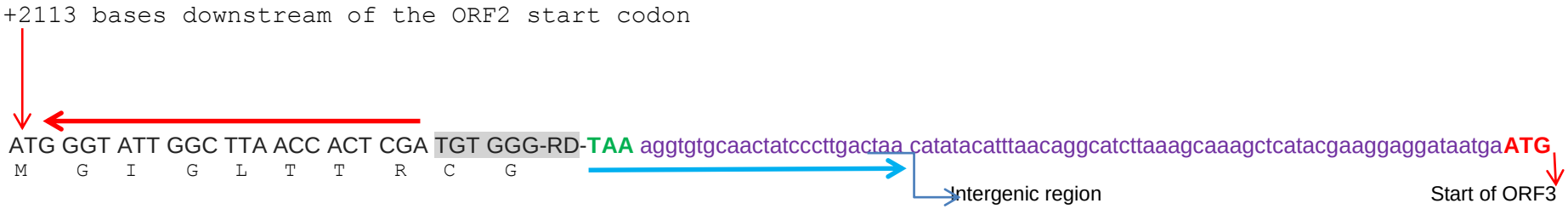

Ligation of amplified pGEMCry41Aa with deleted ricin domain region

ATG GGT ATT GGC TTA ACC ACT CGA TAAaggtgtgcaactatccctgactaacatatacatttaacaggcatcttaaagcaaagctcatacgaaggaggataatgaATG
M G I G L T T R

Figure 4.18. Schematic depiction of binding of the primers to pGEMCry41Aa/ORF2ORF3 for deletion of the ricin domain. RD represents ricin domain. The region highlighted in grey was deleted. The intergenic region is depicted by small purple letters.

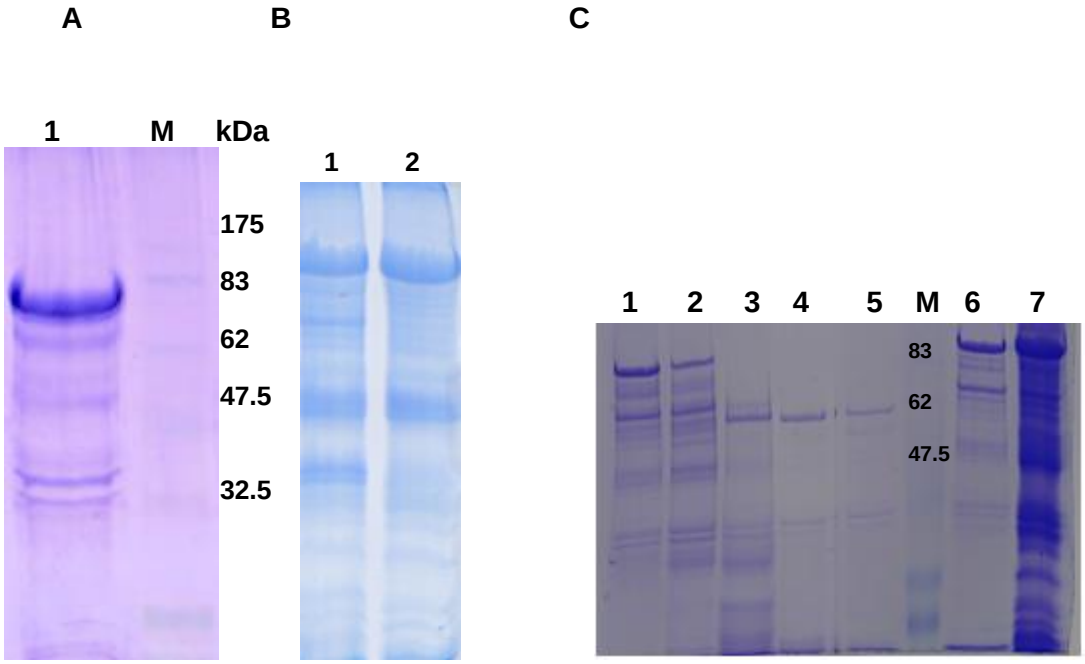

Figure 4.19. SDS-PAGE profile of the expression of Cry41AaΔRD in *E. coli* JM109. A. Cry41AaΔRD inclusions (Lane 1). B. Comparison of the inclusions of the mutant Cry41AaΔRD (Lane 1) with the non-mutant Cry41Aa (Lane 2). C. Protease-treated *E. coli* expressed Cry41AaΔRD. The solubilised samples were treated with 0.002 mg/ml (Lane 1), 0.002 mg/ml (Lane 2), 0.02 mg/ml (Lane 3), 0.2 mg/ml (Lane 4) or 0.4 mg/ml (Lane 5) proteinase K; solubilised sample (Lane 6); total protein sample (Lane 7); protein marker (Lane M).

4.2.3.2 Fusion of ricin domain on to insecticidal pGEMCry1Ac

The ricin domain was amplified from *cry41AaORF2* gene and fused into the insecticidal *cry1Ac* after the conserved block 5 to assess if this particular domain confers any cytotoxic properties or changes the specificity of the insecticidal Cry1Ac thus verifying the involvement of HA-33 like domain in cytotoxicity. The formation of the desired chimeric construct referred to as pGEMCry1AcIg is

schematically represented in Figure 4.20. 519 base pairs of ricin region which encompasses the conserved ricin domain of Cry41AaORF2 including 105 base pairs before the start of the ricin domain (+2041 nucleotides downstream of the start codon of ORF2), 78 base pairs of the intergenic region and the start codon of ORF3 was amplified from pGEMCry41Aa using the forward primer 41IGF 5' CCAGTATATCCTGGTACCTATC 3' and the reverse primer 41IGR 5' **CAT**TCATTATCCTCCTTCG 3' which includes the start codon ATG at its 5'end indicated in red letters (Figure 4.21A). 7103 base pairs of pGEMCry1Ac was amplified by using the forward primer which binds to the region before the conserved block 6 1AcIGF 5'GAATATAATCTGGAAAGAGCG 3' and the reverse primer which binds to regions in and around block 5 1ACIGR 5' AGCCTCGAGTGTTGCAG 3'. This is in order to accommodate the ricin region amplified from Cry41Aa after the block 5 of the insecticidal Cry1Ac and render it as a split toxin by incorporating the start codon before its block 6 (Figure 4.21B).

The expression of the Cry1AcIg was analysed in *E. coli* strain JM109. An approximately 75 kDa band was detected on the gel (Figure 4.22, lane 2), the predicted molecular weight being 84 kDa. The recombinant toxin was expressed as inclusion bodies in *E. coli* JM109 as visible under the phase contrast microscope. However attempts to solubilise inclusion bodies were not met with success (data not shown).

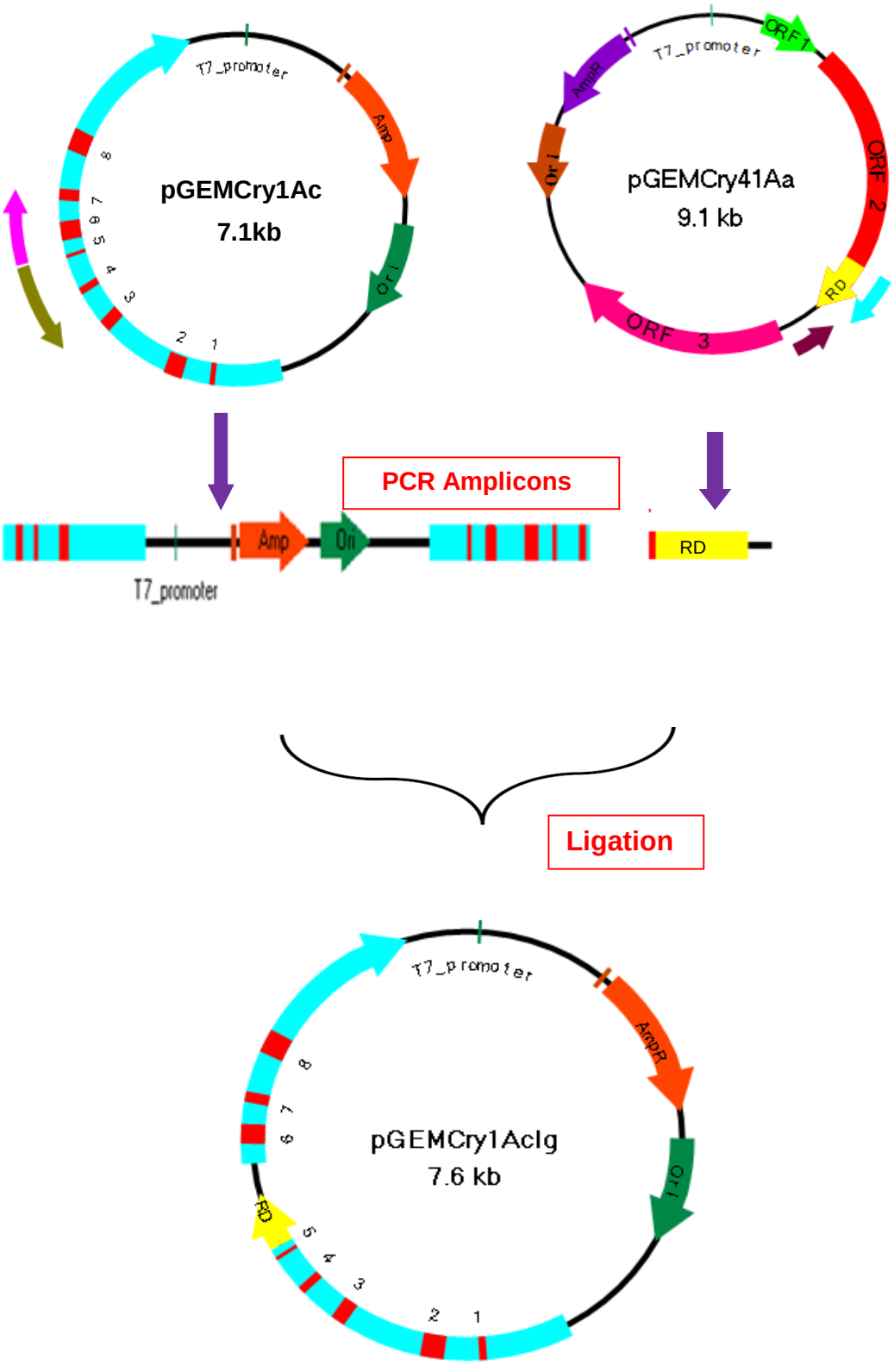

Figure 4.20. Schematic representation of the construction of pGEMCry1AcIg.

A

Forward primer

5’-CCA-GTA-TAT-ATC-CTG-GTA-CCT-ATC -3’

Reverse primer (includes a start codon)

Start codon

↓

5’-**CAT**-TCA-TTA-TCC-TGG-TAC-CTA-TC -3’

Primers annealing to Cry41Aa ORF2 DNA (Part of Cry41Aa ORF2 sequence):

Forward Primer

+2,041 bases downstream of ORF2 start codon

Amplified region

P V Y P G T Y Q I V T A L N N S S V V --RD-

5’-cca gta tat cct ggt acc tat caa atcg tga cag ctt taa ata ata gta gtg ttg taa- - -RD- TAA-3’- intergenic sequence-5’-**ATG**ORF3-3’

Reverse primer

Amplified PCR amplicon (highlighted in grey):

Start codon which was included in the reverse primer

↓

5' CCA-RD –intergenic region-**ATG** 3'

B

Forward primer

5’ GAATATAATCTGGAAAGAGCG 3’

Reverse primer

5’- AGCCTCGAGTGTTGCAG-3’

Primers annealing to pGEMCry1Ac

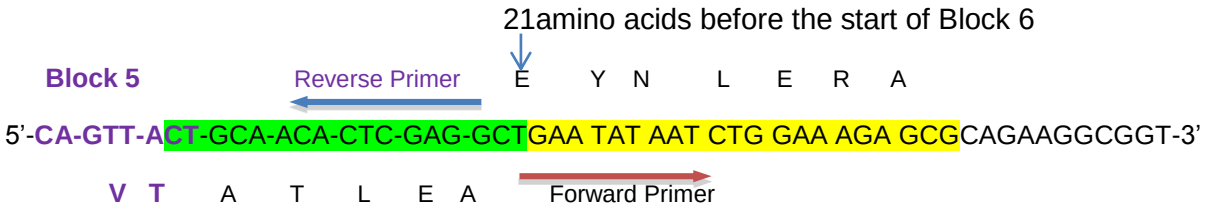

Fusion of amplified Cry41Aa ricin domain region onto pGEMCry1Ac DNA in between the conserved blocks 5 and 6 which includes addition of the start codon before block 6 :

Figure 4.21. Creation of fusion construct pGEMCry1AcIg. (A) Schematic representation of the strategy to amplify ricin domain from ORF2 of Cry41Aa. **(B)** Schematic depiction of the binding of primers to pGEMCry1Ac and intended fusion of Cry41Aa ricin domain region onto pGEMCry1Ac DNA in between the conserved blocks 5 and 6. The fused region from *cry41Aa* is highlighted in grey.

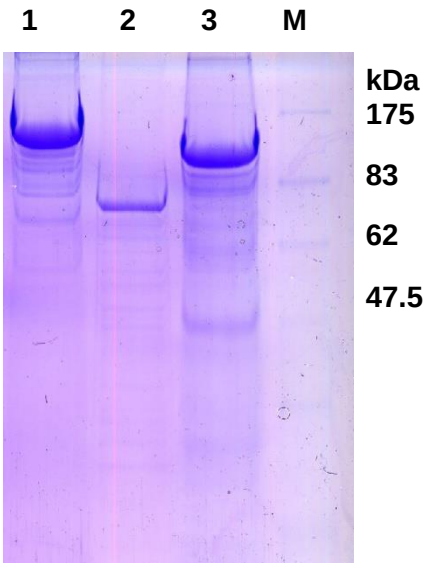

Figure 4.22. 7.5% SDS-PAGE analysis of the expression of the recombinant fusion protein in *E. coli* JM109. Lane 1, recombinant Cry1Ac inclusions; lane 2, fusion recombinant Cry1AcIg inclusions; lane 3, recombinant Cry41Aa inclusions; lane 4, protein marker.

4.2.4 Purification and biological activity of Cry41Aa protein expressed in *E. coli* JM109

Recombinant Cry41Aa toxin devoid of ORF1 was solubilised in 50 mM carbonate buffer, pH 9.5 and purified using AKTA FPLC. The fractions were analysed on 7.5% SDS-PAGE. The solubilised protein was present in fractions B9, B10 and B11 (Figure 4.23). After purification, the samples were treated with various concentrations of trypsin which processed the toxin to ~64 kDa (Figure 4.24).

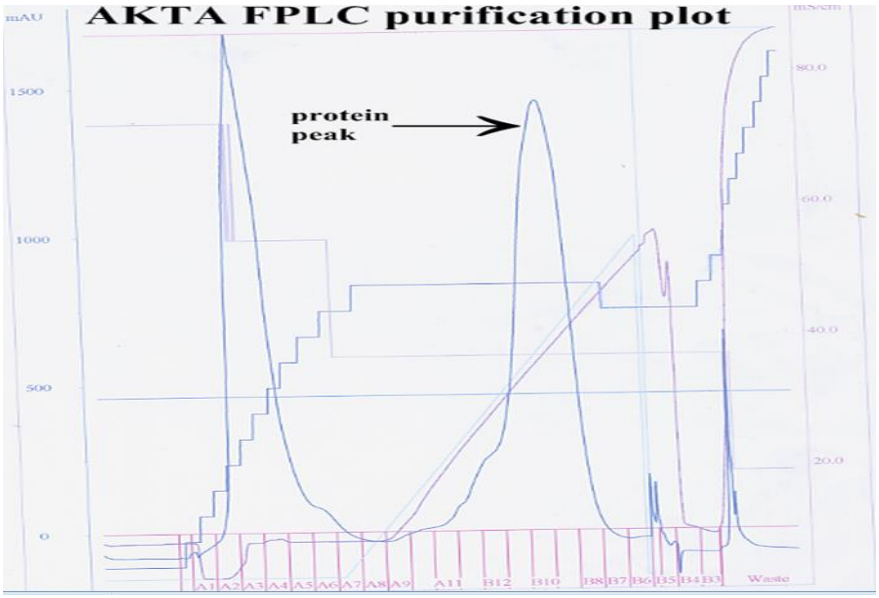

FLOWTHROUGH ELUTION (1ml/min)

Figure 4.23. Purification of recombinant Cry41Aa toxin expressed in *E.coli* JM109. Elution profile of the recombinant toxin on anion exchange chromatography.

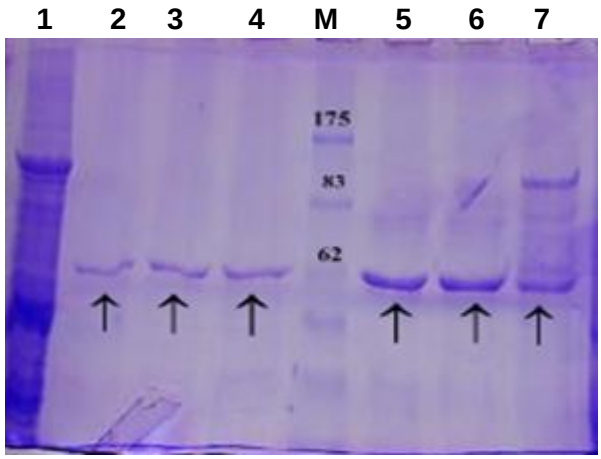

Figure 4.24. 7.5% SDS-PAGE depicting trypsin treatment of Cry41AaΔORF1 expressed in *E. coli* JM109. Lane 1, untreated Cry41AaΔORF1 sample; lanes 2, 3 and 4, B10 fraction of purified Cry41AaΔORF1 samples treated with 0.5, 1 and 2 µl of trypsin (2mg/ml) respectively; lanes 5, 6, 7, B11 fraction of purified Cry41AaΔORF1 sample treated with 2, 1 and 0.5 µl of trypsin (2 mg/ml) respectively; lane M, protein marker. Arrows indicate the activated 64 kDa band.

4.2.4.1 Assessment of biological activity

The toxicity of the pGEMCry41 protein was tested against insecticidal Cry1Ac susceptible G88 and resistant populations KARAK and NO-QA of *Plutella xylostella* using leaf–dip and diet based assays according to the protocols described in Section 2.2.15.1. No mortality was observed in case of G88 or KARAK or NO-QA populations treated with solubilised or trypsin treated protein inclusions. Trypsin-treated Cry1Ac toxic to the cabbage pest, *Plutella xylostella* was used as a positive control.

Dye Exclusion viability assay using Trypan blue (0.4%) was used to assess the cytotoxic activity of solubilised and trypsin treated recombinant Cry41Aa (Section 2.2.15.2.1). The soluble and the trypsin treated proteins at 10 µg/ml failed to demonstrate toxicity against human liver cancer, HepG2 cells and A549 (Human lung cancer cell) (data not shown). Cry41Aa at this concentration has shown to be cytocidal against HepG2 cells (Yamashita et al., 2005).

4.2.4.2 Mass spectrometry analysis

Since the recombinant Cry41A expressed in *E. coli* failed to demonstrate any cytocidal effects against cancer cells and since the deletions made in ORF2 resulted in no change in the size of the proteins on the SDS-PAGE and any mutagenesis in ORF3 resulted in the disruption of the protein produced in *E. coli* JM109, the protein sample was analysed by mass spectrometry to confirm its identity. The data revealed that pGEMCry41Aa resulted in the expression of ORF3 in *E. coli* JM109.

Expressing the ORFs in *E. coli JM109 r*esulted in production of ORF3 as the dominant protein which is similar in size to the desired 88 kDa ORF2 protein. The required ORF2 was not expressed as a major protein in *E. coli* JM109.

We then attempted to develop an alternative method for over-expressing Cry41A proteins. We attempted to express Cry41AORF2 with/without ORF3 in *E. coli* by using T7RNA polymerase/T7 promoter expression systems.

4.2.5 Expression of Cry41Aa ORF2 with/without ORF3 using T7 RNA polymerase promoter

c*ry41AaORF2* and *cry41AaORF2ORF3* genes were amplified from the genomic DNA to yield PCR amplicons of 2.7 kb and 4.9 kb respectively. High Fidelity PCR master mix (Roche) was used. Purified amplicons were ligated into pGEM-T Easy vector to form the plasmids referred to as pGEMCry41Aa/ORF2 and pGEMCry41Aa/ORF2ORF3. The expression of the proteins were analysed in *E. coli* strain BL21(DE3).

An attempt to express *cry41Aa* gene in *E. coli* BL21(DE3) under T7 promoter resulted in overproduction of β-galactosidase (Figure 4.25), a product of Lac Z gene upon induction with IPTG as identified by mass spectrometry. No expression of *cry41Aa* gene was obtained in spite of varying various conditions including media, IPTG concentration, growth- time.

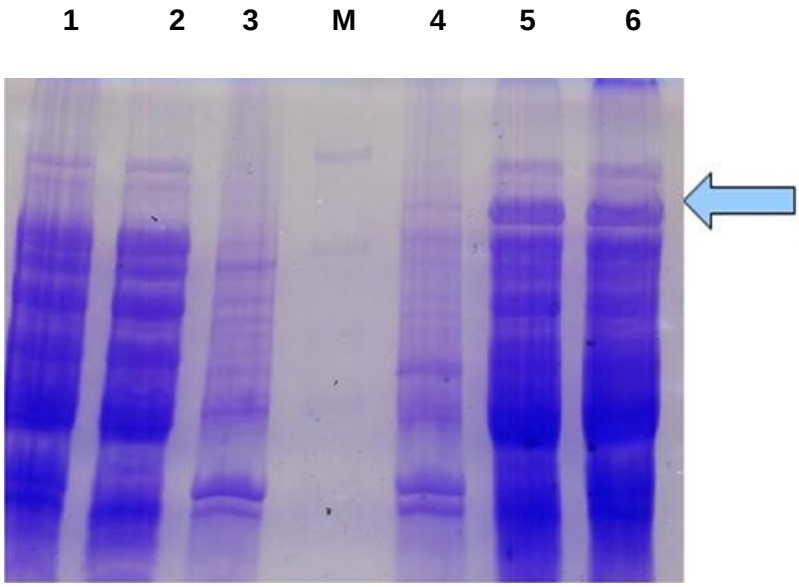

Figure 4.25. SDS-PAGE analysis of Cry41Aa/ORF2ORF3 protein expression in *E. coli* BL21(DE3). Lanes 1-3, No IPTG added; lane 1, total protein sample; lane 2, supernatant; lane 3, pellet resuspended in water; lane M, protein marker. Lanes 4-6; protein harvested after 24 hours of addition of IPTG; lane 5, supernatant fraction; lane 4, pellet resuspended in water; lane 6, total protein. The β-galactosidase over expressed is shown by arrow.

4.2.6 Development of pET Expression systems

4.2.6.1 Expression of Cry41Aa ORF2 with/without ORF3

Since attempts to express *cry41Aa* gene using T7 promoter of pGEM-T in *E. coli* strain BL21(DE3) met with little success, we attempted to express the target gene in a tightly regulated T7 RNA polymerase-based pET vector expression system as diagrammatically represented in Figure 4.26 and Figure 4.27. *cry41AaORF2ORF3* gene was PCR amplified to be ligated in-frame at the BamHI site of pET3a vector. Similarly, *cry41AaORF2* gene was amplified by PCR and ligated in-frame at the NdeI-BamHI sites of pET3 vector allowing fusion of the leader peptide to the gene of interest. Using High fidelity PCR master mix from Roche according to the manufacturer's instructions, ORF2 and ORF3 of *cry41Aa* gene were amplified by PCR using genomic DNA from the Bt strain A1462 with the primers incorporating BamHI restriction sites to the PCR amplicons to be ligated at the BamHI site of pET3a expression plasmid. The forward or 5' PCR primers BamF 5' AATGGAGGATCCTCAATGAATCAAAATTG 3'and the 3' reverse 3BamR 5' GCTTCGGGGATCCTGCTACC 3' were used to generate PCR amplicon of 5 kb. Both the primers contained BamHI restriction site, letters shown in red. Similarly ORF2 of *cry41Aa* gene was amplified by PCR to be ligated in-frame at the NdeI and BamHI sites of pET3a expression plasmid. The forward 5' PCR primer 5'AATGGAGGATTGCATATGAATCAAAATTG 3' containing NdeI site (coloured green) and the 3' reverse primer 2BamR 5' TTAGTCAGGGATCCTTGCACACC 3' containing the BamHI site (coloured red) were employed to yield a PCR product of 2.5 kb. The PCR amplicons were column purified and subjected to restriction digestion. The PCR product of Cry41Aa containing ORF2 and ORF3 was digested with BamHI whereas Cry41Aa containing ORF2 without ORF3 was digested with NdeI and BamHI and

gel purified (Section 2.2.3.2). The 4640 bp expression plasmid, pET3a was digested with the respective enzymes and gel purified as described in Section 2.2.3.2. The genes and the vectors were ligated according to the manufacturer's instructions and used to transform competent *E. coli* JM109 cells by electroporation. The colony containing the correct inserts were identified by rapid size screen (Section 2.2.6) and further verified by restriction digestion and sequencing. The expression of the proteins were analysed in *E. coli* strain BL21(DE3). However, no proteins of interest were obtained on the 7.5% SDS-PAGE (data not shown). Varying several culture conditions did not further aid in obtaining the expression of the desired recombinant proteins, thus suggesting that the cloning of *cry41AaORF2 and cry41AaORF2ORF3* genes in pET expression system resulted in no expression.

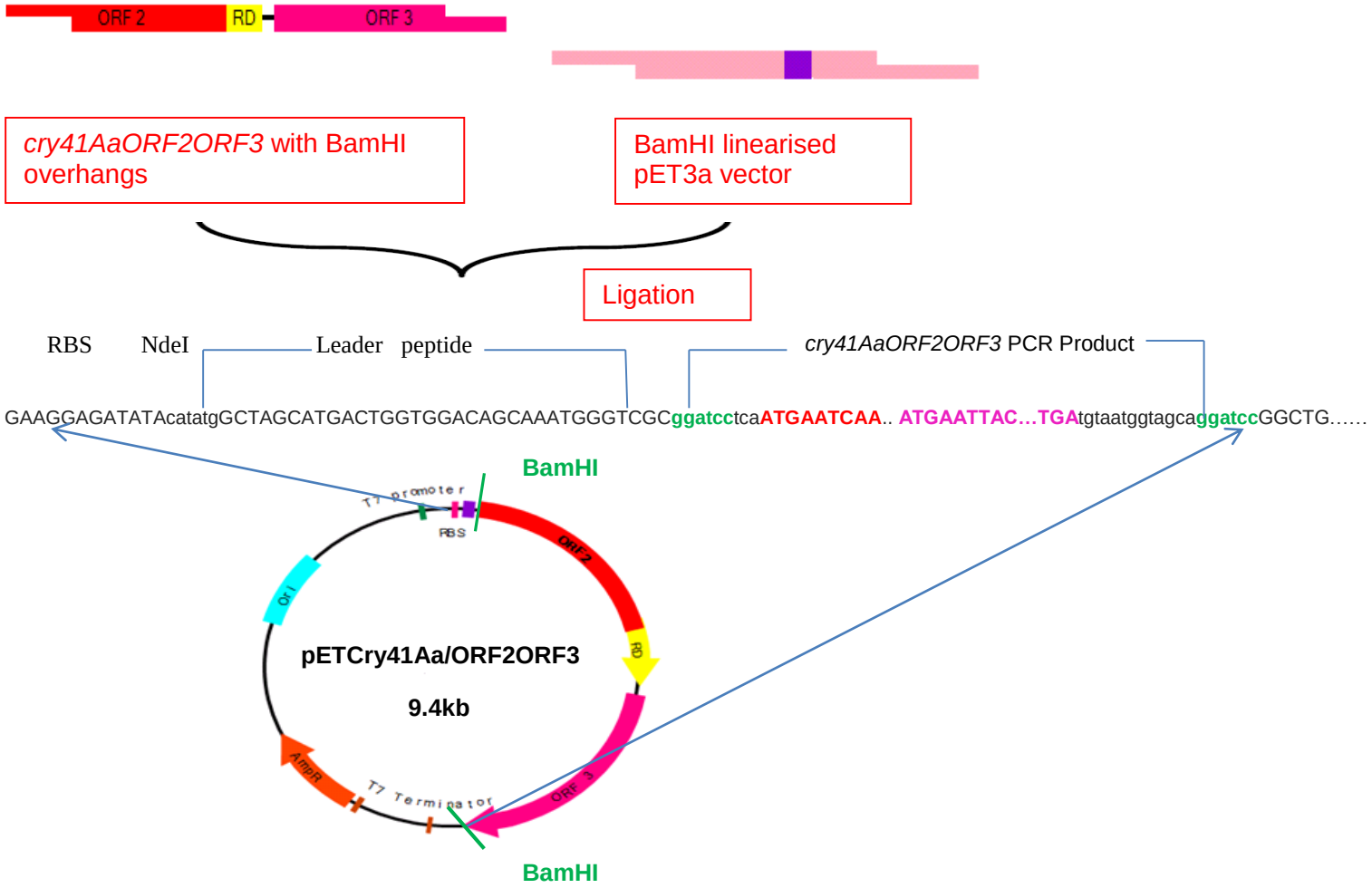

Figure 4.26. Diagrammatic representation of the construction of plasmid pET3aCry41Aa/ORF2ORF3.

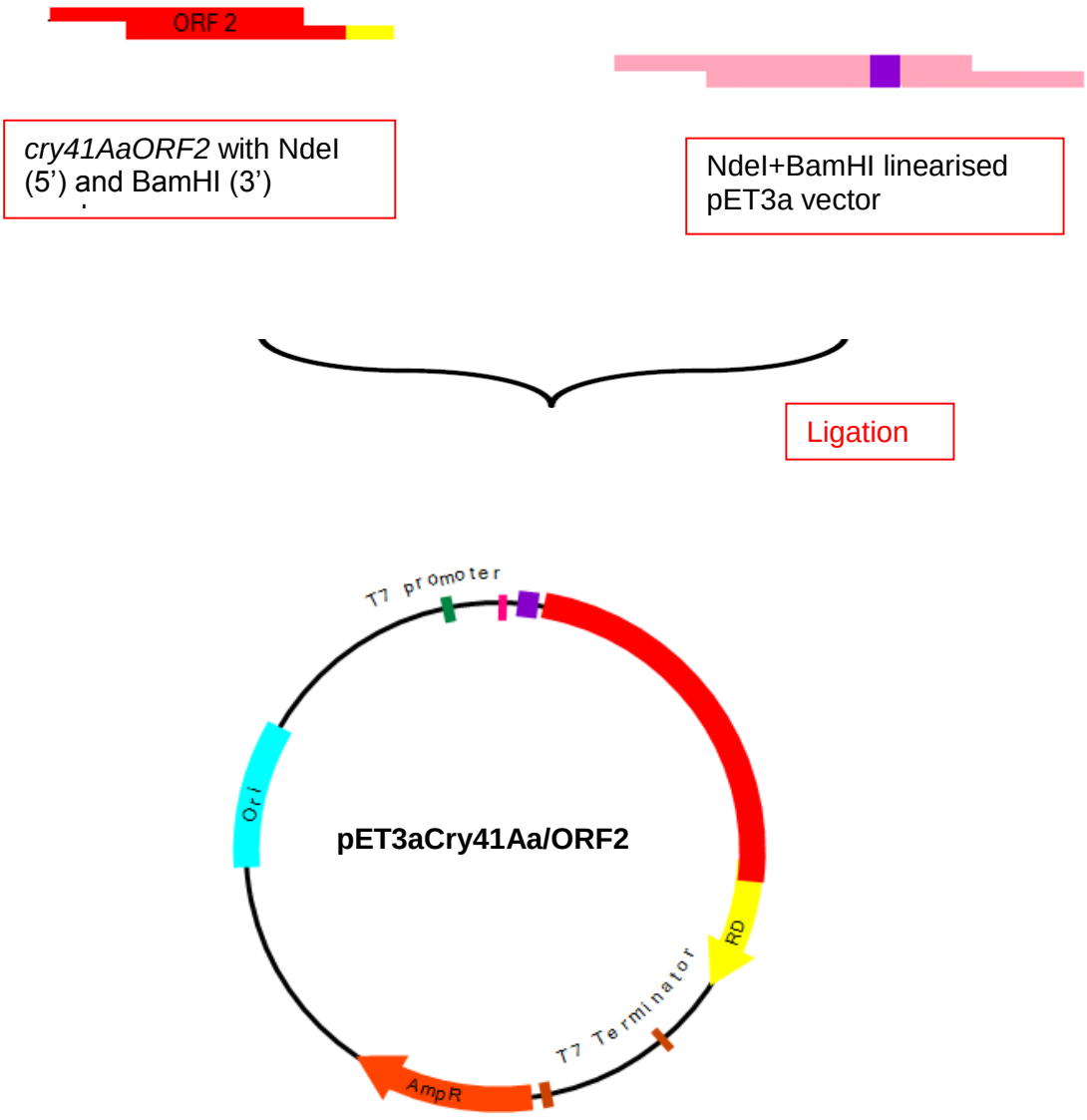

Figure 4.27. Diagrammatic representation of the construction of the plasmid pET3aCry41Aa/ORF2.

4.2.6.2 Expression of Cry1AcIg by pET3 expression system

Since several attempts to solubilise Cry1AcIg failed, we attempted an alternative expression system for the expression of Cry1AcIg in order to obtain the recombinant toxin in the soluble functional form. We designed to express the target gene in a tightly regulated T7 RNA polymerase-based pET vector expression system in *E. coli* strain BL21(DE3) as illustrated schematically in Figure 4.28. The coding sequence of *cry1AcIg* before the conserved block 6 was subjected to PCR amplification and ligated in frame at the BamHI site of pET3a expression vector allowing fusion of the leader peptide for an efficient translation, forming the construct, pETCry1AcIg. However, no protein expression was apparent on the SDS-PAGE suggesting that T7 bacteriophage promoter is most likely unable to drive the expression of the recombinant pETCry1AcIg. The desired 84 kDa recombinant protein was not detected by SDS-PAGE analysis (data not shown).

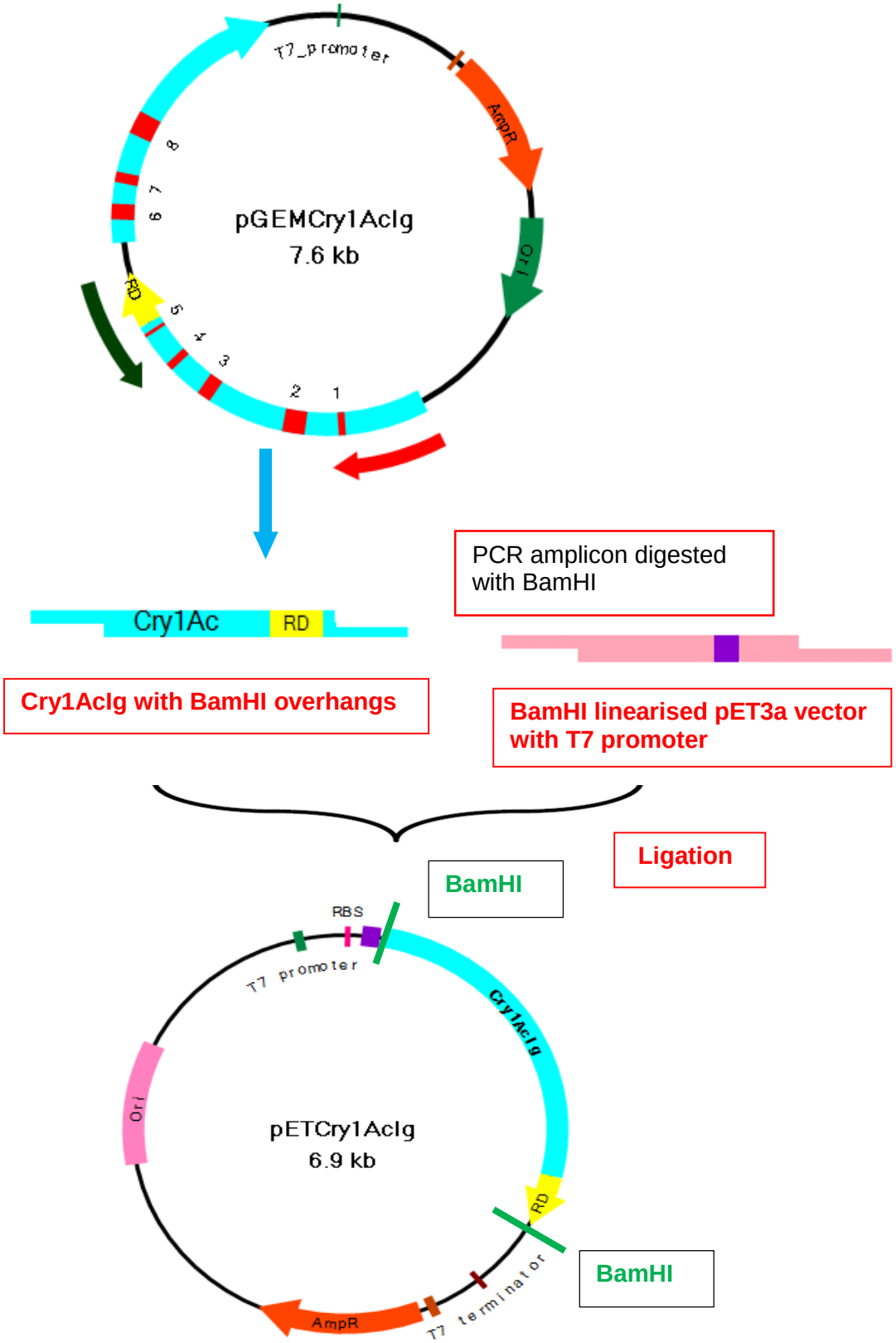

Figure 4.28. Diagrammatic representation of construction of pETCry1AcIg.

4.3 Discussion

E. coli was evaluated as a heterologous host capable of expression of the *cry41A* cytotoxic genes of A1462. *cry41Aa1* gene was cloned into pGEM-T vector and expressed in *E. coli* JM109. Attempts to express *cry41Aa* gene with its own promoter and ribosome binding site in *E. coli* JM109 resulted in expression of ORF3 as major protein. Inclusion bodies were formed in *E. coli*.

Peptide sequencing by mass spectrometry identified the expressed protein in *E. coli* JM109 as the ORF3 (equivalent to C-terminus in longer Cry1A type proteins). The size of ORF3 protein is similar to the size of the ORF2, the desired protein which is around 88 kDa. The trypsin treatment resulted in ~64 kDa protein which was consistent with the previous report that Cry41Aa is cleaved to 64 kDa protein. Toxicity bioassays revealed that these proteins were non-toxic to cabbage insect pest, *Plutella xylostella*. Dye-exclusion cell viability assay confirmed that the ORF3 protein was not cytotoxic to human liver carcinoma, HepG2 cells. The protein thus expressed in *E. coli* JM109 was solubilised and processed efficiently by the protease treatment. However, the protein lacked any biological activity against insect pest and /or against cancer cells. Furthermore, deleting ORF1 from pGEMCry41A did not affect the protein expression. However, deleting ORF3 resulted in no protein expression. Any mutagenesis in ORF3 interfered with protein expression. This further validated that cloning in pGEMCry41Aa resulted in overexpression of ORF3.

To investigate the role of ricin-like domain in toxicity, the particular domain from the plasmid pGEMCry41Aa was fused to the insecticidal pGEMCry1Ac between its conserved blocks 5 and 6. The expression of pGEMCry1AcIg in *E. coli* JM109 was successful yielding a band of approximately 75 kDa as suggested by SDS-PAGE analysis. However, solubilisation of the recombinant protein in various buffers could not be accomplished. The recombinant protein failed to demonstrate the activity defining the insecticidal pGEMCry1Ac toxin suggesting the improper folding of the recombinant Cry1AcIg. Hence, it is pertinent to conclude that fusion of HA-33 domain from cytotoxic Cry41Aa on to Cry1Ac has an adverse impact on its folding and structure resulting in the generation of a non-functional protein. Altering the relative position of the ricin domain between the conserved boxes 5 and 6 of pGEMCry1Ac might aid in expression of functional protein. Further, usage of different expression vectors might enable us to get the functional protein.

We desired to create a hybrid toxin using domains I and III of the three-domain insecticidal Cry1Ac and Domain II of cytotoxic Cry41A gene. Previous studies have successfully conducted domain swaps for generating new specificities (Widner & Whiteley, 1990, Masson et al., 1994, de Maagd et al., 1996). The domain swapping resulted in successful creation of a hybrid that entailed domain II of Cry41Ab and domains I and III of Cry1Ac. No recombinant protein was however, obtained. This could be due to no protein expression or unstable protein due to erroneous folding. Hybrid domains of the construct created have not evolved together. Hence, the protein lacks the specific intramolecular interactions

that are necessary for a stable protein. de Maagd et al. (2000) suggested that Domains I, II and in certain cases Domain III appears to have co-evolved towards certain specificities. Domain swapping by homologous recombination or restriction-fragment exchange leads to the generation of new specificities in Bt toxins. For instance, replacement of domain III in Cry1 toxins (Cry1Ab, Cry1Ac, Cry1Ba, Cry1Ea) by that of Cry1Ca conferred the toxins activity against *Spodoptera exigua* (beet armyworm) which they originally lacked (de Maagd et al., 2000). Further, studies have demonstrated that hybrids of Cry1Ac and Cry1Fa possess wider target spectra than their parent toxins (Malvar & Gilmer, 1998). The presence of salt bridges between domain I and domain II could be responsible for maintaining the protein in a globular form during solubilisation and activation by protease. The residues involved in salt bridges are contained in the conserved block 2 in Cry proteins that entails helix 7 of domain I and first β strand of domain II. These interactions might play a role in specificity. The last β strand of domain II is contained in conserved block 3 and maintains interaction between domains I and III. Disruption of these interactions during hybrid creation might result in unstable protein (Schnepf et al., 1998). Altering the expression system could help us achieve our desired recombinant protein. Alternative hybrids could be attempted with closely related Cry proteins for instance Cry3Aa, Cry3B and Cry3C. Thus, disruption of a large domain of the protein could be a factor resulting in the incompatibility of the hybrid that we created affecting the overall protein folding process. Mutagenesis of a more focussed region of domain II could be attempted.

Further, since Cry41Aa expression using pGEM-T T7 promoter in *E. coli* BL21(DE3) resulted in overexpression of β-galactosidase upon induction with

IPTG, we attempted to clone *cry41Aa* gene in a pET plasmid under control of the strong bacteriophage T7 promoter. The cloning of *cry41Aa* gene into pET expression vector was successful, albeit resulting in no protein expression in *E. coli* host BL21(DE3). Similarly, an attempt to express recombinant pETCry1AcIg in *E. coli* host BL21 was met with little success. Varying growth conditions for instance temperature, media, concentration of the inducer, IPTG did not aid in the expression of the desired protein. Altering the host strain from BL21(DE3) to an alternative *E. coli* host might lead to expression of a functional protein. Usage of a different *E. coli* host strain in conjunction with pET vectors might aid in protein expression. Similar effects were observed by Miroux and Walker (1996), who were unable to produce recombinant bacterial membrane proteins in BL21(DE3) host used en masse with pET3a expression vector owing to bacterial cell death. However on switching over to an alternative host *E. coli* C41(DE3), they were able to achieve the desired expression (Miroux & Walker, 1996). The proposed mechanism for lethality of over expression of protein was generation of large amounts of mRNA from the plasmid by T7 RNA polymerase as compared to *E. coli* RNA polymerase. Hence, translation being outstripped by transcription lead to generation of unstable naked RNA stretches. By an unascertained process, over expression of β-galactosidase from LacZ gene or an inactive form of elongation factor Tu leads to the degradation of ribosomal RNAs (Iost & Dreyfus, 1995). Hence, it is imperative to opt for a strain where the transcripts are synthesised slowly by either the affected activity of T7RNA polymerase or due to the reduced amount of polymerase produced, thereby procrastinating the onset of transcription further preventing uncoupling of transcription and translation (Dong et al., 1995; Miroux & Walker, 1996). However, eliminating the lethality of

protein expression does not guarantee over expression of protein. Additionally, numerous other parameters need to be considered for instance preventing the degradation of mRNA and ensuring that undesirable features in the coding sequence for instance rare or low-usage codons which lead to misincorporation of amino acids do not impede the translation (Kane, 1995; Miroux & Walker, 1996).

Since attempts to obtain the desired functional protein in *E. coli* met with little success, we aimed at devising strategies to establish a stable homologous expression system for Cry41A and its mutants.

5. Homologous expression, characterisation and mutagenesis of Parasporin-3 genes

5.1 Introduction

Heterologous expression efforts in *E. coli* resulted in either expression of ORF3 or lack of expression of the desired recombinant protein. Similar results were obtained by Yamashita et al. when attempting expression of PS-3 genes in *E. coli* (personal communication). The plasmids pCG-I and pCG-III harbouring the genes of parasporin-3 viz., *cry41Aa* and *cry41Ab* respectively in an *E. coli-Bt* shuttle vector pHT3101 were transferred to us by Yamashita (Yamashita et al., 2005). However, our attempts to express *cry41Aa and cry41Ab* genes from pCG-I and pCG-III respectively proved unsuccessful (data not shown). Since the expression of recombinant *cry41Aa* gene could not be repeated using Yamashita's previous established expression system (Yamashita et al., 2005), we demonstrate here the successful homologous expression of *cry41Aa* gene in *B. thuringiensis* under a strong promoter and further characterisation of the genes. We further elucidate the roles of the ORF2 and ORF3 of the split toxin in protein stability and function.

Similarly, since preliminary screening of *B. thuringiensis* isolate Sbt021 demonstrated activity against HepG2 (Figure 3.10A, p. 97), we intended to study its molecular organisation and further clone and express the relevant gene / genes involved in the cytotoxicity of the strain. Two major proteins of molecular masses 140 kDa and 80 kDa were obtained on 7.5% SDS-PAGE from the native

strain Sbt021 as shown previously in Figure 3.2, Chapter 3. Since an 80 kDa protein similar in size to the cytotoxic protein from A1462 was detected on SDS-PAGE, we decided to assess the cytotoxicity of the gene expressing the 80 kDa protein. The 80 kDa protein from Sbt021 has been classed as Cry41Ba1 (Crickmore et al., 2013) and had been identified following sequencing of the strain. However, in the absence of any published upstream and downstream regions, the sequence of Cry41Ba from Sbt021 was deduced from the reference sequence of closely related Bt *serovar andalousiensis* BGSC4AW1 producing Cry41Ba2. Nucleotide analysis of *cry41Ba* revealed three open reading frames in close proximity to each other in the same orientation with short intergenic regions between them. Cry41Ba was found to be a split toxin bearing semblance to Cry41Aa with conserved blocks 1-5 contained in ORF2 and conserved blocks 6-8 being present in ORF3. The upstream flanking region of all the ORF's contained the putative translational signals, ribosome binding sites. The presumed translational start site for the ORF2 is 5'aaaa**aggagg**tttatacATGAATCCA 3' with a ribosome binding site indicated in bold red letters. The ORF2 yields a polypeptide of 840 amino acids with a predicted molecular mass of 95 kDa. Upstream of ORF2 is located ORF1 that encodes a protein of 120 amino acids. An intergenic, non-coding region was located between ORF1 and ORF2. Downstream of ORF2 is another open reading frame, ORF3 separated by short intergenic sequence, with its own ribosome binding site. The ORF3 yields a polypeptide of 607 amino acids with a calculated molecular mass of 68 kDa.

Conserved domain analysis in the protein sequence of Cry41Ba1ORF2 by Conserved Domain search, NCBI (Marchler-Bauer & Bryant, 2004; Marchler-Bauer et al., 2009; Marchler-Bauer et al., 2011), detected the presence of a ricin-like lectin domain [pfam 00652] in its carboxy terminus, referred to as ricin domain (RD) as in previous chapters. The amino acid sequence of Cry41Ba ORF2 contained the signature Q-X-W/F motifs which form the defining characteristics of a member of the "Ricin Superfamily" [cd00161]. This was analogous to the domain present in Cry41AaORF2 derived from Bt strain A1462 (Figure 5.1). The absence of this domain from insecticidal Cry1Ac prompted us to further create mutants of the Cry41Aa and Cry41Ba toxins as done previously. However, since no expression could be achieved in *E. coli*, we illustrate here, the cloning and expression of Cry41Aa and Cry41Ba without the ricin domain assigned as Cry41AaΔRD and Cry41BaΔRD respectively, in *Bacillus thuringiensis*. We further investigate the contribution of this domain to the biological activity of the two proteins.

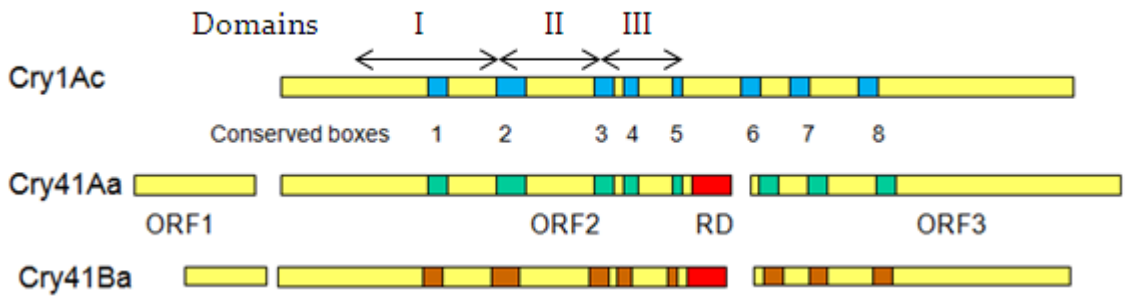

Figure 5.1. Diagrammatic representation of Cry41Ba, Cry41Aa and insecticidal Cry1Ac. RD (red box) denotes the ricin-like domain found at the end of ORF2 in Cry41Aa and Cry41Ba which most closely resembles HA-33 from *Clostridium botulinum.*

5.2 Results

5.2.1 Expression of *cry41Aa* and *cry41Ba* genes in *Bacillus thuringiensis*

Since attempts to express the *cry41* gene in *E. coli* were met with little success, a strategy to express the target gene in *B. thuringiensis* was devised. The *E. coli* / *B. thuringiensis* shuttle vector pSVP27 with the *cyt1A* promoter upstream of the cloned target gene was employed (Crickmore & Ellar, 1992; Crickmore et al., 1994). The strategy was to individually clone *cry41AaORF2ORF3* and *cry41BaORF2ORF3* genes into the pSVP27 vector to form the recombinant plasmids referred to as pSVP27Cry41Aa/ORF2ORF3 (Figure 5.2) and pSVP27Cry41Ba/ORF2ORF3 (Figure 5.4) respectively. Further, it was aimed at cloning ORF2 without ORF3 of each *cry41Aa* and *cry41Ba* operon into pSVP27 designated as pSVP27Cry41Aa/ORF2 and pSVP27Cry41Ba/ORF2 (Figure 5.3).

Using PfuUltra Hotstart Master mix from Stratagene, *cry41AaORF2* and *ORF3* were amplified by PCR from genomic DNA from the Bt strain A1462. Primers were designed to amplify 21 bp upstream of the start codon of ORF2 which includes the ribosome binding site. Similarly, genomic Sbt021 DNA was used a template for PCR amplification of *cry41Ba* gene. The primer sets were designed from the DNA sequence of Bt *serovar andalousiensis* BGSC4AW1 and employed in PCR to amplify the region encoding *cry41BaORF2* and *ORF3*. Primers were designed to amplify 57 bp upstream of the start codon of ORF2 which includes the ribosome binding site. Various restriction sites were included in the primers. The PCR amplicons were column purified and subjected to restriction digestion by the respective enzymes as outlined in Table 5.1.

The vector pSVP27 was subjected to digestion with corresponding restriction enzymes as the template DNA and gel purified (Section 2.2.3.2). The genes and the vectors were ligated according to the manufacturer's instructions (Section 2.2.4) and transformed into *E. coli* JM109 competent cells by electroporation (Section 2.2.5.1). The *E. coli* transformants were isolated by selection on LB-agar-ampicillin plates (100 µg/ml) at 37°C. The colonies containing the correct inserts were identified by rapid size screen (Section 2.2.6). The single colonies with the correct insert obtained were further streaked on to LB-agar-ampicilin plates (100 µg/ml) at 37°C for increased plasmid yield. Small -scale plasmid preparations were carried using QIAprep Spin Miniprep Kit (Qiagen) and extracted plasmids were subjected to restriction analysis (Section 2.2.8) to check for colonies harbouring the desired *cry41Aa and cry41Ba* genes. The correct plasmid pSVP27Cry41Aa/ORF2 was corroborated by digesting it with restriction enzyme HaeIII and further by NdeI and KpnI (Figure 5.5A & B). Similarly, plasmids pSVP27Cry41Aa/ORF2ORF3 (Figure 5.6) and pSVP27Cry41Ba/ORF2 and pSVP27Cry41Ba/ORF2ORF3 (Figure 5.7) were subjected to HaeIII restriction analysis. The colony thus containing the correct inserts was further transformed into *E. coli* GM2163 to obtain unmethylated DNA for ease of transformation in *B. thuringiensis.*

The colonies thus obtained in GM2163 were confirmed for the correct construct by restriction analysis as aforementioned and introduced into various acrystalliferous strains of *B. thurinigiensis* including IPS78/11, 4Q7 and 4D7 by electroporation. Different strains of Bt were used as strain-dependent expression of other Bt toxin genes had been observed in our lab. The *B. thuringiensis* transformants were isolated by selection on LB-agar-chloramphenicol plates (5

µg/ml) at 30°C. Any colony thus obtained in Bt with the desired plasmid was purified using QIAprep Spin Miniprep Kit (Qiagen). Additionally, lysozyme (10 mg/ml) was added to the resuspension buffer to lyse the cell wall (Section 2.2.7.2). The plasmid was re-transformed back into competent *E. coli* JM109 cells to obtain a clean preparation of the DNA for verification of the final construct by restriction analyses as mentioned above. The final construct was further ascertained by sequencing.

Genomic DNA	Primers	Sequence (5'->3')	Product
A1462	BamrbsF	GAAGAAggatccAAATGGAATGGAGG	Cry41Aa/ORF2
	2BamR	TTAGTCAGggatccTTGCACACC	
	BamrbsF	GAAGAAggatccAAATGGAATGGAGG	Cry41Aa/ORF2ORF3
	Cry41Orf3XbaR	CGCTtctagaAGCCTGCTACCATTAC	
Sbt021	41BaF	GTTCgtcgacTATAAAAGTGAACACAC	Cry41Ba/ORF2
	41BaOrf2R	CATTCgcatgcGAATACATATTTTTAC	
	41BaF	GTTCgtcgacTATAAAAGTGAACACAC	Cry41Ba/ORF2ORF3
	41BaOrf2+3R	GAATCgcatgcAGACTCCCTAC	

Table 5.1. PCR primers used for amplification of *cry41* genes. Restriction sites introduced in the amplified fragments are indicated by lower-case letters. BamHI: ggatcc; XbaI: tctaga; SalI: gtcgac; SphI: gcatgc

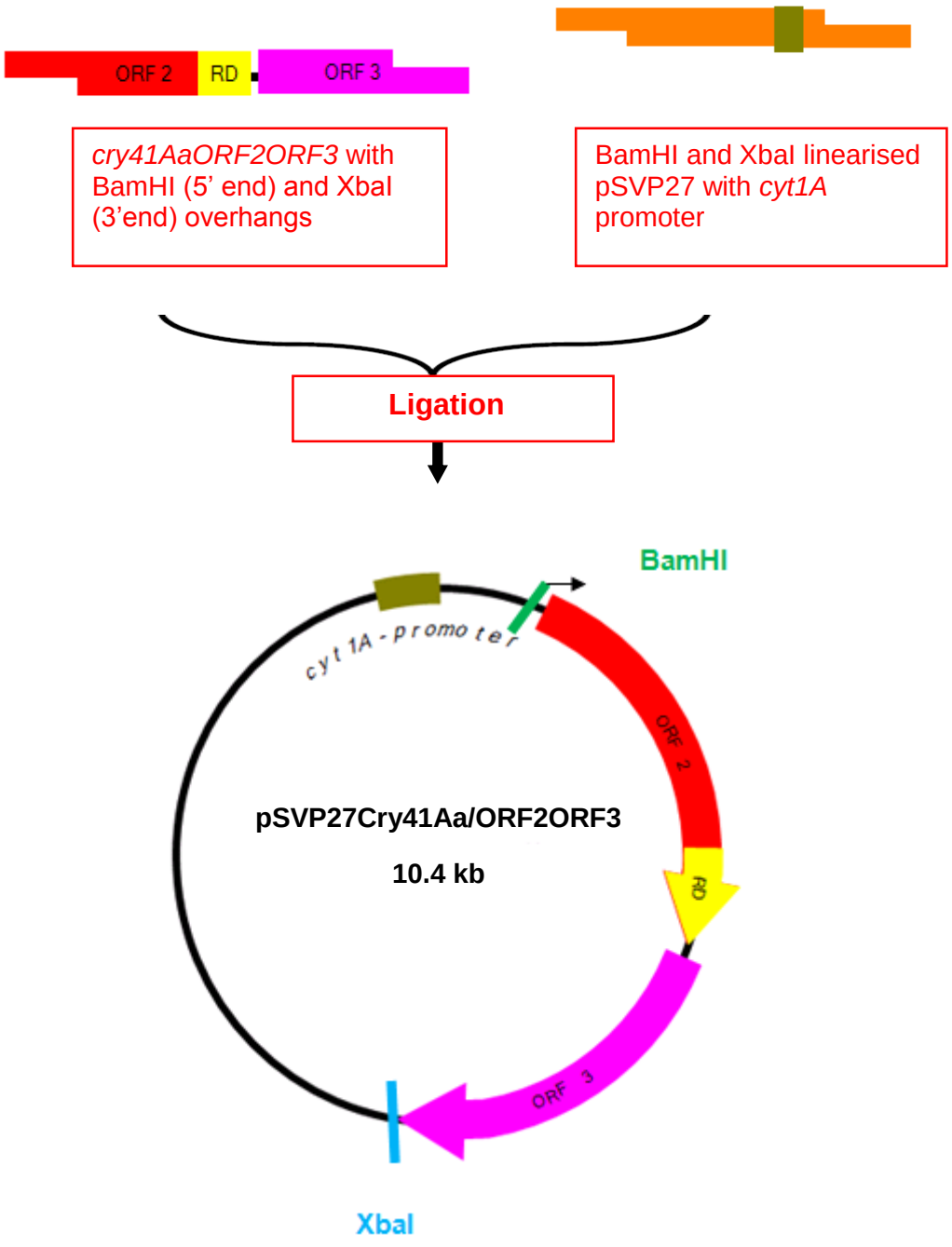

Figure 5.2. Schematic illustration of the construction of plasmid pSVP27Cry41Aa/ORF2ORF3. Location of BamHI and XbaI sites are indicated on the plasmid.

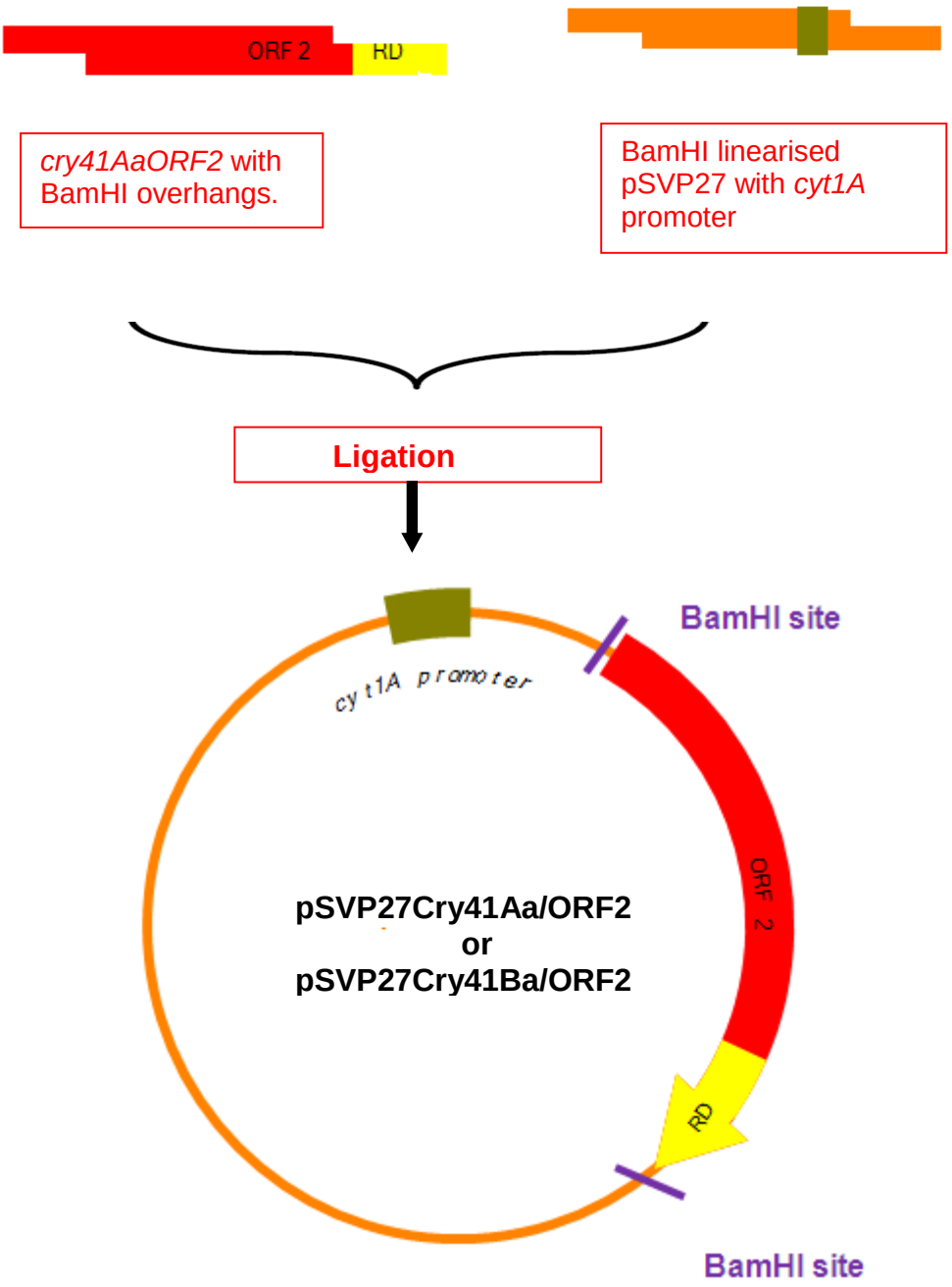

Figure 5.3. Schematic representation of the construction of plasmid pSVP27Cry41Aa/ORF2. Location of BamHI sites are indicated on the plasmid.

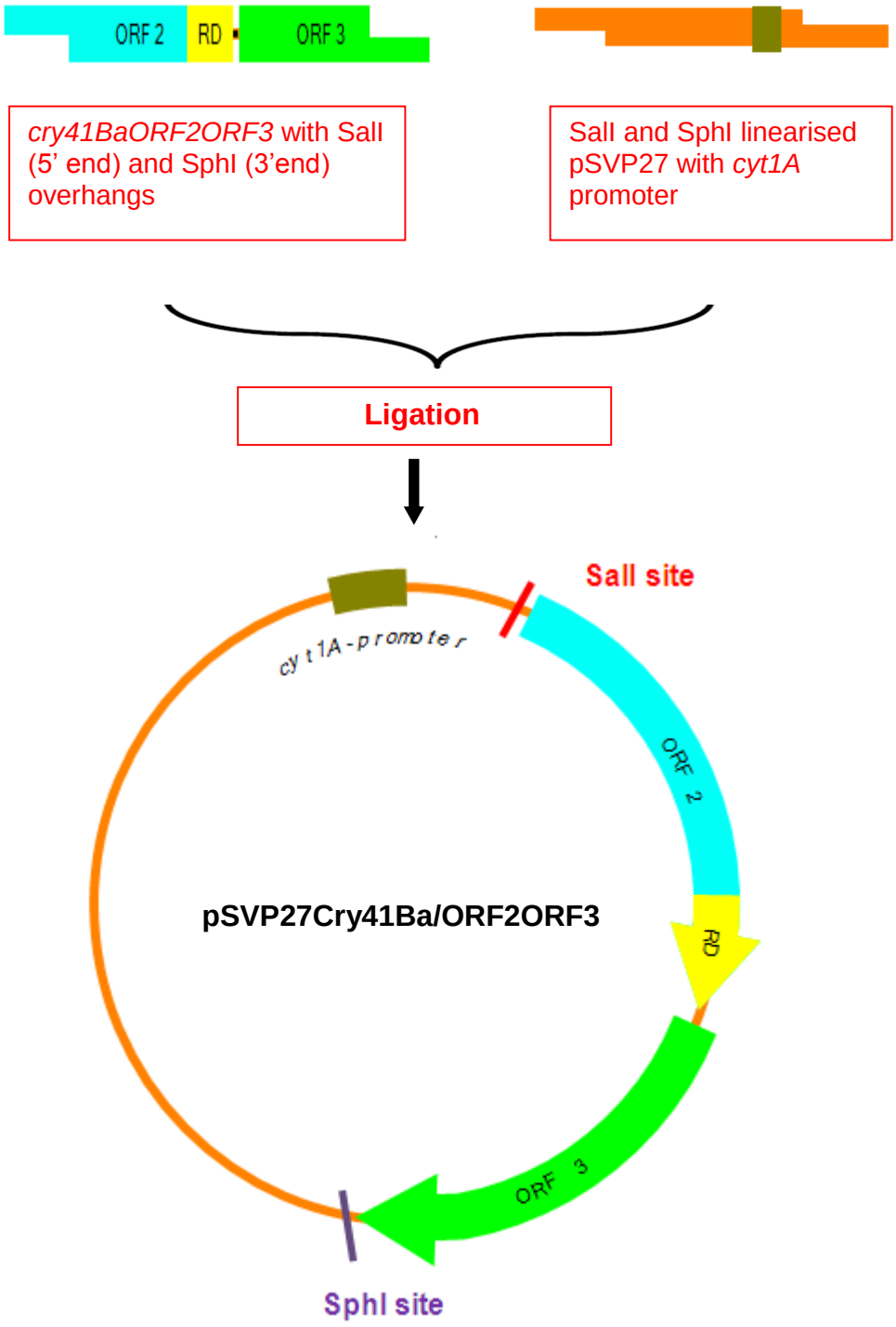

Figure 5.4. Schematic representation of the construction of plasmid pSVP27Cry41Ba/ORF2ORF3. Location of restriction sites SalI and SphI are indicated on the plasmid.

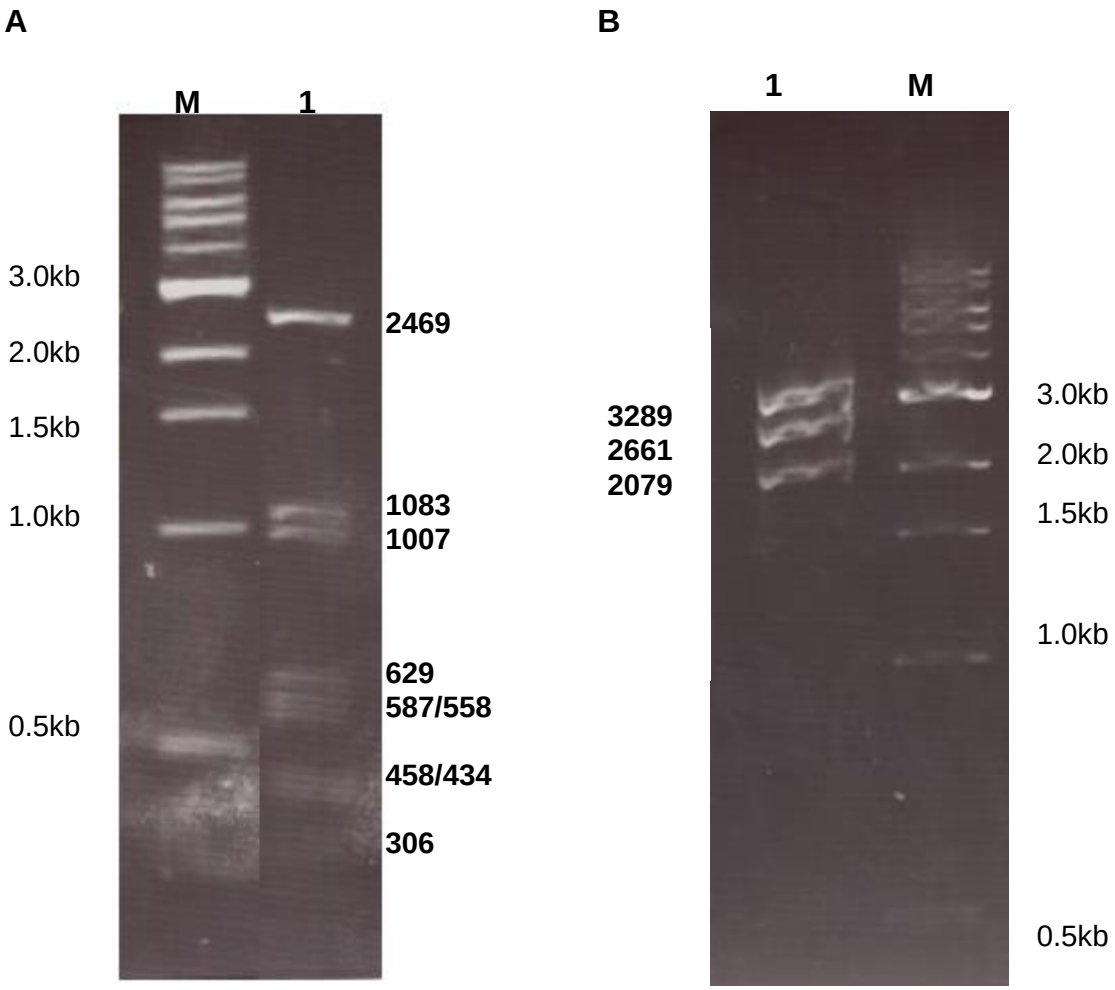

Figure 5.5. 1% Agarose gel depicting restriction patterns for recombinant pSVP24Cry41Aa/ORF2.

(A) Lane 1, HaeIII restriction profile. **(B)** Lane 1, NdeI and KpnI digestion fragments. Lane M is the 1 kb DNA ladder. The fragment sizes predicted by NEB cutter are shown to the sides.

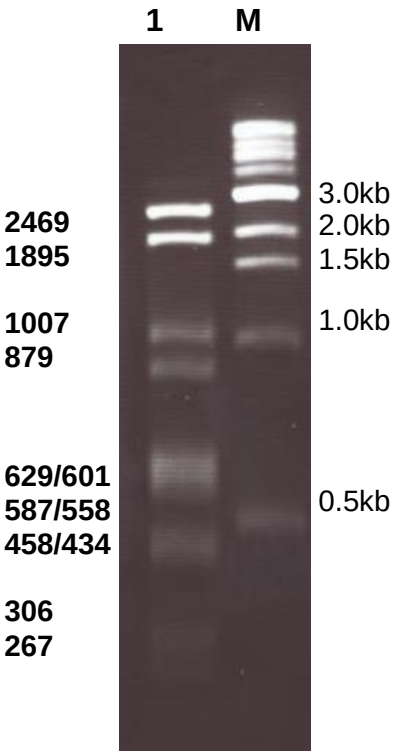

Figure 5.6. 1% Agarose gel illustrating the results of HaeIII restriction analysis of the construct pSVP27Cry41Aa/ORF2ORF3. Lane 1 is the HaeIII fragments of the recombinant pSVP27Cry41Aa/ORF2ORF3 and lane M is the 1 kb molecular mass marker. The corresponding base pair length values of each DNA fragment as predicted by NEB cutter are shown to the left.

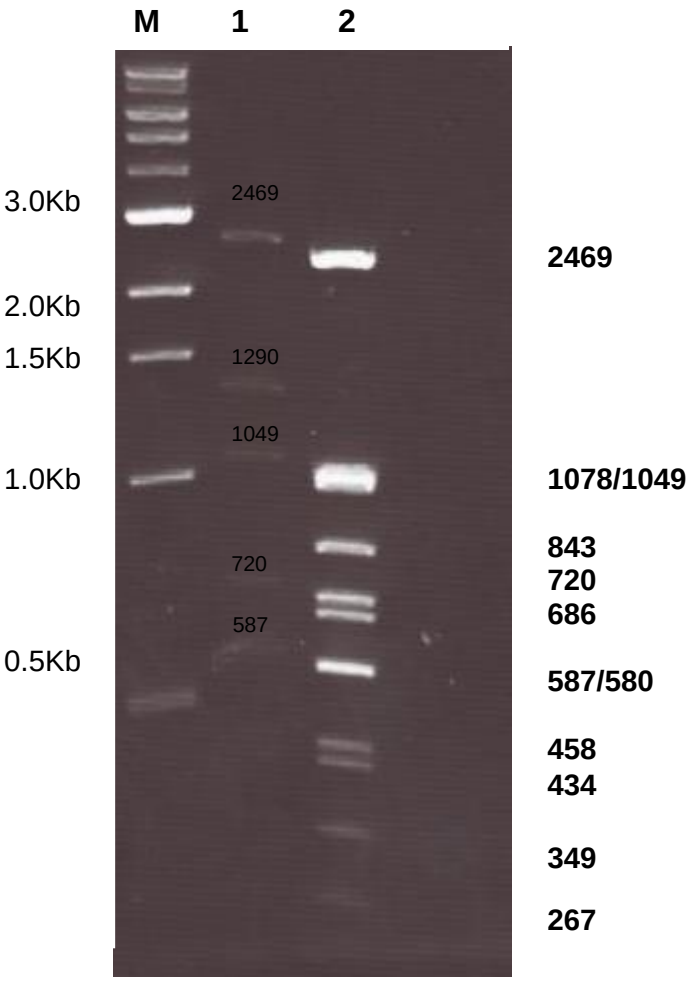

Figure 5.7. HaeIII restriction fragment patterns of recombinant plasmid pSVP27 carrying *cry41Ba* genes. Lane 1, HaeIII fragments of the construct pSVP27Cry41Ba/ORF2; lane 2, HaeIII fragments of the construct pSVP27Cry41Ba/ORF2ORF3; lane M, 1 kb DNA ladder. The corresponding base pair length values of each DNA fragment as predicted by NEB cutter are indicated next to the respective bands.

5.2.2 Preparation and characterisation of inclusion proteins from the recombinants

The recombinants obtained were grown on nutrient agar plates containing chloramphenicol (5 µg/ml) at 30°C for 4 days. Sporulation was checked by microscope and the sporulated cells were harvested as described in Section 2.2.9.3. Different crystal cured (Cry-) *B. thuringiensis* strains were evaluated for production of recombinant proteins. The proteins were analysed on 7.5% SDS-PAGE gel.

No parasporal inclusions or expressed proteins were observed in Bt strains IPS78/11 or 4Q7 (data not shown). However, the recombinant Cry41Aa/ORF2ORF3 yielded major bands with apparent molecular weights of of 80 kDa and 125 kDa when harvested from the 4D7 strain (Figure 5.8). Cry41Aa/ORF2 expressed devoid of ORF3, yielded a major band of 80 kDa (Figure 5.8). Hence the 80 kDa band is ORF2 observed in the expression of the two components of the split toxin Cry41Aa in Bt 4D7. The predicted molecular weight of ORF2 which consists of 825 amino acid residues is 93.7 kDa. The protein runs as 80 kDa band in our gel system. ORF3 which is composed of 737 amino acid residues with a predicted molecular weight of 83 kDa appears to migrate slower than its predicted molecular weight at approximately 125 kDa (Figure 5.8).

A weak expression of recombinant Cry41Ba was detected in 4Q7 (data not shown). No expression was obtained in IPS 78/11 and a strong expression was obtained in 4D7. Cry41Ba/ORF2ORF3 yielded a major band of 80 kDa in 4D7; the predicted molecular weight of ORF2 which consists of 840 amino acid residues is 95.6 kDa. ORF3 which is composed of 688 amino acid residues does not appear to migrate at its expected molecular weight of 78.5 kDa instead yielding a band at 62 kDa (Figure 5.9A). Recombinant Cry41Ba/ORF2 expressed without the ORF3 yielded a major band of 80 kDa (Figure 5.9B). Thus, expression of the recombinant proteins appeared to be strain-specific in *B. thuringiensis*.

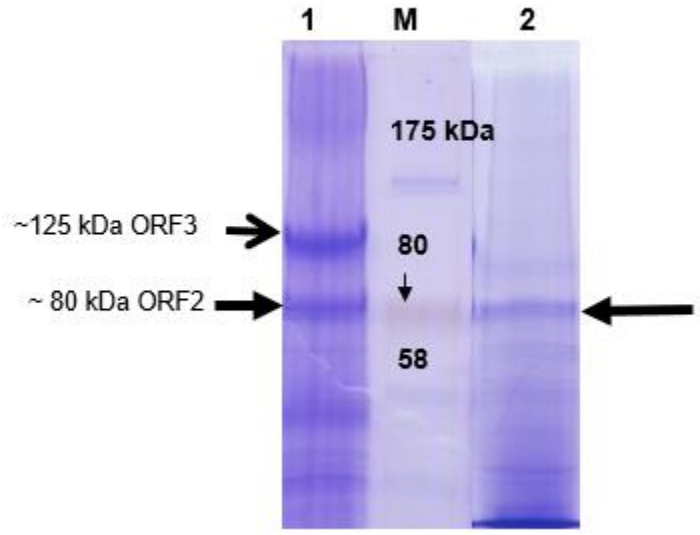

Figure 5.8. SDS-PAGE (7.5%) analysis of protein inclusions extracted from *B. thuringiensis* strain 4D7 expressing recombinant Cry41Aa at 30°C. Lane 1, recombinant Cry41Aa/ORF2ORF3; lane 2, recombinant Cry41Aa/ORF2; lane M, protein marker.

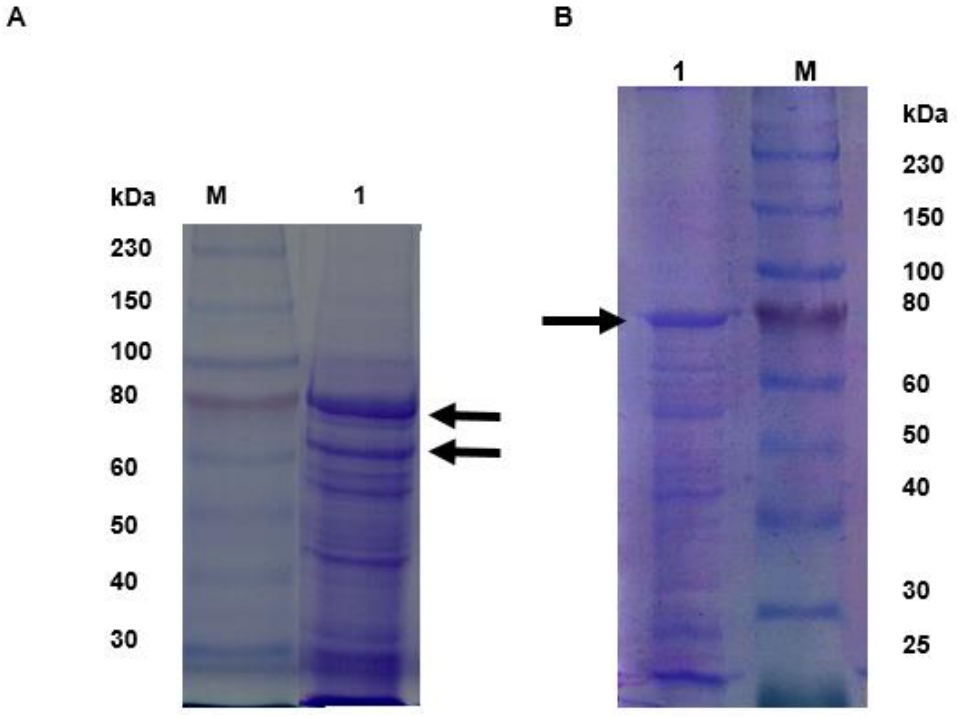

Figure 5.9. SDS-PAGE (7.5%) analysis of recombinant Cry41Ba inclusions extracted from *B. thuringiensis* strain 4D7 grown at 30°C. (A) Lane1, recombinant Cry41Ba/ORF2ORF3 showing ~80 kDa ORF2 and ~62 kDa ORF3. **(B)** Lane 1, recombinant Cry41Ba/ORF2 expressed without ORF3. Lane M is the protein marker.

5.2.2.1 Solubilisation and proteolytic processing of the toxins

In order to study the activity of the expressed recombinant proteins on mammalian cancer cells, we aimed at obtaining large quantities of the desired proteins in soluble and processed forms. Various buffers at different pH were used to solubilise the proteins as mentioned in Section 2.2.12. The protein was subjected to proteolytic treatment with trypsin at 1 mg/ml as described in Section 2.2.12. Attempts were made to solubilise and trypsin-activate the proteins in presence or absence of a reducing agent. The solubilisation assays suggested that 50 mM sodium carbonate buffer at pH 10.9 solubilised the protein in presence of 1 mM DTT. *In vitro* proteolytic processing of recombinant Cry41Aa/ORF2ORF3 by 1 mg/ml trypsin in the presence of DTT resulted in the partial digestion of 80 kDa protein band generating bands of about 60 kDa and 78 kDa (Figure 5.10A). Trypsin treatment of recombinant Cry41Ba/ORF2ORF3 yielded a major protein band of ~58 kDa (Figure 5.10B).

Deleting ORF3 resulted in expression of Cry41Aa/ORF2 which could not be obtained in the soluble form. Initial attempts at solubilising the recombinant Cry41Aa/ORF2 were not successful. Several buffers at different pH ranging from 2-11 were employed (data not shown). On the contrary, Cry41Ba/ORF2 could be readily solubilised and processed efficiently with trypsin in absence of ORF3 (data not shown). The trypsin-treated recombinant Cry41Aa and recombinant Cry41Ba protein samples containing DTT were dialysed against 50 mM Tris buffer pH 8 overnight (Section 2.2.13.2). The dialysed samples were analysed on the 7.5% SDS-PAGE. The dialysed fraction of solubilised recombinant Cry41Aa/ORF2ORF3 contained bands of ~125 kDa (ORF3) and 80 kDa (ORF2) (Figure 5.11, lane 2). The trypsin–treated dialysed fraction of

Cry41Aa/ORF2ORF3 contained a band of ~78kDa (Figure 5.11, lane 3). In case of Cry41BA/ORF2ORF3, a 80 KDa band was obtained in the dialysed fraction of the solubilised protein (Figure 5.11, lane 5) and a processed fragment of ~58 kDa was seen in the dialysed fraction of the trypsin-treated protein (Figure 5.11, lane 6). Protein quantitation was accomplished through Bradford assay. The dialysed samples were stored at -20°C until use in the toxicity assays.

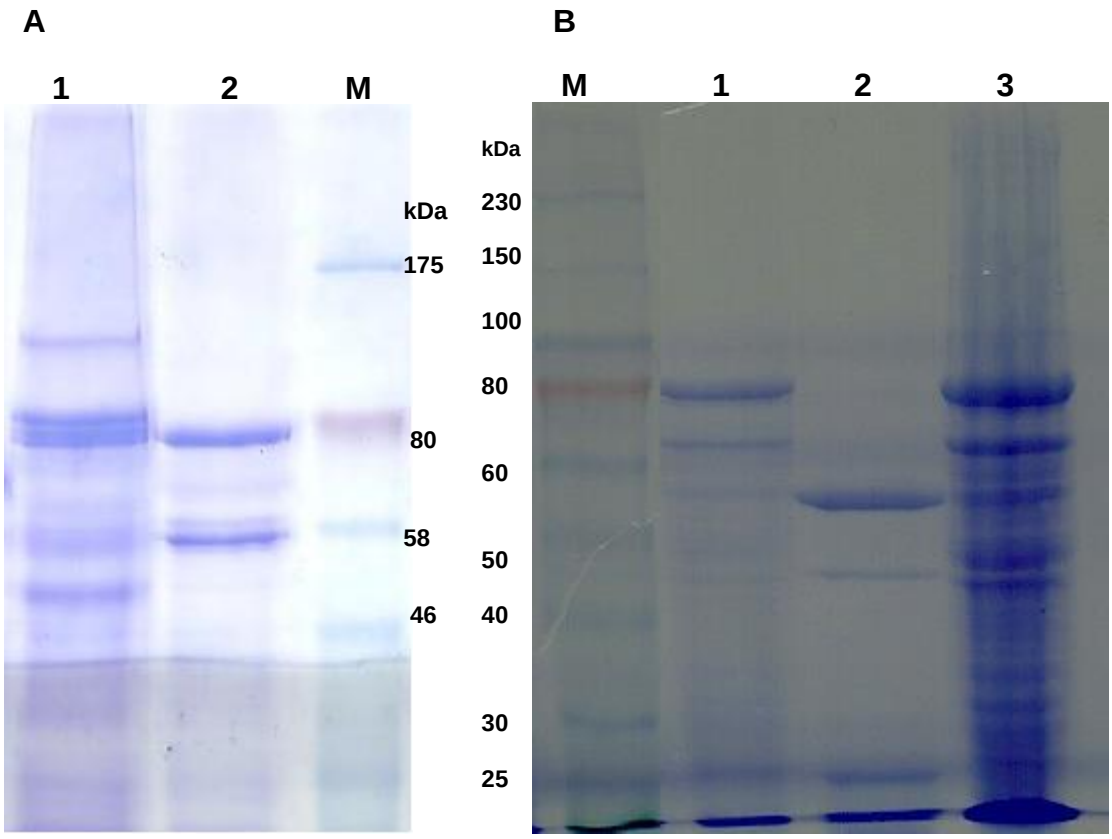

Figure 5.10. Solubilisation and trypsin-treatment of recombinant protein inclusions extracted from *B. thuringiensis* strain 4D7.

(A) Lane 1; solubilsed recombinant Cry41Aa/ORF2ORF3 in carbonate buffer pH 10.9 in presence of DTT; lane 2, trypsin- treated Cry41Aa/ORF2ORF3.

(**B)** Lane 1, solubilised recombinant Cry41Ba/ORF2ORF3 in carbonate buffer pH 11.0; lane 2, trypsin-treated Cry41Ba/ORF2ORF3; lane 3, untreated Cry41Ba/ORF2ORF3. Lane M is the protein marker.

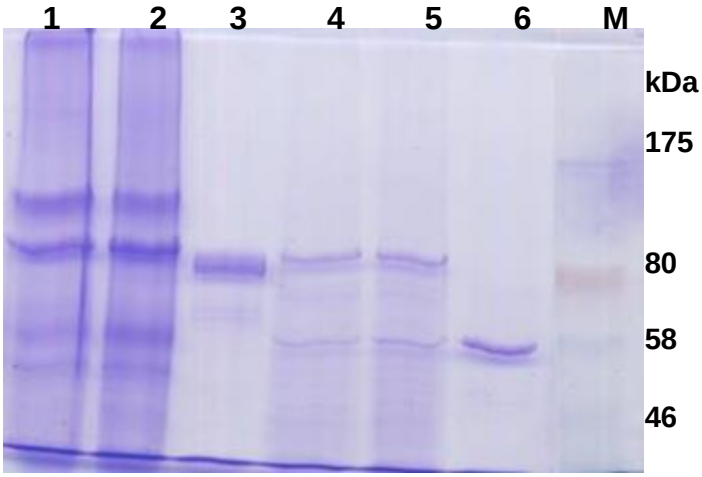

Figure 5.11. 7.5% SDS-PAGE analysis of the dialysis of the solubilised and trypsin-treated samples of recombinant Cry41Aa and Cry41Ba extracted from Bt 4D7. Lane1, solubilised recombinant Cry41Aa/ORF2ORF3 in carbonate buffer pH 11.0 in presence of DTT; lane 2, dialysed solubilised recombinant Cry41Aa/ORF2ORF3; lane 3, dialysed trypsin-treated recombinant Cry41Aa/ORF2ORF3; lane 4, solubilised recombinant Cry41Ba/ORF2ORF3 in carbonate buffer pH 11.0 in presence of DTT; lane 5, dialysed solubilised recombinant Cry41Ba/ORF2ORF3; lane 6, dialysed trypsin-treated recombinant Cry41Ba/ORF2ORF3; lane M, protein marker.

5.2.3 *In vitro* cytotoxic activity of the recombinant Bt toxins

The solubilised and the trypsin-treated proteins were tested on human cancer cell lines, HepG2 and HeLa. Cytotoxicity testing was performed using the Promega CellTIter-Blue cell viability assay (Section 2.2.15.2.2). Cytopathic effects were observed by phase-contrast microscopy. Since Yamashita et al. (2005) observed selective cytocidal effects of the parasporal protein at a final concentration of 10 µg/ml or 1 µg per well, we aimed at using the desired treatments within similar range in each well.

The trypsin-treated recombinant Cry41Aa/ORF2ORF3 protein induced marked morphological changes and cytotoxicity in HepG2 cells resulting in spillage of the intracellular contents into the extracellular milieu as observed under inverted phase contrast microscope (data not shown) and significant reduction in the number of viable cells (Figure 5.12) but exhibited no detectable morphological changes and only a weak toxicity against HeLa cells as seen by the CellTiter-blue assay (Figure 5.13B) and inverted phase-contrast microscopy (data not shown). The trypsin-treated purified recombinant Cry41Ba/ORF2ORF3 did not show any cytotoxic activity (Figure 5.12). No cell-killing activity was observed when HepG2 and HeLa cells were treated with a negative control of activated Cry8 toxins expressed in 4D7 (Figure 5.12). Cell viabilities of HepG2 and HeLa cells when treated with processed recombinant Cry 8, 4D7 and recombinant Cry41Ba protein inclusions were not affected (Figure 5.12). The positive control etoposide brought about significant cell-killing when used at a concentration of 0.2 mg/ml (Figure 5.12) or 0.1 mg/ml (Figure 5.13A). However, trypsin-treated

recombinant Cry41Aa/ORF2ORF3 was able to induce significantly greater cytotoxic effects when used at a two-fold lower concentration of 50 µg/ml than the etoposide. No cytopathic effects were observed on treatment with recombinant Cry41Ba/ORF2 even when used at higher concentrations (data not shown).

A dose-response study conducted showed that cell viability was significantly reduced in a dose-dependent manner after exposure of HepG2 cells to recombinant Cry41Aa/ORF2ORF3 trypsin- treated proteins using the CellTiter-Blue assay (Figure 5.13A & B). Dose-dependent cytotoxicity was induced in HepG2 cells by the trypsin-treated recombinant Cry41Aa/ORF2ORF3. Four-fold dilutions of trypsin-treated recombinant Cry41Aa/ORF2ORF3 exerted greater cytotoxic effects than etoposide (0.1 mg/ml) in HepG2 cells (Figure 5.13A). Cell death was observed with exposure of HepG2 cells to as low as 10 fold dilution of trypsin-treated recombinant Cry41Aa/ORF2ORF3. This dose-response study suggests a great variation in the susceptibility between the cell lines HepG2 and HeLa with HepG2 being highly susceptible to the trypsin-treated recombinant Cry41Aa/ORF2ORF3. Four-fold dilutions of trypsin-treated recombinant Cry41Aa/ORF2ORF3 did not exhibit any cytotoxic effects on HeLa cells (Figure 5.13B).

Effect of Bt recombinant proteins on HepG2 cells: 2h incubation with CellTiter-Blue

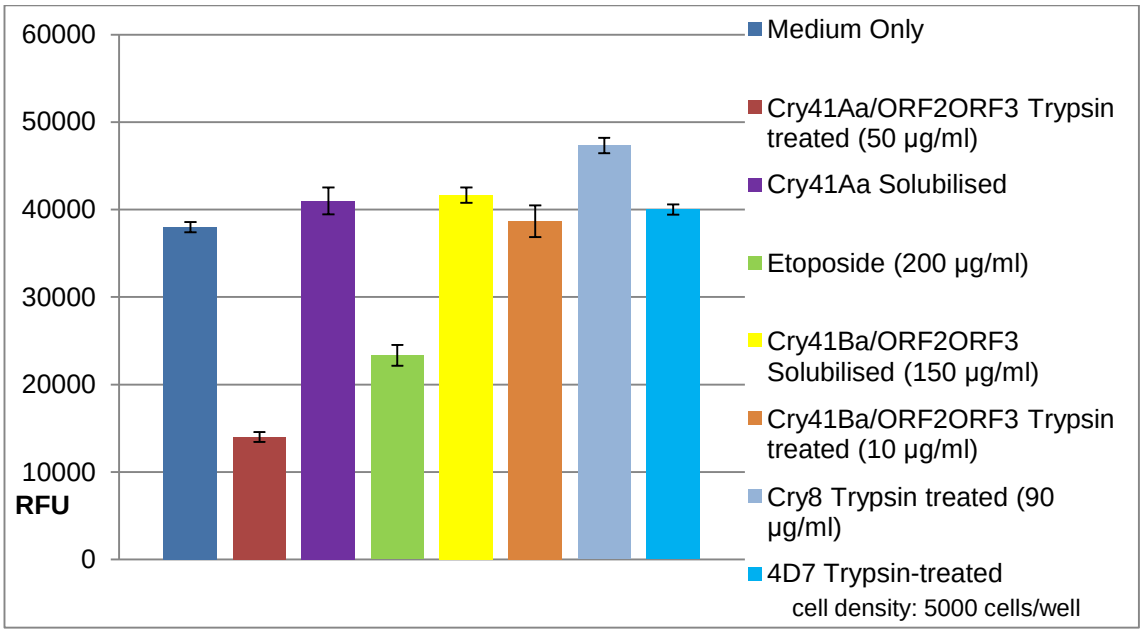

Figure 5.12. Effect of recombinant Bt proteins on cell viability of HepG2 cells.

Y- axis represents Relative Fluorescence Unit (RFU). Fluorescence was measured using a green filter with an excitation wavelength at 525 nm and emission wavelength 580-640 nm. Error bars denote SD of the mean of triplicate wells. Experiments are representative of at least five independent assays with each treatment.

A. Dose-response effect of trypsin-treated Cry41Aa/ORF2ORF3 on HepG2 cells: 4h incubation with CellTiter-Blue

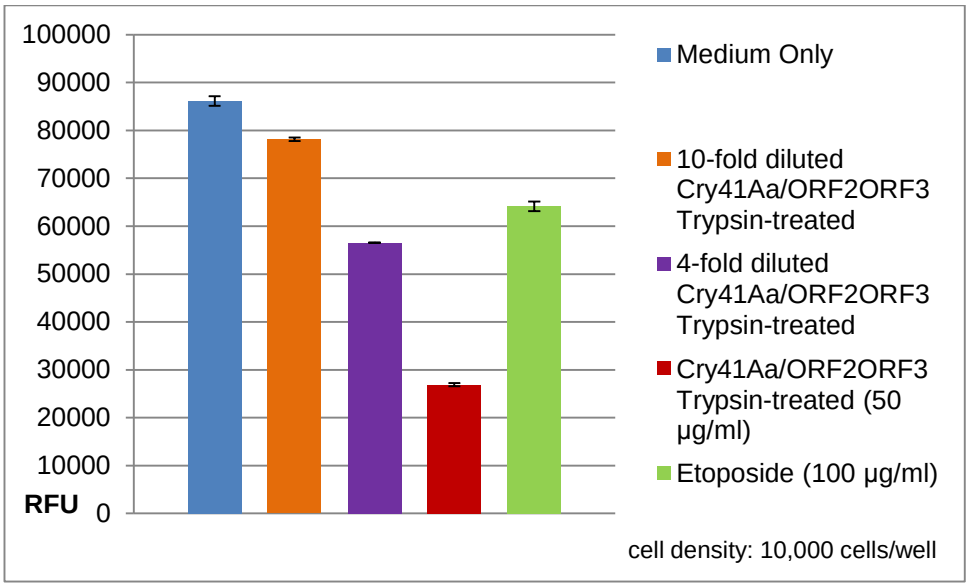

B. Dose-response effect of trypsin-treated Cry41Aa/ORF2ORF3 on HeLa cells: 4h incubation with CellTiter- Blue

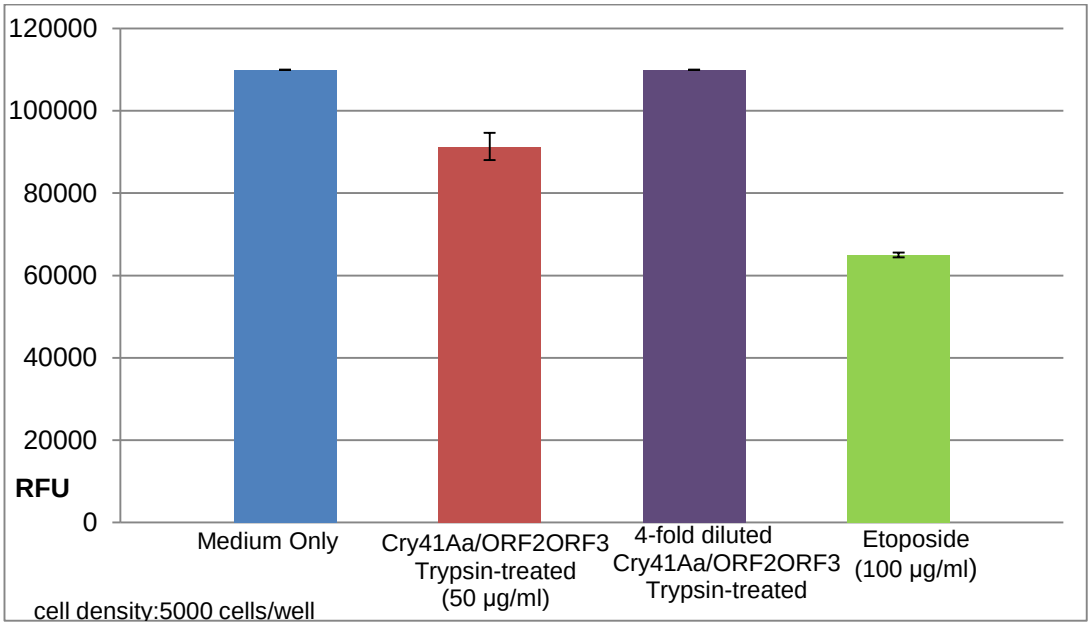

Figure 5.13. CellTiter- Blue assay indicating a dose-response analysis of trypsin-treated recombinant Cry41Aa/ORF2ORF3 protein on A. HepG2 cells B. HeLa cells. Y-axis represents Relative Fluorescence Unit (RFU). Effect of various dilutions of proteins were checked on HepG2 and HeLa cells. Error bars denote SD for the data derived from the individual wells (triplicates). Experiments are representative of at least three independent assays with each treatment.

5.2.4 Investigating the role of the ricin domain

Having analysed the cytotoxic activities of recombinants Cry41Aa and Cry41Ba, we further intended to investigate the factors that contribute to the cytotoxicity. We intended to investigate the role of ricin region contained within the ORF2 of the recombinants. Although the recombinant Cry41Ba did not show activity against HepG2 cells, since it contained the ricin domain as present in Cry41Aa and showed remarkable similarity to Cry41Aa, we decided to investigate the significance of the conserved domain.

PCR-mediated deletion of the ricin domain from ORF2 of pSVP27Cry41Aa/ORF2ORF3 and pSVP27Cry41Ba/ORF2ORF3 was carried out as schematically represented in Figure 5.14. PfuUltra Hotstart Master mix from Stratagene was used for the PCR. Primers were designed to amplify the entire toxin encoding plasmid but excluding the ricin domain. The forward primer (TAAAGGTGTGCAACTATCCCTTGAC) included the stop codon (red letters) of ORF2 at its 5' end whereas the 5' end of the reverse primer (TCGAGTGGTTAAGCCAATACCC) encoded the 713th codon of ORF2 (Figure 5.15A). Following amplification the PCR product was self-ligated to give a plasmid (pSVP27Cry41AaΔricin) encoding the Cry41Aa toxin with amino acids 714-825 deleted. Similarly, pSVP27Cry41BaΔRD mutant was created using the primers 5' TAAGTCGAGTTAAAAATATGTATTCGC 3' and 5' AGCTTGTGTTGTTGGAATGAACTCGA 3' which was intended to delete 453 base pairs of residues after conserved block 5 to include the ricin domain. The primers were also designed to encode a HindIII restriction site (AAGCTT) at the

ligation point thus allowing confirmation of the deletion of ricin domain from the parental *cry41Ba* gene as illustrated schematically in Figure 5.15B. Briefly, the reverse primer 41BaDelRR was designed to encode a part of the HindIII restriction site viz., AAGCT + 2066 bp downstream of the ORF2 start codon. The forward primer contained the missing T from the stop codon at its 5'end. Upon excision of the ricin domain, the resultant PCR amplicon thus had an engineered HindIII site (Figure 5.15B) to ascertain the successful excision of the ricin domain.

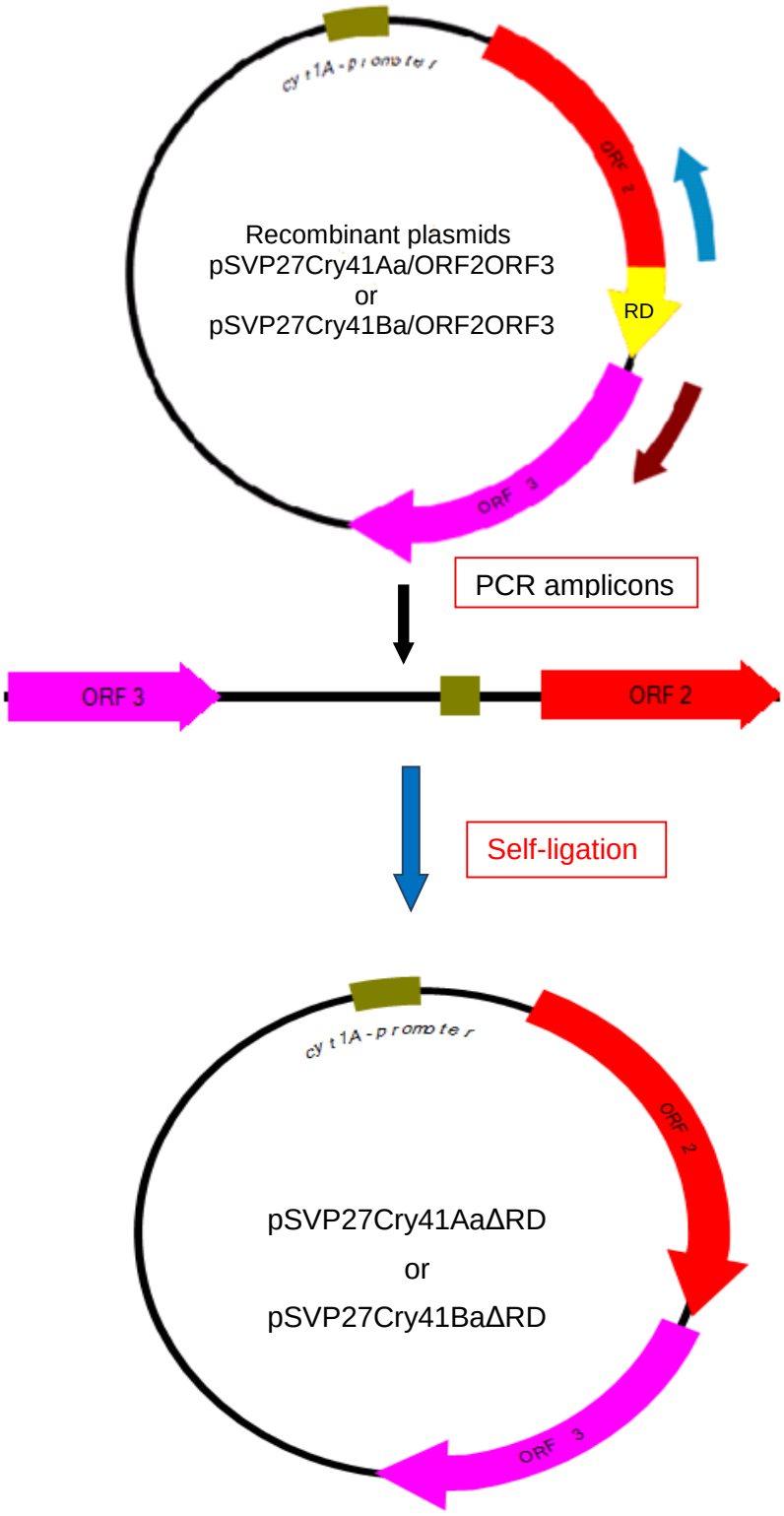

Figure 5.14. Schematic representation of the PCR-mediated deletion of the ricin domain from ORF2 of pSVP27Cry41Aa/ORF2ORF3 and pSVP27Cry41Ba/ORF2ORF3.

A

Forward primer

41rddelF 5’ TAAAGGTGTGCAACTATCCCTTGAC 3’

Reverse primer

41rddelR 5’ TCGAGTGGTTAAGCCAATACCC 3’

Primers annealing to pSVP27Cry41Aa/ORF2ORF3

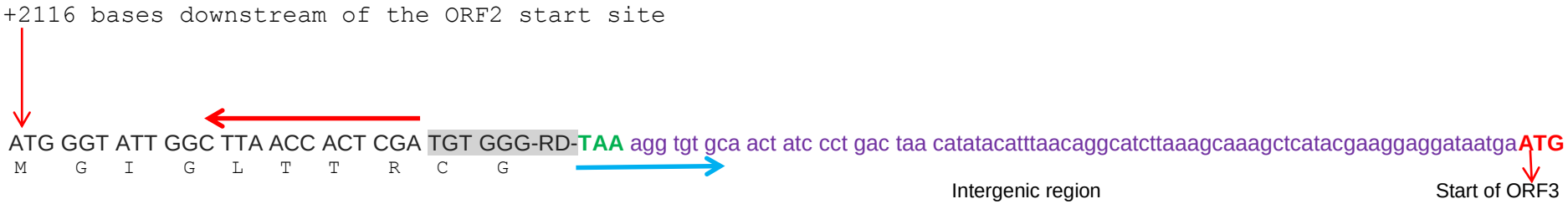

Ligation of amplified PCR amplicon with deleted ricin domain region

ATG GGT ATT GGC TTA ACC ACT CGA **TAA**aggtgtgcaactatccctgactaacatatacatttaacaggcatcttaaagcaaagctcatacgaaggaggataatga**ATG**
M G I G L T T R

B

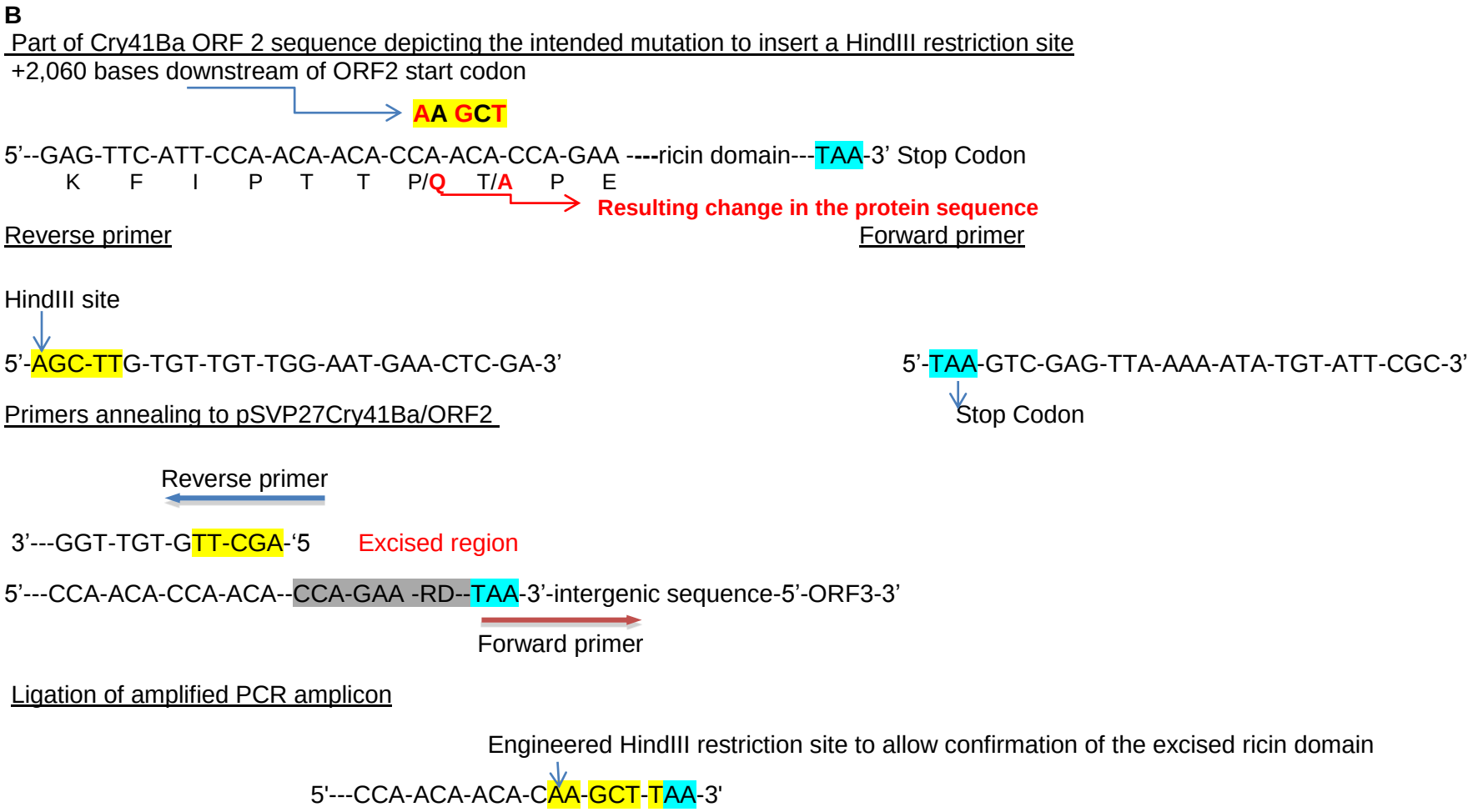

Figure 5.15. Ricin domain deletion. (A) Schematic depiction of binding of the primers to pSVP27Cry41Aa/ORF2ORF3 for deletion of the ricin domain. **(B)** Schematic representation of the strategy to excise ricin domain from ORF2 of *cry41Ba* gene. Ricin domain is denoted by RD and the excised region is highlighted in grey.

PCR amplicons were DpnI digested to remove the template DNA, gel purified, self-ligated using T4 DNA ligase and transformed into *E. coli* GM2163 to obtain unmethylated DNA for ease of transformation in *B. thuringiensis*. Transformants obtained were screened for the correct plasmid by restriction digestion. NdeI and KpnI restriction digestion profile differentiated the mutant pSVP27Cry41AaΔRD which lacked band of 1531 bp from the non-mutant template pSVP27Cry41Aa/ORF2ORF3 (Figure 5.16).

Similarly, pSVP27Cry41BaΔRD was digested with HindIII and HaeIII. The HaeIII restriction fragments differentiated the mutant from the non-mutant (Figure 5.17). However, further digestion with HindIII yielded bands of sizes 5949 and approximately 3000 base pairs instead of 5949, 1949 and 1743 as predicted by NEB cutter suggesting possible deletion in the HindIII site (data not shown). The construct was sequenced and this revealed the loss of 2 bases TA at 5' end of the forward primer. The deletion thus shifted the reading frame downstream to the intended mutation, encountering the further in-frame stop codon in the intergenic region between ORF2 and ORF3, thus extending the reading frame by further adding 14 amino acids onto the C-terminus of the protein as schematically demonstrated in Figure 5.18. Hoping that this wouldn't have an impact on the functionality of the desired mutant protein, as the frameshift caused changes only at the C-terminus of the protein; we decided to proceed further with the construct.

The constructs were transformed into *B. thringiensis* 4D7 strain for expression. The colony thus obtained in Bt with the desired plasmid was purified (Section 2.2.5.2) and re-transformed back in competent *E. coli* 109 to verify the transformant by restriction analysis.

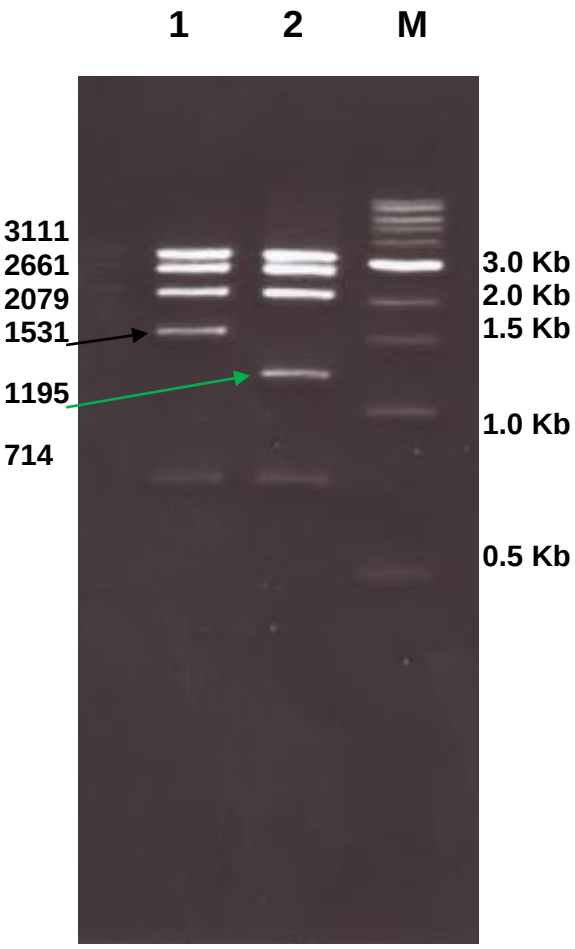

Figure 5.16. Restriction digestion profile confirming the deletion of the ricin domain from pSVP27Cry41Aa/ORF2ORF3.

Template pSVP27Cry41Aa/ORF2ORF3 (Lane 1) and mutant pSVP27Cry41AaΔRD (Lane 2) were digested with NdeI and KpnI. The mutant lacks the 1531 bp band (indicated by black arrow) as seen in the template DNA. Instead the mutant possesses the 1195 bp band (indicated by green arrow). Lane M is the 1 kb marker. The corresponding base pair length values of each DNA fragment as predicted by NEB cutter are shown to the left.

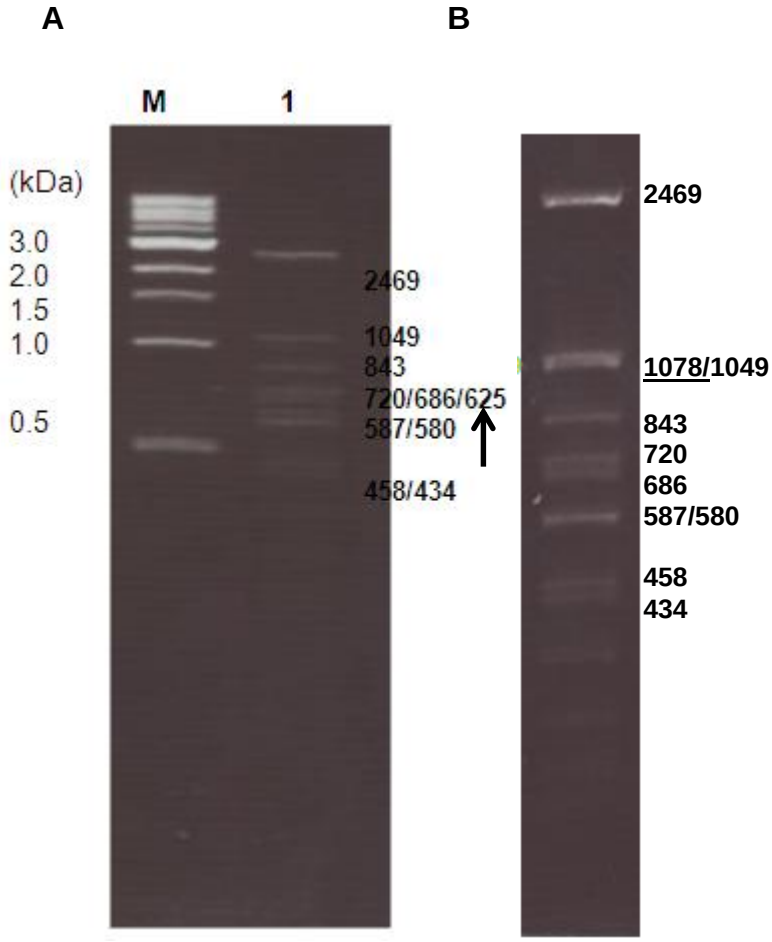

Figure 5.17. HaeIII restriction digestion profile confirming the deletion of the ricin domain from pSVP27Cry41Ba.

(A) pSVP27Cry41BaΔRD HaeIII fragments (Lane 1) **(B)** pSVP27Cry41Ba/ORF2ORF3 HaeIII fragments. The mutant has a band of 625 bp (black arrow) which is lacking from the template. The template has a band of 1078 bp (underlined) which is lacking from the mutant. Lane M is the 1 kb marker. The corresponding base pair length values of each DNA fragment as predicted by NEB cutter are shown to the right.

Intended pSVP27Cry41BaΔRD

+2042 bases downstream of ORF2 start codon

```
E   F   I   P   T   T   Q   A   *                    Intergenic region
GAG TTC ATT CCA ACA ACA CAA gCt TAA gtc gag tta aaa ata tgt att cgc aaaccgaatgttatctaaaaggagagtgttcaATG
                                                                                    Start codon ORF3
```

pSVP27Cry41BaΔRD after sequencing

```
  E   F   I   P   T   T   Q   A   S   R   V   K   N   M   Y   S   Q   T   N   V   I   *
GAG TTC ATT CCA ACA ACA CAA gCt Agt cga gtt aaa aat atg tat tcg caa acg aat gtt atc taa
```

Figure 5.18. Frameshift mutation in pSVP27Cry41BaΔRD. Deletion of ricin domain resulted in frameshift mutation in ORF2 in recombinant Cry41Ba encountering the further in-frame stop codon in the intergenic region before ORF3 thus extending the reading frame.

5.2.5 Preparation and characterisation of recombinant mutant proteins, Cry41AaΔRD and Cry41BaΔRD for activity on human cancer cells

The recombinants obtained were grown on nutrient agar plates containing chloramphenicol (5 µg/ml) at 30°C for 4 days. Sporulation was checked under the microscope and the sporulated cells were harvested as described in Section 2.2.9.3. The proteins were analysed on 7.5% SDS-PAGE gel.

Parasporal inclusions of the mutant Cry41AaΔRD yielded major bands of approximately 70 kDa and 125 kDa when harvested from 4D7 (Figure 5.19, lane 4). 70 kDa is the modified ORF2. 125 kDa band which is also seen in the recombinant Cry41Aa/ORF2ORF3 is ORF3 migrating slower than its predicted molecular weight at 125 kDa. The mutant Cry41BaΔRD yielded a major protein band of ~75 kDa (Figure 5.19, lane 7).

In order to study the activity of the recombinant mutant proteins thus expressed on mammalian cancer cells, we aimed at obtaining large quantities of the desired proteins in soluble and processed forms. Various buffers at different pH were used to solubilise the proteins. The proteins were processed with trypsin at 1 mg/ml as described in Section 2.2.12. Attempts were made to solubilise and trypsin activate the proteins in presence or absence of a reducing agent. The solubilisation assays suggested that 50 mM carbonate buffer at pH 11 solubilised the proteins efficiently in presence of 1 mM DTT. Trypsin in the presence of DTT

resulted in the partial digestion of 70 kDa protein band of mutant Cry41AaΔRD generating a band of about ~68 kDa (Figure 5.20, lane 2). Trypsin-treatment of mutant Cry41BaΔRD yielded a band of ~40 kDa (Figure 5.21, lane 6).

The solubilised and the trypsin-treated samples containing DTT were dialysed against 50 mM Tris buffer pH 8.0 overnight (Section 2.2.13.2). The dialysed solubilised protein samples when subjected to trypsin treatment at 1 mg/ml without DTT yielded the same results as above. Bradford method was employed to estimate the concentration of the protein samples (Section 2.2.11). The dialysed samples were frozen at -20 °C for further cell assays.

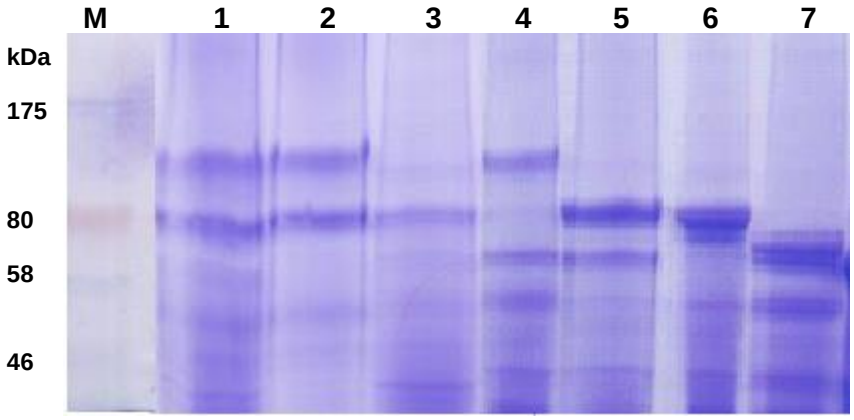

Figure 5.19. Solubilisation of the recombinant mutants of Cry41Aa and Cry41Ba toxins extracted from *B. thuringiensis* strain 4D7. Lane1; the total protein sample of Cry41Aa/ORF2ORF3 at pH 11; lane 2, the soluble fraction of Cry41Aa/ORF2ORF3 at pH 11; lane 3, the total protein sample of Cry41Aa/ORF2; lane 4, the soluble fraction of mutant Cry41AaΔRD; lane 5, the soluble fraction of Cry41Ba/ORF2ORF3; lane 6, the total protein sample of Cry41Ba/ORF2; lane 7, the soluble fraction of the mutant Cry41BaΔRD; lane M, protein marker.

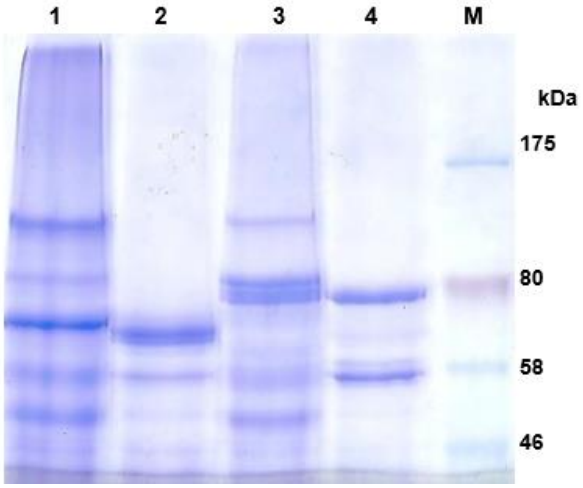

Figure 5.20. Solubilisation and proteolytic processing of Bt 4D7 expressed recombinant proteins Cry41Aa and mutant Cry41AaΔRD in a reducing environment. Lane1, solubilisation of the mutant Cry41AaΔRD in carbonate buffer, pH 11.0 (supernatant fraction); lane 2, trypsin-treatment of the mutant Cry41AaΔRD; lane 3; solubilisation of Cry41Aa/ORF2ORF3 in carbonate buffer, pH 11.0; lane 4; trypsin-treatment of Cry41Aa/ORF2ORF3. Note for the sake of clarity, data for recombinant Cry41Aa/ORF2ORF3 is presented again from Figure 5.10A.

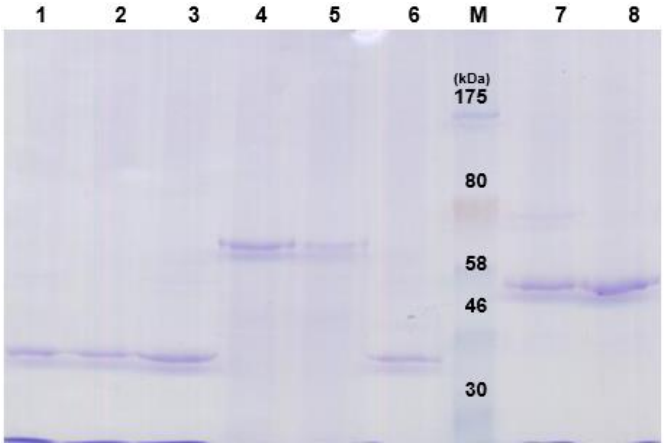

Figure 5.21. Solubilisation and proteolytic processing of the Bt 4D7 expressed mutant Cry41BaΔRD protein inclusions. Sodium carbonate buffers at various pH were used to solubilise and process the proteins. Lanes 1-3 are tryptic fragments of Cry41BaΔRD. Lane 1, trypsin-treatment overnight, pH 10; lane 2, trypsin-treatment overnight at pH 11; lane 3, trypsin-treatment for 1 h, pH 11; lane 4, soluble fraction of Cry41BaΔRD at pH 11; lane 5, soluble fraction of Cry41BaΔRD at pH 10; lane 6, trypsin-treatment at pH 10.5; lane M, protein marker; lane 7, trypsin treatment of the non-mutant recombinant Cry41Ba/ORF2ORF3 at pH 11; lane 8, trypsin treatment of the recombinant Cry41Ba/ORF2ORF3 at pH 10.

5.2.6 *In vitro* cytotoxic activity of the recombinant mutant Bt toxins

The solubilised and the trypsin-treated Cry41AaΔRD and Cry41BaΔRD proteins were tested on human cancer cell lines, HepG2 and HeLa. Effect on cell viability was assessed using the CellTIter-Blue cell viability assay kit (Section 2.2.15.2.2). Cytopathic effects were observed by phase-contrast microscopy.

The mutant trypsin-treated recombinant Cry41AaΔRD when used at a total protein concentration of 40 µg/ml exhibited cytotoxicity significantly reducing viability of HepG2 cells (Figure 5.22). This indicates lack of change of toxicity of Cry41Aa/ORF2ORF3 even when the ricin domain is deleted. The recombinant trypsin-treated Cry41AaΔRD induced cytotoxicity in HepG2 cells as seen in Figure 5.22 which shows the cell viability graphs for trypsin-treated Cry41AaΔRD and Cry41Aa/ORF2ORF3 used at concentrations of 40 and 50 µg/ml respectively on HepG2 cells with CellTiter-Blue assay. The trypsin-treated Cry41AaΔRD exhibited greater reduction in cell viability as compared to the soluble Cry41AaΔRD (Figure 5.22) indicating that N-terminal processing is required for enhanced cytocidal activity. Only a weak toxicity against HeLa cells were observed on treatment with trypsin-treated Cry41AaΔRD (Figure 5.23B) and inverted phase-contrast microscopy (data not shown). The trypsin-treated recombinant Cry41BaΔRD did not show any cytotoxic activity against HepG2 or HeLa cells (data not shown).

A dose-response study conducted showed that cell viability was significantly reduced in a dose-dependent manner after exposure of HepG2 cells to varying concentrations of recombinant mutant Cry41AaΔRD trypsin-treated proteins using the CellTiter-Blue assay as seen in case of Cry41Aa/ORF2ORF3 (Figure

5.23A). The dose response study further suggests a great variation in the susceptibility between the cell lines HepG2 and HeLa with HepG2 being highly susceptible to the trypsin-treated mutant Cry41AaΔRD. Four-fold dilutions of trypsin-treated recombinant Cry41AaΔRD did not exhibit any cytotoxic effects on HeLa cells (Figure 5.23B).

Dose-dependent cytotoxicity was induced in HepG2 cells by the trypsin-treated recombinant Cry41AaΔRD which was comparable to trypsin-treated Cry41Aa/ORF2ORF3. Trypsin-treated recombinant Cry41AaΔRD and Cry41Aa/ORF2ORF3 at concentrations of 1 µg per well each exerted comparable cytotoxic effects to etoposide (100 µg/ml) in HepG2 cells (Figure 5.24). Toxicity decreased with decreasing concentration of the trypsin-treated proteins. Two-fold dilution of trypsin-treated recombinant Cry41AaΔRD and Cry41Aa/ORF2ORF3 exerted lesser degree of cytotoxicity in HepG2. The cytotoxic effects effects were comparable to etoposide in HepG2 cells at two-fold dilution. Cell death was observed with exposure of HepG2 cells to as low as four-fold dilution of trypsin-treated recombinant proteins, Cry41AaΔRD and Cry41Aa/ORF2ORF3 (Figure 5.24).

Effect of Bt recombinant proteins on HepG2 cells: 2h incubation with CellTiter-Blue

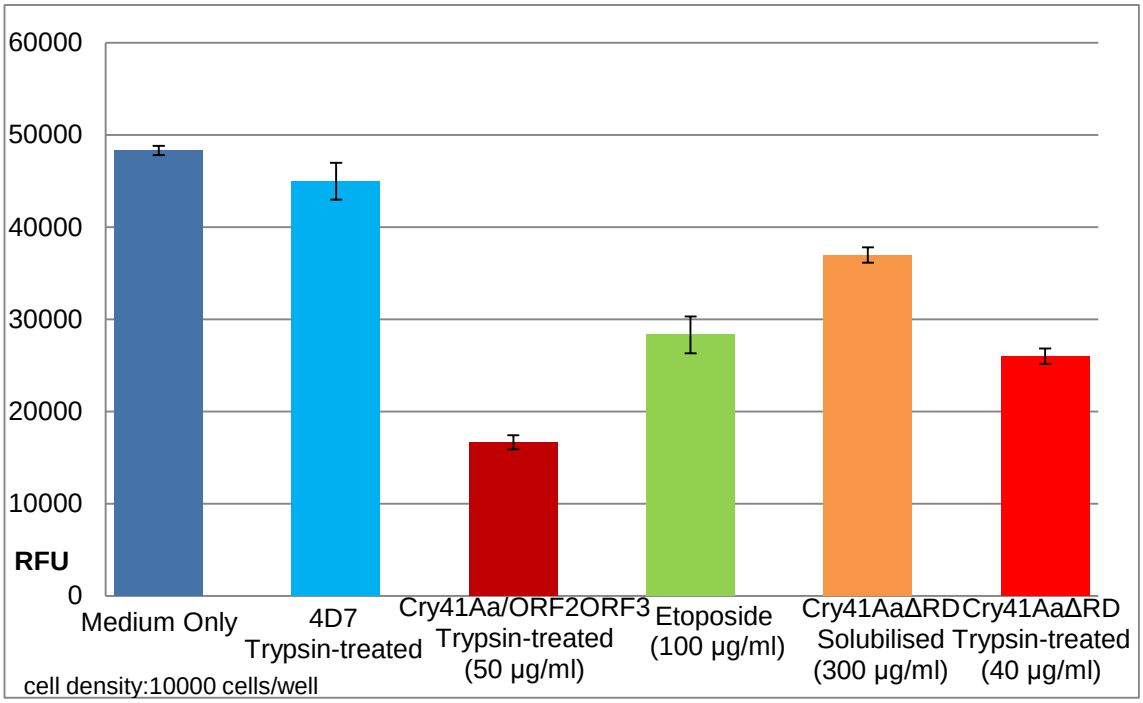

Figure 5.22. Effect of recombinant Cry41Aa protein and the mutant Cry41AaΔRD on viability of HepG2 cells. Y-axis represents Relative Fluorescence Unit (RFU). Error bars denote SD of the mean of triplicate wells. Experiments are representative of at least five independent assays with each treatment.

A. Dose-response effect of trypsin-treated recombinant mutant protein Cry41AaΔRD on HepG2 cells: 2h incubation with CellTiter- Blue

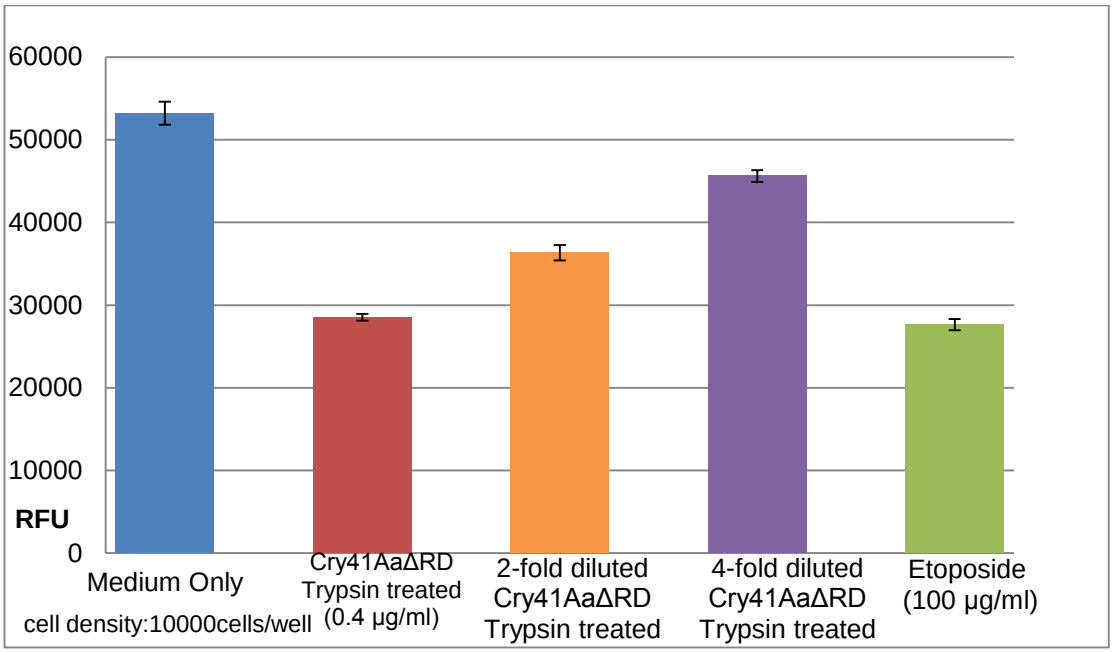

B. Dose-response effect of trypsin-treated recombinant mutant protein Cry41AaΔRD on HeLa cells: 2h incubation with CellTiter-Blue

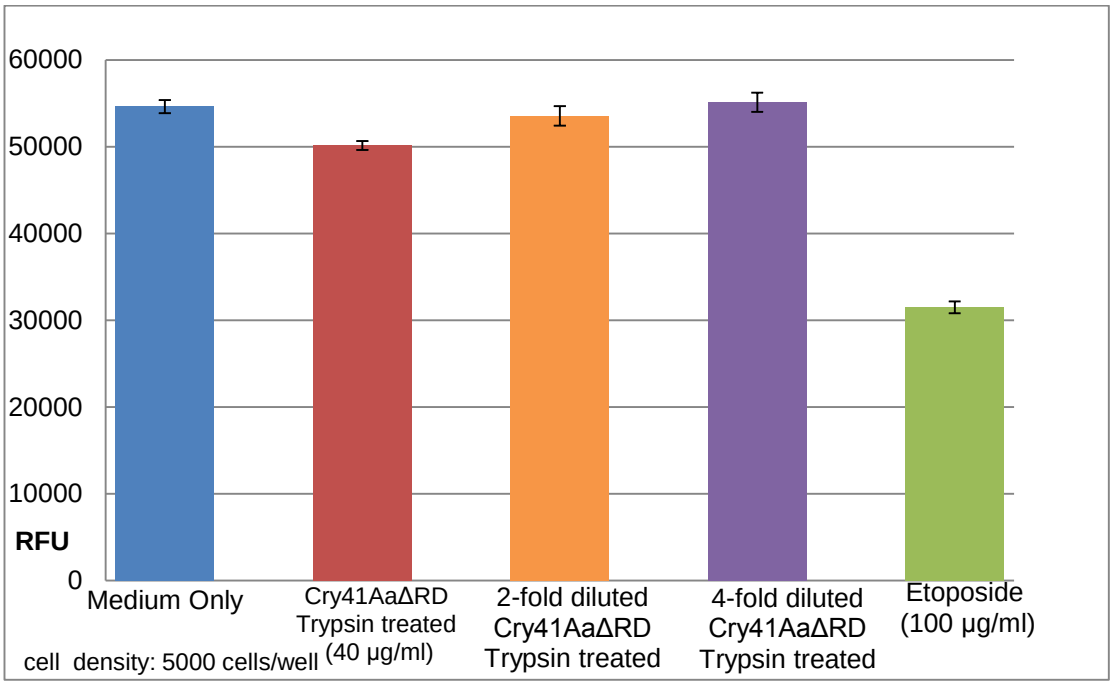

Figure 5.23. Dose-response curves of cytocidal activity associated with varying concentrations of trypsin-treated mutant Cry41AaΔRD on A. HepG2 cells & B. HeLa cells. Y-axis represents Relative Fluorescence Unit (RFU). Error bars denote SD for the data derived from the individual wells (triplicates). Experiments are representative of at least three independent assays with each treatment.

Comparison of dose-response effects of trypsin-treated recombinant Cry41Aa/ORF2ORF3 with mutant protein Cry41AaΔRD on HepG2 cells: 2h incubation with CellTiter-Blue

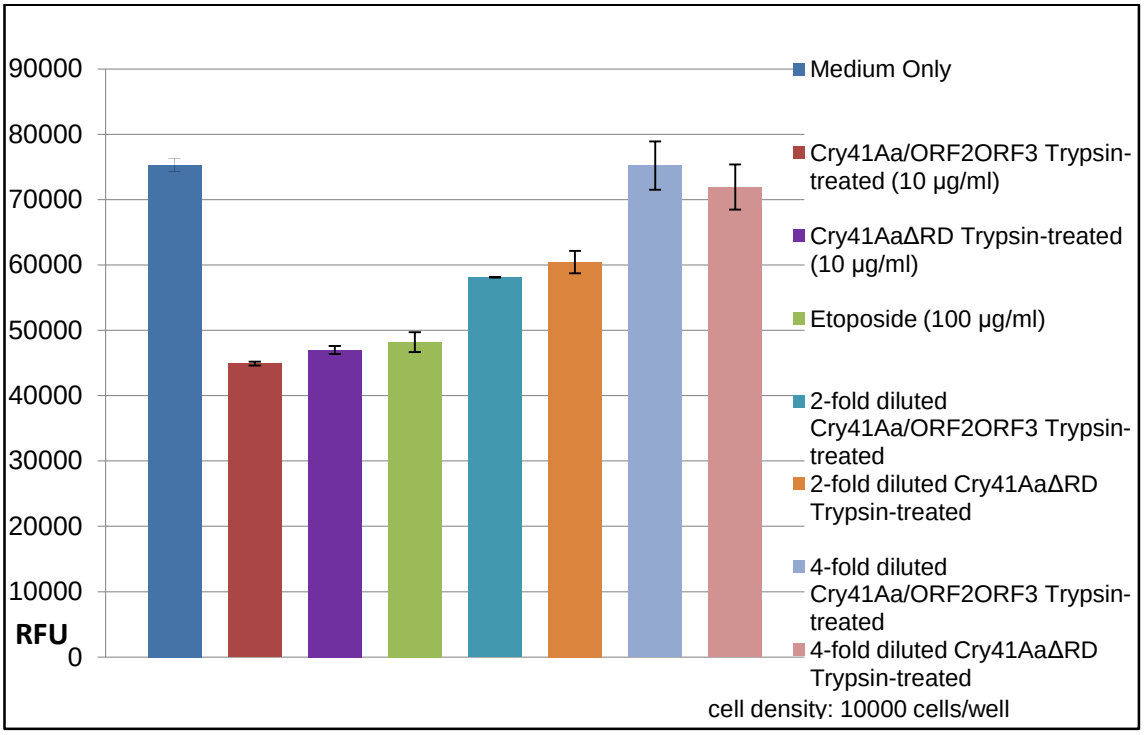

Figure 5.24. Dose-response curves of cytocidal activity associated with varying concentrations of trypsin-treated Cry41Aa and mutant Cry41AaΔRD on HepG2 cells. Y-axis represents Relative Fluorescence Unit (RFU). Error bars denote SD for the data derived from the individual wells (triplicates). Experiments are representative of at least three independent assays with each treatment.

5.3 Discussion

Successful overexpression of *cry41Aa* and *cry41Ba* genes were obtained in acrystalliferous *B. thuringiensis* strain 4D7 when cloned downstream of the Cyt promoter of the expression vector pSVP27. The recombinant protein Cry41Aa/ORF2ORF3 when treated with trypsin was cytotoxic to mammalian cancer cells. However no cytotoxicity was obtained in case of Cry41Ba which possesses significant similarity in overall sequence and in gene-organisation to Cry41Aa.

The recombinant protein Cry41Aa/ORF2ORF3 expressed in acrystalliferous Bt 4D7 was able to solubilise and be processed efficiently to a protease-resistant core by the proteolytic treatment in a reducing environment. Deleting ORF3 resulted in expression of Cry41Aa/ORF2 which could not be solubilised. Hence, suggesting that ORF3 is required for solubility. The solubility assays carried out are congruent with the assumed function of C-terminal ends of longer Cry δ-endotoxins. Proteolytic activation of Bt protoxins cleaves the C-terminal ends containing the conserved homology blocks 6-8 (Lightwood et al., 2000; Bravo et al., 2002). The C-terminal ends are implicated in crystal formation and efficient solubilisation by ensuring a high pH environment for certain protoxins (Park et al., 2000; Naimov et al., 2006; Barboza-Corona et al., 2012). However, Lenane et al. (2008) suggested that Orf2-5Ad derived from *B. thuringiensis* strain L366, being the primary component of the protein crystals, could still accomplish all the functions ascribed to the C-terminus. The Cry5A proteins are nematocidal proteins. Albeit *E. coli* expressed Cry5Ad and Orf2-5Ad proteins lack such

activity. To be noted is that Cry5Ad and Orf2-5Ad are produced as two separate proteins and hence is a split toxin similar to Cry41Aa and Cry41Ba. Vazquez-Padron et al. (2004) further reported that C-terminus containing variants of homology blocks 6-8 of Cry1Ab lacking the toxic core exhibits strong toxicity to *Bt* , *E. coli* and *Agrobacterium tumefaciens* when cloned and expressed in these bacteria. However, the ORF3 of Cry41Aa that was obtained in *E. coli* JM109 was devoid of any biological activity.

Rosso & Delecluse (1997) observed that just Orf2 of the otherwise toxic Cry19Aa to *Culex pipens* and *Anopheles stephensilarvae* exhibited no larvicidal activity. A combination of both proteins synergised the toxic effect of the split toxin Cry19Aa. In order to assess if ORF3 contributed to the cytotoxity of recombinant Cry41Aa/ORF2ORF3, the protein was expressed without ORF3. However, the solubility of ORF2 was severely affected when expressed without ORF3. Thus Cry41Aa/ORF2 could not be obtained in soluble form. On the contrary, Cry41Ba/ORF2 could be readily solubilised and processed efficiently with trypsin in absence of ORF3. It is pertinent to conclude that S-S linkages and cysteine residues present in the open reading frames imparts biological function to the C-terminus and hence varies between the various Cry proteins.

The present results demonstrate that the soluble recombinant Cry41Aa did not exhibit toxicity to the HepG2 cells. Trypsin-treatment was essential for the required cytocidal activity. This is in congruent with reports of activity of other parasporin toxins' against mammalian cell lines. For instance, Ito et al. (2004)

observed that the full length Cry46Aa protoxin from Bt strain A1547 demonstrated no apparent cytotoxic activity. However, the N-terminal truncated protein generated proteolytic processing with a relative molecular mass of 31 kDa exhibited cytocidal activity against MOLT-4 cells. The protease resistant core of approximately 78 kDa of recombinant Cry41Aa generated by trypsin treatment showed preferential activity against HepG2 cells. The solubilised form of the toxin lacked such activity. This is in accordance with previous studies conducted on *M. sexta* which suggested that presence of N-terminal peptide might preclude binding of the toxin to non-target membranes (Martens et al., 1995) inkling that pore forming ability of domain I is achieved only after proteolytic removal of the N-terminal peptide (Bravo et al., 2002). Similar studies ascribe the reduced toxicity of mutant insecticidal Cry1Ac protoxin in which N-terminal tryptic cleavage site has been removed by site-directed mutagenesis to the reduced rate of N-terminal activation (Bravo et al., 2002). In the homologous Cry1Ab protoxins, a mutation preventing N-terminal processing also demonstrated low toxicity to *M. sexta* larvae (Martens et al., 1995). Cry41Aa protoxins that bears a striking similarity to the insecticidal Bt Cry1A toxins might function in a similar manner. This is further validated by the fact that the solubilised mutant Cry41AaΔRD in which the ricin domain has been deleted from the C-terminus of ORF2 exhibits a moderate cytotoxicity as compared to the trypsin treated Cry41AaΔRD and the non-mutant trypsin-treated recombinant Cry41Aa/ORF2ORF3 toxin. This suggests that N-terminal activation is essential for the enhanced cytotoxic activity of the toxin Cry41Aa/ORF2ORF3.

The result of this study however differs with the previous study conducted by Yamashita et al. (2005) who found that solubilised Cry41Aa was not toxic to HepG2 cells whereas toxin treated with proteinase K / trypsin (yielding a 64 kDa fragment) was. The 64 kDa toxin derived from 88-kDa on protease treatment, is the cytocidal toxin in their case. However, when we treated our recombinant Cry41Aa toxin with trypsin we did not get a 64 kDa fragment but instead one that was only marginally smaller than the unprocessed toxin. We did though find that whilst the trypsin-activated toxin showed activity against HepG2 even a large excess of unprocessed toxin had no activity.

Evolutionary process has repeatedly coalesced $(QxW)_3$ scaffolds with proteins of diverse functionality imparting them with novel attributes thus evolving new proteins (Hazes, 1996). This domain has been observed in many unrelated proteins and it has been proposed that it adds carbohydrate binding functionality to these proteins and hence can confer specificity to proteins (Hazes, 1996). In an effort to further elucidate the role of the ricin domain, the domain was deleted from the recombinant Cry41Aa and Cry41Ba. The present results demonstrate that Cry41Aa retains / preserves its cytotoxic activity when expressed without the ricin domain. Ricin domain is not pre-requisite for cytotoxic activity of the inclusion proteins. Unlike Cry41Aa, the ricin domain-containing, and apoptotic-inducing, toxin pierisin is capable of killing HeLa cells (Matsushima-Hibiya et al., 2003). Mutagenesis studies suggested that the conserved QxW sequences in this domain were essential for toxicity, and most likely involved in binding to glycosphingolipid receptors on the cell surface. However our data indicate that this domain is not responsible for the HepG2 specificity. Although the non-toxic

components of botulinum neurotoxin that entails HA-33 comprising of two $(QxW)_3$ -like domains are presumed to have the role of protecting the neurotoxin against acidity and protease in the digestive tract thus facilitating transport of the toxin complex across the intestinal epithelium (Fujinaga et al., 2004). Whether the ricin domain possesses such protective role in case of cytocidal Cry41Aa needs to be ascertained.

Dose-dependent activity was observed in case of recombinant Cry41Aa/ORF2ORF3 and mutant Cry41AaΔRD. Amongst the cell lines assayed, the proteins were highly cytotoxic to HepG2 cells, which were more sensitive to the proteins than HeLa cells. This result is in accordance with other studies on parasporins that demonstrate a preferential activity against certain mammalian cancer cells. No defined rule for specificity of the parasporin toxins and no common features for resistant or sensitive cells to these toxins have been deduced so far.

6. The quest for new cytotoxic genes from *B. thuringiensis*

6.1 Introduction

In pursuit of new cytocidal toxins from Bt, we illustrate in this chapter the screening of novel recombinant Bt toxins isolated from collaborators in China. Recombinant Cry51Aa1 was delivered from Ming Sun's lab, Huazhong Agricultural University, Wuhan, China for the evaluation of its toxicity against cancer cell lines and insects. The gene (GenBank accession number DQ836184) was isolated from the *B. thuringiensis* strain F14-1. The gene was cloned into the shuttle vector, pHT304 and expressed in the acrystalliferous *B. thuringiensis* strain BMB171 (Huang et al., 2007). The protein showed toxicity to *Bombyx mori* (Sun et al., unpublished data). The *cry51Aa* gene is 930 bp in length yielding a polypeptide of 309 amino acid residues. Analysis of the protein sequence of Cry51Aa by Conserved Domain (CD) search (NCBI) (Marchler-Bauer & Bryant, 2004; Marchler-Bauer et al., 2009; Marchler-Bauer et al., 2011) revealed the presence of a putative ETX_MTX2 [pfam03318] domain. Cry51 shows a low sequence similarity to the known existing Bt Cry toxins with 21% identity to Cry15Aa being the highest and only 11% was shown to parasporin-2 and parasporin-4.

Cry65Aa1 was isolated from *B. thuringiensis* strain SBt003 by Sun et al., 2010 (unpublished). A Bt clone expressing Cry65 was obtained from China to evaluate its toxicity against human cancer cells and against insect pests. Cry65Aa1 is a three-domain toxin. The 118 kDa Cry65 protein occurs in crystals with a 54 kDa accompanying protein encoded in the same operon as Cry65. A 5.3 kb PCR

product containing Cry65 and a gene encoding 54 kDa poplypeptide was cloned and expressed in the Bt recombinant strain BMB1281. The recombinant BMB1281 co-expresses both the polypeptides from the native toxin operon.

Blast search by NCBI indicates 100% identity to the protein annotated as cancer-cell killing Cry protein from Bt serovar Pakistani strain T13001. Cry65Aa1 shows 29% identity to parasporin-3 and 24% identity to Cry1Ac. Since no known insecticidal activity of Cry65 against crop pests was identified, its activity against cancer cell lines was assessed.

6.2 Results

6.2.1 Preparation of Cry51Aa δ-endotoxin inclusion proteins, solubilisation and proteolytic processing of the toxins

Acrystalliferous Bt strain BMB171 harbouring recombinant pHT3101Cry51Aa1 was grown on nutrient agar plates containing erythromycin at 5 µg/ml at 30°C for 2 days. Sporulation was checked under the microscope and the sporulated cells were harvested as described in Section 2.2.9.3. Crystals were observed under the microscope. The proteins were analysed on 12.5% SDS-PAGE gel. A major band of 34 kDa was observed which was in accordance with the predicted theoretical molecular weight of the protein calculated using ProtParam tool of ExPASy (http://web.expasy.org/protparam/) (Bjellqvist et al., 1993; Bjeallqvist et al., 1994; Gasteiger et al., 2005) (Figure 6.1).

Cry51Aa crystals were purified by sucrose density gradient (Section 2.2.13.1). Various buffer solutions over a broad pH range of 2.0-11.0 were used to solubilise the crystals. Solubility of the purified recombinant Cry51 tended to be higher in both alkaline and acidic solutions but low at pH 8.3 (Figure 6.2). Solubilisation of the purified Cry51Aa was most efficiently accomplished by treatment with 50 mM sodium carbonate pH 10.9 for 1 h at 37°C and also by treatment with 10 mM HCl pH 3 as observed in case of Cry45Aa (parasporin-4) (Okumura et al., 2006). However, since in most studies the inclusion bodies of Bt are solubilised in alkaline conditions mimicking the alkaline midgut of insects, further experiments were carried out in alkaline conditions. The toxin was processed by trypsin (2 mg/ml) prepared in 50 mM sodium carbonate pH 10.9 to a lower molecular weight approximately 28 kDa protein as expected (Figure 6.2). The solubilised and the

trypsin-treated Cry51Aa toxin were applied to an anion-exchange column, Resource Q (Amersham Pharmacia Biotech, UK) at a flow rate of 1 ml/min at 4°C. The yield of the purified protein was determined by Bradford method by using BSA as the standard (Section 2.2.11). The concentration of purified solubilised sample was found to be 1.0 mg/ml. The concentration of the purified trypsin-treated sample which showed two bands of approximate sizes of 28 kDa and 26 kDa (Figure 6.3) was found to be 0.5 mg/ml. The samples were frozen at -20 °C for toxicity assays.

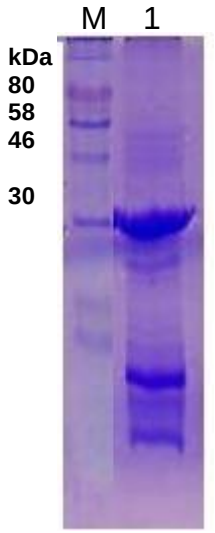

Figure 6.1. 12.5% SDS-PAGE profile of recombinant Cry51Aa expressed in acrystalliferous *B. thuringiensis* strain BMB171. Lane 1, Cry51Aa protein inclusions; lane M, protein marker.

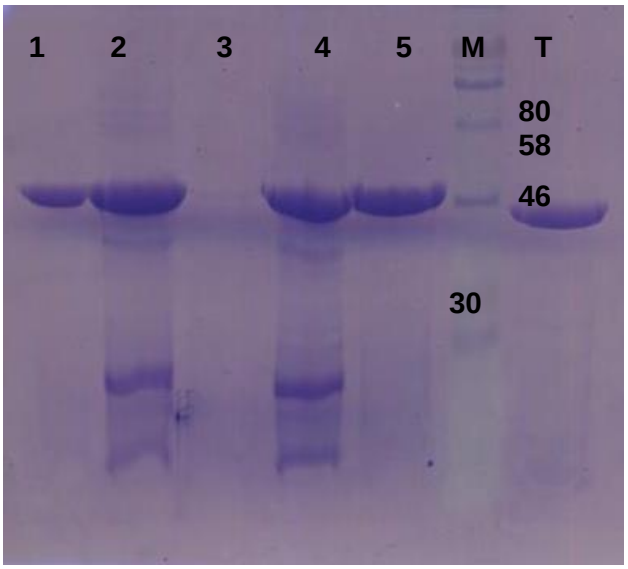

Figure 6.2. 12.5% SDS-PAGE depicting solubility profile and proteolytic processing of recombinant Cry51Aa. Recombinant Cry51Aa solubilised with 10 mM hydrochloric acid, supernatant fraction (Lane 1); sodium hydrogen carbonate pH 8.3, total sample (Lane 2); soluble fraction (Lane 3); sodium carbonate pH 10.9 total sample (Lane 4); soluble fraction (Lane 5). Lane M is the protein marker in kDa. Lane T is the trypsin- treated sample.

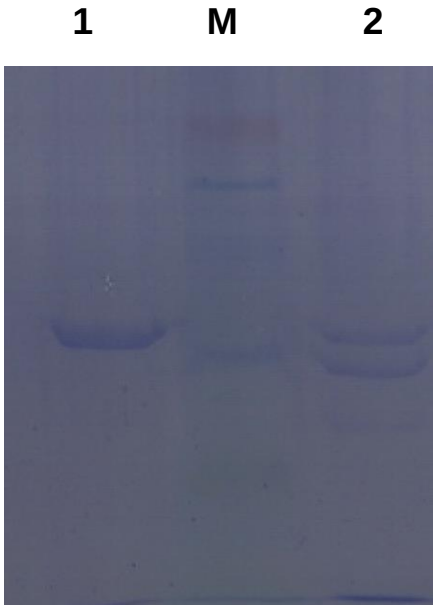

Figure 6.3. 12.5% SDS-PAGE analysis of resource Q purified Cry 51 used for toxicity assays. Lane 1, solubilised Cry51; lane 2, trypsin-treated Cry51; lane M, protein marker.

6.2.2 Preparation of Cry65Aa δ-endotoxin inclusion proteins, solubilisation and proteolytic processing of the toxin

Acrystalliferous Bt strain BMB1281 harbouring recombinant Cry65Aa1 was grown on sterile nutrient agar plates containing chloramphenicol at 5 µg/ml at 30°C for 2 days. Sporulation was checked under the microscope and the sporulated cells were harvested as described in Section 2.2.9.3. Crystals were observed under the microscope. The proteins were analysed on 7.5% SDS-PAGE gel. Two major bands of expected sizes of 118 kDa and 54 kDa were observed (Figure 6.4). Both the polypeptides were co-expressed from the native toxin operon. The 118 kDa protein represents Cry65Aa1.

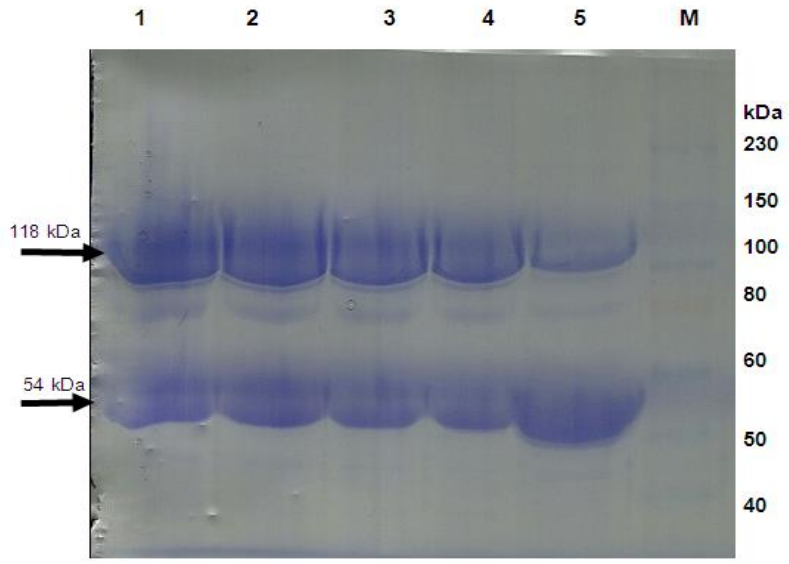

Figure 6.4. 7.5% SDS-PAGE profile of recombinant Cry65Aa1 expressed in Bt strain BMB1281. Lanes 1-5, various dilutions of the recombinant Cry65Aa1 protein viz., 5, 4, 3, 2 and 1 µl of the protein samples were run on the gel. The samples were diluted with sterile distilled water to make up to a total volume of 5 µl. Lane M is the protein marker.

Attempts were made to solubilise and trypsin activate the proteins in the presence as well as absence of a reducing agent. The solubilisation assays suggested that 50 mM Carbonate buffer at pH 10.9 solubilised the proteins in the presence of 1 mM DTT. Trypsin in presence of DTT resulted in the generation of two conspicuous bands with estimated sizes of 60 and 45 kDa (Figure 6.5). The solubilised and the trypsin treated samples containing DTT were dialysed against 50 mM sodium carbonate buffer, pH 10.9 (Section 2.2.13.2). Bradford method was employed to estimate the total protein concentration (Section 2.2.11). The total protein concentration was found to be approximately 5 mg/ml. The dialysed samples were frozen at -20°C for further cell assays.

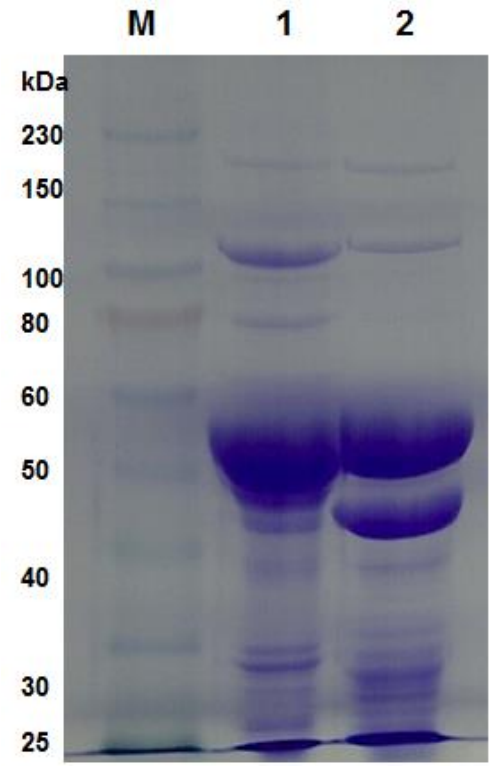

Figure 6.5. 7.5% SDS-PAGE analysis of the dialysed Cry65 samples. Lane 1, soluble fraction of Cry65; lane 2, tryptic fragments of Cry65; lane M, protein marker.

6.2.3 Toxicity evaluation of *B. thuringiensis* proteins

6.2.3.1 Assessment of insecticidal activity against *Plutella xylostella*

The toxicity of recombinant proteins Cry51Aa and Cry65Aa was tested against insecticidal Cry1Ac susceptible G88 and resistant NO-QA populations using leaf –dip and diet based assays according to the protocol described in Section 2.2.15.1. No mortality was observed in the case of either population treated with crystals, solubilised or trypsin-treated recombinant Cry51 and Cry65 toxins at a concentration of 1 mg/ml.

6.2.3.2 *In vitro* cytocidal activity of the *B. thuringiensis* toxins

The solubilised and the trypsin-treated proteins were tested on human cancer cell line, HepG2. Cytocidal activities of Cry51 and Cry65 were evaluated using the CellTiter- Blue assay (Section 2.2.15.2.2). Cytopathic effects were observed under a phase-contrast microscopy. The degree of cytotoxicity was further verified by CellTiter-Glo luminescent cell viability assays kit (Promega). The experiments were set up in 96-well opaque white flat-bottomed microplates (Costar) (Section 2.2.15.2.3). No cytotoxicity was observed in case of solubilised at 100 µg/ml or trypsin treated Cry51 at 50 µg/ml (Figure 6.6). The positive control etoposide at 100 µg/ml brought about significant cell killing. The trypsin-treated Bt protein from A1462, the parasporin-3 producer bought about significant cell killing when used at 50 µg/ml (Figure 6.6). Trypsin-treated recombinant Cry51 did not induce any morphological changes to HepG2 cells as observed using a phase-contrast microscope (data not shown). Cytotoxic activity of trypsin-treated

Cry51 was further assessed by CellTiter-Glo luminescent cell viability assay. However, no cytotoxicity was observed with Cry51 (Figure 6.7).

Phase contrast microscopy (data not shown) coupled with the CellTiter Blue assay revealed that recombinant solubilised Cry65 and the trypsin-treated Cry65 did not exhibit any cytocidal effects on HepG2 cells when used at a concentration of 1 mg/ml (Figure 6.8). A lower concentration of etoposide at 0.01 mg/ml was used to predict any equivalent activity by the recombinant Cry65. The positive control, etoposide brought about significant cell-killing (Figure 6.8).

Effect of solubilised and trypsin-treated recombinant Cry51 on HepG2 cells: 2h incubation with CellTiter- Blue

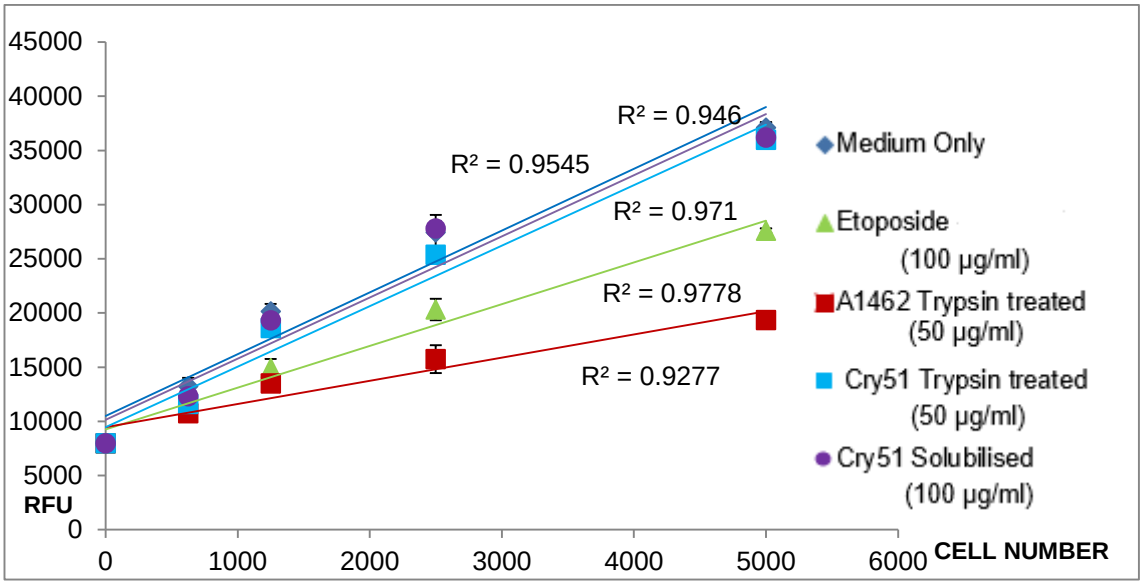

Figure 6.6. Effect of recombinant Cry51 on viability of HepG2 cells. X-axis represents the cell number and Y- axis represents Relative Fluorescence Unit (RFU). Fluorescence was measured using a green filter with an excitation wavelength at 525nm and emission wavelength 580-640nm. Error bars denote SD of the mean of triplicate wells.

Effect of trypsin-treated recombinant Cry 51 on HepG2 cells: CellTiter- Glo assay

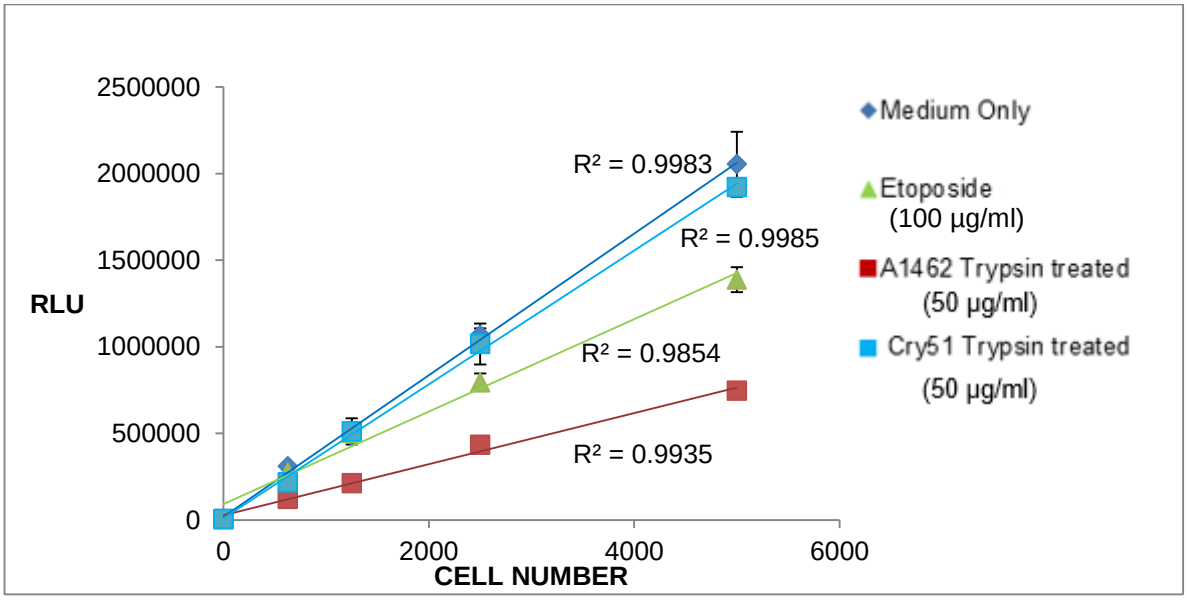

Figure 6.7. Cytotoxicity of trypsin treated Cry51 was further assessed by bioluminescent detection of ATP. X-axis represents the cell number and Y- axis represents Relative Luminescence Unit (RLU). Error bars denote SD for the data derived from the individual wells (triplicates). An integration time of 0.5 s was used.

Effect of solubilised and trypsin-treated recombinant Cry65 on HepG2 cells: 2h incubation with CellTiter- Blue

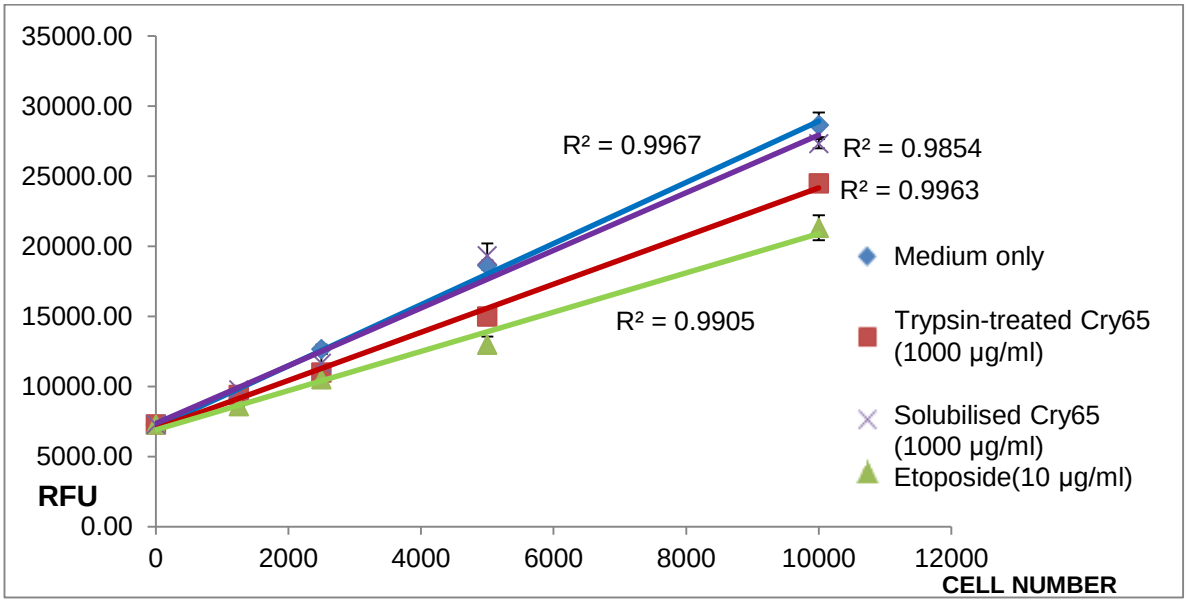

Figure 6.8. Effect of recombinant Cry65 proteins on viability of HepG2 cells. X-axis represents the cell number and Y-axis represents Relative Fluorescence Unit (RFU). Error bars denote SD of the mean of triplicate wells.

6.3 Discussion

We hereby present efficient solubilisation and proteolytic processing of recombinants Cry51Aa and Cry65Aa with unknown toxicity profiles. The 34 kDa recombinant Cry51Aa was obtained in soluble forms in both alkaline and acidic solutions. The protein dissolved well in buffers above pH 10 and below pH 4. It remained in the crystal form at pH 8.5. The solubility profile of the recombinant Cry51Aa demonstrated pH dependence similar to that of the recombinant parasporin-4, Cry45Aa precursor (Okumura et al., 2006) and to the native crystals of *B. thuringiensis* var *san diego*, a coleopteran specific δ-endotoxin (Koller et al., 1992). Koller et al. (1992) observed that the native crystals from the *B. thuringiensis* var *san diego* dissolved well in the universal buffers at above pH 10 and below pH 4 but remained in crystal form between pH 5.0 and pH 9.5. The recombinant Cry51 toxin was processed by trypsin (2 mg/ml) to a lower molecular weight protein approximately 28 kDa protein. Recombinant Cry65Aa1 was efficiently solubilised by treatment with sodium carbonate, pH 10.9 yielding bands of 117 kDa and 60 kDa in the supernatant fraction. Trypsin-treatment generated two major bands at circa 60 kDa and 45 kDa which need further investigation.

Initial screens performed here suggested that the recombinant Cry51A and Cry65 are not cytotoxic to the human cancer cell line, HepG2. The trypsin- treated Cry51Aa and Cry65Aa proteins showed no cytopathic effects as observed using phase-contrast microscopy and further corroborated by CellTiter-Blue and

CellTiter-Glo assays. The recombinant proteins were not toxic to the cabbage pest, *Plutella xylostella*. Whether they exert toxicity on other insects or cell lines, need to be further ascertained.

In order to harness the potency of Bt proteins possessing cytocidal activity against human cancer cells and in order to evaluate the ecological risk assessment Bt proteins exerting undesirable effects in non-target organisms , a wide toxicity screening of the Bt isolates are required. It is imperative that proper *in vitro* toxicity assays are carried out to avoid misleading results. Screening would also lead to understanding of the diversity of the parasporin genes, their occurrence, distribution and frequency. The toxicity screening would also further evaluate the safety of *B. thuringiensis* δ-endotoxins used in agriculture in transgenic plants or as biopesticides. Hence, for maximal utilisation of these toxins, it is vital that cytotoxic activities are properly assessed.

7. Discussion

The present work has implications not only for the ecological risk assessment of *B. thuringiensis* toxins used in agricultural products but also for the development of anti-cancer drugs.

A variety of insect resistant genetically modified crops, particularly cotton and maize, in which *B. thuringiensis* toxins are expressed are cultivated globally particularly in Africa, Asia and America (Gatehouse, 2008; Sanahuja et al., 2011). The knowledge that some of the *B. thuringiensis* toxins exhibit cytocidal activity against mammalian cells is of natural concern. This not only threatens the usage of new toxins in agricultural products but also requires risk assessment of food derived from genetically engineered plants. Recently, there has been a report of a modified *B. thuringiensis* toxin affecting non-target human cells. *In vitro* cytotoxic effects of modified Cry1Ab toxins were observed on a human embryonic kidney 259 cell line. The modified Cry1Ab toxin extracted from GM plants caused plasma membrane disruption, thus inducing necrotic effects at 100 ppm (Mesnage et al., 2011).

In nature, plants and bacteria protect themselves with potent toxins that can kill mammalian cells non-specifically (Goodsell, 2001). Several pharmaceutical drugs are based upon secondary metabolites produced by such plants and bacteria. Understanding the interaction of the Bt cancer killing toxins with their

host may help in deriving useful products and pharmaceuticals. Since the ecological role of the cytocidal toxins from Bt is unclear, it would be intriguing to study the interactions that lead to production of the cytotoxic proteins from *B. thuringiensis*. Understanding the diversity and distribution pattern of the parasporin producing *B. thuringiensis* like that of other microbes would be a vital tool in bioprospecting (the quest for novel biological samples for use in medicine and industry).

The present research evaluated the cytotoxic activity of several native *B. thuringiensis* strains, and further examined the cytotoxicity of several δ-endotoxins from *B. thuringiensis*. Cytotoxic activity was not found in all the crystal proteins investigated thus suggesting that the unique activity is present in only a few. These cytocidal toxins were found to be nontoxic to the crucifer pest, *Plutella xylostella*.

The present study resulted in establishment of an expression system for the overproduction of recombinant Cry41Aa protein that belongs to parasporin-3 family. The *cry41Aa* gene was cloned and homologously expressed in the host bacterium Bt. The *cry41Ba* gene from SBt021 with 49% identity to *cry41Aa* gene was cloned and expressed for comparative studies. Successful overexpression of the *cry41Aa* and *cry41Ba* genes were obtained in the acrystalliferous *B. thuringiensis* strain 4D7 when cloned downstream of the *cyt1A* promoter. The recombinant Cry41Aa/ORF2ORF3 when treated with trypsin was cytotoxic to hepatic cell line, HepG2. However no cytotoxicity was obtained in case of recombinant Cry41Ba which possess a similar gene organisation to Cry41Aa.

The recombinant Cry41Aa toxin when treated with trypsin exhibited preferential cytotoxic activity resulting in significant killing of HepG2 cells whilst HeLa cells were unaffected, by the same concentration of toxin. No cytotoxic activity was demonstrated by the solubilised but non- proteolytically treated protein. Further, our studies demonstrated that it is not the 64 kDa band resulting from proteolytic degradation of 88 kDa band that is cytotoxic to the cells as reported by Yamashita et al., 2005. But the cytotoxic activity is demonstrated by the protease resistant core of approximately 78 kDa resulting from the trypsin treatment of 80 kDa Cry41Aa toxin. This is in congruence with reports of activity of other parasporin toxins against mammalian cell lines. For instance, Ito et al. (2004) observed that the full length Cry46Aa protoxin from Bt strain A1547 demonstrated no apparent cytotoxic activity. However, the N-terminal truncated protein generated by proteolytic processing, and with a relative molecular mass of 31kDa exhibited cytocidal activity against MOLT-4 cells (Ito et al., 2004). A similar phenomenon was also observed in the case of insecticidal Cry1 toxins. The crystalline inclusions ingested by the susceptible insect pests are dissolved in the alkaline milieu of the insect gut and the solubilised protoxins are inactive until cleaved by midgut proteases to yield a protease- resistant core of 60-70 kDa (Schnepf et al., 1998). Bravo et al. (2002) suggested that N-terminal activation is essential for the mechanism of Bt Cry1Ac insecticidal toxin**.** This is in accordance with previous studies conducted on crop pest *M. sexta* which suggested that presence of N-terminal peptide might preclude binding of the toxin to non-target membranes (Martens et al., 1995) suggesting that pore forming ability of domain I is achieved only after proteolytic removal of the N-terminal peptide (Bravo et al., 2002). The studies ascribed the reduced toxicity of mutant insecticidal Cry1Ac protoxin in

which N-terminal tryptic cleavage site has been removed by site-directed mutagenesis to the reduced rate of N-terminal activation (Bravo et al., 2002). In the homologous Cry1Ab protoxins, a similar mutation preventing N-terminal processing also demonstrated low toxicity to *M. sexta* larvae (Martens et al., 1995). It can be inferred from the results that the cytotoxic activity is modulated by N-terminal activation during proteolysis as suggested in case of Bt Cry1Ac insecticidal toxins in which the N-terminus of the toxin modulates the activity of the toxin (Kouskoura et al., 2001). Cry41Aa protoxins which bear a striking sequence similarity to the insecticidal Bt Cry1A toxin might function in a similar manner. This is further substantiated by our result that the solubilised mutant Cry41AaΔRD in which the ricin domain has been deleted from the C-terminal of ORF2 also only exhibits a moderate cytotoxicity as compared to the trypsin treated Cry41AaΔRD and the non-mutant trypsin-treated recombinant Cry41Aa toxin. This suggests that N-terminal activation is essential for the enhanced cytotoxic activity of the toxin Cry41Aa.

Since these toxins exhibit cytotoxic effects against cancer cells, they could potentially be particularly useful as cancer drugs as modifications that alter a healthy cell into cancerous ones are extremely subtle. Since parasporins studied thus far are endowed with ability to identify unique cancer cell attributes that distinguishes them from healthy cells, these toxins can potentially be used in anticancer therapy facilitating selective eradication of cancer whilst minimizing side effects to normal cells. There have been reports of usage of bacterial proteins for cancer therapy. In late 1800's vaccines comprised of two attenuated bacterial species *Streptococcus pyogenes* and *Serratia marcescents* were used

to successfully treat carcinomas, lymphomas, melanomas and sarcomas (Richardson et al., 1999; Zacharski & Sukhatme, 2005). Bacterial endotoxins for instance lipopolysaccharides have also been tested for cancer treatment. Pathogenic species of anaerobic *Clostridia* were shown to proliferate preferentially within the necrotic tumour regions in animals resulting in tumour regression. However, it was accompanied by acute systemic side effects resulting in the death of the subject (Malmgren & Flanigan, 1955; Minton, 2003). The non-pathogenic strain of *Clostridia* for instance M55, however did not result in significant tumour regression (Carey et al., 1967). Bacterial toxins *per se* or in conjunction with anticancer drugs or irradiation could possibly result in effective cancer treatment (Carswell et al., 1975). The bacterial spores of the genetically modified strain *C. novyi*-NT that lacks lethal toxin have demonstrated specific target activity without causing any toxic side effects. Mice injected intravenously with spores of *Clostridium sporogene* or *C. histolyticum* resulted in marked lysis of tumour tissues. Additionally, *Clostridium* was undetected in the normal tissues of the injected mice (Thiele et al., 1963). Bacterial spores have been engineered to deliver anticancer agents, cytotoxic peptides and therapeutic proteins and as vectors for gene therapy (Patyar et al., 2010). Since Cry41Aa toxins demonstrate selective activity against hepatic carcinoma, it has potential to be developed as a promising drug. Further, there are reports that parasporin-2 proteins have limited toxicity to normal tissues and are able to discriminate between leukemic and normal T cells (Ito et al., 2004). Hence, the cancer-killing proteins from *B. thuringiensis* can potentially be used in cancer treatment.

The present work expands our understanding of various open reading frames of the *cry41Aa* and *cry41Ba* genes. The recombinant Cry41Aa/ORF2ORF3 expressed in acrystalliferous Bt 4D7 was solubilised and processed efficiently to a protease-resistant core by the proteolytic treatment in a reducing environment. Deleting ORF3 resulted in expression of Cry41Aa/ORF2 with an altered solubility. Hence, suggesting that ORF3 is required for solubility. The solubility assays carried out are congruent with the assumed function of C-terminal ends of longer Cry δ-endotoxins. Proteolytic activation of *B. thuringiensis* protoxins cleaves the C-terminal ends containing the conserved homology blocks 6-8 (Schnepf et al., 1998). The C-terminal ends are implicated in crystal formation and efficient solubilisation (Park et al., 2000). However, Lenane et al. (2008) suggested that Orf2-5Ad derived from *B. thuringiensis* strain L366, being the primary component of the protein crystals could still accomplish all the functions ascribed to the C-terminus. Vazquez-Padron et al. (2004) reported that the C-terminus containing homology blocks 6-8 of Cry41Ab lacking the toxic core exhibits strong toxicity to Bt, *E. coli* and *Agrobacterium tumefaciens* when cloned and expressed in these bacteria. However, we found that the ORF3 of Cry41Aa that was obtained in *E. coli* JM109 was devoid of any biological activity.

The present study assessed if ORF3 synergised the cytotoxicity of recombinant Cry41Aa as it was observed by Ross & Delecuse (1997) that a combination of Cry19Aa and its non-toxic component Orf2 synergised the toxic effect of the split toxin Cry19Aa against *Culex pipens* and *Anopheles stephensilarvae*. In order to assess if ORF3 contributed to the cytotoxity of recombinant Cry41Aa, the protein was expressed without the C-terminus. However, the solubility of ORF2 was

severely affected when expressed without ORF3. Thus Cry41Aa/ORF2 could not be obtained in soluble form. On the contrary, Cry41Ba/ORF2 could be readily solubilised and processed efficiently with trypsin in absence of ORF3.

In this study we investigated the role of the $(QxW)_3$ scaffold, that belongs to the ricin superfamily, in imparting cytotoxic properties to recombinant Cry41Aa. Evolutionary process has repeatedly coalesced $(QxW)_3$ scaffolds with proteins of diverse functionality imparting them with novel attributes thus evolving new proteins (Hazes, 1996). In an attempt to further elucidate the role of the ricin domain, the domain was deleted from the recombinant pSVP27Cry41Aa and pSVP27Cry41Ba. The present results demonstrate that Cry41Aa retains / preserves its cytotoxic activity when expressed without the ricin domain. Ricin domain is not pre-requisite for cytotoxic activity of the crystal proteins. Though the non-toxic components of *C. botulinum* neurotoxin that entails HA-33 comprising of two $(QxW)_3$ like domains are presumed to have the role of protecting the neurotoxin against acidity and protease in the digestive tract (Fujinaga et al., 2004). Whether ricin domain possesses such protective role in case of cytocidal Cry41Aa needs to be ascertained.

The research attempted various domain swaps and mutations in the domain II loop regions in order to evaluate their role in cytotoxicity. Domain swaps have been used for generating new specificities in Bt toxins (de Maagd et al., 2001). Liu & Dean (2006) redesigned Cry1A domain II loop regions to resemble that of Cry4Ba resulting in a Cry1Aa mutant with moderate insecticidal activity against *C. pipiens*. Abdullah et al. (2003) carried out mutagenesis of the loop 3 region of

Cry4Ba to mimic that of Cry4Aa introducing toxicity against Culex species. Similar research needs to be carried out with the Bt parasporins which might lead to generation of new specificities as in case of insecticidal Bt toxins.

Our investigation has opened several avenues for future research which would look into the mechanism of the cytotoxicity, assess *in vitro* cytotoxicity and conduct structural studies. Further, identification and isolation of the receptors involved in the cytotoxicity of these toxins would lead to a better understanding of the mode of action. An in depth understanding of parasporin diversity and mechanism of action would aid in their effective utilization. Thus, the possibility of mimicking molecules based on the architecture of parasporins to be used as a novel chemotherapy drug in cancer treatments cannot be ruled out.

8. Cited References

Abe, Y., Shimada, H. & Kitada, S. 2008. Raft-targeting and Oligomerization of Parasporin-2, a *Bacillus thuringiensis* Crystal Protein with Anti-Tumour Activity. *Journal of Biochemistry,* 143**,** 269-275.

Agaisse, H., Gominet, M., Økstad, O. A., Kolstø, A.-B. & Lereclus, D. 1999. PlcR is a pleiotropic regulator of extracellular virulence factor gene expression in *Bacillus thuringiensis*. *Molecular Microbiology,* 32**,** 1043-1053.

Agaisse, H. & Lereclus, D. 1994. Expression in *Bacillus subtilis* of the *Bacillus thuringiensis* cryIIIA toxin gene is not dependent on a sporulation-specific sigma factor and is increased in a spo0A mutant. *J Bacteriol,* 176**,** 4734-4741.

Agaisse, H. & Lereclus, D. 1995. How does *Bacillus thuringiensis* produce so much insecticidal crystal protein? *J. Bacteriol.,* 177**,** 6027-6032.

Ahmed, A. S., Gogal Jr, R. M. & Walsh, J. E. 1994. A new rapid and simple non-radioactive assay to monitor and determine the proliferation of lymphocytes: an alternative to [3H]thymidine incorporation assay. *Journal of Immunological Methods,* 170**,** 211-224.

Akhurst, R. J., Lyness, E. W., Zhang, Q. Y., Cooper, D. J. & Pinnock, D. E. 1997. A 16S rRNA gene oligonucleotide probe for identification of *Bacillus thuringiensis* isolates from sheep fleece. *J Invertebr Pathol,* 69**,** 24-30.

Akiba, T., Abe, Y., Kitada, S., Kusaka, Y., Ito, A., Ichimatsu, T., Katayama, H., Akao, T., Higuchi, K., Mizuki, E., Ohba, M., Kanai, R. & Harata, K. 2009. Crystal Structure of the Parasporin-2 *Bacillus thuringiensis* Toxin That Recognizes Cancer Cells. *Journal of Molecular Biology,* 386**,** 121-133.

Armstrong, J. L., Rohrmann, G. F. & Beaudreau, G. S. 1985. Delta endotoxin of *Bacillus thuringiensis* subsp. *israelensis*. *J Bacteriol,* 161**,** 39-46.

Arnold, K., Bordoli, L., Kopp, J. & Schwede, T. 2006. The SWISS-MODEL workspace: a web-based environment for protein structure homology modelling. *Bioinformatics,* 22**,** 195-201.

Aronson, A. I. 1993. The two faces of *Bacillus thuringiensis*: insecticidal proteins and post-exponential survival. *Molecular microbiology,* 7**,** 489-96.

Aronson, A. I., Han, E. S., Mcgaughey, W. & Johnson, D. 1991. The solubility of inclusion proteins from *Bacillus thuringiensis* is dependent upon protoxin composition and is a factor in toxicity to insects. *Appl. Environ. Microbiol.,* 57**,** 981-986.

Aronson, A. I. & Shai, Y. 2001. Why *Bacillus thuringiensis* insecticidal toxins are so effective: unique features of their mode of action. *FEMS Microbiology Letters,* 195**,** 1-8.

Arora, N., Ahmad, T., Rajagopal, R. & Bhatnagar, R. K. 2003. A constitutively expressed 36 kDa exochitinase from *Bacillus thuringiensis* HD-1. *Biochem Biophys Res Commun,* 307**,** 620-625.

Ash, C., Farrow, J. a. E., Dorsch, M., Stackebrandt, E. & Collins, M. D. 1991. Comparative Analysis of *Bacillus anthracis*, *Bacillus cereus*, and Related Species on the Basis of Reverse Transcriptase Sequencing of 16S rRNA. *International Journal of Systematic Bacteriology,* 41**,** 343-346.

Barboza-Corona, J. E., De La Fuente-Salcido, N., Alva-Murillo, N., Ochoa-Zarzosa, A. & Lopez-Meza, J. E. 2009. Activity of bacteriocins synthesized by *Bacillus thuringiensis* against *Staphylococcus aureus* isolates associated to bovine mastitis. *Vet Microbiol,* 138**,** 179-183.

Barboza-Corona, J. E., Park, H. W., Bideshi, D. K. & Federici, B. A. 2012. The 60-kilodalton protein encoded by *orf2* in the *cry19A* operon of *Bacillus*

thuringiensis subsp. *jegathesan* functions like a C-terminal crystallization domain. *Appl Environ Microbiol,* 78**,** 2005-2012.

Barloy, F., Lecadet, M. M. & Delecluse, A. 1998. Distribution of clostridial *cry*-like genes among *Bacillus thuringiensis* and *Clostridium* strains. *Curr Microbiol,* 36**,** 232-237.

Barton, K. A., Whiteley, H. R. & Yang, N.-S. 1987. *Bacillus thuringiensis* δ-Endotoxin Expressed in Transgenic *Nicotiana tabacum* Provides Resistance to Lepidopteran Insects. *Plant Physiology,* 85**,** 1103-1109.

Battisti, L., Green, B. D. & Thorne, C. B. 1985. Mating system for transfer of plasmids among *Bacillus anthracis*, *Bacillus cereus*, and *Bacillus thuringiensis*. *J Bacteriol,* 162**,** 543-550.

Baum, J. A., Chu, C. R., Rupar, M., Brown, G. R., Donovan, W. P., Huesing, J. E., Ilagan, O., Malvar, T. M., Pleau, M., Walters, M. & Vaughn, T. 2004. Binary toxins from *Bacillus thuringiensis* active against the western corn rootworm, *Diabrotica virgifera virgifera* LeConte. *Appl Environ Microbiol,* 70**,** 4889-4898.

Baum, J. A. & Gonzalez, J. M., Jr. 1992. Mode of replication, size and distribution of naturally occurring plasmids in *Bacillus thuringiensis*. *FEMS Microbiol Lett,* 75**,** 143-148.

Baum, J. A. & Malvar, T. 1995. Regulation of insecticidal crystal protein production in *Bacillus thuringiensis*. *Mol Microbiol,* 18**,** 1-12.

Becker, N. 2000. Bacterial control of vector-mosquitoes and black flies. *In Entomopathogenic Bacteria: From Laboratory to Field Application (ed. J.-F. Charles, A. Delécluse and C. Nielsen-LaRoux), Dordrecht,The Netherlands: Kluwer,* 383-398.

Bjellqvist, B., Hughes, G.J., Pasquali, J. Ch., Paquet, N., Ravier, F., Sanchez, J.-Ch., Frutiger, S. & Hochstrasser, D.F. 1993. The focusing positions of

polypeptides in immobilized pH gradients can be predicted from their amino acid sequences. *Electrophoresis*. 14, 1023-1031.

Bjellqvist, B., Basse, B., Olsen, E. and Celis, J.E. 1994. Reference points for comparisons of two-dimensional maps of proteins from different human cell types defined in a pH scale where isoelectric points correlate with polypeptide compositions. *Electrophoresis*. 15, 529-539.

Bernhard, K., Jarrett, P., Meadows, M., Butt, J., Ellis, D. J., Roberts, G. M., Pauli, S., Rodgers, P. & Burges, H. D. 1997. Natural Isolates of *Bacillus thuringiensis*: Worldwide Distribution, Characterization, and Activity against Insect Pests. *Journal of Invertebrate Pathology,* 70**,** 59-68.

Berry, C., O'neil, S., Ben-Dov, E., Jones, A. F., Murphy, L., Quail, M. A., Holden, M. T., Harris, D., Zaritsky, A. & Parkhill, J. 2002. Complete sequence and organization of pBtoxis, the toxin-coding plasmid of *Bacillus thuringiensis* subsp. *israelensis*. *Appl Environ Microbiol,* 68**,** 5082-5095.

Bietlot, H. P., Vishnubhatla, I., Carey, P. R., Pozsgay, M. & Kaplan, H. 1990. Characterization of the cysteine residues and disulphide linkages in the protein crystal of *Bacillus thuringiensis*. *Biochem J,* 267**,** 309-315.

Bizzarri, M. F. & Bishop, A. H. 2007. Recovery of *Bacillus thuringiensis* in vegetative form from the phylloplane of clover (*Trifolium hybridum*) during a growing season. *J Invertebr Pathol,* 94**,** 38-47.

Boonserm, P., Davis, P., Ellar, D. J. & Li, J. 2005. Crystal Structure of the Mosquito-larvicidal Toxin Cry4Ba and Its Biological Implications. *Journal of Molecular Biology,* 348**,** 363-382.

Boonserm, P., Mo, M., Angsuthanasombat, C. & Lescar, J. 2006. Structure of the Functional Form of the Mosquito Larvicidal Cry4Aa Toxin from *Bacillus thuringiensis* at a 2.8-Angstrom Resolution. *J. Bacteriol.,* 188**,** 3391-3401.

Bouillaut, L., Ramarao, N., Buisson, C., Gilois, N., Gohar, M., Lereclus, D. & Nielsen-Leroux, C. 2005. FlhA influences *Bacillus thuringiensis* PlcR-regulated gene transcription, protein production, and virulence. *Appl Environ Microbiol,* 71**,** 8903-8910.

Bourne, Y., Zamboni, V., Barre, A., Peumans, W. J., Van Damme, E. J. & Rouge, P. 1999. Helianthus tuberosus lectin reveals a widespread scaffold for mannose-binding lectins. *Structure,* 7**,** 1473-1482.

Bradford, M. M. 1976. A rapid and sensitive method for the quantitation of microgram quantities of protein utilizing the principle of protein-dye binding. *Anal Biochem*, 72, 248-254.

Brar, S. K., Verma, M., Tyagi, R. D., Valero, J. R. & Surampalli, R. Y. 2009. Entomotoxicity, protease and chitinase activity of *Bacillus thuringiensis* fermented wastewater sludge with a high solids content. *Bioresour Technol,* 100**,** 4317-4325.

Bravo, A., Gill, S. S. & Soberon, M. 2007. Mode of action of *Bacillus thuringiensis* Cry and Cyt toxins and their potential for insect control. *Toxicon,* 49**,** 423-435.

Bravo, A., Gomez, I., Conde, J., Munoz-Garay, C., Sanchez, J., Miranda, R., Zhuang, M., Gill, S. S. & Soberon, M. 2004. Oligomerization triggers binding of a *Bacillus thuringiensis* Cry1Ab pore-forming toxin to aminopeptidase N receptor leading to insertion into membrane microdomains. *Biochim Biophys Acta,* 1667**,** 38-46.

Bravo, A., Gomez, I., Porta, H., Garcia-Gomez, B. I., Rodriguez-Almazan, C., Pardo, L. & Soberon, M. 2012. Evolution of *Bacillus thuringiensis* Cry toxins insecticidal activity. *Microb Biotechnol*, 17-26.

Bravo, A., Likitvivatanavong, S., Gill, S. S. & Soberon, M. 2011. *Bacillus thuringiensis*: A story of a successful bioinsecticide. *Insect Biochem Mol Biol,* 41**,** 423-431.

Bravo, A., Sanchez, J., Kouskoura, T. & Crickmore, N. 2002. N-terminal activation is an essential early step in the mechanism of action of the *Bacillus thuringiensis* Cry1Ac insecticidal toxin. *J Biol Chem,* 277**,** 23985-23987.

Bravo, A. & Soberón, M. 2008. How to cope with insect resistance to Bt toxins? *Trends in biotechnology,* 26**,** 573-579.

Brizzard, B. L., Schnepf, H. E. & Kronstad, J. W. 1991. Expression of the *cryIB* crystal protein gene of *Bacillus thuringiensis*. *Molecular & general genetics : MGG,* 231**,** 59-64.

Broadwell, A., Baumann, L. & Baumann, P. 1990. Larvicidal properties of the 42 and 51 kilodalton *Bacillus sphaericus* proteins expressed in different bacterial hosts: Evidence for a binary toxin. *Current Microbiology,* 21**,** 361-366.

Brown, K. L. 1993. Transcriptional regulation of the *Bacillus thuringiensis* subsp. *thompsoni* crystal protein gene operon. *Journal of bacteriology,* 175**,** 7951-7957.

Brown, K. L. & Whiteley, H. R. 1992. Molecular characterization of two novel crystal protein genes from *Bacillus thuringiensis* subsp. *thompsoni*. *J. Bacteriol.,* 174**,** 549-557.

Budarina, Z. I., Sinev, M. A., Mayorov, S. G., Tomashevski, A. Y., Shmelev, I. V. & Kuzmin, N. P. 1994. Hemolysin II is more characteristic of *Bacillus thuringiensis* than *Bacillus cereus*. *Arch Microbiol,* 161**,** 252-257.

Bulla, L. A., Rhodes, R. A. & St. Julian, G. 1975. Bacteria as Insect Pathogens. *Annual Review of Microbiology,* 29**,** 163-190.

Butko, P. 2003. Cytolytic Toxin Cyt1A and Its Mechanism of Membrane Damage: Data and Hypotheses. *Appl. Environ. Microbiol.,* 69**,** 2415-2422.

Caquet, T., Roucaute, M., Le Goff, P. & Lagadic, L. 2011. Effects of repeated field applications of two formulations of *Bacillus thuringiensis* var. *israelensis* on non-target saltmarsh invertebrates in Atlantic coastal wetlands. *Ecotoxicol Environ Saf,* 74**,** 1122-1130.

Carey, R., Holland, J., Whang, H., Neter, E. & Bryant, B. 1967. Clostridial oncolysis in man. *Eur J Cancer,* 3**,** 37-46.

Carlberg, G., Tikkanen, L. & Abdel-Hameed, A. H. 1995. Safety testing of *Bacillus thuringiensis* preparations, including thuringiensin, using the Salmonella assay. *J Invertebr Pathol,* 66**,** 68-71.

Carlson, C. R., Caugant, D. A. & Kolsto, A. B. 1994. Genotypic Diversity among *Bacillus cereus* and *Bacillus thuringiensis* Strains. *Appl Environ Microbiol,* 60**,** 1719-1725.

Carlson, C. R., Johansen, T. & Kolsto, A. B. 1996. The chromosome map of *Bacillus thuringiensis* subsp. canadensis HD224 is highly similar to that of the *Bacillus cereus* type strain ATCC 14579. *FEMS Microbiol Lett,* 141**,** 163-167.

Carlson, C. R. & Kolsto, A. B. 1993. A complete physical map of a *Bacillus thuringiensis* chromosome. *J Bacteriol,* 175**,** 1053-1060.

Carozzi, N. B., Kramer, V. C., Warren, G. W., Evola, S. & Koziel, M. G. 1991. Prediction of insecticidal activity of *Bacillus thuringiensis* strains by polymerase chain reaction product profiles. *Appl. Environ. Microbiol.,* 57**,** 3057-3061.

Carroll, J., Convents, D., Van Damme, J., Boets, A., Van Rie, J. & Ellar, D. J. 1997. Intramolecular Proteolytic Cleavage of *Bacillus thuringiensis* Cry3A

[delta]-Endotoxin May Facilitate Its Coleopteran Toxicity. *Journal of Invertebrate Pathology,* 70**,** 41-49.

Carswell, E., Old, L., Kassel, R., Green, S., Fiore, N. & Williamson, B. 1975. An endotoxin-induced serum factor that causes necrosis of tumors. *Proc Natl Acad Sci,* 72**,** 3666 - 3670.

Charles, J.-F., Nielson-Leroux, C. & Delecluse, A. 1996. *Bacillus Sphaericus* Toxins: Molecular Biology and Mode of Action. *Annual Review of Entomology,* 41**,** 451-472.

Choma, C. T., Surewicz, W. K. & Kaplan, H. 1991. The toxic moiety of the *Bacillus thuringiensis* protoxin undergoes a conformational change upon activation. *Biochem Biophys Res Commun,* 179**,** 933-938.

Cole, A. R., Gibert, M., Popoff, M., Moss, D. S., Titball, R. W. & Basak, A. K. 2004. *Clostridium perfringens* ε-toxin shows structural similarity to the pore-forming toxin aerolysin. *Nature Structural and Molecular Biology,* 11**,** 797-798.

Collier, F. A., Elliot, S. L. & Ellis, R. J. 2005. Spatial variation in *Bacillus thuringiensis/cereus* populations within the phyllosphere of broad-leaved dock (*Rumex obtusifolius)* and surrounding habitats. *FEMS Microbiol Ecol,* 54**,** 417-425.

Crickmore, N. & Ellar, D. J. 1992. Involvement of a possible chaperonin in the efficient expression of a cloned CryIIA δ-endotoxin gene in *Bacillus thuringiensis*. *Molecular Microbiology,* 6**,** 1533-1537.

Crickmore, N., Wheeler, V. C. & Ellar, D. J. 1994. Use of an operon fusion to induce expression and crystallisation of a *Bacillus thuringiensis* δ-endotoxin encoded by a cryptic gene. *Molecular and General Genetics MGG,* 242**,** 365-368.

Crickmore, N., Zeigler, D. R., Feitelson, J., Schnepf, E., Van Rie, J., Lereclus, D., Baum, J. & Dean, D. H. 1998. Revision of the Nomenclature for the *Bacillus thuringiensis* Pesticidal Crystal Proteins. *Microbiology and Molecular Biology Reviews,* 62**,** 807-813.

Crickmore, N., Zeigler, D. R., Schnepf, E., Van Rie, J., Lereclus, D., Baum, J., Bravo, A. & Dean, D. H. 2013. *Bacillus thuringiensis* toxin nomenclature. http://www.btnomenclature.info/

Crouch, S. P., Kozlowski, R., Slater, K. J. & Fletcher, J. 1993. The use of ATP bioluminescence as a measure of cell proliferation and cytotoxicity. *J. Immunol. Meth*, 160, 81-88.

Daffonchio, D., Cherif, A. & Borin, S. 2000. Homoduplex and Heteroduplex Polymorphisms of the Amplified Ribosomal 16S-23S Internal Transcribed Spacers Describe Genetic Relationships in the "*Bacillus cereus* Group". *Applied and Environmental Microbiology,* 66**,** 5460-5468.

Damgaard, P. H., Hansen, B. M., Pedersen, J. C. & Eilenberg, J. 1997. Natural occurrence of *Bacillus thuringiensis* on cabbage foliage and in insects associated with cabbage crops. *J Appl Microbiol,* 82**,** 253-258.

Damgaard, P. H., Larsen, H. D., Hansen, B. M., Bresciani, J. & Jorgensen, K. 1996. Enterotoxin-producing strains of *Bacillus thuringiensis* isolated from food. *Lett Appl Microbiol,* 23**,** 146-150.

de Maagd, R. A., Bravo, A., Berry, C., Crickmore, N. & Schnepf, H. E. 2003. Structure, diversity, and evolution of protein toxins from spore-forming entomopathogenic bacteria. *Annual Review of Genetics,* 37**,** 409-433.

de Maagd, R. A., Bravo, A. & Crickmore, N. 2001. How *Bacillus thuringiensis* has evolved specific toxins to colonize the insect world. *Trends in Genetics,* 17**,** 193-199.

de Maagd, R. A., D, B. & Stiekema, S. 1999. *Bacillus thuringiensis* toxin-mediated insect resistance in plants. *Trends Plant Sci.,* 4**,** 9-13.

de Maagd, R. A., Kwa, M. S., Van Der Klei, H., Yamamoto, T., Schipper, B., Vlak, J. M., Stiekema, W. J. & Bosch, D. 1996. Domain III substitution in *Bacillus thuringiensis* delta-endotoxin CryIA(b) results in superior toxicity for *Spodoptera exigua* and altered membrane protein recognition. *Appl Environ Microbiol,* 62**,** 1537-1543.

de Maagd, R. A., Weemen-Hendriks, M., Stiekema, W. & Bosch, D. 2000. *Bacillus thuringiensis* Delta-Endotoxin Cry1C Domain III Can Function as a Specificity Determinant for *Spodoptera exigua* in Different, but Not All, Cry1-Cry1C Hybrids. *Applied and Environmental Microbiology,* 66**,** 1559-1563.

Delucca, A. J., Palmgren, M. S. & De Barjac, H. 1984. A new serovar of *Bacillus thuringiensis* from grain dust: *Bacillus thuringiensis* serovar *colmeri* (Serovar 21). *Journal of Invertebrate Pathology,* 43**,** 437-438.

Delucca, A. J., 2nd, Simonson, J. & Larson, A. 1979. Two new serovars of *Bacillus thuringiensis*: Serovars *dakota* and *indiana* (Serovars 15 and 16). *Journal of Invertebrate Pathology,* 34**,** 323-324.

Delucca, A. J., 2nd, Simonson, J. G. & Larson, A. D. 1981. *Bacillus thuringiensis* distribution in soils of the United States. *Can J Microbiol,* 27**,** 865-870.

Dervyn, E., Poncet, S., Klier, A. & Rapoport, G. 1995. Transcriptional regulation of the cryIVD gene operon from *Bacillus thuringiensis* subsp. *israelensis*. *Journal of bacteriology,* 177**,** 2283-2291.

Dong, H., Nilsson, L. & Kurland, C. G. 1995. Gratuitous overexpression of genes in *Escherichia coli* leads to growth inhibition and ribosome destruction. *Journal of Bacteriology,* 177**,** 1497-504.

Donovan, W. P., Donovan, J. C., Slaney, A. C. 2000. *U.S. Patent No. 6063756.*

Drobniewski, F. A. 1993. *Bacillus cereus* and related species. *Clin. Microbiol. Rev.,* 6**,** 324-338.

Drobniewski, F. A. 1994. The safety of Bacillus species as insect vector control agents. *Journal of Applied Microbiology,* 76**,** 101-109.

Eilenberg, J., Damgaard, P. H., Hansen, B. M., Pedersen, J. C., Bresciani, J. & Larsson, R. 2000. Natural coprevalence of *Strongwellsea castrans, Cystosporogenes deliaradicae*, and *Bacillus thuringiensis* in the host, *Delia radicum*. *J Invertebr Pathol,* 75**,** 69-75.

Ellis, R. T., Stockhoff, B. A., Stamp, L., Schnepf, H. E., Schwab, G. E., Knuth, M., Russell, J., Cardineau, G. A. & Narva, K. E. 2002. Novel *Bacillus thuringiensis* binary insecticidal crystal proteins active on western corn rootworm, *Diabrotica virgifera virgifera* LeConte. *Appl Environ Microbiol,* 68**,** 1137-1145.

Ermolaeva, M.D., Khalak, H.G., White, O., Smith, H.O. & Salzberg, S.L. 2000.Prediction of transcription terminators in bacterial genomes. J Mol Biol, 301, 27-33.

Espinasse, S., Chaufaux, J., Buisson, C., Perchat, S., Gohar, M., Bourguet, D. & Sanchis, V. 2003. Occurrence and linkage between secreted insecticidal toxins in natural isolates of *Bacillus thuringiensis*. *Curr Microbiol,* 47**,** 501-507.

Estruch, J. J., Warren, G. W., Mullins, M. A., Nye, G. J., Craig, J. A. & Koziel, M. G. 1996. Vip3A, a novel *Bacillus thuringiensis* vegetative insecticidal protein with a wide spectrum of activities against lepidopteran insects. *Proceedings of the National Academy of Sciences,* 93**,** 5389-5394.

Fang, J., Xu, X., Wang, P., Zhao, J.-Z., Shelton, A. M., Cheng, J., Feng, M.-G. & Shen, Z. 2007. Characterization of Chimeric *Bacillus thuringiensis* Vip3 Toxins. *Appl. Environ. Microbiol.,* 73**,** 956-961.

Fedhila, S., Gohar, M., Slamti, L., Nel, P. & Lereclus, D. 2003. The *Bacillus thuringiensis* PlcR-regulated gene *inhA2* is necessary, but not sufficient, for virulence. *J Bacteriol,* 185**,** 2820-2825.

Fedhila, S., Nel, P. & Lereclus, D. 2002. The InhA2 metalloprotease of *Bacillus thuringiensis* strain 407 is required for pathogenicity in insects infected via the oral route. *J Bacteriol,* 184**,** 3296-3304.

Fernandez, L. E., Aimanova, K. G., Gill, S. S., Bravo, A. & Soberón, M. 2006. A GPI-anchored alkaline phosphatase is a functional midgut receptor of Cry11Aa toxin in *Aedes aegypti* larvae. *Biochem J,* 394**,** 77-84.

Frederiksen, K., Rosenquist, H., Jorgensen, K. & Wilcks, A. 2006. Occurrence of natural *Bacillus thuringiensis* contaminants and residues of Bacillus *thuringiensis*-based insecticides on fresh fruits and vegetables. *Appl Environ Microbiol,* 72**,** 3435-3440.

Fujinaga, Y., Inoue, K., Shimazaki, S., Tomochika, K., Tsuzuki, K., Fujii, N., Watanabe, T., Ohyama, T., Takeshi, K. & Oguma, K. 1994. Molecular Construction of *Clostridium botulinum* Type C Progenitor Toxin and Its Gene Organization. *Biochemical and Biophysical Research Communications,* 205**,** 1291-1298.

Galitsky, N., Cody, V., Wojtczak, A., Ghosh, D., Luft, J. R., Pangborn, W. & English, L. 2001. Structure of the insecticidal bacterial δ-endotoxin Cry3Bb1 of *Bacillus thuringiensis*. *Acta Crystallographica Section D,* 57**,** 1101-1109.

Gasteiger, E., Hoogland, C., Gattike, R. A., Duvaud, S., Wilkins, M. R., Appel, R. D., Bairoch, A. 2005. Protein Identification and Analysis Tools on the

ExPASy Server. *In John M. Walker (ed): The Proteomics Protocols Handbook, Humana Press,* 571-607.

Gatehouse, J. A. 2008. Biotechnological prospects for engineering insect-resistant plants. *Plant Physiol,* 146, 881-887.

Gill, S. S., Cowles, E. A. & Francis, V. 1995. Identification, isolation, and cloning of a *Bacillus thuringiensis* CryIAc toxin-binding protein from the midgut of the lepidopteran insect *Heliothis virescens*. *J Biol Chem,* 270**,** 27277-27282.

Gill, S. S., Cowles, E. A. & Pietrantonio, P. V. 1992. The mode of action of *Bacillus thuringiensis* endotoxins. *Annu Rev Entomol,* 37**,** 615-636.

Gill, S. S. & Hornung, J. M. 1987. Cytolytic activity of *Bacillus thuringiensis* proteins to insect and mammalian cell lines. *J Invertebr Pathol,* 50**,** 16-25.

Gill, S. S., Singh, G. J. & Hornung, J. M. 1987. Cell membrane interaction of *Bacillus thuringiensis* subsp. *israelensis* cytolytic toxins. *Infect Immun,* 55**,** 1300-1308.

Gohar, M., Faegri, K., Perchat, S., Ravnum, S., Okstad, O. A., Gominet, M., Kolstø, A.-B. & Lereclus, D. 2008. The PlcR Virulence Regulon of *Bacillus cereus*. *PLoS One,* 3**,** e2793.

Gomez, I., Miranda-Rios, J., Rudino-Pinera, E., Oltean, D. I., Gill, S. S., Bravo, A. & Soberon, M. 2002. Hydropathic complementarity determines interaction of epitope (869)HITDTNNK(876) in Manduca sexta Bt-R(1) receptor with loop 2 of domain II of *Bacillus thuringiensis* Cry1A toxins. *J Biol Chem,* 277**,** 30137-30143.

Gonzalez, E., Granados, J. C., Short, J. D., Ammons, D. R. & Rampersad, J. 2011. Parasporins from a Caribbean Island: Evidence for a Globally Dispersed *Bacillus thuringiensis* Strain. *Curr Microbiol*, 1643-1648.

González, J. M., Brown, B. J. & Carlton, B. C. 1982. Transfer of *Bacillus thuringiensis* plasmids coding for delta-endotoxin among strains of *B. thuringiensis* and *B. cereus. Proceedings of the National Academy of Sciences,* 79**,** 6951-6955.

Gonzalez, J. M., Jr. & Carlton, B. C. 1980. Patterns of plasmid DNA in crystalliferous and acrystalliferous strains of *Bacillus thuringiensis. Plasmid,* 3**,** 92-98.

Gonzalez, J. M., Jr., Dulmage, H. T. & Carlton, B. C. 1981. Correlation between specific plasmids and delta-endotoxin production in *Bacillus thuringiensis*. *Plasmid,* 5**,** 352-365.

Gonzalez, J. M., Jr., H. T. Dulmage & B. C. Carlton 1981. Correlation between specific plasmids and delta-endotoxin production in *Bacillus thuringiensis*. *Plasmid***,** 352-365.

Gonzalez, R. J. & Tarloff, J. B. 2001. Evaluation of hepatic subcellular fractions for Alamar blue and MTT reductase activity. *Toxicology in Vitro,* 15**,** 257-259.

Goodsell, D. S. 2001. The Molecular Perspective: Targeted Toxins. *STEM CELLS,* 19**,** 161-162.

Green, B. D., Battisti, L. & Thorne, C. B. 1989. Involvement of Tn4430 in transfer of *Bacillus anthracis* plasmids mediated by *Bacillus thuringiensis* plasmid pXO12. *J Bacteriol,* 171**,** 104-113.

Griffitts, J. S., Haslam, S. M., Yang, T., Garczynski, S. F., Mulloy, B., Morris, H., Cremer, P. S., Dell, A., Adang, M. J. & Aroian, R. V. 2005. Glycolipids as receptors for *Bacillus thuringiensis* crystal toxin. *Science,* 307**,** 922-925.

Grochulski, P., Masson, L., Borisova, S., Pusztai-Carey, M., Schwartz, J.-L., Brousseau, R. & Cygler, M. 1995. *Bacillus thuringiensis* CrylA(a) Insecticidal Toxin: Crystal Structure and Channel Formation. *Journal of Molecular Biology,* 254**,** 447-464.

Guex, N. & Peitsch, M. C. 1997. SWISS-MODEL and the Swiss-Pdb Viewer: An environment for comparative protein modeling. *Electrophoresis,* 18**,** 2714-2723.

Guo, S., Liu, M., Peng, D., Ji, S., Wang, P., Yu, Z. & Sun, M. 2008. New strategy for isolating novel nematicidal crystal protein genes from *Bacillus thuringiensis* strain YBT-1518. *Appl Environ Microbiol,* 74**,** 6997-7001.

Guo, S., Ye, S., Liu, Y., Wei, L., Xue, J., Wu, H., Song, F., Zhang, J., Wu, X., Huang, D. & Rao, Z. 2009. Crystal structure of *Bacillus thuringiensis* Cry8Ea1: An insecticidal toxin toxic to underground pests, the larvae of Holotrichia parallela. *J Struct Biol,* 168**,** 259-266.

Hang'ombe, M. B., Mukamoto, M., Kohda, T., Sugimoto, N. & Kozaki, S. 2004. Cytotoxicity of *Clostridium septicum* alpha-toxin: its oligomerization in detergent resistant membranes of mammalian cells. *Microbial Pathogenesis,* 37**,** 279-286.

Hansen, B. M., Damgaard, P. H., Eilenberg, J. & Pedersen, J. C. 1998. Molecular and phenotypic characterization of *Bacillus thuringiensis* isolated from leaves and insects. *J Invertebr Pathol,* 71**,** 106-114.

Hansen, B. M. & Salamitou, S. 2000. Virulence of *Bacillus thuringiensis*. *In Entomopathogenic Bacteria: From Laboratory to Field Application (Charles, J. et al.,eds).Kluwer Academic Publishers***,** 41–64.

Hastowo, S., Lay, B. W. & Ohba, M. 1992. Naturally occurring *Bacillus thuringiensis* in Indonesia. *Journal of Applied Microbiology,* 73**,** 108-113.

Hazes, B. 1996. The (QxW)3 domain: A flexible lectin scaffold. *Protein Science,* 5**,** 1490-1501.

Heierson, A., Siden, I., Kivaisi, A. & Boman, H. G. 1986. Bacteriophage-resistant mutants of *Bacillus thuringiensis* with decreased virulence in pupae of *Hyalophora cecropia*. *J Bacteriol,* 167**,** 18-24.

Heimpel, A. & Angus, T. A. 1958. The taxonomy of insect pathogens related to *Bacillus cereus* Frankland and Frankland. *Can J Microbiol,* 4**,** 531-541.

Helgason, E., Okstad, O. A., Caugant, D. A., Johansen, H. A. & Fouet, A. 2000. *Bacillus anthracis*, *Bacillus cereus*, and *Bacillus thuringiensis*—One species on the basis of genetic evidence. *Appl. Environ. Microbiol.,* 66**,** 2627-2630.

Hendriksen, N. B. & Hansen, B. M. 2002. Long-term survival and germination of *Bacillus thuringiensis* var. kurstaki in a field trial. *Can J Microbiol,* 48**,** 256-261.

Henner, D. J., Yang, M., Chen, E., Hellmiss, R., Rodriguez, H. & Low, M. G. 1988. Sequence of the *Bacillus thuringiensis* phosphatidylinositol specific phospholipase C. *Nucleic Acids Res,* 16**,** 10383.

Hernandez-Soto, A., Del Rincon-Castro, M. C., Espinoza, A. M. & Ibarra, J. E. 2009. Parasporal body formation via overexpression of the Cry10Aa toxin of *Bacillus thuringiensis* subsp. *israelensis*, and Cry10Aa-Cyt1Aa synergism. *Appl Environ Microbiol,* 75**,** 4661-4667.

Hirabayashi, J., Dutta, S. K. & Kasai, K.-I. 1998. Novel Galactose-binding Proteins in Annelida. Characterization of 29-kDa tandem repeat-type lectins from the earthworm *Lumbricus terrestris*. *J. Biol. Chem.,* 273**,** 14450-14460.

Hodgman, T. C. & Ellar, D. J. 1990. Models for the structure and function of the *Bacillus thuringiensis* delta-endotoxins determined by compilational analysis. *DNA Seq,* 1**,** 97-106.

Hofmann, C. & Luthy, P. 1986. Binding and activity of *Bacillus thuringiensis* delta-endotoxin to invertebrate cells. *Arch Microbiol,* 146**,** 7-11.

Hofmann, C., Vanderbruggen, H., Höfte, H., Van Rie, J., Jansens, S. & Van Mellaert, H. 1988. Specificity of *Bacillus thuringiensis* delta-endotoxins is correlated with the presence of high-affinity binding sites in the brush border membrane of target insect midguts. *Proceedings of the National Academy of Sciences,* 85**,** 7844-7848.

Hofte, H. & Whiteley, H. R. 1989. Insecticidal crystal proteins of *Bacillus thuringiensis*. *Microbiol. Mol. Biol. Rev.,* 53**,** 242-255.

Hossain, D. M., Shitomi, Y., Moriyama, K., Higuchi, M., Hayakawa, T., Mitsui, T., Sato, R. & Hori, H. 2004. Characterization of a Novel Plasma Membrane Protein, Expressed in the Midgut Epithelia of *Bombyx mori*, That Binds to Cry1A Toxins. *Applied and Environmental Microbiology,* 70**,** 4604-4612.

Hossain, M. A., Ahmed, S. & Hoque, S. 1997. Abundance and Distribution of *Bacillus thuringiensis* in the Agricultural Soil of Bangladesh. *J Invertebr Pathol,* 70**,** 221-225.

Hu, X., Swiecicka, I., Timmery, S. & Mahillon, J. 2009. Sympatric soil communities of *Bacillus cereus* sensu *lato*: population structure and potential plasmid dynamics of pXO1- and pXO2-like elements. *FEMS Microbiology Ecology,* 70**,** 344-355.

Huang, D.-F., Zhang, J., Song, F.-P. & Lang, Z.-H. 2007. Microbial control and biotechnology research on *Bacillus thuringiensis* in China. *Journal of Invertebrate Pathology,* 95**,** 175-180.

Ichikawa, M., Uemori, A., Ohgushi, K., Yasutake, K., Kagoshima, K., Mizuki, E., Binh , N. D. & Ohba, M. 2007. Phenotypic and morphometric characterization of *Bacillus thuringiensis* parasporin-1 producers: a comparison with insecticidal Cry-protein producers. *J. Fac. Agric. Kyushu Univ.,* 52**,** 307–313.

Ichikawa, M., Uemori, A., Yasutake, K., Kagoshima, K., Mizuki, E. & Ohba, M. 2008. Failure to phenotypically discriminate between non-insecticidal *Bacillus thuringiensis* strains with anticancer parasporins (PS2, PS3, and PS4) and *Bacillus thuringiensis* strains that produce insecticidal Cry proteins. *Applied Entomology and Zoology,* 43**,** 421-426.

Ihara, H. & Himeno, M. 2008. Study of the irreversible binding of *Bacillus thuringiensis* Cry1Aa to brush border membrane vesicles from *Bombyx mori* midgut. *J Invertebr Pathol,* 98**,** 177-183.

Inoue, K., Fujinaga, Y., Watanabe, T., Ohyama, T., Takeshi, K., Moriishi, K., Nakajima, H., Inoue, K. & Oguma, K. 1996. Molecular composition of *Clostridium botulinum* type A progenitor toxins. *Infection and Immunity,* 64**,** 1589-1594.

Isaac, B. C., Krieger, E.K., Mettus-Light, AM., Sivasupramanium, S., Moshiri, F. 2001. *PCT Int. Appl. WO 0187940.*

Ito, A., Sasaguri, Y., Kitada, S., Kusaka, Y., Kuwano, K., Masutomi, K., Mizuki, E., Akao, T. & Ohba, M. 2004. A *Bacillus thuringiensis* Crystal Protein with Selective Cytocidal Action to Human Cells. *Journal of Biological Chemistry,* 279**,** 21282-21286.

Ito, T., Ikeya, T., Sahara, K., Bando, H. & Asano, S.-I. 2006. Cloning and Expression of Two Crystal Protein Genes, *cry30Ba1* and *cry44Aa1*, Obtained from a Highly Mosquitocidal Strain, *Bacillus thuringiensis* subsp. entomocidus INA288. *Appl. Environ. Microbiol.,* 72**,** 5673-5676.

Jackson, P. J., Hill, K. K., Laker, M. T., Ticknor, L. O. & Keim, P. 1999. Genetic comparison of *Bacillus anthracis* and its close relatives using amplified fragment length polymorphism and polymerase chain reaction analysis. *Journal of Applied Microbiology,* 87**,** 263-269.

Jensen, G. B., Hansen, B. M., Eilenberg, J. & Mahillon, J. 2003. The hidden lifestyles of *Bacillus cereus* and relatives. *Environmental Microbiology,* 5**,** 631-640.

Jung, Y. C., Mizuki, E., Akao, T. & Cote, J. C. 2007. Isolation and characterization of a novel *Bacillus thuringiensis* strain expressing a novel crystal protein with cytocidal activity against human cancer cells. *Journal of Applied Microbiology,* 103**,** 65-79.

Kane, J. F. 1995. Effects of rare codon clusters on high-level expression of heterologous proteins in *Escherichia coli*. *Current Opinion in Biotechnology,* 6**,** 494-500.

Kanintronkul, Y., Srikhirin, T., Angsuthanasombat, C. & Kerdcharoen, T. 2005. Insertion behavior of the *Bacillus thuringiensis* Cry4Ba insecticidal protein into lipid monolayers. *Archives of Biochemistry and Biophysics,* 442**,** 180-186.

Kapur, M., Bhatia, R., Pandey, G., Pandey, J., Paul, D. & Jain, R. K. 2010. A Case Study for Assessment of Microbial Community Dynamics in Genetically Modified Bt Cotton Crop Fields. *Curr Microbiol*, 118-124.

Katayama, H., Kusaka, Y., Yokota, H., Akao, T., Kojima, M., Nakamura, O., Mekada, E. & Mizuki, E. 2007. Parasporin-1, a novel cytotoxic protein from *Bacillus thuringiensis*, induces Ca^{2+} influx and a sustained elevation of the cytoplasmic Ca^{2+} concentration in toxin-sensitive cells. *J Biol Chem,* 282**,** 7742-7752.

Katayama, H., Yokota, H., Akao, T., Nakamura, O., Ohba, M., Mekada, E. & Mizuki, E. 2005. Parasporin-1, a novel cytotoxic protein to human cells from non-insecticidal parasporal inclusions of *Bacillus thuringiensis*. *J Biochem,* 137**,** 17-25.

Keim, P., Kalif, A., Schupp, J., Hill, K., Travis, S. E., Richmond, K., Adair, D. M., Hugh-Jones, M., Kuske, C. R. & Jackson, P. 1997. Molecular evolution and diversity in *Bacillus anthracis* as detected by amplified fragment length polymorphism markers. *Journal of Bacteriology,* 179**,** 818-824.

Kim, H. S., Yamashita, S., Akao, T., Saitoh, H., Higuchi, K., Park, Y., Mizuki, E. & Ohba, M. 2000. *In vitro* cytotoxicity of non-Cyt inclusion proteins of a *Bacillus thuringiensis* isolate against human cells, including cancer cells. *Journal of Applied Microbiology,* 89**,** 16-23.

Kitada, S., Abe, Y., Maeda, T. & Shimada, H. 2009. Parasporin-2 requires GPI-anchored proteins for the efficient cytocidal action to human hepatoma cells. *Toxicology,* 264**,** 80-88.

Kitada, S., Abe, Y., Shimada, H., Kusaka, Y., Matsuo, Y., Katayama, H., Okumura, S., Akao, T., Mizuki, E., Kuge, O., Sasaguri, Y., Ohba, M. & Ito, A. 2006. Cytocidal Actions of Parasporin-2, an Anti-tumor Crystal Toxin from *Bacillus thuringiensis*. *Journal of Biological Chemistry,* 281**,** 26350-26360.

Knight, P. J. K., Crickmore, N. & Ellar, D. J. 1994. The receptor for *Bacillus thuringiensis* CrylA(c) delta-endotoxin in the brush border membrane of the lepidopteran *Manduca sexta* is aminopeptidase N. *Molecular Microbiology,* 11**,** 429-436.

Knowles, B. H. & Farndale, R. W. 1988. Activation of insect cell adenylate cyclase by *Bacillus thuringiensis* delta-endotoxins and melittin. Toxicity is independent of cyclic AMP. *Biochem J,* 253**,** 235-241.

Koni, P. A. & Ellar, D. J. 1994. Biochemical characterization of *Bacillus thuringiensis* cytolytic δ-endotoxins. *Microbiology,* 140**,** 1869-1880.

Kramer, K. J. & Muthukrishnan, S. 1998. Insect Chitinases: Molecular Biology and Potential Use as Biopesticides. *Insect Biochemistry and Molecular Biology,* 27**,** 887-900.

Krieg, A. 1971. Concerning α-exotoxin produced by vegetative cells of *Bacillus thuringiensis* and *Bacillus cereus*. *Journal of Invertebrate Pathology,* 17**,** 134-135.

Kronstad, J. W., Schnepf, H. E. & Whiteley, H. R. 1983. Diversity of locations for *Bacillus thuringiensis* crystal protein genes. *J Bacteriol,* 154**,** 419-428.

Laemmli, U. K. 1970. Cleavage of structural proteins during the assembly of the head of bacteriophage T4. *Nature*, 227,680-685.

Lecadet, M. M. & Dedonder, R. 1967. Enzymatic hydrolysis of the crystals of *Bacillus thuringiensis* by the proteases of *Pieris brassicae* I. Preparation and fractionation of the lysates. *Journal of Invertebrate Pathology,* 9**,** 310-321.

Lechner, M., Kupke, T., Stefanovic, S. & Gotz, F. 1989. Molecular characterization and sequence of phosphatidylinositol-specific phospholipase C of *Bacillus thuringiensis*. *Mol Microbiol,* 3**,** 621-626.

Lechner, S., Mayr, R., Francis, K. P., Prüß, B. M., Kaplan, T., Wießner-Gunkel, E., Stewart, G. S. a. B. & Scherer, S. 1998. *Bacillus weihenstephanensis* sp. nov. is a new psychrotolerant species of the *Bacillus cereus* group. *International Journal of Systematic Bacteriology,* 48**,** 1373-1382.

Lee, D. W., Akao, T., Yamashita, S., Katayama, H., Maeda, M., Saitoh, H., Mizuki, E. & Ohba, M. 2000. Noninsecticidal Parasporal Proteins of a *Bacillus thuringiensis* Serovar *shandongiensis* Isolate Exhibit a Preferential

Cytotoxicity against Human Leukemic T Cells. *Biochemical and Biophysical Research Communications,* 272**,** 218-223.

Lenane, I. J., Bagnall, N. H., Josh, P. F., Pearson, R. D., Akhurst, R. J. & Kotze, A. C. 2008. A pair of adjacent genes, *cry5Ad* and *orf2-5Ad*, encode the typical N- and C-terminal regions of a Cry5Aδ-endotoxin as two separate proteins in *Bacillus thuringiensis* strain L366. *FEMS Microbiology Letters,* 278**,** 115-120.

Lereclus, D., Lecadet, M. M., Ribier, J. & Dedonder, R. 1982. Molecular relationships among plasmids of *Bacillus thuringiensis*: conserved sequences through 11 crystalliferous strains. *Mol Gen Genet,* 186**,** 391-398.

Levinson, B. L., Kasyan, K. J., Chiu, S. S., Currier, T. C. & Gonzalez, J. M., Jr. 1990. Identification of beta-exotoxin production, plasmids encoding beta-exotoxin, and a new exotoxin in *Bacillus thuringiensis* by using high-performance liquid chromatography. *J Bacteriol,* 172**,** 3172-3179.

Li, J., Carroll, J. & Ellar, D. J. 1991. Crystal structure of insecticidal δ-endotoxin from *Bacillus thuringiensis* at 2.5 A resolution. *Nature,* 353**,** 815-821.

Li, J., Koni, P. A. & Ellar, D. J. 1996. Structure of the Mosquitocidal δ-Endotoxin CytB from *Bacillus thuringiensis* sp. *kyushuensis* and Implications for Membrane Pore Formation. *Journal of Molecular Biology,* 257**,** 129-152.

Li, R. S., Jarrett, P. & Burges, H. D. 1987. Importance of spores, crystals, and [delta]-endotoxins in the pathogenicity of different varieties of *Bacillus thuringiensis* in *Galleria mellonella* and *Pieris brassicae*. *Journal of Invertebrate Pathology,* 50**,** 277-284.

Lightwood, D. J., Ellar, D. J. & Jarrett, P. 2000. Role of proteolysis in determining potency of *Bacillus thuringiensis* Cry1Ac delta-endotoxin. *Appl Environ Microbiol,* 66**,** 5174-5181.

Liu, M., Cai, Q. X., Liu, H. Z., Zhang, B. H., Yan, J. P. & Yuan, Z. M. 2002. Chitinolytic activities in *Bacillus thuringiensis* and their synergistic effects on larvicidal activity. *Journal of applied microbiology,* 93**,** 374-379.

Macaluso, A. & Mettus, A. M. 1991. Efficient transformation of *Bacillus thuringiensis* requires nonmethylated plasmid DNA. *Journal of Bacteriology,* 173**,** 1353-1356.

Malmgren, R. & Flanigan, C. 1955. Localization of the vegetative form of *Clostridium tetani* in mouse tumors following intravenous spore administration. *Cancer Res,* 15**,** 473 - 478.

Mancheño, J. M., Tateno, H., Goldstein, I. J., Martínez-Ripoll, M. & Hermoso, J. A. 2005. Structural Analysis of the *Laetiporus sulphureus* Hemolytic Pore-forming Lectin in Complex with Sugars. *Journal of Biological Chemistry,* 280**,** 17251-17259.

Manonmani, A. M., Rajendran, G. & Balaraman, K. 1991. Isolation of mosquito pathogenic *Bacillus sphaericus* & *B. thuringiensis* from the root surface of hydrophytes. *Indian J Med Res,* 93**,** 111-114.

Marchler-Bauer, A., Lu, S., Anderson, J. B., Chitsaz, F., Derbyshire, M. K., DeWeese-Scott, C., Fong, J. H., Geer, L. Y., Geer, R. C., Gonzales, N. R., Gwadz, M., He, S., Hurwitz, D. I., Jackson, J. D., Ke, Z., Lanczycki, C. J., Lu, F., Marchler, G. H., Mullokandov, M., Omelchenko, M. V., Robertson, C. L., Song, J. S., Thanki, N., Yamashita, R. A., Zhang, D., Zhang, N., Zheng, C. & Bryant, S. H. 2011. CDD: a Conserved Domain Database for the functional annotation of proteins.*Nucleic Acids Res,* 39, 225-229.

Marchler-Bauer, A., Anderson, J. B., Chitsaz, F., Derbyshire, M. K., DeWeese-Scott, C., Fong, J. H., Geer, L. Y., Geer, R. C., Gonzales, N. R., Gwadz, M., He, S. , Hurwitz, D. I. , Jackson, J. D., Ke, Z., Lanczycki, C. J., Liebert,

C. A., Liu, C., Lu, Fu., Lu, S., Marchler, G. H., Mullokandov, M., Song, J. S., Tasneem, A., Thanki, N., Yamashita, R. A., Zhang, D., Zhang, N. & Bryant, S. H.2009. CDD: specific functional annotation with the Conserved Domain Database. *Nucleic Acids Res,* 37, 205-210.

Marchler-Bauer, A. & Bryant, S.H. 2004. CD-Search: protein domain annotations on the fly. *Nucleic Acids Res,* 32, 327-331.

Martens, J. W., Knoester, M., Weijts, F., Groffen, S. J., Hu, Z., Bosch, D. & Vlak, J. M. 1995. Characterization of baculovirus insecticides expressing tailored *Bacillus thuringiensis* CryIA(b) crystal proteins. *J Invertebr Pathol,* 66**,** 249-257.

Martin, P. a. W. & Travers, R. S. 1989. Worldwide Abundance and Distribution of *Bacillus thuringiensis* Isolates. *Appl. Environ. Microbiol.,* 55**,** 2437-2442.

Masson, L., Mazza, A., Gringorten, L., Baines, D., Aneliunas, V. & Brousseau, R. 1994. Specificity domain localization of *Bacillus thuringiensis* insecticidal toxins is highly dependent on the bioassay system. *Molecular Microbiology,* 14**,** 851-860.

Matsushima-Hibiya, Y., Watanabe, M., Hidari, K. I., Miyamoto, D., Suzuki, Y., Kasama, T., Koyama, K., Sugimura, T. & Wakabayashi, K. 2003. Identification of glycosphingolipid receptors for pierisin-1, a guanine-specific ADP-ribosylating toxin from the cabbage butterfly. *J Biol Chem,* 278,9972-9978.

Meadows, M. P., Ellis, D. J., Butt, J., Jarrett, P. & Burges, H. D. 1992. Distribution, Frequency, and Diversity of *Bacillus thuringiensis* in an Animal Feed Mill. *Appl. Environ. Microbiol.,* 58**,** 1344-1350.

Meagher, J. L., Winter, H. C., Ezell, P., Goldstein, I. J. & Stuckey, J. A. 2005. Crystal structure of banana lectin reveals a novel second sugar binding site. *Glycobiology,* 15**,** 1033-1042.

Mendelsohn, M., Kough, J., Vaituzis, Z. & Matthews, K. 2003. Are Bt crops safe? *Nat Biotech,* 21**,** 1003-1009.

Mesnage, R., Clair, E., Gress, S., Then, C., Székács, A. & Séralini, G. E. 2012. Cytotoxicity on human cells of Cry1Ab and Cry1Ac Bt insecticidal toxins alone or with a glyphosate-based herbicide. *Journal of Applied Toxicology***,** 695-699.

Mettus-Light, A-M., Baum, J. 2000. *PCT Int. Appl. WO 0026378.*

Minton, N. 2003. *Clostridia* in cancer therapy. *Nat Rev Microbiol,* 1**,** 237 - 242.

Miroux, B. & Walker, J. E. 1996. Over-production of Proteins in *Escherichia coli*: Mutant Hosts that Allow Synthesis of some Membrane Proteins and Globular Proteins at High Levels. *Journal of Molecular Biology,* 260**,** 289-298.

Mizuki, E., Ohba, M., Akao, T., Yamashita, S., Saitoh, H. & Park, Y. S. 1999. Unique activity associated with non-insecticidal *Bacillus thuringiensis* parasporal inclusions: *in vitro* cell-killing action on human cancer cells. *Journal of Applied Microbiology,* 86**,** 477-486.

Mizuki, E., Park, Y. S., Saitoh, H., Yamashita, S., Akao, T., Higuchi, K. & Ohba, M. 2000. Parasporin, a human leukemic cell-recognizing parasporal protein of *Bacillus thuringiensis*. *Clin Diagn Lab Immunol,* 7**,** 625-634.

Mohd-Salleh, M. B., Beegle, C. C. & Lewis, L. C. 1980. Fermentation media and production of exotoxin by three varieties of *Bacillus thuringiensis*. *Journal of Invertebrate Pathology,* 35**,** 75-83.

Moran, C.P., 1993. RNA polymerase and transcription factors. *In: Sonenshein, A. L., Hoch, J. A., Losick, R. (Eds.), Bacillus subtilis and Other Gram-*

Positive Bacteria. American Society for Microbiology, Washington, DC, 653–667.

Morse, R. J., Yamamoto, T. & Stroud, R. M. 2001. Structure of Cry2Aa Suggests an Unexpected Receptor Binding Epitope. *Structure,* 9**,** 409-417.

Nagamatsu, Y., Koike, T., Sasaki, K., Yoshimoto, A. & Furukawa, Y. 1999. The cadherin-like protein is essential to specificity determination and cytotoxic action of the *Bacillus thuringiensis* insecticidal CryIAa toxin. *FEBS Lett,* 460**,** 385-390.

Nagamatsu, Y., Okamura, S., Saitou, H., Akao, T. & Mizuki, E. 2010. Three Cry toxins in two types from *Bacillus thuringiensis* strain M019 preferentially kill human hepatocyte cancer and uterus cervix cancer cells. *Biosci Biotechnol Biochem,* 74**,** 494-498.

Nagamatsu, Y., Toda, S., Yamaguchi, F., Ogo, M., Kogure, M., Nakamura, M., Shibata, Y. & Katsumoto, T. 1998. Identification of *Bombyx mori* midgut receptor for *Bacillus thuringiensis* insecticidal CryIA(a) toxin. *Biosci Biotechnol Biochem,* 62**,** 718-726.

Naimov, S., Boncheva, R., Karlova, R., Dukiandjiev, S., Minkov, I. & De Maagd, R. A. 2008. Solubilization, activation, and insecticidal activity of *Bacillus thuringiensis* serovar *thompsoni* HD542 crystal proteins. *Appl Environ Microbiol,* 74**,** 7145-7151.

Naimov, S., Martens-Uzunova, E., Weemen-Hendriks, M., Dukiandjiev, S., Minkov, I. & De Maagd, R. A. 2006. Carboxy-terminal extension effects on crystal formation and insecticidal properties of Colorado potato beetle-active *Bacillus thuringiensis* delta-endotoxins. *Mol Biotechnol,* 32**,** 185-196.

Nisnevitch, M., Sigawi, S., Cahan, R. & Nitzan, Y. 2010. Isolation, Characterization and Biological Role of Camelysin from *Bacillus thuringiensis* Subsp. *israelensis*. *Curr Microbiol*, 61, 176-183.

O'brien, J., Wilson, I., Orton, T. & Pognan, F. 2000. Investigation of the Alamar Blue (resazurin) fluorescent dye for the assessment of mammalian cell cytotoxicity. *European Journal of Biochemistry,* 267**,** 5421-5426.

Oestergaard, J., Ehlers, R. U., Martinez-Ramirez, A. C. & Real, M. D. 2007. Binding of Cyt1Aa and Cry11Aa toxins of *Bacillus thuringiensis* serovar *israelensis* to brush border membrane vesicles of *Tipula paludosa* (Diptera: Nematocera) and subsequent pore formation. *Appl Environ Microbiol,* 73**,** 3623-3629.

Ohba, M. 1996. *Bacillus thuringiensis* populations naturally occurring on mulberry leaves: a possible source of the populations associated with silkworm-rearing insectaries. *Journal of Applied Microbiology,* 80**,** 56-64.

Ohba, M. & Aizawa, K. 1986. Insect toxicity of *Bacillus thuringiensis* isolated from soils of Japan. *Journal of Invertebrate Pathology,* 47**,** 12-20.

Ohba, M., Mizuki, E. & Uemori, A. 2009. Parasporin, a new anticancer protein group from *Bacillus thuringiensis*. *Anticancer Res,* 29**,** 427-433.

Ohgushi, A., Saitoh, H., Wasano, N., Uemori, A. & Ohba, M. 2005. Cloning and Characterization of Two Novel Genes, *cry24B* and *s1orf2*, from a Mosquitocidal Strain of *Bacillus thuringiensis* serovar *sotto. Current Microbiology,* 51**,** 131-136.

Okinaka, R., Cloud, K., Hampton, O., Hoffmaster, A., Hill, K., Keim, P., Koehler, T., Lamke, G., Kumano, S., Manter, D., Martinez, Y., Ricke, D., Svensson, R. & Jackson, P. 1999. Sequence, assembly and analysis of pX01 and pX02. *Journal of Applied Microbiology,* 87**,** 261-262.

Okumura, S., Ohba, M., Mizuki, E., Crickmore, N., Côté, J.-C., Nagamatsu, Y., Kitada, S., Sakai, H., Harata, K. and Shin, T. 2013. Parasporin nomenclature. http://parasporin.fitc.pref.fukuoka.jp/

Okumura, S., Saitoh, H., Ishikawa, T., Inouye, K. & Mizuki, E. 2011. Mode of action of parasporin-4, a cytocidal protein from *Bacillus thuringiensis*. *Biochimica et Biophysica Acta (BBA) - Biomembranes,* 1808**,** 1476-1482.

Okumura, S., Saitoh, H., Ishikawa, T., Wasano, N., Yamashita, S., Kusumoto, K.-I., Akao, T., Mizuki, E., Ohba, M. & Inouye, K. 2005. Identification of a Novel Cytotoxic Protein, Cry45Aa, from *Bacillus thuringiensis* A1470 and Its Selective Cytotoxic Activity against Various Mammalian Cell Lines. *Journal of Agricultural and Food Chemistry,* 53**,** 6313-6318.

Okumura, S., Saitoh, H., Wasano, N., Katayama, H., Higuchi, K., Mizuki, E. & Inouye, K. 2006. Efficient solubilization, activation, and purification of recombinant Cry45Aa of *Bacillus thuringiensis* expressed as inclusion bodies in *Escherichia coli*. *Protein Expression and Purification,* 47**,** 144-151.

Pacheco, S., Gómez, I., Arenas, I., Saab-Rincon, G., Rodríguez-Almazán, C., Gill, S. S., Bravo, A. & Soberón, M. 2009. Domain II Loop 3 of *Bacillus thuringiensis* Cry1Ab Toxin Is Involved in a “Ping Pong” Binding Mechanism with *Manduca sexta* Aminopeptidase-N and Cadherin Receptors. *Journal of Biological Chemistry,* 284**,** 32750-32757.

Pardo-López, L., Soberón, M. & Bravo, A. 2013. *Bacillus thuringiensis* insecticidal three-domain Cry toxins: mode of action, insect resistance and consequences for crop protection. *FEMS Microbiology Reviews,* 37**,** 3-22.

Park, H.-W., Bideshi, D. K. & Federici, B. A. 2000. Molecular Genetic Manipulation of Truncated Cry1C Protein Synthesis in *Bacillus thuringiensis* To Improve Stability and Yield. *Applied and Environmental Microbiology,* 66**,** 4449-4455.

Parker, M. W., Buckley, J. T., Postma, J. P. M., Tucker, A. D., Leonard, K., Pattus, F. & Tsernoglou, D. 1994. Structure of the *Aeromonas* toxin proaerolysin in its water-soluble and membrane-channel states. *Nature,* 367**,** 292-295.

Parker, M. W., Postma, J. P. M., Pattus, F., Tucker, A. D. & Tsernoglou, D. 1992. Refined structure of the pore-forming domain of colicin A at 2.4 Å resolution. *Journal of Molecular Biology,* 224**,** 639-657.

Patyar, S., Joshi, R., Byrav, D. P., Prakash, A., Medhi, B. & Das, B. 2010. Bacteria in cancer therapy: a novel experimental strategy. *Journal of Biomedical Science,* 17**:** 21.

Payne, J. M., Kennedy, M. K., Randall, J. B., Meier, H., Uick, H.J., et al. 1997.*U.S. Patent No. 5596071.*

Pendleton, I. R., Bernheimer, A. W. & Grushoff, P. 1973. Purification and partial characterization of hemolysins from *Bacillus thuringiensis*. *J Invertebr Pathol,* 21**,** 131-135.

Perani, M., Bishop, A. H. & Vaid, A. 1998. Prevalence of beta-exotoxin, diarrhoeal toxin and specific delta-endotoxin in natural isolates of *Bacillus thuringiensis*. *FEMS Microbiol Lett,* 160**,** 55-60.

Perez, C., Fernandez, L. E., Sun, J., Folch, J. L., Gill, S. S., Soberon, M. & Bravo, A. 2005. *Bacillus thuringiensis* subsp. *israelensis* Cyt1Aa synergizes Cry11Aa toxin by functioning as a membrane-bound receptor. *Proc Natl Acad Sci U S A,* 102**,** 18303-18308.

Petras, S. F. & Casida, L. E. 1985. Survival of *Bacillus thuringiensis* Spores in Soil. *Appl Environ Microbiol,* 50**,** 1496-1501.

Pigott, C. R. & Ellar, D. J. 2007. Role of receptors in *Bacillus thuringiensis* crystal toxin activity. *Microbiol Mol Biol Rev,* 71**,** 255-281.

Poornima, K., Selvanayagam, P. & Shenbagarathai, R. 2010. Identification of native *Bacillus thuringiensis* strain from South India having specific cytocidal activity against cancer cells. *J Appl Microbiol*, 348-354.

Promdonkoy, B. & Ellar, D. J. 2000. Membrane pore architecture of a cytolytic toxin from *Bacillus thuringiensis*. *Biochem. J. ,* 350**,** 275-282.

Promdonkoy, B. & Ellar, D. J. 2003 Investigation of the pore-forming mechanism of a cytolytic delta-endotoxin from *Bacillus thuringiensis*. *Biochem. J. ,* 374**,** 255-259.

Promdonkoy, B., Promdonkoy, P. & Panyim, S. 2005. Co-expression of *Bacillus thuringiensis* Cry4Ba and Cyt2Aa2 in *Escherichia coli* revealed high synergism against *Aedes aegypti* and *Culex quinquefasciatus* larvae. *FEMS Microbiol Lett,* 252**,** 121-126.

Promega 2009. CellTiter-Blue® Cell Viability Assay. *Technical Bulletin #TB317* Revised 6/09.

Rajamohan, F., Alzate, O., Cotrill, J. A., Curtiss, A. & Dean, D. H. 1996a. Protein engineering of *Bacillus thuringiensis* delta-endotoxin: mutations at domain II of CryIAb enhance receptor affinity and toxicity toward gypsy moth larvae. *Proc Natl Acad Sci U S A,* 93**,** 14338-14343.

Rajamohan, F., Cotrill, J. A., Gould, F. & Dean, D. H. 1996b. Role of domain II, loop 2 residues of *Bacillus thuringiensis* CryIAb delta-endotoxin in reversible and irreversible binding to *Manduca sexta* and *Heliothis virescens*. *J Biol Chem,* 271**,** 2390-2396.

Rang, C., Lacey, L. A. & Frutos, R. 2000. The crystal proteins from *Bacillus thuringiensis* subsp. thompsoni display a synergistic activity against the codling moth, *Cydia pomonella*. *Curr Microbiol,* 40**,** 200-204.

Rang, C., Vachon, V., De Maagd, R. A., Villalon, M., Schwartz, J.-L., Bosch, D., Frutos, R. & Laprade, R. 1999. Interaction between Functional Domains of *Bacillus thuringiensis* Insecticidal Crystal Proteins. *Applied and Environmental Microbiology,* 65**,** 2918-2925.

Raymond, B., Johnston, P. R., Nielsen-Leroux, C., Lereclus, D. & Crickmore, N. 2010. *Bacillus thuringiensis*: an impotent pathogen? *Trends in Microbiology,* 18**,** 189-194.

Read, T. D., Peterson, S. N., Tourasse, N., Baillie, L. W., Paulsen, I. T., Nelson, K. E., Tettelin, H., Fouts, D. E., Eisen, J. A., Gill, S. R., Holtzapple, E. K., Okstad, O. A., Helgason, E., Rilstone, J., Wu, M., Kolonay, J. F., Beanan, M. J., Dodson, R. J., Brinkac, L. M., Gwinn, M., Deboy, R. T., Madpu, R., Daugherty, S. C., Durkin, A. S., Haft, D. H., Nelson, W. C., Peterson, J. D., Pop, M., Khouri, H. M., Radune, D., Benton, J. L., Mahamoud, Y., Jiang, L., Hance, I. R., Weidman, J. F., Berry, K. J., Plaut, R. D., Wolf, A. M., Watkins, K. L., Nierman, W. C., Hazen, A., Cline, R., Redmond, C., Thwaite, J. E., White, O., Salzberg, S. L., Thomason, B., Friedlander, A. M., Koehler, T. M., Hanna, P. C., Kolsto, A.-B. & Fraser, C. M. 2003. The genome sequence of *Bacillus anthracis* Ames and comparison to closely related bacteria. *Nature,* 423**,** 81-86.

Richardson, M., Ramirez, T., Russell, N. & Moye, L. 1999. Coley toxins immunotherapy: a retrospective review. *Altern Ther Health Med,* 5**,** 42 - 47.

Rosenquist, H., Smidt, L., Andersen, S. R., Jensen, G. B. & Wilcks, A. 2005. Occurrence and significance of *Bacillus cereus* and *Bacillus thuringiensis* in ready-to-eat food. *FEMS Microbiol Lett,* 250**,** 129-136.

Rössler, D., Ludwig, W., Schleifer, K. H., Lin, C., Mcgill, T. J., Wisotzkey, J. D., Jurtshuk Jr, P. & Fox, G. E. 1991. Phylogenetic Diversity in the Genus Bacillus as Seen by 16S rRNA Sequencing Studies. *Systematic and Applied Microbiology,* 14**,** 266-269.

Rosso, M. & Delecluse, A. 1997. Contribution of the 65-kilodalton protein encoded by the cloned gene *cry19A* to the mosquitocidal activity of *Bacillus thuringiensis* subsp. *jegathesan*. *Appl. Environ. Microbiol.,* 63**,** 4449-4455.

Rydel, T., Sharamitaro, J., Brown, G.R., Gouzov, V., Seale, J., *Sturman, E.,* Thoma, R., Gruys, K. & English, L. 2001. The crystal structure of a coleopteran insect-active binary B.t. protein toxin complex at 2.5 Å resolution. *Presented at Annu. Meet. Am. Crystallogr. Assoc., Los Angeles.*

Rydel, T., Sturman, E., Williams, J., Moshiri, F., Krieger, E. & Isaac, B. 2003. The crystal structure of a novel 79 kDa, six domain Bt toxin. *Presented at Annu. Meet. Am. Crystallogr. Assoc., Covington.*

Salamitou, S., Agaisse, H., Bravo, A. & Lereclus, D. 1996. Genetic analysis of *cryIIIA* gene expression in *Bacillus thuringiensis*. *Microbiology,* 142 (Pt 8)**,** 2049-55.

Salamitou, S., Ramisse, F., Brehelin, M., Bourguet, D., Gilois, N., Gominet, M., Hernandez, E. & Lereclus, D. 2000. The *plcR* regulon is involved in the opportunistic properties of *Bacillus thuringiensis* and *Bacillus cereus* in mice and insects. *Microbiology,* 146**,** 2825-2832.

Sampson, M. N. & Gooday, G. W. 1998. Involvement of chitinases of *Bacillus thuringiensis* during pathogenesis in insects. *Microbiology,* 144**,** 2189-2194.

Sandvig, K. & Deurs, B. V. 2000. Entry of ricin & shiga toxin into cells: molecular mechanisms and medical perspectives. *The EMBO Journal,* 19**,** 5943-5950.

Sangadala, S., Walters, F. S., English, L. H. & Adang, M. J. 1994. A mixture of *Manduca sexta* aminopeptidase and phosphatase enhances *Bacillus thuringiensis* insecticidal CryIA(c) toxin binding and $^{86}Rb^{+}$-K^{+} efflux *in vitro. J Biol Chem,* 269**,** 10088-10092.

Sayyed, A. H., Haward, R., Herrero, S., Ferré, J. & Wright, D. J. 2000. Genetic and biochemical approach for characterization of resistance to *Bacillus thuringiensis* toxin Cry1Ac in a field population of the diamondback moth, *Plutella xylostella*. *Applied and Environmental Microbiology,* 66, 1509-1516.

Schmitt, C., Meysick, K. & O'brien, A. 1999. Bacterial toxins: friends or foes? *Emerg Infect Disease.,* 5**,** 224-234.

Schnepf, E., Crickmore, N., Van Rie, J., Lereclus, D., Baum, J., Feitelson, J., Zeigler, D. R. & Dean, D. H. 1998. *Bacillus thuringiensis* and Its Pesticidal Crystal Proteins. *Microbiol. Mol. Biol. Rev.,* 62**,** 775-806.

Schwede, T., Kopp, J., Guex, N. & Peitsch, M. C. 2003. SWISS-MODEL: an automated protein homology-modeling server. *Nucleic Acids Research,* 31**,** 3381-3385.

Sher, D., Fishman, Y., Zhang, M., Lebendiker, M., Gaathon, A., Mancheño, J.-M. & Zlotkin, E. 2005. Hydralysins, a New Category of β-Pore-forming Toxins in Cnidaria. *Journal of Biological Chemistry,* 280**,** 22847-22855.

Shi, Y., Xu, W., Yuan, M., Tang, M., Chen, J. & Pang, Y. 2004. Expression of *vip1/vip2* genes in *Escherichia coli* and *Bacillus thuringiensis* and the analysis of their signal peptides. *J Appl Microbiol,* 97**,** 757-765.

Silo-Suh, L. A., Stabb, E. V., Raffel, S. J. & Handelsman, J. 1998. Target Range of Zwittermicin A, an Aminopolyol Antibiotic from *Bacillus cereus*. *Current Microbiology,* 37**,** 6-11.

Slaughter, M. R., Bugelski, P. J. & O'brien, P. J. 1999. Evaluation of Alamar Blue Reduction for the *In Vitro* Assay of Hepatocyte Toxicity. *Toxicology in Vitro,* 13**,** 567-569.

Squatrito, R. C., Connor, J. P. & Buller, R. E. 1995. Comparison of a Novel Redox Dye Cell Growth Assay to the ATP Bioluminescence Assay. *Gynecologic Oncology,* 58**,** 101-105.

Stabb, E. V., Jacobson, L. M. & Handelsman, J. 1994. Zwittermicin A-producing strains of *Bacillus cereus* from diverse soils. *Applied and Environmental Microbiology,* 60**,** 4404-4412.

Swiecicka, I. & De Vos, P. 2003. Properties of *Bacillus thuringiensis* isolated from bank voles. *J Appl Microbiol,* 94**,** 60-64.

Swiecicka, I., Fiedoruk, K. & Bednarz, G. 2002. The occurrence and properties of *Bacillus thuringiensis* isolated from free-living animals. *Lett Appl Microbiol,* 34**,** 194-198.

Swiecicka, I. & Mahillon, J. 2006. Diversity of commensal *Bacillus cereus sensu lato* isolated from the common sow bug (*Porcellio scaber*, Isopoda). *FEMS Microbiology Ecology,* 56**,** 132-140.

Tabashnik, B. E. 2010. Communal Benefits of Transgenic Corn. *Science,* 330**,** 189-190.

Tantimavanich, S., Pantuwatana, S., Bhumiratana, A. & Panbangred, W. 1997. Cloning of a chitinase gene into *Bacillus thuringiensis* subsp. *aizawai* for enhanced insecticidal activity. *J Gen Appl Microbiol,* 43**,** 341-347.

Te Giffel, M. C., Beumer, R. R., Klijn, N., Wagendorp, A. & Rombouts, F. M. 1997. Discrimination between *Bacillus cereus* and *Bacillus thuringiensis* using specific DNA probes based on variable regions of 16S rRNA. *FEMS Microbiol Lett,* 146**,** 47-51.

Thiele, E., Arison, R. & Boxer, G. 1963. Oncolysis by Clostridia IV effect of nonpathogenic Clostridial spores in normal and pathological tissues. *Cancer Res,* 24**,** 234 - 238.

Thomas, W. E. & Ellar, D. J. 1983a. *Bacillus thuringiensis* var *israelensis* crystal delta-endotoxin: effects on insect and mammalian cells *in vitro* and *in vivo*. *Journal of Cell Science,* 60**,** 181-197.

Thomas, W. E. & Ellar, D. J. 1983b. Mechanism of action of *Bacillus thuringiensis* var *israelensis* insecticidal delta-endotoxin. *FEBS Lett,* 154**,** 362-368.

Thompson, M., Knuth, M., Cardineau, G. 2001. *U.S. Patent No. 6303364.*

Thorne, L., Garduno, F., Thompson, T., Decker, D., Zounes, M., Wild, M., Walfield, A. M. & Pollock, T. J. 1986. Structural similarity between the lepidoptera- and diptera-specific insecticidal endotoxin genes of *Bacillus thuringiensis* subsp. "*kurstaki*" and "*israelensis*". *Journal of Bacteriology,* 166**,** 801-811.

Tilley, S. J., Orlova, E. V., Gilbert, R. J., Andrew, P. W. & Saibil, H. R. 2005. Structural basis of pore formation by the bacterial toxin pneumolysin.*Cell,* 121**,** 247–256.

Tojo, A. & Aizawa, K. 1983. Dissolution and Degradation of *Bacillus thuringiensis* δ-Endotoxin by Gut Juice Protease of the Silkworm *Bombyx mori. Applied and Environmental Microbiology,* 45**,** 576-580.

Tsuzuki, K., Kimura, K., Fujii, N., Yokosawa, N., Indoh, T., Murakami, T. & Oguma, K. 1990. Cloning and complete nucleotide sequence of the gene for the main component of hemagglutinin produced by *Clostridium botulinum* type C. *Infection and Immunity,* 58**,** 3173-3177.

Uemori, A., Ohgushi, A., Yasutake, K., Maeda, M., Mizuki, E. & Ohba, M. 2008. Parasporin-1Ab, a novel *Bacillus thuringiensis* cytotoxin preferentially active on human cancer cells *in vitro*. *Anticancer Res,* 28**,** 91-95.

Vachon, V., Laprade, R. & Schwartz, J. L. 2012. Current models of the mode of action of *Bacillus thuringiensis* insecticidal crystal proteins: A critical review. *J Invertebr Pathol*, 111, 1-12.

Vadlamudi, R. K., Ji, T. H. & Bulla, L. A., Jr. 1993. A specific binding protein from *Manduca sexta* for the insecticidal toxin of *Bacillus thuringiensis* subsp. *berliner*. *J Biol Chem,* 268**,** 12334-12340.

Vaeck, M., Reynaerts, A., Hofte, H., Jansens, S., De Beuckeleer, M., Dean, C., Zabeau, M., Montagu, M. V. & Leemans, J. 1987. Transgenic plants protected from insect attack. *Nature,* 328**,** 33-37.

Valaitis, A. P., Mazza, A., Brousseau, R. & Masson, L. 1997. Interaction analyses of *Bacillus thuringiensis* Cry1A toxins with two aminopeptidases from gypsy moth midgut brush border membranes. *Insect Biochemistry and Molecular Biology,* 27**,** 529-539.

Van Rie, J., Jansens, S., Hofte, H., Degheele, D. & Van Mellaert, H. 1989. Specificity of *Bacillus thuringiensis* delta-endotoxins. Importance of specific receptors on the brush border membrane of the mid-gut of target insects. *Eur J Biochem,* 186**,** 239-247.

Walter, C., Fladung, M. & Boerjan, W. 2010. The 20-year environmental safety record of GM trees. *Nat Biotech,* 28**,** 656-658.

Ward, E. S. & Ellar, D. J. 1983. Assignment of the δ-endotoxin gene of *Bacillus thuringiensis* var. *israelensis* to a specific plasmid by curing analysis. *FEBS Letters,* 158**,** 45-49.

Wei, J. Z., Hale, K., Carta, L., Platzer, E., Wong, C., Fang, S. C. & Aroian, R. V. 2003. *Bacillus thuringiensis* crystal proteins that target nematodes. *Proc Natl Acad Sci U S A,* 100**,** 2760-5.

West, A. W., Burges, H. D. & Wyborn, C. H. 1984. Effect of incubation in natural and autoclaved soil upon potency and viability of *Bacillus thuringiensis*. *J. Invertebr. Pathol.,* 44**,** 121-127.

Widner, W. R. & Whiteley, H. R. 1990. Location of the dipteran specificity region in a lepidopteran-dipteran crystal protein from *Bacillus thuringiensis*. *J Bacteriol,* 172**,** 2826-2832.

Wirth, M. C., Walton, W. E. & Delecluse, A. 2003. Deletion of the Cry11A or the Cyt1A toxin from *Bacillus thuringiensis* subsp. *israelensis*: effect on toxicity against resistant *Culex quinquefasciatus* (Diptera: Culicidae). *J Invertebr Pathol,* 82**,** 133-135.

Wirth, M. C., Walton, W. E. & Federici, B. A. 2010. Evolution of resistance to the *Bacillus sphaericus* Bin toxin is phenotypically masked by combination with the mosquitocidal proteins of *Bacillus thuringiensis* subspecies *israelensis*. *Environmental Microbiology,* 12**,** 1154-1160.

Wong, H. C., Schnepf, H. E. & Whiteley, H. R. 1983. Transcriptional and translational start sites for the *Bacillus thuringiensis* crystal protein gene. The Journal of biological chemistry, 258,1960-1967.

Yamashita, S., Akao, T., Mizuki, E., Saitoh, H., Higuchi, K., Park, Y. S., Kim, H. S. & Ohba, M. 2000. Characterization of the anti-cancer-cell parasporal proteins of a *Bacillus thuringiensis* isolate. *Can J Microbiol,* 46**,** 913-919.

Yamashita, S., Katayama, H., Saitoh, H., Akao, T., Park, Y. S., Mizuki, E., Ohba, M. & Ito, A. 2005. Typical Three-Domain Cry Proteins of *Bacillus thuringiensis* Strain A1462 Exhibit Cytocidal Activity on Limited Human Cancer Cells. *Journal of Biochemistry,* 138**,** 663-672.

Yoshisue, H., Fukada, T., Yoshida, K., Sen, K., Kurosawa, S., Sakai, H. & Komano, T. 1993a. Transcriptional regulation of *Bacillus thuringiensis* subsp. *israelensis* mosquito larvicidal crystal protein gene *cryIVA*. *J Bacteriol,* 175**,** 2750-2753.

Yoshisue, H., Nishimoto, T., Sakai, H. & Komano, T. 1993b. Identification of a promoter for the crystal protein-encoding gene *cryIVB* from *Bacillus thuringiensis* subsp. *israelensis*. *Gene,* 137**,** 247-251.

Zacharski, L. & Sukhatme, V. 2005. Coley's toxin revisited: immunotherapy or plasminogen activator therapy of cancer? *Journal of Thrombosis and Haemostasis,* 3**,** 424-427.

Zhang, J., Hodgman, T. C., Krieger, L., Schnetter, W. & Schairer, H. U. 1997. Cloning and analysis of the first *cry* gene from *Bacillus popilliae*. *Journal of Bacteriology,* 179**,** 4336-4341.

Zhang, M. Y., Lovgren, A., Low, M. G. & Landen, R. 1993. Characterization of an avirulent pleiotropic mutant of the insect pathogen *Bacillus thuringiensis*: reduced expression of flagellin and phospholipases. *Infect Immun,* 61**,** 4947-54.

Zhang, X., Candas, M., Griko, N. B., Rose-Young, L. & Bulla, L. A., Jr. 2005. Cytotoxicity of *Bacillus thuringiensis* Cry1Ab toxin depends on specific binding of the toxin to the cadherin receptor BT-R1 expressed in insect cells. *Cell Death Differ,* 12**,** 1407-1416.

Zhang, X., Candas, M., Griko, N. B., Taussig, R. & Bulla, L. A., Jr. 2006. A mechanism of cell death involving an adenylyl cyclase/PKA signaling pathway is induced by the Cry1Ab toxin of *Bacillus thuringiensis*. *Proc Natl Acad Sci U S A,* 103**,** 9897-9902.

Zhang, X., Griko, N. B., Corona, S. K. & Bulla, L. A., Jr. 2008. Enhanced exocytosis of the receptor BT-R(1) induced by the Cry1Ab toxin of *Bacillus thuringiensis* directly correlates to the execution of cell death. *Comp Biochem Physiol B Biochem Mol Biol,* 149**,** 581-588.

Zhuang, M., Oltean, D. I., Gómez, I., Pullikuth, A. K., Soberón, M., Bravo, A. & Gill, S. S. 2002. *Heliothis virescens* and *Manduca sexta* Lipid Rafts Are Involved in Cry1A Toxin Binding to the Midgut Epithelium and Subsequent Pore Formation. *Journal of Biological Chemistry,* 277**,** 13863-13872.

Appendix

Appendix 1. Alignment of Cry1Ac with homologous Cry1Aa whose three-dimensional structure has been resolved by x-ray crystallography to predict the secondary structure elements.

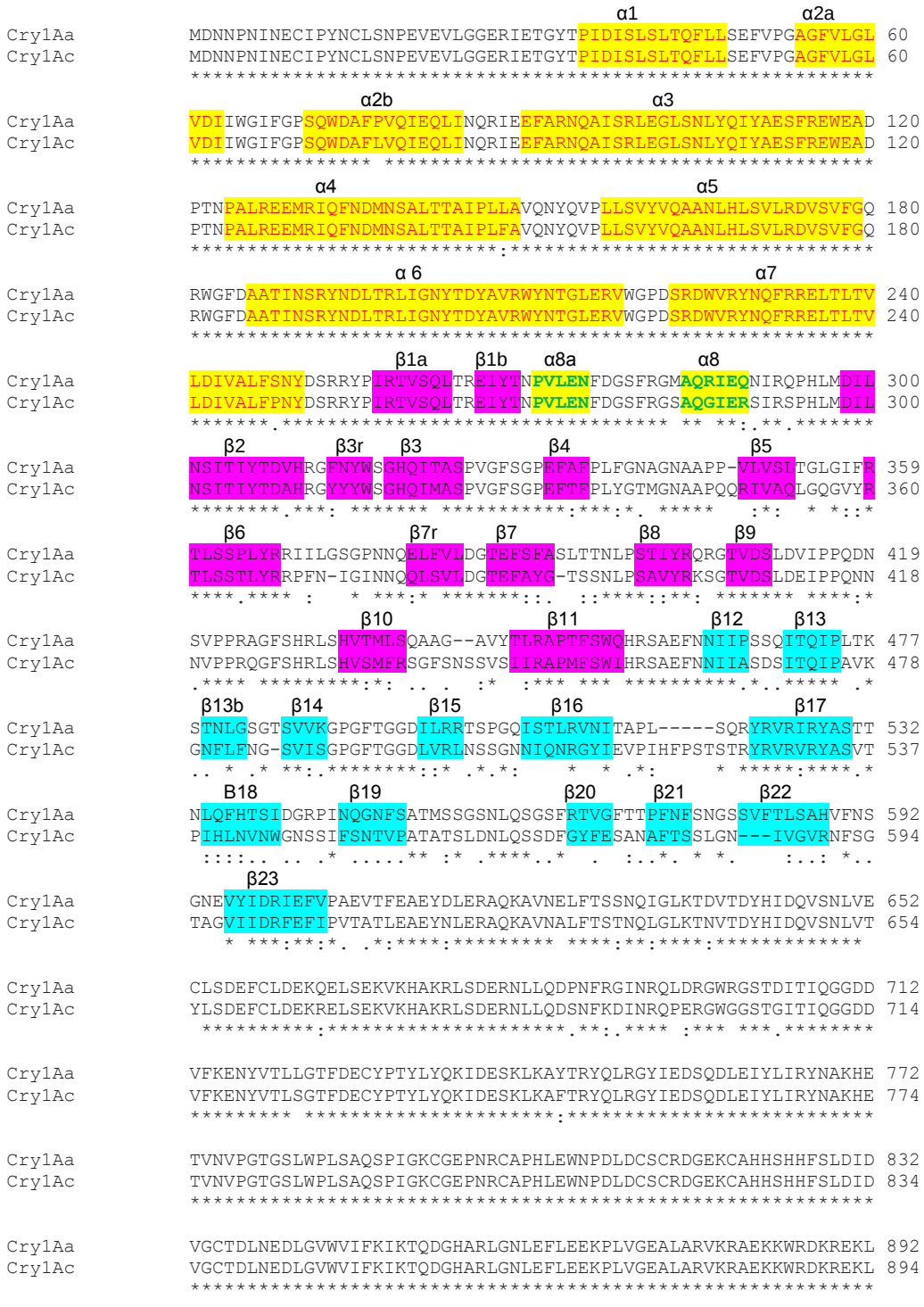

```
Cry1Aa          EWETNIVYKEAKESVDALFVNSQYDQLQADTNIAMIHAADKRVHSIREAYLPELSVIPGV 952
Cry1Ac          EWETNIVYKEAKESVDALFVNSQYDQLQADTNIAMIHAADKRVHSIREAYLPELSVIPGV 954
                ************************************************************


Cry1Aa          NAAIFEELEGRIFTAFSLYDARNVIKNGDFNNGLSCWNVKGHVDVEEQNNQRSVLVLPEW 1012
Cry1Ac          NAAIFEELEGRIFTAFSLYDARNVIKNGDFNNGLSCWNVKGHVDVEEQNNQRSVLVVPEW 1014
                ************************************************************:***

Cry1Aa          EAEVSQEVRVCPGRGYILRVTAYKEGYGEGCVTIHEIENNTDELKFSNCVEEEIYPNNTV 1072
Cry1Ac          EAEVSQEVRVCPGRGYILRVTAYKEGYGEGCVTIHEIENNTDELKFSNCVEEEIYPNNTV 1074
                ************************************************************

Cry1Aa          TCNDYTVNQEEYGGAYTSRNRGYNEAPSVPADYASVYEEKSYTDGRRENPCEFNRGYRDY 1132
Cry1Ac          TCNDYTVNQEEYGGAYTSRNRGYNEAPSVPADYASVYEEKSYTDGRRENPCEFNRGYRDY 1134
                ************************************************************

Cry1Aa          TPLPVGYVTKELEYFPETDKVWIEIGETEGTFIVDSVELLLMEE 1176
Cry1Ac          TPLPVGYVTKELEYFPETDKVWIEIGETEGTFIVDSVELLLMEE 1178
                *********************************************
```

Amino acid residues of Cry1Aa and Cry1Ac in red letters and highlighted in yellow represent the α-helices of domain I (α1-7) and those in green letters and highlighted in yellow represent the α-helices of domain II (α8a and 8) and those highlighted in pink represent the β-strands of domain II (β1a-β11) and the ones highlighted in turquoise represent domain III (β12-23).